Usman Ghani

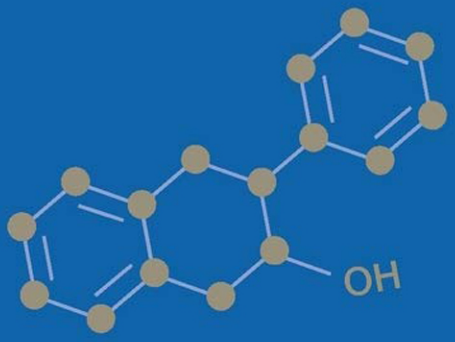

Alpha-Glucosidase Inhibitors

Clinically Promising Candidates for Antidiabetic Drug Discovery

ELSEVIER

Alpha-Glucosidase Inhibitors

Alpha-Glucosidase Inhibitors

Clinically Promising Candidates for Antidiabetic Drug Discovery

USMAN GHANI
Associate Professor of Biochemistry,
Clinical Biochemistry Unit, Department of Pathology,
College of Medicine, King Saud University,
Riyadh, Saudi Arabia

ELSEVIER

Elsevier
Radarweg 29, PO Box 211, 1000 AE Amsterdam, Netherlands
The Boulevard, Langford Lane, Kidlington, Oxford OX5 1GB, United Kingdom
50 Hampshire Street, 5th Floor, Cambridge, MA 02139, United States

Notices
Knowledge and best practice in this field are constantly changing. As new research and experience broaden our understanding, changes in research methods, professional practices, or medical treatment may become necessary.

Practitioners and researchers must always rely on their own experience and knowledge in evaluating and using any information, methods, compounds, or experiments described herein. In using such information or methods they should be mindful of their own safety and the safety of others, including parties for whom they have a professional responsibility.

To the fullest extent of the law, neither the Publisher nor the authors, contributors, or editors, assume any liability for any injury and/or damage to persons or property as a matter of products liability, negligence or otherwise, or from any use or operation of any methods, products, instructions, or ideas contained in the material herein.

British Library Cataloguing-in-Publication Data
A catalogue record for this book is available from the British Library

Library of Congress Cataloging-in-Publication Data
A catalog record for this book is available from the Library of Congress

ISBN: 978-0-08-102779-0

Publisher: Susan Dennis
Acquisition Editor: Emily M. McCloskey
Editorial Project Manager: Kelsey Connors
Production Project Manager: Vijayaraj Purushothaman
Cover Designer: Christian Bilbow

Typeset by MPS Limited, Chennai, India

Quote from the Quran

And it is We Who constructed the Universe with might,
and verily it is We Who are expanding it.

(The Quran: Chapter 51, Verse 47)

To my beloved parents

Dr. Ibrahim Haroon and Mrs. Zubeda Ibrahim

who are my perpetual provenance of
love, care, prayers, and nurturing of
endeavors that define my life.

Contents

About the author

Dr. Usman Ghani is a biochemist with education and training from the University of Karachi, Pakistan and University of Alberta, Canada. Presently, he is Associate Professor of Biochemistry at Clinical Biochemistry Unit, Department of Pathology, College of Medicine, King Saud University, Saudi Arabia. His research interests include enzymology, cellular processes, and endothelial function and repair in disease. Dr. Ghani's current research also involves screening and identification of clinically important enzyme inhibitors and studies on their mechanism of inhibition. His team has identified a number of synthetic and natural inhibitors of α-glucosidase and other enzymes that may become promising candidates for development into drugs for treatment of diabetes mellitus and other diseases. Dr. Ghani has been awarded numerous research grants, and publishes his research work in high impact journals of international repute.

Preface

Diabetes mellitus is a growing global problem in both clinical and economic terms. The disease has been alarmingly ushering clinicians, healthcare authorities, and scientists into finding new avenues to curb its devastating impact on patients and healthcare systems. Consequently, the field of antidiabetic drug discovery has flourished dramatically in recent years witnessing development of promising drugs with broad spectra of modes of action. However, treatment of diabetes mellitus by oral α-glucosidase inhibitors is still confined to acarbose, miglitol, and voglibose. The drug development of antidiabetic α-glucosidase inhibitors is essentially at halt since acarbose, miglitol and voglibose were launched three decades ago. Healthcare authorities and pharmaceutical companies in many countries are phasing them out partly because of their efficacy problems, unwanted gastrointestinal side effects, lack of multiple modes of action, and lack of promising net therapeutic effects including improvement in quality of life.

This does not mean that α-glucosidase inhibitor discovery has stopped; the scientific literature has been witnessing thousands of compounds of natural and synthetic origins exhibiting promising antihyperglycemic and α-glucosidase inhibitory activities. Therefore, there is ample supply of new compounds generating a plethora of α-glucosidase inhibitors simply piling up in the haystack of publications and reports that usually do not undergo further studies involving lead optimization and development. Realizing the gaps and vacuum in antidiabetic α-glucosidase inhibitor drug development, this book addresses the concern by finding "needles" in that ever growing haystack of compounds by identifying promising α-glucosidase inhibitors and presenting them to the drug development

community to come forward and further gauge their potential candidacy for lead optimization, preclinical or even clinical trials. The book will serve as a valuable tool for biochemists, synthetic and medicinal chemists, enzymologists, pharmacologists, structural and computational biologists, and pharmaceutical companies who have interest or would like to direct their interest toward developing new α-glucosidase inhibitors as antidiabetic drugs.

For this purpose, the groundwork for identifying promising inhibitors is already laid in the present work so that the target audience does not have to go through that tedious process of selecting lead inhibitors. New, safer and efficacious α-glucosidase inhibitors may be just around the corner, if re-explored. This work identifies 390 promising α-glucosidase inhibitors of natural and synthetic origins that may qualify for antidiabetic drug candidacy based on their enzyme kinetic data, potency of inhibition, ability to reduce blood glucose levels *in vivo*, and computational and structural biology.

The book is composed of seven chapters that discuss a wide range of α-glucosidase inhibitors of diverse chemistry encompassing sugar mimics, polyphenols, terpenoids and steroids, azoles and cyclitols. It also addresses the general problems associated with drug development with special focus on relevant background and factors which are potentially responsible for challenges in the α-glucosidase drug development. The book discusses acarbose, miglitol and voglibose against a broader perspective of current antidiabetic drugs, and identifies supporting and contrasting avenues that provide insights into the future of α-glucosidase inhibitor drug discovery.

Sugar mimics are a major class of α-glucosidase inhibitors that include iminosugars, thiosugars, aminosugars, and carbasugars. Previous research on sugar mimics has led to the development of acarbose, miglitol, and voglibose as antidiabetic drugs. They still bear potential for new antidiabetic drug

development since many new and promising sugar mimicking α-glucosidase inhibitors have been discovered to date including polyhydroxylated pyrrolidines, pyrrolizidines, quinolizidines, indolizidines, and nojirimycin derivatives.

Recently, the scientific literature has witnessed a significant surge in reports on antidiabetic polyphenols with antihyperglycemic and α-glucosidase inhibitory activities. Polyphenols, isolated from the plants of medicinal value, are active against a number of clinical targets including diabetes mellitus. Plants used for treatment of diabetes in traditional medicine contain potent polyphenol α-glucosidase inhibitors such as xanthones, chalcones and flavonoids with ability to lower blood glucose levels and stimulate insulin secretion *in vivo*.

Natural and synthetic terpenoids and steroids are gaining interest due to their antidiabetic effects since they regulate glucose metabolism and inhibit α-glucosidase. Synthetic approaches involving various combinations of chemical moieties incorporated into the terpenoid structure have yielded lupine, oleanane, ursane, oleanolic acid, and ursolic acid derivatives with promising α-glucosidase inhibitory activity and *in vivo* antihyperglycemic effects. The book also highlights azole and cyclitol α-glucosidase inhibitors that include thiadiazole, oxadiazole, triazole, oxindole, polycyclitol, aminocyclitol, conduritol, and inositol derivatives.

Lastly, a special chapter has been dedicated to computational and structural biology of α-glucosidase inhibitors that aims to explore structural and functional clues to drug optimization and development. It also provides insights into the mechanism of α-glucosidase inhibition based on x-ray crystal structures of enzyme-inhibitor complexes and computational simulations. These approaches will provide new avenues for drug development involving designing and developing leads with better efficacies.

I hope this work will be of great help to relevant audiences, especially the drug discovery community either in academia or industry who would like to take drug development of α-glucosidase inhibitors to advanced levels.

Usman Ghani

Acknowledgments

I am deeply grateful to the Almighty God who gave me inspiration and courage to conceive the importance of writing this book and accomplish it successfully.

My deepest gratitude to all my family members who are my source for love and inspiration. I am thankful to my wife Yasmeen for her motivation and support that kept me resolute in the writing process.

I am obliged to thank my sons Abdur Raafay (in A2 level) and Abdul Hadi (in grade 9) who took keen interest in drawing some of the chemical structures of the inhibitors discussed in the book.

Of course I cannot forget to mention my 5-year old daughter Aaminah whose inquisitive company I used to enjoy while writing the manuscript.

Thanks to my colleagues at our unit and department for their good wishes.

Thanks to Kelsey Connors, the Editorial Project Manager at Elsevier, Boston, MA, United States, for her excellent coordination, follow-up, and patience throughout the project.

Thanks to all authors and publishers for permission to reproduce some figures for the book.

CHAPTER ONE

Introduction, rationale and the current clinical status of oral α-glucosidase inhibitors

Contents

1.1 Introduction

Reducing mortality and improving quality of life is one of the crucial aims of therapeutic agents. Continuing research in the field of drug discovery has been attracting the attention of researchers focusing on development of drugs with safer and better efficacy profiles since these two targets are compulsively explored as part of the drug optimization process. However, need for drugs with safer treatment options and better efficacy has always been challenging to the drug discovery community, which is generally addressed by alluring temptation of screening the rich and still unexplored molecular diversity of candidate compounds of natural and synthetic origins. Despite all these valuable efforts, there exists a downturn in the drug screening process. These efforts have been generating no more than a plethora of active compounds piled up and forgotten in the ether without being given ample consideration for further development into therapeutic candidacy.

Alpha-glucosidase Inhibitors.
DOI: https://doi.org/10.1016/B978-0-08-102779-0.00001-0

This perspective is especially important for diseases or clinical conditions including AIDS, cancer, and hepatitis that have been facing a dilemma of limited and inefficacious treatment choices. Even the treatment of a range of diseases with relatively broader spectra of therapeutic options is currently threatened with efficacy problems and unwanted side effects.

It is unfortunate to mention that majority of the lead compounds identified against a number of clinically important targets do not get beyond the bounds of mass production of publications and reports, thus creating a haystack destined to be forgotten in the scientific literature. For one reason, it appears that the bridge connecting the field of drug screening to further development is somewhere broken. Traditionally, research involving drug candidate design and screening against a clinical target follows a rational approach to identifying promising leads, which undergoes kinetic, structure–activity analyses, toxicity, pharmacokinetic, and optimization studies aided by X-ray crystallography or computational and combinatorial chemistry followed by preclinical or clinical trials (Fig. 1.1). The rational approach is designed to rule out unpromising leads with low activity or potency or high toxicity. However, majority of identified promising leads are not subjected to the optimization cycle that involves structure–activity refinement and other studies before being eligible for preclinical or clinical trials. Therefore in the rational approach to discovery and modification of leads, the optimization cycle is missing out in most of the drug screening attempts.

Another approach to drug discovery is to use traditional medicine as a beacon for identification of active compounds against a disease, combined with optimization. The molecular mechanism of action of majority of plant extracts or their active compounds used in traditional medicine is still unknown despite the fact that they possess safe and proven therapeutic effects which people have been witnessing for centuries in different cultures of the world. As mentioned earlier,

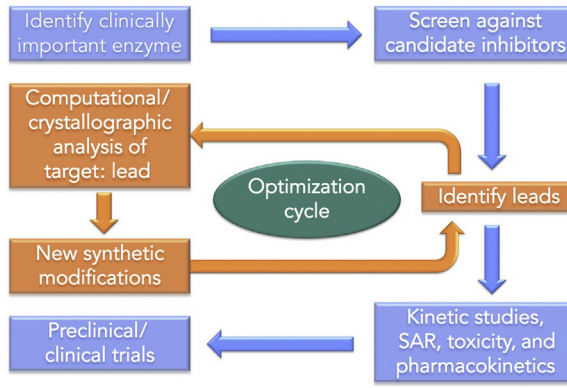

Figure 1.1 A rational approach to screening, identification, and optimization of drug candidates or enzyme inhibitors directed toward clinically important targets. In drug screening efforts, majority of identified promising leads do not enter the phase of studies involving structure–activity relationship, toxicity, pharmacokinetics, preclinical or clinical trials, and lead optimization cycle.

the most common drug development strategy is to identify targets and leads followed by optimization. However, this approach often results in major obstacles that make the optimization process more challenging chiefly in the areas of synthesis, pharmacokinetics, and toxicity. In order to curb such challenges, it is important to first explore the mechanism of action of plant extracts and the compounds therein because their therapeutic effects in the treatment of diseases have already been proven for centuries, followed by focused optimization cycle involving synthetic chemistry, pharmacokinetics, toxicity, and structural and computational biology.

There exists a spectrum of conceivable reasons to address the challenges in further development of promising leads including, but not limited to, obstacles in the university–industry relationships, conflicts in the practice of intellectual property ethics, limited in-house drug development programs at university level, limited funding for specialized research, and, last but not least, the budget cutdowns. One of the

convincing facts that can also aggravate severity of the challenge is that in the perspective of moving forward in the field of drug discovery, the scientific community is somewhat reluctant to look backward to find "needles" in that ever-growing haystack of active compounds. There may be tens or hundreds of compounds that could become promising candidates for drug development if re-explored. Re-exploring is indeed a challenging work, nevertheless, it can be equally rewarding, especially in the perspective of diseases or clinical conditions awaiting promising drugs for their treatment for decades.

One such target that this book intends to highlight to the scientific community is urge for re-exploring α-glucosidase inhibitors for potential development into oral antidiabetic drugs, because this area has been witnessing no significant progress for years. Development of antidiabetic drugs is yet to see launching of new oral α-glucosidase inhibitors since no new drug has been developed in the last two decades.

Therefore, this work intends to create a groundwork for identifying promising α-glucosidase inhibitors of natural and synthetic origins by gauging their potential for becoming suitable candidates for optimization and, if applicable, for preclinical or clinical trials based on available *in vitro* and *in vivo* data. Moreover, it will also draw the attention of the scientific community, especially the drug development scientists, to look back, reconsider, and take the challenge of transforming promising lead α-glucosidase inhibitors into potential antidiabetic drugs.

1.2 Diabetes mellitus and the antidiabetic drugs

Diabetes mellitus is one of the most prevalent metabolic diseases in the world. Type 1 diabetes is due to insulin

deficiency affecting around 5%–10% of the diabetic population, whereas type 2 is most common and mainly due to insulin resistance [1]. Diabetes is one of the leading causes of morbidity and mortality characterized by hyperglycemia that is associated with a number of complications including neuropathy, nephropathy, heart disease, stroke, and vascular diseases [2]. The worldwide prevalence of diabetes in all age groups has been rising and it is estimated that it might increase from 2.8% (171 million) in the year 2000 to 4.4% (366 million) in the year 2030. According to the World Health Organization projection, there will be a 42% increase in diabetes cases (from 51 to 72 million) in the developed countries, while 170% increase (from 84 to 228 million) in the developing countries. The occurrence of diabetic complications in the developing world is more common and is partly due to socioeconomic reasons [3].

Alarmingly, the Middle East and North Africa have the highest comparative prevalence of diabetes worldwide (11%). In Saudi Arabia alone, approximately 25% of the adult population is suffering from the disease making it seventh highest in the world [3,4]. The trend has been rising, and the country has witnessed a ten-fold increase in the disease over the last three decades. It is estimated that by the year 2030, there will be about 5.5 million cases of diabetes in the country [5–10]. Furthermore, diabetes has been a continuous cause of rising health-care costs globally. According to the American Diabetes Association, in United States alone, the total costs of diagnosed cases of diabetes were estimated to be $245 billion in 2012 compared to $174 billion in 2007 [11].

Current therapeutic approaches to treat type 2 diabetes include oral antidiabetic drugs such as sulfonylureas, thiazolidinediones, metformin, α-glucosidase inhibitors, and glycosurics. New therapies include peptides such as glucagon-like peptide-1 agonists (exenatide and liraglutide), and dipeptidyl peptidase-IV inhibitors (sitagliptin and vildagliptin), whereas emerging

therapies include cannabinoid receptor type 1 antagonists and bile acid sequestrants [12]. Retarding or inhibiting the digestion and absorption of carbohydrates has therapeutic implications for controlling postprandial hyperglycemia in type 2 diabetes. In this regard, inhibition of digestive α-glucosidase is one therapeutic approach that slows down carbohydrate digestion and glucose absorption, therefore, stabilizing blood glucose levels and preventing hyperglycemia in diabetic patients [13].

1.3 α-Glucosidase inhibitors—past and present

Glucosidases belong to the diverse class of glycoside hydrolase (GH) enzymes that cleave the glycosidic bond to release glucose from the nonreducing end of their oligosaccharide substrates. Glucosidases including α-glucosidases (α-*D*-glucoside glucohydrolase; EC 3.2.1.20) are a group of enzymes that play pivotal roles in carbohydrate metabolism and glycoprotein processing. α-Glucosidases specifically hydrolyze the α-glucopyranosidic bond (α-1,4) in complex carbohydrates to release glucose. Their functions in mammals include glycogen degradation, *N*-linked oligosaccharide processing for glycoprotein folding and maturation, and intestinal digestion of dietary carbohydrates. There are five GH families in which α-glucosidases are distributed: GH4, GH13, GH31, GH63, and GH97 [14].

The GH13 and GH31 families are composed of two major classes of α-glucosidases with different substrate specificities. In the predigestion phase, the salivary and gastric α-amylases hydrolyze carbohydrates into maltose, maltotriose, α-1,6- and α-1,4-oligoglucans [15], which are then hydrolyzed in the intestinal lumen by maltase-glucoamylase (MGAM; EC 3.2.1.20, 3.2.1.3) and sucrose-isomaltase (SI; EC 3.2.1.48,

3.2.1.10) enzymes anchored on the small-intestinal brush border membrane through an *O*-glycosylated link from their *N*-terminal [16]. These enzymes are divided into two categories bearing the *N*-terminal (MGAM-N and SI-N) and the *C*-terminal (MGAM-C and SI-C) catalytic subunits [17]. The carbohydrate-active enzymes (CAZY) classification designates the enzymes as members of the GH31 family subgroup 1 with conserved catalytic centers [18]. The three-dimensional structure and carbohydrate recognition by the enzymes in the GH13 family have been extensively studied that include the most widely characterized enzymes such as α-xylosidase, 6-α-glucosyltransferase, 3-α-isomaltosyltransferase, and α-glucosidases. The catalytic function of the GH31 family of enzymes is common to all members, that is, hydrolysis of a terminal carbohydrate moiety. However, they catalyze a wide range of hydrolytic activities due to their preference for substrates that vary in size from disaccharides to large storage polymers such as starch and glycogen [19,20].

Management of hyperglycemia in diabetes mellitus by oral α-glucosidase inhibitors is currently limited to acarbose, voglibose, and miglitol aimed at delaying digestion of dietary carbohydrates to maintain postprandial blood glucose at normal levels (Fig. 1.2). The drugs inhibit the membrane-bound α-glucosidase at the brush border of the small intestine that catalyzes the hydrolysis of di-, tri-, and oligosaccharides to glucose and other monosaccharides. The inhibition subsequently reduces the intestinal digestion of dietary starch and other sugars thereby preventing hyperglycemia and its complications and maintaining normal blood glucose levels [21].

Acarbose (Glucobay™), a bacterial oligosaccharide analogous to α-glucosidase substrate, was the first α-glucosidase inhibitor launched in 1990 for treatment of type 2 diabetes. It is a potent sucrase inhibitor ($IC_{50} = 0.5\ \mu M$) first isolated from the *Actinoplanes utahensis* bacteria that reduced postprandial

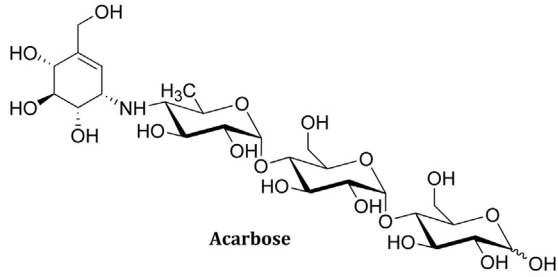

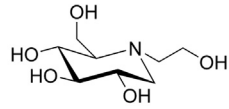

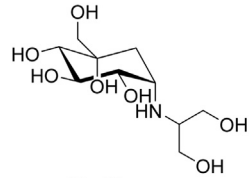

Figure 1.2 The chemical structures of acarbose, miglitol, and voglibose. Currently these drugs are the only oral α-glucosidase inhibitors that are clinically prescribed for the management of hyperglycemia in diabetes mellitus.

blood glucose and increased insulin secretion in rats and healthy human volunteers [22–24]. Acarbose prevents digestion of starch and oligosaccharides by competitively inhibiting α-glucosidases and other digestive enzymes present in the brush border of the enterocyte lining of the intestine thus reducing blood glucose levels [21].

Voglibose and miglitol are structurally unrelated to glucosidase substrate possessing the piperidine-3,4,5-triol and tetraol-cyclohexane moieties, respectively. Previous studies reported that *Streptomyces hygroscopicus* bacteria produced valiolamine with promising inhibitory activity against intestinal maltase and sucrase ($IC_{50} = 2.2$ and $0.049\,\mu M$, respectively) [25].

Voglibose (Basen™) is one of the synthetic derivatives of *N*-substituted valiolamine that was selected as potential antidiabetic agent in 1994. It delays the digestion of complex carbohydrates and oligosaccharides by inhibiting the maltase and sucrase enzymes ($IC_{50} = 15$ and 4.6 nM, respectively) [26]. Voglibose is the newest addition to the battery of α-glucosidase inhibitors launched in 2009 in Japan for treatment of type 2 diabetes [24]. A randomized double-blind trial on voglibose involving 1780 Japanese patients found that it significantly regulated blood glucose to normal levels and delayed the progression of the disease [27], with fewer side effects than other α-glucosidase inhibitors but with lesser efficacy than that of acarbose [28].

Further research on natural inhibitors of α-glucosidase led to the identification of nojirimycin (NJ), which was first reported in 1966 as antibiotic produced by the *Streptomyces roseochromogenes* bacteria [29]. NJ is a potent inhibitor of α- and β-glucosidases from different species [30–34]. A variety of derivatives and analogues of NJ was synthesized later and studied for α-glucosidase inhibition. 1-Deoxynojirimycin (DNJ), also called moranoline (Fig. 1.3), was synthesized from NJ which was later isolated from the roots of mulberry plant [35], particularly the *N*-hydroxyethyl derivatives of DNJ that showed strong *in vitro* inhibitory activity against α-glucosidase, however, their *in vivo* efficacy was proved to be moderate [36]. Out of these derivatives, miglitol (Glyset™) was selected to be the most effective inhibitor for therapeutic use in 1999. It inhibits carbohydrate digestive enzymes at the intestinal border thereby preventing the digestion and absorption of glucose. Unlike acarbose, miglitol is almost completely absorbed through the intestine indicating that it may have systemic effects [37,38]. However, previous studies showed no evidence to support that it exerts extraintestinal therapeutic effects [39].

Oral α-glucosidase inhibitors are generally well tolerated because their gastrointestinal side effects are mainly

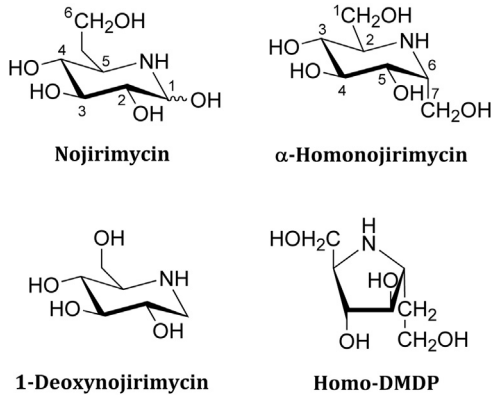

Figure 1.3 The chemical structures of NJ, DNJ, α-homonojirimycin, and homo-2,5-dideoxy-2,5-imino-*D*-*L*-glycero-*D*-manno-heptitol. These promising α-glucosidase inhibitors were discovered during the early pioneering work on oral antidiabetic drug discovery leading to identification of a number of new inhibitors. *DNJ*, 1-Deoxynojirimycin; *NJ*, nojirimycin.

nonsystemic compared to that of other antidiabetic drugs. Since they inhibit the digestion of complex carbohydrates in the intestine, the side effects are usually confined to flatulence, abdominal pain, and diarrhea due to bacterial action on undigested carbohydrates [40]. One of the greatest advantages of α-glucosidase inhibitors over other antidiabetic drugs is that they exhibit localized action accompanied by minimal absorption hence limiting the systemic side effects. Since their discovery more than two decades ago, less attention has been paid to development of new α-glucosidase inhibitors with ability to exert localized therapeutic effects and minimal systemic absorption despite publication of hundreds of reports on α-glucosidase inhibitors to date.

1.4 Rationale

In the past few decades much of the interest has been diverted toward screening of antidiabetic drugs possessing a

broad spectrum of mode of action that resulted in the development of a number of promising drugs currently prescribed by clinicians. However, the area of α-glucosidase inhibitor drug development has been unattended since the launch of acarbose, voglibose, and miglitol with no significant progress to date, leaving a wide gap in the field. This demands the need for re-exploration and development of new α-glucosidase inhibitors with minimal side effects and better efficacy.

While it is convincing to accept that other antidiabetic drugs do exhibit promising therapeutic benefits, new α-glucosidase inhibitors may provide a better therapeutic output when used in combination with those drugs [41]. Therefore, their importance cannot be undermined when taken into the perspective of nonsystemic side effects or combination therapy.

On the contrary, the treatment of type 2 diabetes with acarbose, voglibose, and miglitol in various patient populations has been currently facing challenges pertaining to efficacy, side effects, and improving quality of life despite relative benefits. These have been attested by a number of clinical trials conducted on the drugs. A survey of 41 clinical trials on oral α-glucosidase inhibitors was conducted to evaluate mortality or morbidity in patients with type 2 diabetes that included 30 trials on acarbose, seven on miglitol, one on voglibose, and three that compared various α-glucosidase inhibitors. The drugs reduced fasting and postprandial blood glucose levels that eventually reduced glycated hemoglobin (HbA1c) levels. However, the survey found no statistically significant effects of the drugs on the mortality, morbidity, and quality of life in patients with type 2 diabetes. Moreover, there were no significant therapeutic effects of the drugs on the plasma lipid profile and body weight of the patients. The overall gastrointestinal side effects of the drugs were more adverse than that of other drugs specifically sulfonylureas. The efficacy of sulfonylureas in terms of glycemic control along with the side effects was

better than that of α-glucosidase inhibitors, but the efficacy of α-glucosidase inhibitors was better than that of some sulfonylureas in terms of decreasing the fasting and postprandial insulin levels [42,43].

In this work, searching through that haystack of active compounds has revealed a significant number of natural and synthetic α-glucosidase inhibitors identified to date. Some of the compounds have been found to be more efficacious than acarbose, miglitol, and voglibose in terms of potency and *in vivo* antihyperglycemic activity. Despite existence of a wide chemical diversity of α-glucosidase inhibitors identified to date, unfortunately majority of them are solely piled up in publications and reports let alone considered for further development into drugs. Based on this rationale, the primary objective of writing the book is to utilize a focused approach to pinpoint selective promising α-glucosidase inhibitors that may become potential candidates for development into antidiabetic drugs.

The Clarivate Analytics Web of Science database search from 1900 to 2019 identified a number of α-glucosidase inhibitors. Out of these, 390 natural and synthetic promising inhibitors have been selected to be discussed in the book. The criteria for selection are based on the availability of *in vitro* and/or *in vivo* data that include inhibition potency and ability to reduce blood glucose levels. The book also highlights and discusses chemically diverse pharmacophores or active moieties or chemical groups identified from the compounds that significantly contribute to potent α-glucosidase inhibition including the ones that are unfavorable to the inhibitory activity. Inhibitors with IC_{50} or K_i values in nanomolar or low micromolar ranges are considered and discussed along with their structure–activity relationship, structural biology and/or computational simulations where available. A comprehensive list of α-glucosidase inhibitors discussed in the book is presented in the Appendix with data on their IC_{50} and/or K_i values, and *in vivo* antihyperglycemic activity where available.

References

[1] Y. Zheng, S.H. Ley, F.B. Hu, Global aetiology and epidemiology of type 2 diabetes mellitus and its complications, Nat. Rev. Endocrinol. 14 (2018) 88–98.

[2] D.V. Nguyen, L.C. Shawand, M.B. Grant, Inflammation in the pathogenesis of microvascular complications in diabetes, Front. Endocrinol. (Lausanne) 3 (2012) 1–7.

[3] S. Wild, G. Roglic, A. Green, R. Sicree, H. King, Global prevalence of diabetes: estimates for the year 2000 and projections for 2030, Diabetes Care 27 (2004) 1047–1053.

[4] M.M. Al-Nozha, et al., Diabetes mellitus in Saudi Arabia, Saudi Med. J. 25 (2004) 1603–1610.

[5] A. Alzaid, Diabetes: a tale of two cultures, Br. J. Diabetes Vas. Dis 12 (2012) 57–59.

[6] R.A. Bacchus, J.L. Bell, M. Madkour, B. Kilshaw, The prevalence of diabetes mellitus in male Saudi Arabs, Diabetologia 23 (1982) 330–332.

[7] H.H. Fatani, S.A. Mira, A.G. El-Zubier, Prevalence of diabetes mellitus in rural Saudi Arabia, Diabetes Care 10 (1987) 180–183.

[8] H.A. Abu-Zeid, A.S. Al-Kassab, Prevalence and health-care features of hyperglycemia in semiurban-rural communities in southern Saudi Arabia, Diabetes Care 15 (1992) 484–489.

[9] M.A. El-Hazmi, et al., Diabetes mellitus and impaired glucose tolerance in Saudi Arabia, Ann. Saudi Med. 16 (1996) 381–385.

[10] A.R. Al-Nuaim, Prevalence of glucose intolerance in urban and rural communities in Saudi Arabia, Diabet. Med. 14 (1997) 595–602.

[11] American Diabetes Association, USA. <https://www.diabetes.org/resources/statistics/cost-diabetes> (accessed November 2019).

[12] B.T. Srinivasan, J. Jarvis, K. Khunti, M.J. Davies, Recent advances in the management of type 2 diabetes mellitus: a review, Postgrad. Med. J. 84 (2008) 524–531.

[13] K.C. Maki, M.L. Carson, M.P. Miller, M. Turowski, M. Bell, D.M. Wilder, et al., High-viscosity hydroxypropylmethylcellulose blunts postprandial glucose and insulin responses, Diabetes Care 30 (2007) 1039–1043.

[14] H.A. Ernst, et al., Structure of the *Sulfolobus solfataricus* α-glucosidase: implications for domain conservation and substrate recognition in GH3, J. Mol. Biol. 358 (2006) 1106–1124.

[15] G.D. Brayer, G. Sidhu, R. Maurus, E.H. Rydberg, C. Braun, Y. Wang, et al., Subsite mapping of the human pancreatic alpha-amylase active site through structural, kinetic, and mutagenesis techniques, Biochemistry 39 (2000) 4778–4791.

[16] L. Sim, R. Quezada-Calvillo, E.E. Sterchi, B.L. Nichols, D.R. Rose, Human intestinal maltase-glucoamylase: crystal structure of the N-terminal catalytic subunit and basis of inhibition and substrate specificity, J. Mol. Biol. 375 (2008) 782–792.

[17] (a) B.L. Nichols, S. Avery, P. Sen, D.M. Swallow, D. Hahn, E. Sterchi, The maltase-glucoamylase gene: common ancestry to sucrase-isomaltase with complementary starch digestion activities, Proc. Natl. Acad. Sci. U.S.A. 100 (2003) 1432–1437.
(b) B.L. Nichols, J. Eldering, S. Avery, D. Hahn, A. Quaroni, E. Sterchi, Human small intestinal maltase-glucoamylase cDNA cloning. Homology to sucrase-isomaltase, J. Biol. Chem. 273 (1998) 3076–3081.
[18] H.A. Ernst, L. Leggio, M. Willemoës, G. Leonard, P. Blum, S. Larsen, Structure of the *Sulfolobus solfataricus* alphaglucosidase: implications for domain conservation and substrate recognition in GH31, J. Mol. Biol. 358 (2006) 1106–1124.
[19] B. Henrissat, A classification of glycosyl hydrolases based on amino-acid sequence similarities, Biochem. J. 280 (1991) 309–316.
[20] B. Henrissat, A. Bairoch, New families in the classification of glycosyl hydrolases based on amino acid sequence similarities, Biochem. J. 293 (1993) 781–788.
[21] A.J. Krentz, C.J. Bailey, Oral antidiabetic agents: current role in type 2 diabetes mellitus, Drugs 65 (2005) 385–411.
[22] D.O. Schmidt, W. Frommer, L. Muller, E. Truscheit, Glucosidase inhibitors from bacilli, Natunlinenschafien 66 (1979) 584–585.
[23] W. Puts, U. Keup, I.J.P. Krause, G. Thomas, F. HoO'meister, Glucosidase inhibition: a new approach to the treatment of diabetes, obesity and hyperlipoproteinaemia, Naturwissenschafien 64 (1977) 536–537.
[24] N. Asano, Naturally occurring iminosugars and related compounds: structure, distribution, and biological activity, Current Topics Med. Chem. 3 (2003) 471–484.
[25] Y. Kameda, et al., Valiolamine, a new alpha-glucosidase inhibiting aminocyclitol produced by *Streptomyces hygroscopicus*, J. Antibiot. 37 (1984) 1301–1307.
[26] S. Horii, H. Fukase, T. Matsuo, Y. Kameda, N. Asano, K. Matsui, Synthesis and α-D-glucosidase inhibitory activity of *N*-substituted valiolamine derivatives as potential oral antidiabetic agents, J. Med. Chem. 29 (1986) 1038–1046.
[27] R. Kawamori, N. Tajima, Y. Iwamoto, A. Kashiwagi, K. Shimamoto, K. Kaku, Voglibose Ph-3 Study Group. Voglibose for prevention of type 2 diabetes mellitus: a randomised, doubleblind trial in Japanese individuals with impaired glucose tolerance, Lancet 373 (2009) 1607–1614.
[28] A. Vichayanrat, S. Ploybutr, M. Tunlakit, P. Watanakejorn, Efficacy and safety of voglibose in comparison with acarbose in type 2 diabetic patients, Diabetes Res. Clin. Pract. 55 (2002) 99–103.
[29] S. Inoue, T. Tsuruoka, T. Niida, The structure of nojirimycin, a piperidinose sugar antibiotic, J. Antibiot 19 (1966) 288–292.

[30] T. Niwa, T. Tsuruoka, H. Goi, Y. Kodama, J. Ltoh, S. Lnoue, et al., Novel glycosidase inhibitors, nojirimycin B and D-mannonic delta-lactam. Isolation, structure determination and biological property, J. Antibiot. 37 (1984) 1579–1586.
[31] T. Niwa, S. Inoue, T. Tsuruoka, Y. Koaze, T. Niida, "Nojirimycin" as a potent inhibitor of glucosidase, Agric. Biol. Chem. 34 (1970) 966–968.
[32] Y. Kodama, T. Tsuruoka, T. Niwa, S. Inoue, Molecular structure and glycosidase inhibitory activity of nojirimycin bisulfite adduct, J. Antibiot. 38 (1985) 116–118.
[33] G. Legler, S. Pohl, Synthesis of 5-amino-5-deoxy-D-galactopyranose and 1,5-dideoxy-1,5-imino-D-galactitol, and their inhibition of α- and α-galactosidases, Carbohydr. Res. 155 (1986) 119–129.
[34] Y. Miyake, M. Ebata, Inhibition of α-galactosidase by galactostatin, galactostatin-lactam and 1-deoxygalactostatin, Agric. Biol. Chem. 52 (1988) 1649–1654.
[35] M. Yagi, T. Kouno, Y. Aoyagi, H. Murai, The structure of moranoline, a piperidine alkaloid from *Morus* species, Nippon Nougei Kagaku Kaishi 50 (1976) 571–572.
[36] B. Junge, M. Matzke, J. Stohefuss, Chemistry and structure-activity relationships of glucosidase inhibitors, in: J. Kuhlmann, W. Puis (Eds.), Handbook of Experimental Pharmacology, vol. 119, Springer-Verlag, Berlin, Heidelberg, New York, 1996, pp. 411–482.
[37] P.H. Joubert, G.N. Foukaridis, M.L. Bopape, Miglitol may have a blood glucose lowering effect unrelated to inhibition of α-glucosidase, Eur. J. Clin. Pharmacol. 31 (1987) 723–724.
[38] P.H. Joubert, H.L. Venter, G.N. Foukaridis, The effect of miglitol and acarbose after an oral glucose load: a novel hypoglycaemic mechanism? Br. J. Clin. Pharmacol. 30 (1990) 391–396.
[39] J.P.J.E. Sels, J.J.P. Nauta, P.P.C.A. Menheere, B.H.R. Wolfenbuttel, A. C. Nieuwenhuijzen Kruseman, Miglitol (Bay m 1099) has no extraintestinal effects on glucose control in healthy volunteers, Br. J. Clin. Pharmacol 42 (1996) 503–506.
[40] J.L. Chiasson, et al., Acarbose for prevention of type 2 diabetes mellitus: the STOPNIDDM randomised trial, Lancet 359 (2002) 2072–2077.
[41] J.A. Balfour, D. McTavish, Acarbose, an update of its pharmacology and therapeutic use in diabetes mellitus, Drugs 46 (1993) 1025–1054.
[42] F.A. van de Laar, P.L. Lucassen, R.P. Akkermans, E.H. van de Lisdonk, G.E. Rutten, C. van Weel, Alpha-glucosidase inhibitors for patients with type 2 diabetes: results from a Cochrane systematic review and meta-analysis, Diabetes Care 28 (2005) 154–163.
[43] F.A. van de Laar, P.L. Lucassen, R.P. Akkermans, E.H. van de Lisdonk, G.E. Rutten, C. van Weel, Alpha-glucosidase inhibitors for type 2 diabetes mellitus, Cochrane Database Syst. Rev. 2 (2005). CD003639.

CHAPTER TWO

Natural and synthetic sugar mimics

Contents

2.1 Introduction

The sugar-mimicking inhibitors of glycosidases including that of α-glucosidase are of particular interest due to their structural and transition state analogy to sugar substrates. They are promising candidates for treatment of diabetes mellitus, immune disorders, viral infections, neoplasia, and lysosomal storage diseases [1–3]. Sugar mimics and their derivatives are divided into three major types: iminosugars, thiosugars, and carbaglycosylamines. In imino and thiosugars, a nitrogen and sulfur atom replaces the ring oxygen of monosaccharides, respectively, whereas in carbaglycosylamines a methylene group replaces the ring oxygen. Sugar mimics are the most widely studied class of α-glucosidase inhibitors with promising *in vitro* and *in vivo* biological activity profiles.

Alpha-glucosidase Inhibitors.
DOI: https://doi.org/10.1016/B978-0-08-102779-0.00002-2

2.2 Iminosugars

Iminosugars are found in nature and are generally classified into two groups: monocyclic iminosugars that include five-membered pyrrolidines, six-membered piperidines, and seven-membered azepanes, and bicyclic iminosugars that include pyrrolizidines, indolizidines, and nortropanes [4]. Iminosugars are the most widely studied class of compounds among other sugar mimics, which exhibit promising therapeutic potential for treatment of hyperglycemia in type 2 diabetes by inhibiting α-glucosidases to slow down carbohydrate digestion and absorption [3,5–8]. This is witnessed by a number of patents registered to date specifically for imino and thiosugars due to their promising oral bioavailability [9]. Sugar-mimicking α-glucosidase inhibitors have been discussed in great detail in the literature [1,2,4,9–11]; some of which are classic and well-known inhibitors of α-glucosidase that are presented at the beginning of this chapter for reference purposes followed by a discussion on other promising sugar mimics recently identified as α-glucosidase inhibitors.

2.2.1 Polyhydroxylated pyrrolidines

Natural iminosugar glycosides have been reported to inhibit a range of glycosidase enzymes. β-Fructofuranose analogs such as 1,4-dideoxy-1,4-imino-D-arabinitol (DAB) (**1**) and *2R,5R*-dihydroxymethyl-*3R,4R*-dihydroxypyrrolidine (DMDP) (**2**) [12] were first isolated from the fruit of *Angylocalyx boutiqueanus* [13] and the leaves of *Derris elliptica* [14], respectively. Naturally occurring 2,5-dideoxy-2,5-iminoheptitol such as homo-DMDP was first isolated from the leaves of *Hyacinthoides nonscripta* (bluebell) belonging to the Hyacinthaceae family [15]. Since their discovery more than three decades ago, a number of natural and synthetic derivatives of iminosugars

have been studied for a wide range of biological activities including α-glucosidase inhibitory activity. Kato et al. [16] studied α-glucosidase inhibitory activity of natural derivatives of DMDP and compared it with DAB (Fig. 2.1). *Baphia nitida*, an African medicinal tree, is reported to contain a variety of polyhydroxylated pyrrolidines, piperidines, and their glycosides particularly iminosugar glycosides that inhibit a number of glycosidases. DAB is a more potent inhibitor of yeast α-glucosidase ($IC_{50} = 0.15\ \mu M$) and rat intestinal isomaltase ($IC_{50} = 5.8\ \mu M$) than DMDP (compound **2**; yeast α-glucosidase $IC_{50} = 0.71\ \mu M$; rat intestinal isomaltase $IC_{50} = 91\ \mu M$) that lacks one hydroxymethyl group. 3-*O*-β-*D*-Glucopyranosyl-DMDP (**3**) is found to show promising inhibitory activity against rice α-glucosidase ($IC_{50} = 0.79\ \mu M$), rat intestinal maltase ($IC_{50} = 4.7\ \mu M$), and sucrase ($IC_{50} = 5\ \mu M$). In these compounds, presence of β-*D*-fructofuranosyl residue at C_1 or C_6 of

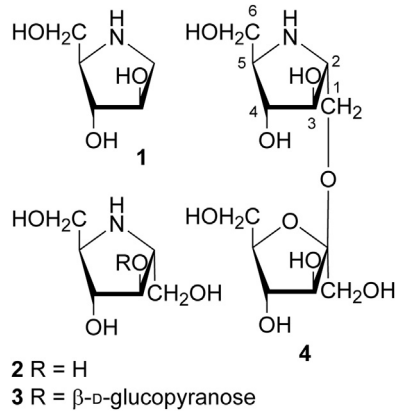

Figure 2.1 DMDP (**2**) and its natural derivatives: DAB (**1**), 3-*O*-β-*D*-glucopyranosyl-DMDP (**3**), and β-*D*-fructofuranosyl-DMDP (**4**). Some of these compounds are promising inhibitors of α-glucosidase with antihyperglycemic effects *in vivo*. *Reproduced from U. Ghani, Re-exploring promising α-glucosidase inhibitors for potential development into oral anti-diabetic drugs: finding needle in the haystack, Eur. J. Med. Chem. 103 (2015) 133–162. © 2015 French Société de Chimie Thérapeutique published by Elsevier Masson SAS. All rights reserved.*

DMDP (as in compound **4**), substantially lowered its yeast α-glucosidase inhibitory activity. However, it possessed more specificity to α-glucosidase ($IC_{50} = 22\ \mu M$) and rat intestinal maltase ($IC_{50} = 65\ \mu M$) than that of DMDP alone.

Jenkinson et al. [17] synthesized carbon branched iminosugars including enantiomeric pairs of isoDMDP, isoDGDP, and isoDAB, and evaluated their inhibitory activities on various glycosidases. The activities of the compounds were compared to that of linear isomeric natural products such as DMDP, DGDP, and DAB. Comparison of the iso-*D*-iminosugar activity with that of natural unbranched analogs showed that both types of compounds exhibited weak inhibition of glycosidases, including some that were inactive against the target enzymes. Comparison of iso-*L*-iminosugars with their natural product analogs showed that both forms inhibited the same type of enzymes. It is important to highlight *L*-iso-DMDP (**5**) presented in Fig. 2.2, which was identified as competitive inhibitor of rat intestinal maltase ($IC_{50} = 0.19\ \mu M$; $K_i = 0.081\ \mu M$), sucrase ($IC_{50} = 0.38\ \mu M$), isomaltase ($IC_{50} = 8.8\ \mu M$), and rice α-glucosidase ($IC_{50} = 2.0\ \mu M$); however, its *D*-iminosugar, iso-DMDP showed no activity against any of these enzymes. Additionally, it exerted *in vivo* antihyperglycemic effects by significantly decreasing blood glucose levels within 15−30 minutes in maltose-loaded mice at a

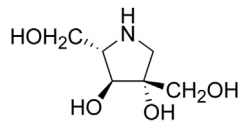

5

Figure 2.2 *L*-Iso-DMDP: a competitive inhibitor of rat intestinal maltase, sucrase, isomaltase, and rice α-glucosidase. *Reproduced from U. Ghani, Re-exploring promising α-glucosidase inhibitors for potential development into oral anti-diabetic drugs: finding needle in the haystack, Eur. J. Med. Chem. 103 (2015) 133−162. © 2015 French Société de Chimie Thérapeutique published by Elsevier Masson SAS. All rights reserved.*

dose of 1.0 mg/mL bodyweight similar to that of miglitol but with better efficacy. The *Iso*-iminosugars are promising α-glucosidase inhibitors that may be regarded as future-generation candidates for antidiabetic drug development due to their high efficacy of reducing postprandial glucose levels and inhibiting α-glucosidase. Moreover, none of these iminosugars inhibit endoplasmic reticulum (ER) glucosidases, therefore the probability of developing unwanted side effects similar to that of miglitol would be lower.

Studies on 1,4-dideoxy-1,4-imino-*L*-arabinitol (LAB) (**6**) (Fig. 2.3), an *L*-enantiomer of DAB, revealed that it is a potent inhibitor of rat intestinal isomaltase ($IC_{50} = 0.08\ \mu M$) [18]. Structural modification of DAB including enantiomerization, epimerization at C_2 or C_3, substitution at C_1, and introduction of a sulfur to replace ring nitrogen drastically lowered or abolished its inhibitory activity against various glucosidases. Addition of a hydroxymethyl group in the β-orientation at C_1 of DAB has been shown to significantly lower its enzyme inhibitory activity. Moreover, the imino group substitution by a sulfur atom in DAB also decreased the activity [18,19].

Further synthetic work by Natori et al. [20] on derivatives of LAB yielded α-1-*C*-alkyl-*L*-arabinoiminofuranoses (α-1-*C*-alkyl-LAB) containing alkyl groups substituted at the anomeric position (Fig. 2.4). These imino-*C*-glycosides were prepared by replacing the oxygen atom of the *N*,*O*-acetal function by a methylene group. The compounds exhibited selective inhibition

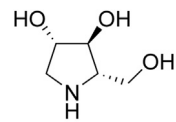

6

Figure 2.3 1,4-Dideoxy-1,4-imino-*L*-arabinitol (LAB) is an *L*-enantiomer of DAB that exhibits promising inhibitory activity against rat intestinal isomaltase.

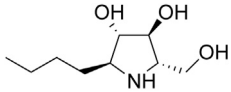

7

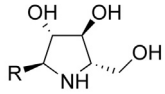

8 R=$CH_3(CH_2)_4$
9 R=$CH_3(CH_2)_5$
10 R=$CH_3(CH_2)_6$
11 R=$CH_3(CH_2)_7$

Figure 2.4 The α-1-*C*-Butyl-LAB and its derivatives. In these derivatives, a strong correlation is observed between the chain length of the aglycone group and the extent of enzyme inhibition. Regarded as new class of α-glucosidase inhibitors, the compounds also lower postprandial blood glucose levels with higher efficacy than that of miglitol. *Reproduced from U. Ghani, Re-exploring promising α-glucosidase inhibitors for potential development into oral anti-diabetic drugs: finding needle in the haystack, Eur. J. Med. Chem. 103 (2015) 133–162.*

of various intestinal α-glucosidase showing a strong correlation between the chain length of the aglycone group and the potency of inhibition. The α-1-*C*-butyl-LAB derivative (**7**) strongly inhibits rat intestinal sucrase ($IC_{50} = 0.032\ \mu M$) and maltase ($IC_{50} = 0.2\ \mu M$). Its promising sucrase inhibitory activity is more promising than that of oral α-glucosidase inhibitors currently prescribed clinically. The activity of other compounds such as **8**, **9**, **10**, and **11** carrying linear alkyl chains from C_5 to C_8 reasonably compared with that of the oral α-glucosidase inhibitors. These compounds potently inhibited rat intestinal maltase ($IC_{50} = 0.71$, 0.51, 0.38, and $0.32\ \mu M$, respectively) and sucrase ($IC_{50} = 0.19$, 0.11, 0.24, and $0.45\ \mu M$, respectively). In general, the activity of the compounds was inversely proportional to a specific alkyl chain length; however, compounds with

shortest (C_2-C_3) and longest (C_9-C_{11}) chains showed lower enzyme inhibitory activities.

Recently, investigators from the same group further extended their work on the α-1-*C*-alkyl-LAB derivatives by conducting *in vivo* and molecular docking studies. α-1-*C*-Butyl-LAB, identified as highly potent inhibitor of intestinal α-glucosidase, strongly suppressed postprandial hyperglycemia at early stage similar to that of miglitol but at a dose 10 times lower than that of miglitol to exhibit the same effect. It certainly differs from miglitol in that it does not interfere with oligosaccharide processing and maturation of glycoproteins as revealed from the proteomic analysis. Molecular docking studies showed that despite being competitive inhibitors of α-glucosidases, the orientation and enzyme interaction of the alkyl chains in miglitol and α-1-*C*-butyl-LAB are distinct. Each of the alkyl groups in these inhibitors has been proposed to preferably interact with different hydrophobic pockets of the enzyme. The α-1-*C*-alkyl-LAB derivatives particularly α-1-*C*-butyl-LAB are regarded as a new class of promising α-glucosidase inhibitors with higher efficacy for treating postprandial hyperglycemia than that of miglitol [21].

In continuation of their work on arabinoiminofuranoses, Natori et al. [22] also synthesized a number of α-1-*C*-40-aryl-butyl-*L*-arabinoiminofuranoses carrying functional groups on the phenyl ring demonstrating comparable potency of α-glucosidase inhibition to that of α-1-*C*-butyl-LAB (**7**). Compound **12**, a difluorophenylbutyl derivative, shown in Fig. 2.5, exhibited more promising activity against rat intestinal isomaltase ($IC_{50} = 0.22\ \mu M$) than that of α-1-*C*-butyl-LAB and oral α-glucosidase inhibitors. Furthermore, its activity against rat intestinal sucrase ($IC_{50} = 0.026\ \mu M$) compares well with that of α-1-*C*-butyl-LAB ($IC_{50} = 0.032\ \mu M$) and more improved than that of oral α-glucosidase inhibitors that are in current clinical practice [22].

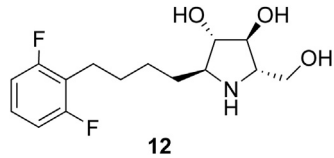

12

Figure 2.5 The difluorophenylbutyl derivative of α-1-C-butyl-LAB. *Reproduced from U. Ghani, Re-exploring promising α-glucosidase inhibitors for potential development into oral anti-diabetic drugs: finding needle in the haystack, Eur. J. Med. Chem. 103 (2015) 133–162.*

A number of natural and synthetic derivatives of radicamines exhibiting potent α-glucosidase inhibitory activity have been reported. Radicamines are natural polyhydroxylated pyrrolidines possessing an aromatic substituent on the iminosugar ring. The compounds were originally isolated from *Lobelia chinensis* LOUR (*Campanulaceae*) whole plant by Shibano and coworkers [23]. The plant is used as antidote, diuretic, hemostat, and as remedy for stomach cancer in Chinese herbal medicine. Radicamine A (**13**) and B (**14**) isolated from the plant potently inhibited yeast α-glucosidase ($IC_{50} = 6.7$ and 9.3 μM, respectively) (Fig. 2.6). Similarity of the aromatic ring of these compounds to that of deoxynojirimycin (DNJ) appears to be partially responsible for their inhibitory activity [23].

Li et al. [24] recently synthesized eight fluorinated derivatives of radicamine A and B and evaluated their inhibitory activity against α-glucosidases from yeast and rice, and rat intestinal maltase. In these derivatives (**15–18**), the position of the fluorine atom played a central role in the activity (Fig. 2.7). Fluorination at C_7 and C_{11} was proves to be unfavorable to the activity, however, at C_8 and C_{10} positions, it is optimal for the enzyme inhibition. The C_{10}-fluorinated derivative (**15**) ($IC_{50} = 1.4$ μM) of radicamine A exhibited more potent yeast α-glucosidase

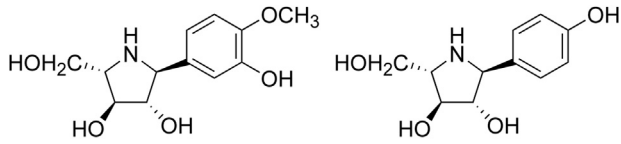

Figure 2.6 Natural polyhydroxylated pyrrolidines: radicamine A and B. The aromatic rings of the compounds bear similarity to that of DNJ. *Reproduced from U. Ghani, Re-exploring promising α-glucosidase inhibitors for potential development into oral anti-diabetic drugs: finding needle in the haystack, Eur. J. Med. Chem. 103 (2015) 133–162.* © *2015 French Société de Chimie Thérapeutique published by Elsevier Masson SAS. All rights reserved.*

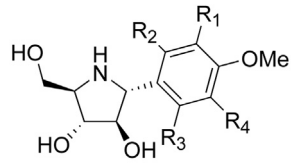

15. R_1= F, R_2,R_3= H, R_4= OH
16. R_1,R_2,R_3= H, R_4= F
17. R_1,R_3= H, R_2= F, R_4= OH
18. R_1,R_2= H, R_3= F, R_4= OH

Figure 2.7 The fluorinated derivatives of radicamine A and B show α-glucosidase inhibitory activity similar to their natural counterparts.

inhibitory activity than that of radicamine A alone, whereas the C_8-fluorinated derivative (**16**) ($IC_{50} = 4.9$ μM) showed comparable level of yeast α-glucosidae inhibition to that of radicamine A.

Conversely, fluorination at C_7 and C_{11} positions significantly reduced the inhibitory activity most likely due to the bonding of fluorine with the adjacent N–H group of the same compound. This bonding apparently interferes with the interaction of the group with enzyme active site residues by changing the interfacial angle between the sugar ring and the aryl group, which is not the case with C_8- and C_{10}-fluorinated derivatives. Fluorine may act as a chemical isostere of either hydrogen or

hydroxyl group resulting in no influence of the compounds on reducing the inhibitory activity. Therefore, these derivatives exhibited inhibitory activities similar to that of their natural counterparts.

Broussonetines are naturally occurring iminosugars (polyhydroxylated pyrrolidine alkaloids), isolated from the branches of the deciduous tree *Broussonetia kazinoki* that commonly grows in China and Japan. The plant has been used as diuretic, detoxicating, and hemostatic agent in Chinese medicine [25]. Shibano et al. reported six new natural pyrrolidine alkaloids including broussonetines and broussonetinines from the branches of the *Broussonetia kazinoki* tree with inhibitory activities against various glycosidases. Two of the alkaloids namely broussonetine E (**19**) and F (**20**) were found to be promising inhibitors of yeast α-glucosidase ($IC_{50} = 3.3$ and $1.5\,\mu M$, respectively; Fig. 2.8). In these compounds, presence of a hydroxyl group at the C_1' position is significant for high inhibition potency [25].

Further interest in exploring the structure−activity diversity of broussonetine yielded first total synthesis of broussonetine I (**21**) and J_2 (**22**), and their enantiomers *ent*-broussonetine I (**23**) and J_2 (**24**) (Fig. 2.9) exhibiting α-glucosidase inhibitory activity [26]. Both types of compounds displayed different activity profiles; broussonetine I (**21**) J_2 (**22**) inhibited bovine liver β-glucosidase, whereas their corresponding enantiomers **23** and **24** inhibited rat intestinal maltase ($IC_{50} = 0.33$ and $0.53\,\mu M$, respectively). The enantiomers were more selective to α-glucosidase inhibition than their corresponding compounds.

Moreover, the first total synthesis of (+)-broussonetine W (**25**) and its analogs has been recently reported (Fig. 2.10). The analogs were also evaluated for their inhibitory activity against a number of glycosidases including yeast and rice α-glucosidases, rat intestinal maltase and sucrase, intestinal isomaltase, and ER α-glucosidase II. The enantiomer of

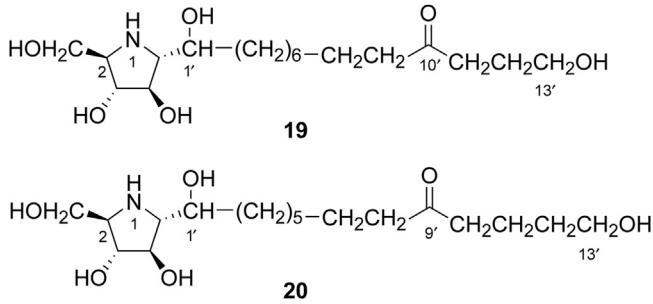

Figure 2.8 The broussonetine E and F alkaloids. Presence of a hydroxyl group at the C_1' position is central to high inhibitory potency exhibited by the alkaloids. *Reproduced from U. Ghani, Re-exploring promising α-glucosidase inhibitors for potential development into oral anti-diabetic drugs: finding needle in the haystack, Eur. J. Med. Chem. 103 (2015) 133–162. © 2015 French Société de Chimie Thérapeutique published by Elsevier Masson SAS. All rights reserved.*

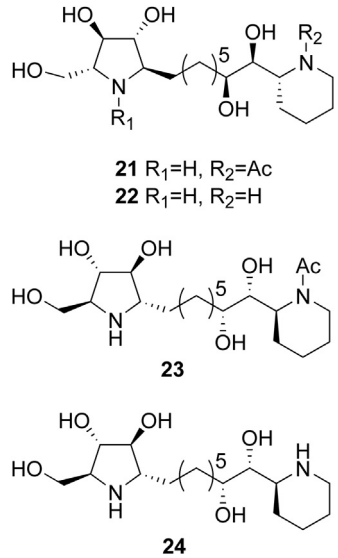

Figure 2.9 Broussonetine I and J_2, and their enantiomers. The enantiomers are more selective to α-glucosidase inhibition than their corresponding compounds. *Reproduced from U. Ghani, Re-exploring promising α-glucosidase inhibitors for potential development into oral anti-diabetic drugs: finding needle in the haystack, Eur. J. Med. Chem. 103 (2015) 133–162. © 2015 French Société de Chimie Thérapeutique published by Elsevier Masson SAS. All rights reserved.*

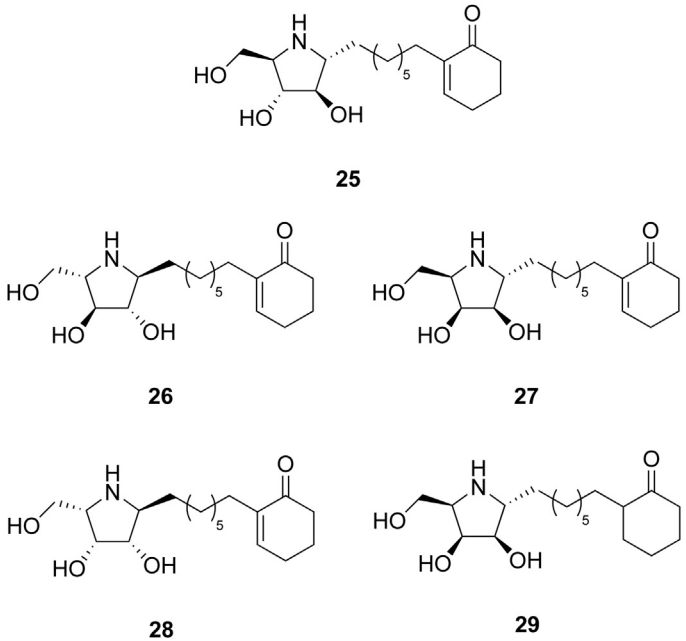

Figure 2.10 (+)-Broussonetine W and its synthetic analogs. Their α-glucosidase inhibition potency depends on the configuration of the polyhydroxylated pyrrolidine, the length of the side chain, and presence of the α,β-unsaturated ketone group functionality.

(+)-broussonetine W (**26**) demonstrated strong and selective inhibition of rat intestinal maltase ($IC_{50} = 0.047$ μM). A general correlation of the inhibitory activities of the analogs with the configuration of the polyhydroxylated pyrrolidine ring was observed. Furthermore, the length of the side chain and the α,β-unsaturated ketone group functionality played minor roles in glycosidase inhibition.

Compound **26** also displayed promising inhibitory activities against rice α-glucosidase and rat intestinal sucrase and isomaltase ($IC_{50} = 0.73$, 0.20, and 1.5 μM, respectively), which were comparable to that of L-DMDP since both compounds share similar features at the core pyrrolidine structural level.

Compound **27** was found to be a weaker inhibitor of α-glucosidase than its natural counterpart (+)-broussonetine

W mainly due to differences in the C_3 configuration of the polyhydroxylated pyrrolidine ring. In contrast, its enantiomer **28** remarkably exhibited more potency of inhibition against rat intestinal maltase and sucrase ($IC_{50} = 3.5$ and 3.4 μM, respectively) than (+)-broussonetine W ($IC_{50} = 67$ and 216 μM, respectively).

Attempts involving modifications of the side-chains of the analogs did not dramatically change the levels of activity of the compounds rather the activity was merely directly proportional to the side-chain length. Moreover, the terminal substitutions of the side chain did not impart a significant effect on the pattern of glycosidase inhibition. Compounds bearing the saturated cyclohexanone group were slightly weaker inhibitors than the natural (+)-broussonetine W and its analogs containing the same group. However, it is noteworthy to mention that relative to compound **27** that holds the unsaturated cyclohexenone group, compound **29** exhibited much more inhibitory activity against rice α-glucosidase, rat intestinal maltase, and sucrase ($IC_{50} = 7.9$, 1.6, and 3.1 μM, respectively) [27].

Novel α-geminal dihydroxymethyl piperidine and pyrrolidine iminosugar inhibitors of various glucosidase enzymes have been recently synthesized (Fig. 2.11). All pyrrolidine iminosugars (e.g., **30** and **31**) and piperidine iminosugars (e.g., **32**, **33**, and **34**) inhibited rice α-glucosidase ($IC_{50} = 0.028-5.0$ μM; $K_i = 0.083-3.0$ μM). The hydroxymethyl group at C_5 position of compound **33** is crucial for promising rice α-glucosidase inhibitory activity when compared to DNJ. However, compounds **30** and **33** exhibited moderate inhibition of yeast α-glucosidase. Molecular docking confirmed that the higher affinity of **30**, **33**, and **34** to rice α-glucosidase is due to strong hydrogen bonding with the enzyme as indicated by their lower free energies. Each of the inhibitors forms approximately five to six strong and stable hydrogen bonds with the active site residues of the enzyme [28].

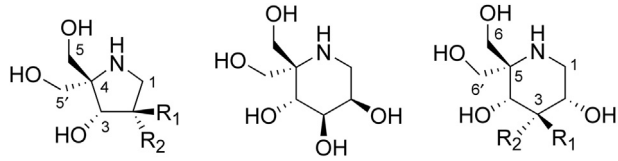

30 R_1=OH, R_2=H
31 R_1=H, R_2=OH
32
33 R_1=OH, R_2=H
34 R_1=H, R_2=OH

Figure 2.11 The α-geminal dihydroxymethyl piperidine and pyrrolidine iminosugars. The compounds form strong hydrogen bonding with yeast α-glucosidase active site as revealed by molecular docking studies. *Reproduced from U. Ghani, Re-exploring promising α-glucosidase inhibitors for potential development into oral anti-diabetic drugs: finding needle in the haystack, Eur. J. Med. Chem. 103 (2015) 133–162. © 2015 French Société de Chimie Thérapeutique published by Elsevier Masson SAS. All rights reserved.*

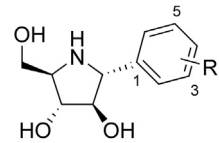

35 R=4-methoxyphenyl
36 R=3-methoxyphenyl
37 R=3,4-dimethoxyphenyl
38 R=2,4-dimethoxyphenyl
39 R=2,5-dimethoxyphenyl

Figure 2.12 The substitutions on the aryl ring of the 2-aryl polyhydroxylated pyrrolidine derivatives are important for inhibition and selectivity to different glucosidases. *Reproduced from U. Ghani, Re-exploring promising α-glucosidase inhibitors for potential development into oral anti-diabetic drugs: finding needle in the haystack, Eur. J. Med. Chem. 103 (2015) 133–162. © 2015 French Société de Chimie Thérapeutique published by Elsevier Masson SAS. All rights reserved.*

Tsou et al. [29] synthesized and screened a library of 2-aryl polyhydroxylated pyrrolidines against various glucosidases including bacterial (*Bacillus stearothermophilus*) and yeast α-glucosidases (Fig. 2.12). In these compounds, the substitutions on the aryl ring determined the potency of inhibition and selectivity to different glucosidases. Compounds with the

D-gluco configuration were found to be more selective inhibitors of α-glucosidases than β-glucosidases and mannosidases. Compounds with mono-substitution on the aryl ring with *para* (**35**) ($IC_{50} = 0.5$ μM) and *meta* (**36**) ($IC_{50} = 2.4$ μM) methoxy groups showed higher levels of yeast α-glucosidase inhibition than those containing a *para*-hydroxyl group only.

Compounds with the 3,4-dimethoxy-substitution, such as in **37**, showed more promising activity than those possessing the same substitution at the 2,4- or 2,5-positions as in compounds **38** and **39**, respectively. Compound **37**, a competitive inhibitor of yeast α-glucosidase ($K_i = 0.7$ μM), behaves like a transition state analog in glycosidic catalysis since its conformation and the orientation of its hydroxyl groups are ideal for optimal inhibition of the enzyme. Increasing the hydrophobicity of the compounds by incorporating a methyl or a butyl group to the imino moiety resulted in a significant loss of inhibitory activity, further confirming that the hydroxyl groups in these compounds that apparently participate in the interactions with the enzyme active site residues are crucial for potent inhibition.

Recently, a limited library of alkaloids and scaffolds, based on natural bicyclic iminosugars bearing the polyhydroxylated pyrrolidine and varied ring skeletons, have been synthesized [30]. Polyhydroxylated pyrrolizidines and piperidines are monocyclic iminosugars that have been widely studied [31,32] due to their broad spectrua of biological activities including inhibition of various glucosidases that are implicated in diabetes, cancer, and lysosomal storage diseases [33]. In their work, Cheng et al. [30] identified two libraries with promising α-glucosidase inhibitory activity, which showed a general pattern of structure-dependent inhibition. In these libraries, the structural features responsible for promising enzyme inhibition include the stereocenter on the ring B and the structure of the substituent. Furthermore, the inhibitors carrying phenyl moieties exhibited more potent enzyme inhibition than those

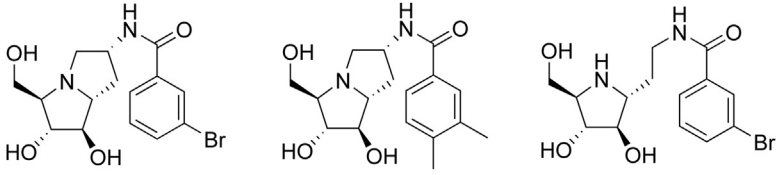

Figure 2.13 The bicyclic iminosugar-based alkaloids and scaffolds mainly inhibit α-glucosidase through their stereocenter on the ring B and the type of the substituent group.

bearing the alkyl, benzyl, or alicyclic groups. Comparison of the structures and activity of inhibitors **40** (possessing a bromo group at the *meta* position; $IC_{50} = 0.2\ \mu M$) and **41** (possessing methyl groups at the *meta* and *para* positions; $IC_{50} = 0.4\ \mu M$) revealed that the hydrophobic substituents on the phenyl moiety tend to enhance the potency of inhibition. These compounds inhibited α-glucosidase with more potency than DAB, particularly compound **40** whose potency also exceeded that of monocyclic DMDP. The compound competitively inhibited bacterial α-glucosidase ($K_i = 71$ nM), which appears to be a mechanism-based inhibitor since it mimics the transition state during catalysis. The monocyclic compound **42** inhibited α-glucosidase, albeit 500 times weaker than the bicyclic compound **40** (Fig. 2.13). It appears that the inhibitory activity of both compounds is generally due to protonation of their amine groups in the acidic assay conditions in which they, most likely, act as transition state analogs. However, the discriminating factor that dictates potent activity is the bicyclic conformationally restricted scaffold (as in compound **40**) rather than charge distribution.

2.2.2 Polyhydroxylated pyrrolizidines

Polyhydroxylated pyrrolizidines are naturally occurring alkaloid inhibitors of glucosidases with potential therapeutic effects for treatment of diabetes mellitus, cancer, and HIV [34–36].

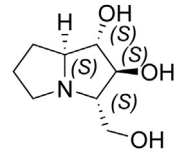

43

Figure 2.14 (−)-Hyacinthacine A_2. *Reproduced from U. Ghani, Re-exploring promising α-glucosidase inhibitors for potential development into oral anti-diabetic drugs: finding needle in the haystack, Eur. J. Med. Chem. 103 (2015) 133–162. © 2015 French Société de Chimie Thérapeutique published by Elsevier Masson SAS. All rights reserved.*

Asano et al. [37] first isolated hyacinthacines A_1 and A_2 from the bulbs of *Muscari armeniacum* (Hyacinthaceae) with significant inhibitory activities against rat intestinal lactase, rat epididymis α-L-fucosidase, and amyloglucosidase enzymes. Later, Calveras and coworkers [38] attempted the first chemoenzymatic synthesis of these alkaloids particularly the stereoisomers of hyacinthacines A_1 and A_2. (−)-Hyacinthacine A_2 (**43**), an enantiomer of (+)-hyacinthacine A_2, is a competitive inhibitor of rice α-glucosidase ($K_i = 4.7$ μM) (Fig. 2.14); conversely, (+)-hyacinthacine A_2 is inactive. The exclusive inhibition of the enzyme by (−)-hyacinthacine A_2 obviously explains their preferred selectivity of the active site for that specific stereochemistry.

Natural bicyclic iminosugars such as (+)-casuarine (**44**; $IC_{50} = 0.7$ μM) and casuarine 6-O-α-glucoside (**45**; $IC_{50} = 1.1$ μM) are of interest in terms of their promising biological activities especially α-glucosidase inhibition (Fig. 2.15). (+)-Casuarine and casuarine 6-O-α-glucoside, isolated from the bark of *Casuarina equisetifolia* and the leaves of *Eugenia jambolana*, respectively, were originally identified as inhibitors of fungal maltase–glucoamylase originating from *Aspergillus niger* [39]. Casuarine is also a promising inhibitor of rice α-glucosidase ($IC_{50} = 1.2$ μM) and rat intestinal maltase ($IC_{50} = 0.7$ μM) [40]. The first total synthesis of casuarine and

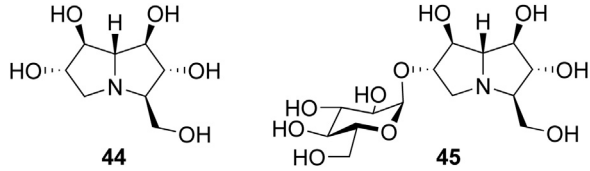

Figure 2.15 Casuarine and its glycoside. *Reproduced from U. Ghani, Re-exploring promising α-glucosidase inhibitors for potential development into oral anti-diabetic drugs: finding needle in the haystack, Eur. J. Med. Chem. 103 (2015) 133–162.*

casuarine 6-*O*-α-glucoside has been reported by Denmark and Hurd [41], and Cardona et al. [42], respectively. Further work on its biological activities revealed that casuarine also potently inhibits the *N*-terminal domain of human intestinal maltase–glucoamylase (MGAM-N) ($K_i = 0.45$ μM) [42]. Discussion on the crystal structure of casuarine in complex with MGAM-N will follow in Chapter 7: Computational and structural biology of α-glucosidase-inhibitor complexes: clues to drug optimization and development.

2.2.3 Polyhydroxylated quinolizidines

There are several reports on the synthetic polyhydroxylated quinolizidine iminosugars exhibiting moderate α-glucosidase inhibitory activity [43,44]. However, no natural polyhydroxylated quinolizidine has been isolated and studied to date. Recent work by Da Cruz et al. on the synthesis and biological activity of quinolizidine iminosugar derivatives carrying a hydroxymethyl group at the ring junction has identified a number of highly potent α-glucosidase inhibitors with IC_{50} values in nanomolar range [45]. The derivatives (**46**, **47**, **48**, and **49**) were synthesized using the *L*-sorbose-derived ketonitrones as starting material, which were also evaluated for α-glucosidase inhibitory activity (Fig. 2.16). All *D*-gluco configured quinolizidines (**46**, **48**, and **49**) potently and selectively

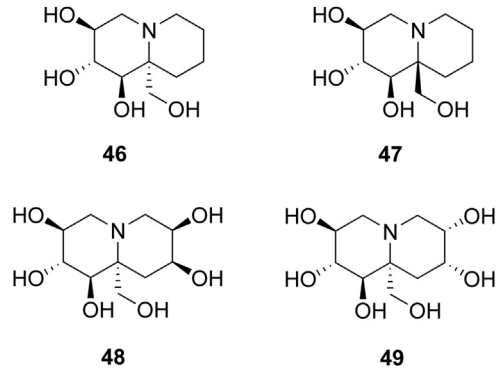

Figure 2.16 The polyhydroxylated quinolizidine iminosugars.

inhibited the enzyme, particularly the compound **46** that demonstrated highest inhibitory activity against rice α-glucosidase ($IC_{50} = 47$ nM) compared to that of DNJ ($IC_{50} = 35$ nM). The compound, a mixed-type inhibitor, showed tight binding affinity with the enzyme active site ($K_i = 57$ nM). Additionally, it also inhibited yeast α-glucosidase but with much lower potency ($IC_{50} = 300$ μM). Compound **47** with the *L-ido* configuration for the polyhydroxylated ring exhibited modest inhibitory activity against rice α-glucosidase ($IC_{50} = 107$ μM). It is important to mention that the hexahydroxylated quinolizidines (**48** and **49**) were found to be promising inhibitors of rice α-glucosidase ($IC_{50} = 0.26$ and 0.79 μM, respectively). Kinetic studies showed that these compounds bind to the enzyme with much lower affinity than that of **46** since they contain an additional dihydroxylated cyclic structure. Interestingly, presence of these additional hydroxyl groups in **48** and **49** markedly suppressed their yeast α-glucosidase inhibitory activity.

2.2.4 Hydroxymethyl-branched polyhydroxylated indolizidines

The piperidine and polyhydroxylated indolizidine derivatives have shown to be promising α-glucosidase inhibitors. The former are analogs of DNJ with an improved α-glucosidase

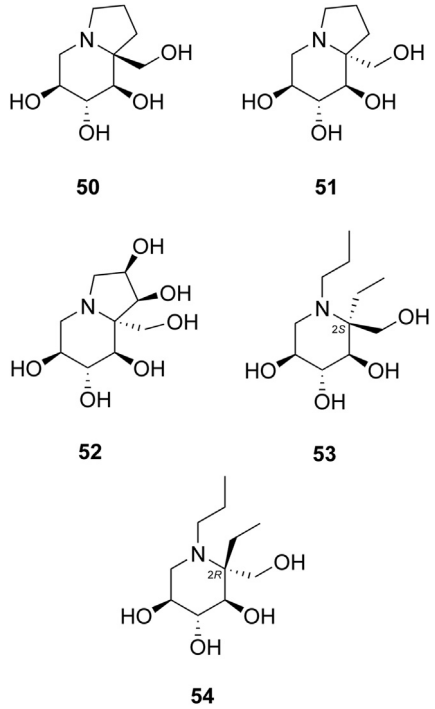

Figure 2.17 The α,α-disubstituted piperidine and 8α-branched polyhydroxylated indolizidine derivatives.

inhibitory profile than that of DNJ. Boisson et al. [46] synthesized and evaluated α,α-disubstituted piperidine and 8α-branched polyhydroxylated indolizidine derivatives for α-glucosidase inhibitory activity (Fig. 2.17). The tetrahydroxylated indolizidines such as **50** ($IC_{50} = 2.2$ μM) and **51** ($IC_{50} = 0.052$ μM/$K_i = 31$ nM) have shown to inhibit rice α-glucosidase with high potency. Dihydroxylation of these derivatives yielded compound **52** exhibiting comparable levels of rice α-glucosidase inhibition ($IC_{50} = 1.5$ μM) indicating that the dihydroxylation exerted similar inhibitory effects despite carrying six hydroxyl groups. The tetrahydroxylated *N*-propyl α,α-disubstituted piperidines (**53** and **54)** showed comparable levels of rice α-glucosidase inhibition as well ($IC_{50} = 2.3$ μM).

2.2.5 Nojirimycin derivatives

α-Homonojirimycin (α-HNJ), a C_1-branched derivative of DNJ, is a natural product first discovered in 1988 [47]. Since then numerous natural derivatives of α-HNJ have been isolated and synthesized, many of which displayed promising α-glucosidase inhibitory activity including its 7-*O*-β-*D*-glucoside with potential for treatment of hyperglycemia in type 2 diabetes [48–51].

Suregada glomerulata, a plant native to China with no report on its medicinal use, has been investigated by Yan et al. for its potential medicinal value [52]. The water extract of its leaves showed α-glucosidase inhibitory activity that led to isolation of 10 new piperidine iminosugars closely related to α-HNJ including one known pyrrolidine (homo-DMDP) and nine known natural derivatives of α-HNJ. All compounds inhibited rat small intestinal maltase including four that also lowered postprandial blood glucose levels in healthy mice. Interestingly, the *N*-methyl, *N*-butyl, and *N*,*N*-dimethyl derivatization of the piperidine compounds resulted in a significant loss of α-glucosidase inhibitory activity. However, the *N*-methylation of α-HNJ, α-7-deoxyhomonojirimycin and 4-deoxy-α-homonojirimycin yielded better inhibitors (e.g., **55**; $IC_{50} = 0.72$ μM).

More importantly, the 4-deoxygentaion of these compounds at the C_4 position remarkably suppressed the activity suggesting a decisive role of the 4-hydroxyl group in enzyme inhibition especially with β orientation. The α-1-*C*-hydroxyoctyl derivative of DNJ (**56**), presented in Fig. 2.18, showed moderate activity ($IC_{50} = 5.53$ μM) suggesting that DNJ bearing long hydroxylated side chains may potentially become a new class of α-glucosidase inhibitors. Some of the known natural derivatives of HNJ were also found to significantly reduce postprandial blood glucose levels in healthy mice using oral starch and sucrose tolerance tests.

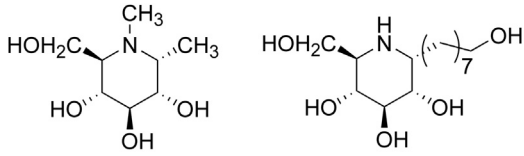

Figure 2.18 Natural derivatives of α-HNJ and DNJ. The 4-hydroxyl group, especially with β orientation, is responsible for promising activity. *Reproduced from U. Ghani, Re-exploring promising α-glucosidase inhibitors for potential development into oral anti-diabetic drugs: finding needle in the haystack, Eur. J. Med. Chem. 103 (2015) 133–162. © 2015 French Société de Chimie Thérapeutique published by Elsevier Masson SAS. All rights reserved.*

In order to study the influence of a variety of chiral centers and conformations on the selectivity and potency of inhibition of glucosidases, Asano et al. [49] synthesized a series of natural epimers of α-HNJ and its *N*-alkylated derivatives, and screened them against various glucosidases (Fig. 2.19). α-HNJ (**57**) showed potent inhibition of a number of α-glucosidases ($IC_{50} = 0.04–8.4$ μM), whereas β-HNJ (**58**), α-homomannojirimycin (**59**), and β-homomannojirimycin (**60**) were inactive against β-glucosidases and mannosidases despite being moderate inhibitors of some mammalian α-glucosidases. β-4,5-di-*epi*-HNJ (**61**), *N*-methyl-α-HNJ (**62**), and *N*-butyl-α-HNJ (**63**) inhibited various α-glucosidases. The structure of α-HNJ features a chair conformation with the C_1 hydroxyl group equatorial to the piperidine ring, whereas the *N*-methyl-α-HNJ (**62**) carries an axial orientation. From these studies, the investigators proposed that the axial conformation of the C_1 hydroxyl group is essential for promising glucosidase inhibition, rendering more specificity to rat liver α-glucosidases I than II unlike *N*-butyl-α-HNJ (**63**) and *N*-butyl-DNJ (**64**), both of which lack this type of conformation. The IC_{50} values of the compounds are listed in the Appendix.

It is noteworthy to mention the synthetic alkylated derivatives of (+)-DNJ especially compounds **65** ($IC_{50} = 0.108$;

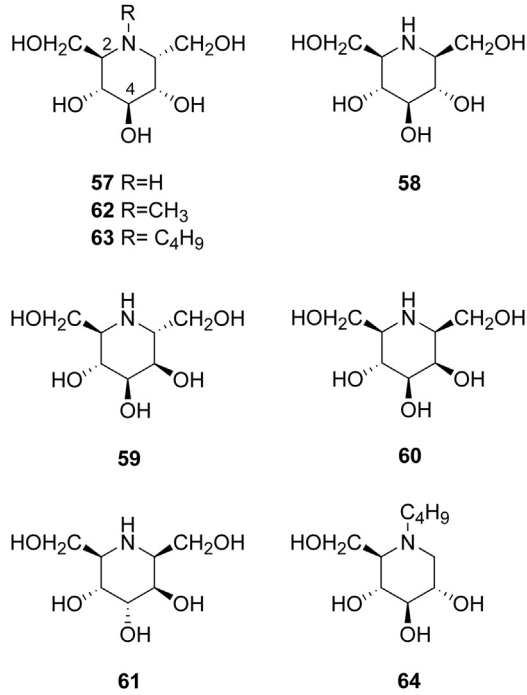

Figure 2.19 The axial conformation of the C_1 hydroxyl group is essential for potent inhibition of α-glucosidase by the natural epimers of α-HNJ and their *N*-alkylated derivatives. *Reproduced from U. Ghani, Re-exploring promising α-glucosidase inhibitors for potential development into oral anti-diabetic drugs: finding needle in the haystack, Eur. J. Med. Chem. 103 (2015) 133–162. © 2015 French Société de Chimie Thérapeutique published by Elsevier Masson SAS. All rights reserved.*

1.9 μM) and **66** ($IC_{50} = 0.017$; 0.3 μM) that exhibited more stronger inhibition of rat liver α-glucosidases I and II than that of *N*-butyl-DNJ ($IC_{50} = 0.68$; 10.8 μM) (Fig. 2.20). Particularly, the aryl azide (**66**) that showed promising inhibition of rat liver α-glucosidase I in nanomolar range ($IC_{50} = 17$ nM), whereas compound **67** inhibited rat liver α-glucosidase II with $IC_{50} = 0.29$ μM [53].

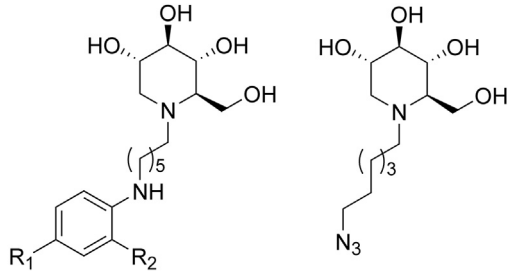

65 R_1=NO_2, R_2=NO_2, *n*=5
66 R_1=N_3, R_2=NO_2, *n*=5

67

Figure 2.20 The alkylated derivatives of (+)-DNJ. *Reproduced from U. Ghani, Re-exploring promising α-glucosidase inhibitors for potential development into oral anti-diabetic drugs: finding needle in the haystack, Eur. J. Med. Chem. 103 (2015) 133–162. © 2015 French Société de Chimie Thérapeutique published by Elsevier Masson SAS. All rights reserved.*

Ardes-Guisot et al. [54] synthesized a series of neoglycoconjugates of DNJ by click connection with functionalized adamantanes (Fig. 2.21).

All compounds (**68–74**) significantly inhibited rice α-glucosidases, rat intestinal maltase, and sucrose with an IC_{50} range of 0.025–7.3 μM showing a direct correlation of the level of inhibition with increasing side-chain length. Compounds containing shorter side chains displayed moderate inhibition of the enzyme when compared to miglitol and DNJ.

Hatano et al. [55] synthesized and characterized five new fluorescent DNJ conjugates (**75–79**) by linking fluorescent molecules to DNJ through click azide–alkyne coupling reaction (Fig. 2.22). This type of conjugation resulted in compounds exhibiting moderate to potent α-glucosidase inhibitory activity. The conjugate **75** was active against rice α-glucosidase, rat intestinal maltase, rat intestinal isomaltase, and rat intestinal sucrase, whereas the inhibitory activity of the conjugate **75** was comparable to that of DNJ and miglitol. The conjugate **76**

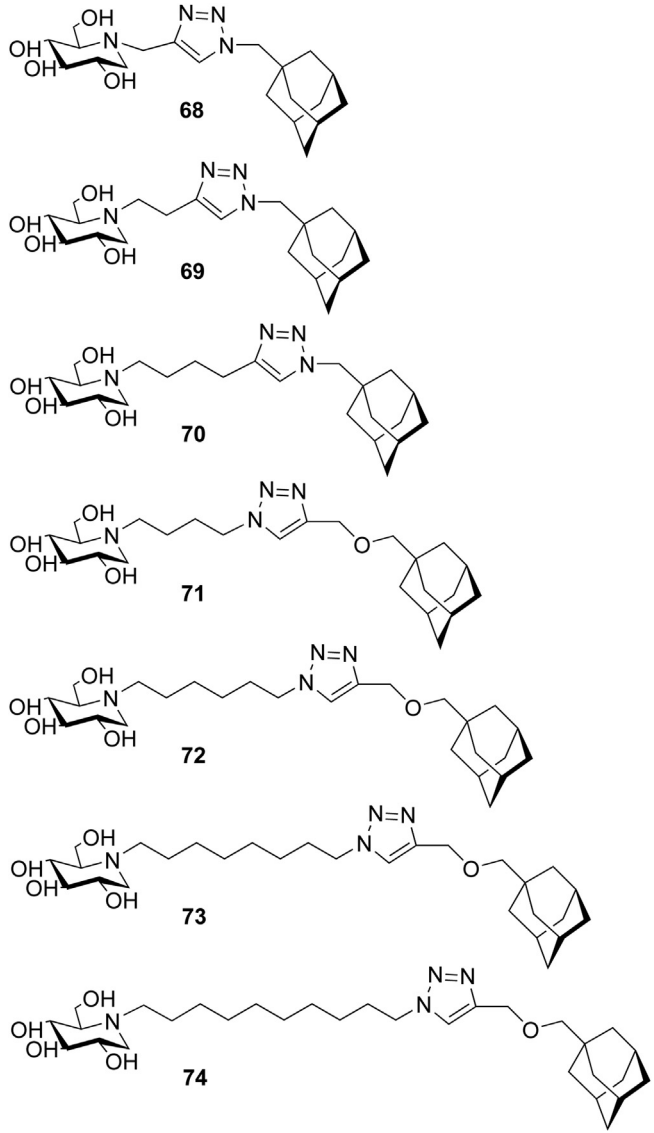

Figure 2.21 There is a direct correlation of inhibition potency to increasing side-chain length of the neoglycoconjugates of DNJ. *Reproduced from U. Ghani, Re-exploring promising α-glucosidase inhibitors for potential development into oral anti-diabetic drugs: finding needle in the haystack, Eur. J. Med. Chem. 103 (2015) 133–162.*

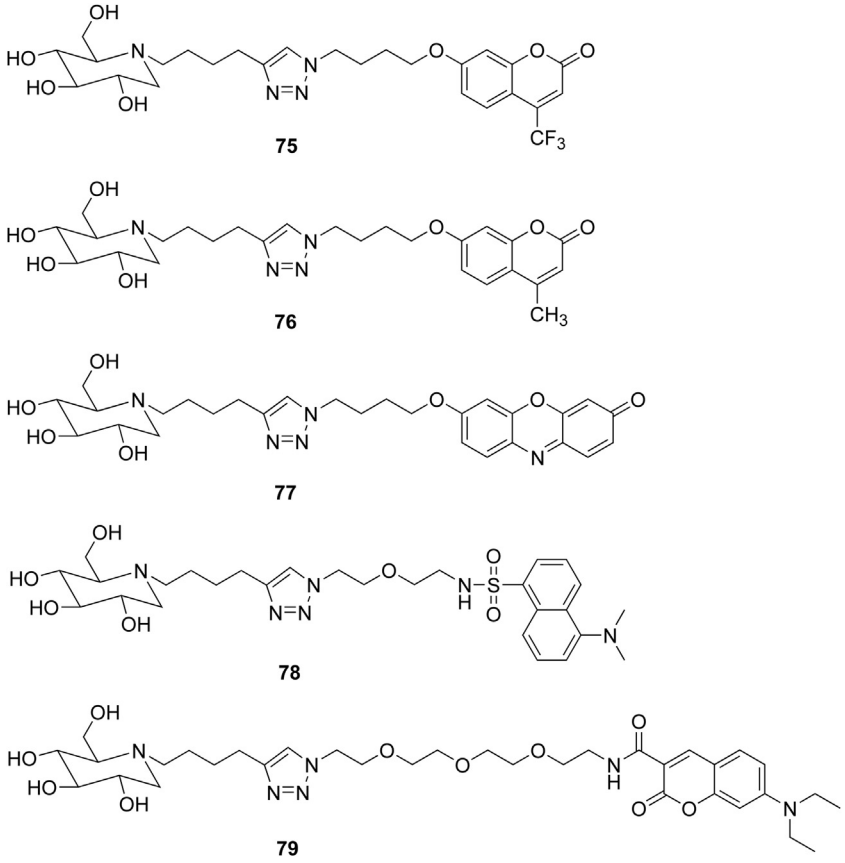

Figure 2.22 The fluorescent deoxynojirimycin conjugates. In these compounds, the DNJ moiety and the linking hydrophobic chromophores act in concert to influence the activity.

exhibited more activity against the above enzymes than that of **75**; it inhibited both α- and β-glucosidases. The activity of conjugates **77** and **78** was found to be lower than that of other conjugates on the target enzymes. Conjugate **79** inhibited rat intestinal maltase with highest potency ($IC_{50} = 0.1\ \mu M$) but exhibited moderate potency of inhibition on rat intestinal isomaltase ($IC_{50} = 13.6\ \mu M$). These DNJ conjugates are an interesting class of compounds that inhibit a variety of

α-glucosidases. Their inhibitory effect on several α-glucosidases is particularly due to the DNJ moiety and the linking hydrophobic chromophores that act in concert for the net effect. Molecular docking studies have confirmed that the conjugates strongly inhibit α-glucosidase by optimally binding to the enzyme active site, and through electrostatic interactions involving the N_1,*N*-alkylation of DNJ at position 1.

2.2.6 Other derivatives

A variety of plants from the *Beilschmiedia* genus have been used in African folklore medicine for treatment of tumors, rheumatism, and lung diseases [56]. Natural compounds isolated from the *Beilschmiedia alloiophylla* plant have shown to possess promising α-glucosidase inhibitory activity. Recently, isolation of a new alkaloid namely 2-hydroxy-9-methoxyaporphine, along with 10 known compounds from the plant with yeast α-glucosidase inhibitory activity, has been reported ($IC_{50} = 8-55\ \mu M$). Since 2-hydroxy-9-methoxyaporphine ($IC_{50} = 40\ \mu M$) contains the aromatic ring system and substitutions similar to that of NJ, its inhibitory activity can be justified by the presence of these structural similarities. Among other compounds oreobeiline, 6-epioreobeiline, β-amyrone, and (*S*)-3-methoxynordomesticine also showed inhibitory activity with IC_{50} values of 8, 10, 20, and 10 μM, respectively [57]. More details of the inhibitor structures have been provided in the original article [57].

It is important to discuss the synthetic *N*-alkylated iminosugar mimics (*S*-alkylated, cyclic sulfonium ions) featuring varying alkyl chain lengths that have been reported to inhibit human intestinal maltase−glucoamylase (K_i range = $6-75\ \mu M$). Example includes compound **80** ($K_i = 6\ \mu M$) (Fig. 2.23) [58].

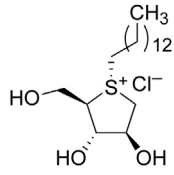

80

Figure 2.23 The cyclic sulfonium ion of *S*-alkylated iminosugars. *Reproduced from U. Ghani, Re-exploring promising α-glucosidase inhibitors for potential development into oral anti-diabetic drugs: finding needle in the haystack, Eur. J. Med. Chem. 103 (2015) 133–162. © 2015 French Société de Chimie Thérapeutique published by Elsevier Masson SAS. All rights reserved.*

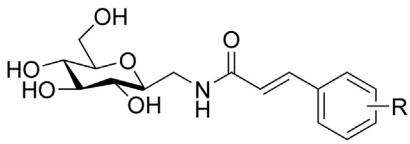

81 R=H
82 R=4-OH
84 R=3,4-diOAc

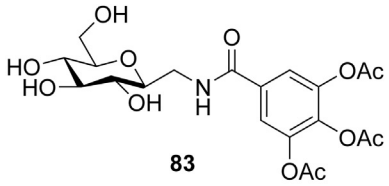

83

Figure 2.24 The benzamide, cinnamide, gallamide, and caffeoyl aminosugars. *Reproduced from U. Ghani, Re-exploring promising α-glucosidase inhibitors for potential development into oral anti-diabetic drugs: finding needle in the haystack, Eur. J. Med. Chem. 103 (2015) 133–162. © 2015 French Société de Chimie Thérapeutique published by Elsevier Masson SAS. All rights reserved.*

2.3 Aminosugars

The synthetic *N*-substituted 1-aminomethyl-β-*D*-glucopyranoside aminosugar derivatives (Fig. 2.24) are of interest since they inhibit a range of glycosidases including yeast α-glucosidase, rat intestinal maltase and sucrase enzymes (IC_{50} range $= 2.3\ \mu M - 2.0\ mM$). In these compounds, the type of *N*-substitution greatly affects the activity. The amidosugar series of the compounds constitute benzamide and cinnamide derivatives; out these, two of the cinnamic amide derivatives

81 ($IC_{50} = 2.3\ \mu M$) and **82** ($IC_{50} = 5.6\ \mu M$) are promising inhibitors of yeast α-glucosidase. Changes in the aromatic ring substituents on the cinnamide moiety resulted in a significant loss of inhibitory activity, specifically the groups incorporated at position 4 impart marked effect on the activity.

The gallamide derivative **83** and the caffeoyl amide derivative **84** inhibited rat intestinal maltase ($IC_{50} = 7.7$ and $5.1\ \mu M$, respectively) and rat intestinal sucrase ($IC_{50} = 15.9$ and $10.4\ \mu M$, respectively). The latter is a competitive inhibitor of rat intestinal maltase and sucrase ($K_i = 4.8$ and $17.1\ \mu M$, respectively). The 3,4,5-triacetoxy motif in the former augments higher inhibitory potency possibly due to favorable role of acetoxy groups in apparent hydrogen bonding with the enzyme. Generally, the amidosugar series of compounds are more promising inhibitors of the target enzymes than aminosugars [59].

Three pseudoaminosugars namely validamine, valienamine, and valiolamine have been tested for rat liver α-glucosidases I and II, and rat liver lysosomal α-glucosidase inhibitory activities. Valiolamine (**85**) (Fig. 2.25) potently inhibited α-glucosidases I and II ($IC_{50} = 12\ \mu M$ each). Moreover, it is also a competitive inhibitor of rat liver lysosomal α-glucosidase ($K_i = 8.1$ and $11\ \mu M$) using maltose and glycogen substrates, respectively) [60]. As discussed earlier, valiolamine was

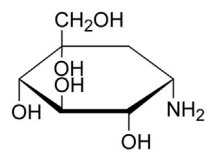

Valiolamine (**85**)

Figure 2.25 Valiolamine—a promising lead compound that paved way for the development of voglibose. *Reproduced from U. Ghani, Re-exploring promising α-glucosidase inhibitors for potential development into oral anti-diabetic drugs: finding needle in the haystack, Eur. J. Med. Chem. 103 (2015) 133–162. © 2015 French Société de Chimie Thérapeutique published by Elsevier Masson SAS. All rights reserved.*

identified as promising lead compound that later resulted in the drug development of voglibose. The compound and its derivatives may still provide further avenues for studying oligosaccharide processing by glucosidases and for developing new antidiabetic drugs.

2.4 Thiosugars

Salacia reticulata has been used in Ayurvedic traditional medicine for treatment of type 2 diabetes mellitus. *In vivo* experiments have shown that the aqueous extract of the stem and roots of the plant significantly reduced blood glucose levels [61] and bodyweight [62] in rats without acute toxicity. Additionally, the plant extract has shown to significantly reduce blood glucose levels in patients with type 2 diabetes [63]. *Salacia reticulata* contains well-known and widely studied α-glucosidase inhibitors such as salacinol, kotalanol, and de-*O*-sulfonated kotalanol, which possess the 1,4-anhydro-4-thio-*D*-arabinitol moiety and the polyhydroxylated acyclic side chain. One of the characteristics of the sulfonium ion inhibitors is that they carry a permanent positively charged sulfur that is assumed to interact with the α-glucosidase active site in a fashion similar to that of protonated amines. This section highlights some of the natural and synthetic thiosugars with promising α-glucosidase inhibitory activity.

In Asian traditional medicine, the stem and roots of *Salacia chinensis* are widely used for treatment of diabetes. Hot-water extract of the plant stem has shown promising *in vivo* antidiabetic activity in a type 2 diabetes mellitus mice model. The extract significantly lowered postprandial glucose as well as HbA1C (glycated hemoglobin) levels [64]. The plant is known to contain kotalanol (**86**), salacinol, and other compounds that

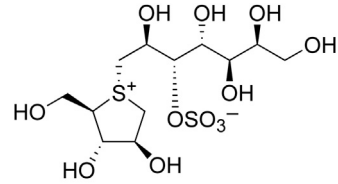

Kotalanol (**86**)

Figure 2.26 Kotalanol—a thiosugar α-glucosidase inhibitor isolated from *Salacia reticulata* featuring the 1-deoxyheptosyl-3-sulfate anion and the 1-deoxy-4-thio-D-arabinofuranosyl sulfonium cation. *Reproduced from U. Ghani, Re-exploring promising α-glucosidase inhibitors for potential development into oral anti-diabetic drugs: finding needle in the haystack, Eur. J. Med. Chem. 103 (2015) 133–162. © 2015 French Société de Chimie Thérapeutique published by Elsevier Masson SAS. All rights reserved.*

are widely recognized as classic glucosidase inhibitors. Kotalanol and salacinol are extensively studied natural thiosugars with potent α-glucosidase inhibitory activity. Yoshikawa and coworkers [65] first isolated kotalanol from the water soluble extract of the roots and stems of *Salacia reticulata*, a woody climbing plant from the submontane forests of Southeast Asia. Use of roots and stems of the plant are common in traditional medicine for treatment of diabetes mellitus. Chemically, kotalanol is a thiosugar derivative composed of the 1-deoxyheptosyl-3-sulfate anion and the 1-deoxy-4-thio-D-arabinofuranosyl sulfonium cation (Fig. 2.26). It is a more potent competitive inhibitor of rat intestinal maltase ($K_i = 0.18$ μM) than acarbose.

Moreover, Yoshikawa and coworkers [66] also first isolated salacinol (**87**) from the same plant and reported its biological activities (Fig. 2.27). Salacinol is a potent competitive inhibitor of rat intestinal maltase, isomaltase, and sucrase ($K_i = 0.31$, 0.47, 0.32 μM, respectively). The water-soluble fraction of the roots and stems of the plant significantly reduced blood glucose levels in rats. Additionally, the same fraction inhibited rat

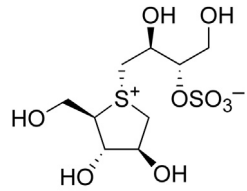

Salacinol (**87**)

Figure 2.27 Salacinol. *Reproduced from U. Ghani, Re-exploring promising α-glucosidase inhibitors for potential development into oral anti-diabetic drugs: finding needle in the haystack, Eur. J. Med. Chem. 103 (2015) 133–162. © 2015 French Société de Chimie Thérapeutique published by Elsevier Masson SAS. All rights reserved.*

intestinal maltase ($IC_{50} = 35$ μM) and sucrase ($IC_{50} = 26$ μM) *in vitro*. High doses of the fraction did not show significant effects on alloxan-induced hyperglycemia in mice indicating that the plant possibly lowers blood glucose levels by inhibiting intestinal α-glucosidase. Bioactive-guided fractionation confirmed salacinol to be the active ingredient responsible for this effect. The inhibitory activities of salacinol on rat intestinal maltase, sucrase, and isomaltase are comparable to that of acarbose ($K_i = 0.12$, 0.37, 75 μM, respectively).

The inhibitory effects of a series of natural thiosugars and their analogs on human recombinant glucosidases (maltase–glucoamylase, sucrase–isomaltase) have been reported recently [67,68]. These include neosalacinol (**88**), neokotalanol (**89**) ponkoranol (**90**), and neoponkoranol (**91**) which potently inhibited human intestinal maltase–glucoamylase ($IC_{50} = 3.9$, 3.9, 5.0, and 4.0 μM, respectively) (Fig. 2.28). The compounds exhibited rat intestinal maltase inhibitory activities similar to that of acarbose, miglitol, and voglibose [62].

Several synthetic derivatives of salacinol and related compounds have been reported since its original isolation from *Salacia reticulata*. Ishikawa et al. [69] utilized a diastereoselective approach to designing of promising salacinol-type α-glucosidase

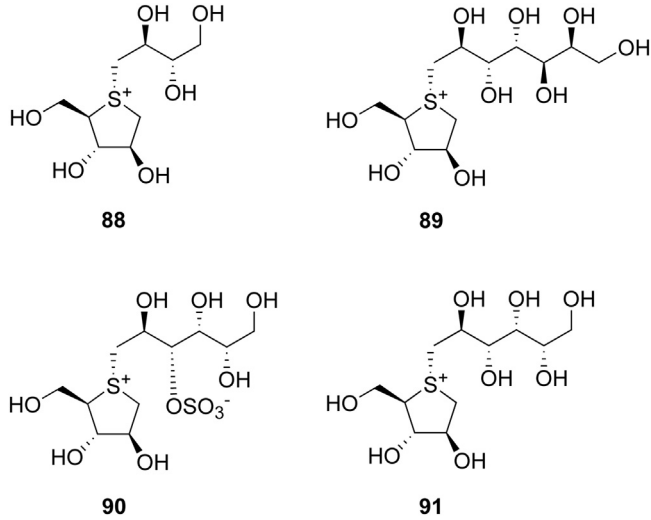

Figure 2.28 Natural thiosugar analogs. *Reproduced from U. Ghani, Re-exploring promising α-glucosidase inhibitors for potential development into oral anti-diabetic drugs: finding needle in the haystack, Eur. J. Med. Chem. 103 (2015) 133–162. © 2015 French Société de Chimie Thérapeutique published by Elsevier Masson SAS. All rights reserved.*

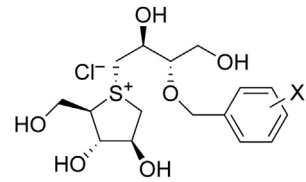

Figure 2.29 Synthetic 3′-*o*-benzylated salacinol analogs.

inhibitors, which were synthesized by *S*-alkylation of thiosugars with epoxides. The salacinol-type natural compounds, originating from the genus *Salacia*, are known to inhibit α-glucosidase and lower blood glucose levels. In this work, the 3′-*o*-benzylated salacinol analogs (Fig. 2.29) were identified as potent inhibitors of α-glucosidase with ability to reduce blood glucose levels in

maltose-loaded mice similar to that of voglibose. Compounds **92**, **93**, **94**, and **95** showed human intestinal maltase inhibitory activities comparable to that of neosalacinol, salacinol, voglibose, acarbose, and miglitol. Compounds **93**, **94**, and **95** ($IC_{50} = 0.11-0.22\ \mu M$) showed 20–45-fold more activity than salacinol. All compounds competitively inhibited human intestinal maltase with a K_i range of 15–73 nM. Additionally, the compounds were also tested for antihyperglycemic effects *in vivo*. Oral administration of the compounds to maltose-loaded mice with high blood glucose levels resulted in a more effective reduction of blood glucose level than that of salacinol.

Although the inhibitory potency of compound **92** ($IC_{50} = 0.58\ \mu M$) was several fold less than that of other target compounds, it displayed comparable level of hypoglycemic activity to that of compounds **93**, **94**, and **95**. Furthermore, compound **95** at a dose of 0.1 mg/kg efficiently reduced blood glucose levels in maltose-loaded mice similar to that of voglibose. These findings imply that the net therapeutic effects of the target compounds is accomplished by inhibiting intestinal α-glucosidase *in vivo* aided by an underlying systemic mechanism through which they reduce blood glucose levels. The compounds show potential for antidiabetic drug development since they demonstrate promising *in vitro* and *in vivo* α-glucosidase and antihyperglycemic activities.

Eskandari et al. [70] modified the structure of ponkoranol (**90**) by replacing its sulfur moiety with a methyl ether and investigated its effects on the inhibition of the *N*-terminal catalytic domain of human maltase–glucoamylase (Fig. 2.30). Previous studies showed that de-*O*-sulfonated kotalanol (**86**) and its stereoisomers are more potent inhibitors of human maltase–glucoamylase than natural kotalanol and its sulfated stereoisomers [71,72].

The de-*O*-sulfonated ponkoranol (**96**) ($K_i = 0.043\ \mu M$) and its 5′-stereoisomer (**97**) ($K_i = 0.015\ \mu M$) were indeed more

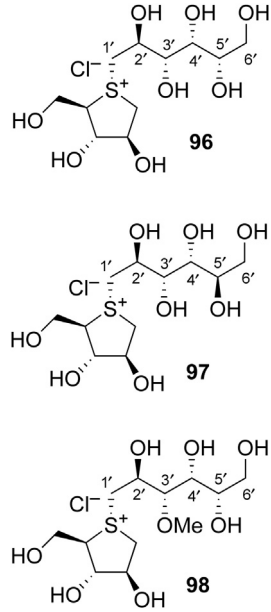

Figure 2.30 Synthetic de-*o*-sulfonated ponkoranol and its derivatives. *Reproduced from U. Ghani, Re-exploring promising α-glucosidase inhibitors for potential development into oral anti-diabetic drugs: finding needle in the haystack, Eur. J. Med. Chem. 103 (2015) 133–162. © 2015 French Société de Chimie Thérapeutique published by Elsevier Masson SAS. All rights reserved.*

promising than natural ponkoranol (**90**) ($K_i = 0.17\ \mu M$). Structural evidence for this comes from the crystal structures of human maltase–glucoamylase in complex with kotalanol and de-*O*-sulfonated kotalanol confirming that the proximity of the sulfate group to the bulky hydrophobic amino acids in the active site restricts its conformational freedom. Therefore, removal of the sulfate renders conformational freedom to the polyhydroxylated chain so that it can optimally interact with the enzyme active site. The activities of compound **96** ($K_i = 43\ nM$) and its 5′-stereoisomer (**97**) ($K_i = 15\ nM$) proved to be more promising than that of 3′-*O*-methyl ponkoranol (**98**; $K_i = 0.5\ \mu M$), asserting that incorporation

of a methyl ether instead of a sulfate is not favorable to the activity [70].

Continuing interest in exploring new derivatives of ponkoranol has led to identification of a number of 3′-benzylated analogs of 3′-*epi*-neoponkoranol bearing a variety of hydrophobic substituent groups at the 3′-position [73]. The purpose of designing the analogs was to determine whether these structural modifications contribute to improvement in their α-glucosidase inhibitory activities. The 3′-*epi*-neoponkoranol analogs, carrying a variety of hydrophobic substituents at the 3′-position, exhibited more potent α-glucosidase inhibitory activity than their natural counterparts mainly those with the *ortho*-substituted benzyl groups. The sulfonium salts of these thiosugars with *ortho*-substituted benzyl groups exhibited most potent enzyme inhibition (**99**—**109**) (Fig. 2.31). Compound **99** exhibited comparable rat antimaltase and antisucrase activities with that of its natural counterpart neoponkoranol. Replacement of the benzyl group with an ethyl (as in compound **100**) culminated in the reduction of its antimaltase activity. However, its antisucrase activity improved six-fold more than that of compound **99**.

The inhibitory activity of the compounds significantly depended on the type of substituents that are present on the phenyl ring of the benzyl group; sulfonium salts possessing *para*-substitutions exhibited less inhibitory potency especially

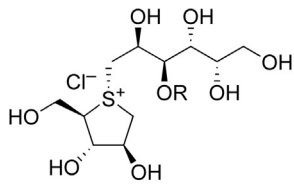

99. R = Bn
100. R = Et
101. R = *o*-Nitrobenzyl
102. R = *m*-Nitrobenzyl
103. R = *p*-Nitrobenzyl
104. R = *o*-Chlorobenzyl
105. R = *m*-Chlorobenzyl
106. R = *p*-Chlorobenzyl
107. R = *o*-(Trifluoromethyl)benzyl
108. R = *m*-(Trifluoromethyl)benzyl
109. R = *p*-(Trifluoromethyl)benzyl

Figure 2.31 The 3′-*epi*-neoponkoranol analogs.

against sucrase. Compound **107** with the *ortho*-substituted trifluoromethyl group on the phenyl ring exhibited more inhibitory potency than that of all natural compounds studied in the series. It is a competitive inhibitor of both maltase and sucrase exhibiting ten-fold more potency than that of acarbose.

Comparison of these compounds with previously studied 3′-alkylated analogs of neosalacinol containing the 3′*S*-*OR* stereochemistry indicated that majority of the *ortho*- and *meta*-substituted analogs showed comparable sucrase inhibitory activity but lower antimaltase activity. Therefore, the stereo inversion and changes in the specific hydrophobic substitutions of these compounds did not further optimize their α-glucosidase inhibitory activity.

2.5 Carbasugars

Pericosines A–E metabolites, produced by the *Periconia byssoides* fungus, are structurally similar to carbasugars. Pericosine E is a novel compound containing an *O*-linked carbasaccharide structure between the pericosine A-like and pericosine B-like moieties with opposite absolute configurations (Fig. 2.32). It is the only natural *O*-linked carbadisaccharide found in nature to date as an enantiomeric mixture. Synthesis of pericosine E is highly challenging due to its complicated stereochemistry. However, attempts have been made recently to synthesize the compound involving first total synthesis of (−)-pericosine E [74]. Usami et al. [75] recently reported the enantiospecific synthesis of both enantiomers and six diastereomers of pericosine E possessing α-glucosidase inhibitory activity. Although all pericosines exhibited some level of α-glucosidase inhibitory activity, (−)-pericosine E (**110**) and (+)-pericosine E (**111**) were distinct in terms of high potency of inhibition (IC_{50} = 12 and 31 μM, respectively).

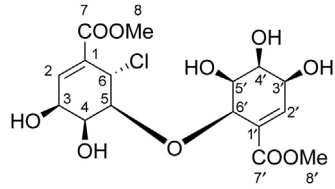

110

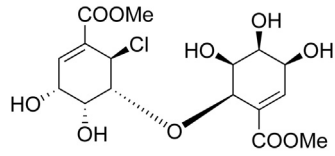

111

Figure 2.32 Pericosine E—an *o*-linked carbadisaccharide found in nature as enantiomeric mixture.

References

[1] N. Asano, R.J. Nash, R.J. Molyneux, G.W.J. Fleet, Sugar-mimic glycosidase inhibitors: natural occurrence, biological activity and prospects for therapeutic application, Tetrahedron: Asymmetry 11 (2000) 1645–1680. 2000.

[2] N. Asano, Glycosidase inhibitors: update and perspectives on practical use, Glycobiology 13 (2003) 93R–104R.

[3] T.D. Butters, R.A. Dwek, F.M. Platt, Iminosugar inhibitors for treating the lysosomal glycosphingolipidoses, Glycobiology 15 (2005) 43R–52R.

[4] N. Asano, Sugar-mimicking glycosidase inhibitors: bioactivity and application, Cell. Mol. Life Sci. 66 (2009) 1479–1492.

[5] B. Henrissat, A. Bairoch, New families in the classification of glycosyl hydrolases based on amino acid sequence similarities, Biochem. J. 293 (1993) 781–788.

[6] A. Trapero, A. Llebaria, A prospect for pyrrolidine iminosugars as antidiabetic α-glucosidase inhibitors, J. Med. Chem. 55 (2012) 10345–10346.

[7] K. Suzuki, T. Nakahara, O. Kanie, 3,4-Dihydroxypyrrolidine as glycosidase inhibitor, Cur. Top. Med. Chem. 9 (2009) 34–57.

[8] R.J. Nash, A. Kato, C.Y. Yu, G.W. Fleet, Iminosugars as therapeutic agents: recent advances and promising trends, Future Med. Chem. 3 (2011) 1513–1521.

[9] N.F. Brás, N.M. Cerqueira, M.J. Ramos, P.A. Fernandes, Glycosidase inhibitors: a patent review (2008–2013), Exp. Opin. Ther. Pat. 24 (2014) 857–874.

[10] Y. Kobayashi, Carbasugars: synthesis and functions. in: B. Fraser-Reid, K. Tatsuta, J. Thiem (Eds.), Glycoscience, Springer-Verlag Berlin Heidelberg, 2008, pp. 1914–1997.
[11] D.J. Wardrop, S.L. Waidyarachchi, Synthesis and biological activity of naturally occurring α-glucosidase inhibitors, Nat. Prod. Rep. 27 (2010) 1431–1468.
[12] N. Asano, et al., Polyhydroxylated pyrrolidine and piperidine alkaloids from *Adenophora triphylla var. japonica (Campanulaceae)*, Phytochemistry 53 (2000) 379–382.
[13] R.J. Nash, E.A. Bell, J.M. Williams, 2-Hydroxymethyl-3,4-dihydroxy-pyrrolidine in fruits of *Angylocalyx boutiqueanus*, Phytochemistry 24 (1985) 1620–1622.
[14] A. Welter, J. Jadot, G. Dardenne, M. Marlier, J. Casimir, 2,5-Dihydroxymethyl-3,4-dihydroxypyrrolidine dans les feuilles de Derris elliptica, Phytochemistry 15 (1976) 747–749.
[15] A.A. Watson, R.J. Nash, M.R. Wonnald, D.J. Harvey, S. Dealler, E. Lees, et al., Glycosidase-inhibiting pyrrolidine alkaloids from *Hyacinthoides non-scripta*, Phytochemistry 2 (1997) 255–259.
[16] A. Kato, N. Kato, S. Miyauchi, Y. Minoshima, I. Adachi, K. Ikeda, et al., Iminosugars from Baphia nitida Lodd, Phytochemistry 69 (2008) 1261–1265.
[17] S.F. Jenkinson, et al., *C*-Branched iminosugars: α-glucosidase inhibition by enantiomers of isoDMDP, isoDGDP, and isoDAB-*L*-isoDMDP compared to miglitol and miglustat, J. Org. Chem. 78 (2013) 7380–7397.
[18] A. Ghavami, B.D. Johnston, B.M. Pinto, A new class of glycosidase inhibitor: synthesis of salacinol and its stereoisomers, J. Org. Chem. 66 (2001) 2312–2317.
[19] E.J. Rossi, et al., Inhibition of recombinant human maltase glucoamylase by salacinol and derivatives, FEBS J. 273 (2006) 2673–2683.
[20] Y. Natori, et al., The synthesis and biological evaluation of 1-*C*-alkyl-*L*-arabinoiminofuranoses, a novel class of α-glucosidase inhibitors, Bioorg. Med. Chem. Lett. 21 (2011) 738–741.
[21] A. Kato, et al., α-1-*C*-Butyl-1,4-dideoxy-1,4-imino-*L*-arabinitol as a second-generation iminosugar-based oral α-glucosidase inhibitor for improving postprandial hyperglycemia, J. Med. Chem. 55 (2012) 10347–10362.
[22] Y. Natori, et al., Synthesis and biological evaluation of α-1-*C*-40-aryl-butyl-*L*-arabinoiminofuranoses, a new class of α-glucosidase inhibitors, Bioorg. Med. Chem. Lett. 24 (2014) 3298–3301.
[23] M. Shibano, D. Tsukamoto, A. Masuda, Y. Tanaka, G. Kusano, Two new pyrrolidine alkaloids, radicamines A and B, as inhibitors of α-glucosidase from *Lobelia chinensis Lour*, Chem. Pharm. Bull. 49 (2001) 1362–1365.

[24] Y. Li, et al., Fluorinated radicamine A and B: synthesis and glycosidase inhibition, Eur. J. Org. Chem. 7 (2016) 1429–1438.
[25] M. Shibano, S. Kitagawa, S. Nakamura, N. Akazawa, G. Kusano, Studies on the constituents of *Broussonetia* species. II. Six new pyrrolidine alkaloids, broussonetine A, B, E, F and broussonetinine A and B, as inhibitors of glycosidases from *Broussonetia kazinoki Sieb*, Chem. Pharm. Bull. (Tokyo) 45 (1997) 700–705.
[26] H. Zhao, A. Kato, K. Sato, Y. Jia, C. Yu, Total synthesis and glycosidase inhibition of broussonetine I and J_2, J. Org. Chem. 78 (2013) 7896–7902.
[27] Y. Song, et al., First total synthesis of (+)-broussonetine W: glycosidase inhibition of natural product and analogs, Org. Biomol. Chem. 14 (2016) 5157–5174.
[28] N.J. Pawar, et al., α-Geminal dihydroxymethyl piperidine and pyrrolidine iminosugars: synthesis, conformational analysis, glycosidase inhibitory activity, and molecular docking studies, J. Org. Chem. 77 (2012) 7873–7882.
[29] E. Tsou, et al., Synthesis and biological evaluation of a 2-aryl polyhydroxylated pyrrolidine alkaloid-based library, Bioorg. Med. Chem. 16 (2008) 10198–10204.
[30] W.C. Cheng, C.W. Guo, C.K. Lin, Y.R. Jiang, Cheng synthesis and inhibition study of bicyclic iminosugar-based alkaloids, scaffolds, and libraries towards glucosidase, Isr. J. Chem. 55 (2015) 403–411.
[31] T.H. Chan, Y.F. Chang, J.J. Hsu, W.C. Cheng, Straightforward synthesis of diverse 1-deoxyazapyranosides via stereocontrolled nucleophilic additions to six-membered cyclic nitrones, Eur. J. Org. Chem. (2010) 5555–5559.
[32] S.M.P. Morwenna, M.A. Monique, F. Valerie, L. Jacques, Recent advances in the total synthesis of piperidine azasugars, Eur. J. Org. Chem. (2005) 2159–2191.
[33] P. Compain, O.R. Martin (Eds.), Iminosugars: From Synthesis to Therapeutic Applications, John Wiley & Sons Ltd., Chichester, 2007.
[34] A. Kato, et al., Polyhydroxylated pyrrolidine and pyrrolizidine alkaloids from *Hyancinthoides* non-scripta and *Scilla campanulata*, Carbohydr. Res. 316 (1999) 95–103.
[35] T.D. Heightman, A.T. Vasella, Recent insights into inhibition, structure, and mechanism of configuration-retaining glycosidases, Angew. Chem. 111 (1999) 794–815.
[36] A.A. Watson, G.W.J. Fleet, N. Asano, R.J. Molyneux, R.J. Nash, Polyhydroxylated alkaloids—natural occurrence and therapeutic applications, Phytochemistry 56 (2001) 265–295.

[37] N. Asano, et al., New polyhydroxylated pyrrolizidine alkaloids from *Muscari armeniacum*: structural determination and biological activity, Tetrahedron: Asymmetry 11 (2000) 1–8.
[38] J. Calveras, J. Casas, T. Parella, J. Joglar, P. Clapes, Chemoenzymatic synthesis and inhibitory activities of hyacinthacines A_1 and A_2 stereoisomers, Adv. Synth. Catal. 349 (2007) 1661–1666.
[39] R.J. Nash, et al., Casuarine: a very highly oxygenated pyrrolizidine alkaloid, Tetrahedron Lett. 35 (1994) 7849–7852.
[40] A. Kato, et al., Australine and related alkaloids: easy structural confirmation by ^{13}C NMR spectral data and biological activities, Tetrahedron: Asymmetry 14 (2003) 325–331.
[41] S.E. Denmark, A.R. Hurd, Synthesis of (+)-casuarine, Org. Lett. 1 (1999) 1311–1314.
[42] F. Cardona, et al., Total syntheses of casuarine and its 6-*O*-α-glucoside: complementary inhibition towards glycoside hydrolases of the GH31 and GH37 families, Chem. Eur. J. 15 (2009) 1627–1636.
[43] T. Tite, F. Jacquelin, L. Bischoff, C. Fruit, F. Marsais, An efficient approach to new dihydroxyquinolizidines, Tetrahedron: Asymmetry 21 (2010) 2032–2036.
[44] N. Saha, S.K. Chattopadhyay, Enantioselective synthesis of polyhydroxyindolizidinone and quinolizidinone derivatives from a common precursor, Beilstein J. Org. Chem. 10 (2014) 3104–3110.
[45] A.V. Da Cruz, A. Kanazawa, J.F. Poisson, J.B. Behr, S. Py, Polyhydroxylated quinolizidine iminosugars as nanomolar selective inhibitors of α-glucosidases, J. Org. Chem. 82 (2017) 9866–9872.
[46] J. Boisson, A. Thomasset, E. Racine, P. Cividino, T. Banchelin Sainte-Luce, J.F. Poisson, et al., Hydroxymethyl-branched polyhydroxylated indolizidines: novel selective α-glucosidase inhibitors, Org. Lett. 17 (2015) 3662–3665.
[47] G.C. Kite, L.E. Fellows, G.W.J. Fleet, P.S. Liu, A.M. Scofield, N.G. Smith, α-Homonojirimycin [2,6-dideoxy-2,6-imino-*d*-glycero-l-gulo-heptitol] from *Omphalea diandra L.*: isolation and glucosidase inhibition, Tetrahedron Lett. 29 (1988) 6483–6485.
[48] N. Asano, M. Nishida, H. Kizu, K. Matsui, A.A. Watson, R.J. Nash, Homonojirimycin isomers and glycosides from *Aglaonema treubii*, J. Nat. Prod. 60 (1997) 98–101.
[49] N. Asano, et al., Homonojirimycin isomers and *N*-Alkylated homonojirimycins: structural and conformational basis of inhibition of glycosidases, J. Med. Chem. 41 (1998) 2565–2571.
[50] N. Asano, A. Kato, M. Miyauchi, H. Kizu, Y. Kameda, A.A. Watson, et al., Nitrogen-containing furanose and pyranose analogs from *Hyacinthus orientalis*, J. Nat. Prod. 61 (1998) 625–628.

[51] O.R. Martin, P. Compain, H. Kizu, N. Asano, Revised structure of a homonojirimycin isomer from *Aglaonema treubii*: first example of a naturally occurring alpha-homoallonojirimycin, Bioorg. Med. Chem. Lett. 9 (1999) 3171–3174.
[52] R.-Y. Yan, H.-Q. Wang, C. Liu, J. Kang, R.-Y. Chen, α-Glucosidase-inhibitory iminosugars from the leaves of *Suregada glomerulata*, Bioorg. Med. Chem. 21 (2013) 6796–6803.
[53] A.J. Rawlings, et al., Synthesis and biological characterisation of novel *N*-alkyl-deoxynojirimycin alpha-glucosidase inhibitors, ChemBioChem 10 (2009) 1101–1105.
[54] N. Ardes-Guisot, et al., Selection of the biological activity of DNJ neoglycoconjugates through click. Length variation of the side chain, Org. Biomol. Chem. 9 (2011) 5373–5388.
[55] A. Hatano, et al., Synthesis and characterization of novel, conjugated, fluorescent DNJ derivatives for α-glucosidase recognition, Bioorg. Med. Chem. 25 (2017) 773–778.
[56] M. Iwu, Handbook of African Medicinal Plants, CRC, Boca Raton, FL, 1993, p. 435.
[57] A. Mollataghi, E. Coudiere, A. Hamid, A. Hadi, M.R. Mukhtar, K. Awang, et al., Anti-acetylcholinesterase, anti-α-glucosidase, anti-leishmanial and anti-fungal activities of chemical constituents of *Beilschmiedia* species, Fitoterapia 83 (2012) 298–302.
[58] S. Mohan, L. Sim, D.R. Rose, B.M. Pinto, Synthesis of *S*-alkylated sulfonium-ions and their glucosidase inhibitory activities against recombinant human maltase glucoamylase, Carbohyd. Res. 342 (2007) 901–912.
[59] X. Bian, X. Fan, C. Ke, Y. Luan, G. Zhao, A. Zeng, Synthesis and α-glucosidase inhibitory activity evaluation of *N*-substituted amino-methyl-β-*D*-glucopyranosides, Bioorg. Med. Chem. 21 (2013) 5442–5450.
[60] M. Takeuchi, K. Kamata, M. Yoshida, Y. Kameda, K. Matsui, Inhibitory effect of pseudo-aminosugars on oligosaccharide glucosidases I and II and on lysosomal α-glucosidase from rat liver, J. Biochem. 108 (1990) 42–46.
[61] H. Shimoda, T. Fujimura, K. Makino, K. Yoshijima, K. Naitoh, H. Ihota, et al., Safety profile of extractive from trunk of *Salacia reticulata* (*Celastraceae*), J. Food Hyg. Soc. Jpn. 20 (1999) 198–205.
[62] R. Im, H. Mano, S. Nakatani, J. Shimizu, M. Wada, Aqueous extract of Kothala himbutu (*Salacia reticulata*) stems promotes oxygen consumption and suppresses body fat accumulation in mice, J. Health Sci. 54 (2008) 645–653.
[63] M.H.S. Jayawardena, N.M.W. de Alwis, V. Hettigoda, D.J.S. Fernando, Double blind randomised placebo controlled cross over study of a herbal

preparation containing *Salacia reticulata* in the treatment of type 2 diabetes, J. Ethnopharmacol. 97 (2005) 215–218.
[64] T. Morikawa, J. Akaki, K. Ninomiya, E. Kinouchi, G. Tanabe, Y. Pongpiriyadacha, et al., Salacinol and related analogs: new leads for type 2 diabetes therapeutic candidates from the Thai traditional natural medicine *Salacia chinensis*, Nutrients 7 (2015) 1480–1493.
[65] M. Yoshikawa, T. Murakami, K. Yashiro, H. Matsuda, Kotalanol, a potent alpha-glucosidase inhibitor with thiosugar sulfonium sulfate structure from antidiabetic ayurvedic medicine Salacia reticulata, Chem. Pharm. Bull. (Tokyo) 46 (1998) 1339–1340.
[66] M. Yoshikawa, T. Murakamia, H. Shimadaa, H. Matsudaa, Y. Yamaharab, G. Tanabe, et al., Salacinol, potent antidiabetic principle with unique thiosugar sulfonium sulfate structure from the Ayurvedic traditional medicine *Salacia reticulata* in Sri Lanka and India, Tetrahedron Lett. 38 (1997) 8367–8370.
[67] R. Nasi, B.O. Patrick, L. Sim, D.R. Rose, B.M. Pinto, Studies directed toward the stereochemical structure determination of the naturally occurring glucosidase inhibitor, kotalanol: synthesis and inhibitory activities against human maltase glucoamylase of seven-carbon, chain-extended homologues of salacinol, J. Org. Chem. 73 (2008) 6172–6181.
[68] L. Sim, K. Jayakanthan, S. Mohan, R. Nasi, B.D. Johnston, B.M. Pinto, et al., New glucosidase inhibitors from an Ayurvedic herbal treatment for type 2 diabetes: structures and inhibition of human intestinal maltase-glucoamylase with compounds from *Salacia reticulata*, Biochemistry 49 (2010) 443–451.
[69] F. Ishikawa, K. Jinno, E. Kinouchi, K. Ninomiya, S. Marumoto, W. Xie, et al., Diastereoselective synthesis of salacinol-type α-glucosidase inhibitors, J. Org. Chem. 83 (2018) 185–193.
[70] R. Eskandari, K. Jones, D.R. Rose, B.M. Pinto, Probing the active-site requirements of human intestinal *N*-terminal maltase glucoamylase: the effect of replacing the sulfate moiety by a methyl ether in ponkoranol, a naturally occurring α-glucosidase inhibitor, Bioorg. Med. Chem. Lett. 20 (2010) 5686–5689.
[71] K. Jayakanthan, S. Mohan, B.M. Pinto, Structure proof and synthesis of kotalanol and de-*O*-sulfonated kotalanol, glycosidase inhibitors isolated from an herbal remedy for the treatment of type-2 diabetes, J. Am. Chem. Soc. 131 (2009) 5621–5626.
[72] S. Mohan, K. Jayakanthan, R. Nasi, D.A. Kuntz, D.R. Rose, B.M. Pinto, Synthesis and biological evaluation of heteroanalogs of kotalanol and de-*O*-sulfonated kotalanol, Org. Lett. 12 (2010) 1088–1091.
[73] D. Liu, et al., Design, synthesis and biological evaluation of 3′-benzylated analogs of 3′-*epi*-neoponkoranol as potent α-glucosidase inhibitors, Eur. J. Med. Chem. 110 (2016) 224–236.

[74] Y. Usami, M. Ohsugi, K. Mizuki, H. Ichikawa, M. Arimoto, Facile and efficient synthesis of naturally occurring carbasugars (+)-pericosines A and C, Org. Lett. 11 (2009) 2699–2701.
[75] Y. Usami, K. Mizuki, R. Kawahata, M. Shibano, A. Sekine, H. Yoneyama, et al., Synthesis of natural *O*-linked carba-disaccharides, (+)- and (−)-pericosine E, and their analogs as α-glucosidase inhibitors, Mar. Drugs 15 (2017) 22.

CHAPTER THREE

Polyphenols

Contents

Polyphenols are secondary metabolites abundant in the plant kingdom with a broad range of biological activities. Due to their diverse therapeutic effects, they are a focus of interest in traditional medicine and drug development. Polyphenols possess a broad spectrum of biological activities such as antioxidant, antihypertensive, and α-glucosidase inhibitory activities. As their name suggests, polyphenols are aromatic compounds that bear one or more hydroxyl groups, which are divided into phenolic acids and flavonoids. Phenolic acids are further classified as hydroxybenzoic acids (e.g., gallic acid and related derivatives) and hydroxycinnamic acids (e.g., caffeic acid and related derivatives). The subtypes of flavonoids include flavonols, flavones, isoflavones, flavans, catechins (flavan-3-ols), anthocyanins, and chalcones. This chapter focuses on polyphenol α-glucosidase inhibitors that are divided into chalcones, xanthones, flavonoids, and others for clarity and organizational purposes [1,2].

3.1 Chalcones

Chalcones are widely distributed in the plant kingdom and have been reported as precursors of flavonoids and

Alpha-glucosidase Inhibitors.
DOI: https://doi.org/10.1016/B978-0-08-102779-0.00003-4

isoflavonoids. They possess a wide range of medicinal properties that include antidiabetic [3], antiinflammatory [4], anticancer [5], and immunomodulatory activities [6]. The chalcone skeleton (1,3-diphenyl-2E-propene-1-one) comprises a benzylideneacetophenone scaffold in which a three-carbon α-,β-unsaturated carbonyl bridge joins the two aromatic structures [7]. In nature, chalcones exist in a number of forms conjugated with other moieties. It is an intermediate featuring an open-chain structure in aurones synthesis of flavones [8,9]. Interest in chalcones as antidiabetic agents has identified various promising α-glucosidase inhibitors. New galloyl, caffeoyl, and hexahydroxydiphenyl esters of dihydrochalcone glucosides identified from the aerial tissues of *Balanophora tobiracola* plant exhibited yeast α-glucosidase inhibition (Fig. 3.1). Compounds **1**, **2**, **3**, **4**, and **5** inhibited the enzyme with IC_{50} values of 0.4, 0.8, 1.1, 1.8, and 1.6 μM, respectively. Compounds containing the 3-*O*-galloyl-4,6-*O*-HHDP-glucose moiety (**1** and **2**) were most potent inhibitors in the series [10].

Ryu et al. [11] isolated and identified various chalcone α-glucosidase inhibitors from *Broussonetia papyrifera* plant (Fig. 3.2). These include broussochalcone B (**6**), 3,4-dihydroxyisolonchocarpin (**7**), 4-hydroxyisolonchocarpin (**8**), kazinol A (**9**), and B (**10**) ($IC_{50} = 11.1-19.1$ μM). All compounds inhibited the enzyme noncompetitively except kazinol A and B which were mixed-type inhibitors ($K_i = 9.7-16.2$ μM). In the target compounds, a free resorcinol motif in the A ring (as in compound **2**) was more selective to enzyme inhibition than the corresponding products of oxidative cyclization of the alcohol group onto the pendant allyl group (as in compounds **3** and **4**).

Seo et al. [12] synthesized a new series of chalcones that includes amino and nonaminochalcones. Aminochalcones specifically the sulfonamide chalcones are reported to be noncompetitive inhibitors of yeast α-glucosidase (**11**, $IC_{50} = 12.4$ μM; **12**, $IC_{50} = 15.6$ μM; **13**, $IC_{50} = 0.98$ μM; and **14**, $IC_{50} = 0.4$ μM;

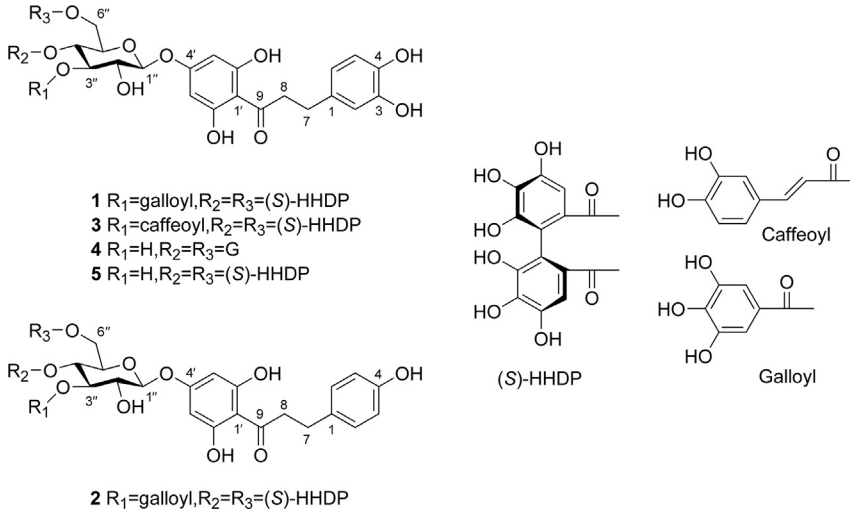

Figure 3.1 The dihydrochalcone glucoside derivatives exhibit promising inhibition of α-glucosidase mainly due to the 3-*o*-galloyl-4,6-*o*-HHDP-glucose moiety. *Reproduced from U. Ghani, Re-exploring promising α-glucosidase inhibitors for potential development into oral anti-diabetic drugs: finding needle in the haystack, Eur. J. Med. Chem. 103 (2015) 133–162. © 2015 French Société de Chimie Thérapeutique published by Elsevier Masson SAS. All rights reserved.*

Fig. 3.3). Sulfonamide chalcones are a new promising class of nonsugar α-glucosidase inhibitors with potential for treatment of type 2 diabetes mellitus.

Wang et al. [13] extended the work on sulfonamide chalcones by incorporating the phenylsulfonamide chalcone substructure into the benzopyran backbone forming the 3-[4-(phenylsulfonamido)benzoyl]-2*H*-1-benzopyran-2-one derivatives (Fig. 3.4). The synthetic approach yielded more potent yeast α-glucosidase inhibitors than the simple sulfonamide chalcones.

In the $R^4 = H$ series, addition of a halogen (F) at C_6 position of compound **15** ($IC_{50} = 7.18\ \mu M$) weakened the inhibitory activity relative to compound **16** ($IC_{50} = 3.28\ \mu M$). The effects of chlorine and bromine halogens was detrimental to the activity of the compounds. Compound **16** was more

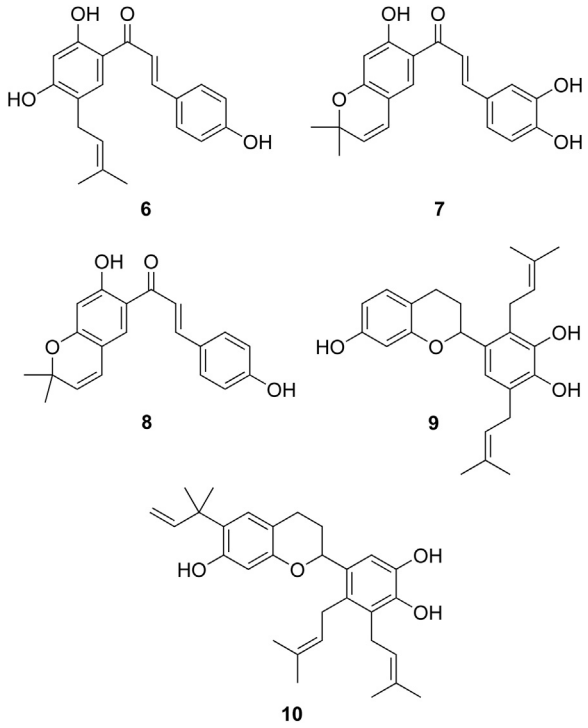

Figure 3.2 Broussochalcone B and other α-glucosidase inhibitors isolated from *Broussonetia papyrifera* plant.

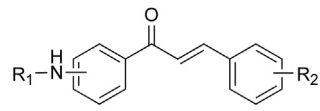

11 R_1=3-*p*-tosyl, R_2=4-hydroxy
12 R_1=3-*p*-tosyl, R_2=3,4-dihydroxy
13 R_1=4-*p*-tosyl, R_2=4-hydroxy
14 R_1=4-*p*-tosyl, R_2=3,4-dihydroxy

Figure 3.3 Sulfonamide chalcones are a promising new class of non-sugar α-glucosidase inhibitors with potential for treatment of type 2 diabetes mellitus. *Reproduced from U. Ghani, Re-exploring promising α-glucosidase inhibitors for potential development into oral anti-diabetic drugs: finding needle in the haystack, Eur. J. Med. Chem. 103 (2015) 133–162.*

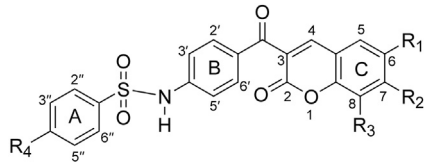

15 R_1=F, R_2=H, R_3=H, R_4=H
16 R_1=H, R_2=H, R_3=H, R_4=H
17 R_1=$C(CH_3)_3$, R_2=H, R_3=$C(CH_3)_3$, R_4=H
18 R_1=H, R_2=OH, R_3=H, R_4=H
19 R_1=OCH_3, R_2=OH, R_3=H, R_4=H
20 R_1=H, R_2=OH, R_3=H, R_4=CH_3
21 R_1=H, R_2=$N(C_2H_5)_2$, R_3=H, R_4=CH_3
22 R_1=OCH_3, R_2=OH, R_3=H, R_4=CH_3

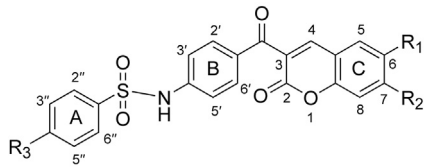

23 R_1=OCH_3, R_2=OH, R_3=F
24 R_1=OCH_3, R_2=OH, R_3=Cl
25 R_1=H, R_2=H, R_3=Br
26 R_1=OCH_3, R_2=OH, R_3=Br
27 R_1=H, R_2=H, R_3=OCH_3
28 R_1=H, R_2=OH, R_3=OCH_3

Figure 3.4 The phenylsulfonamide chalcone substructure with the benzopyran backbone. *Reproduced from U. Ghani, Re-exploring promising α-glucosidase inhibitors for potential development into oral anti-diabetic drugs: finding needle in the haystack, Eur. J. Med. Chem. 103 (2015) 133–162.*

potent than **17** ($IC_{50} = 7.13\ \mu M$) containing the bulky *tert*-butyl groups at C_6 and C_8 positions that are apparently unfavorable for enzyme binding. Interestingly, the activity significantly reduced when the C_7 was substituted with a methoxy group. However, the effect of a hydroxyl substitution at the same position was not much influential on the potency (as in **18**, $IC_{50} = 5.76\ \mu M$). Contrary to the above, the diethylamino substitution at C_7 position appears to be favorable to inhibitory activity (as in **19**, $IC_{50} = 0.19\ \mu M$).

Similar pattern of activity was observed in the $R^4 = CH_3$ series which possessed same substitutions as above. In this series, the promising activities of compounds **20** (IC_{50} = 1.12 μM), **21** (IC_{50} = 0.34 μM), and **22** (IC_{50} = 0.0645 μM) appear to be due to the hydroxy or diethylamino substitutions at C_7 position. Moreover, methylation of the hydroxyl group at the same carbon atom was not favorable to the activity. In contrast, the methoxy group at C_6 position greatly enhanced the activity as shown in compound **22**, which was most potent in both series of inhibitors.

Investigators from the same laboratory synthesized a new series of substituted 3-[4-(phenylsulfonamido)benzoyl]-2*H*-1-benzopyran-2-one derivatives containing methoxy or *tert*-butyl groups and halogen atoms at the *para* position of the A ring (Fig. 3.4). Most of the compounds with or without halogen-substitutions displayed more promising yeast α-glucosidase inhibitory activity than previously studied inhibitor **16**, suggesting an essential role of the *para* position of the A ring in enzyme inhibition. Examples include compounds **23**, **24**, **25**, and **26** (IC_{50} = 0.075, 0.025, 0.014, and 0.036 μM, respectively). Similarly, comparison of **27** (IC_{50} = 0.073 μM) and **28** (IC_{50} = 0.018 μM) in the methoxy series ($R^3 = OCH_3$) with **16** (IC_{50} = 3.28 μM) again confirmed that the methoxy substitution at the same position yields more potent inhibitors than previously studied C-ring-substituted compounds. In contrast, the bulky *tert*-butyl substitution at the *para* position of the A ring was not favorable to the activity, which is in agreement with the C-ring-substituted compounds as well [14].

Ansari et al. [15] synthesized a series of 2,4-diaryl-2,3-dihydro- and tetrahydro-1,5-benzothiazepines from chalcones and evaluated both classes of the compounds for α-glucosidase activity (Fig. 3.5). One chalcone (**29**) and some derivatives of 1,5-benzothiazepines (**30**, **31**, **32**, and **33**) have been found to

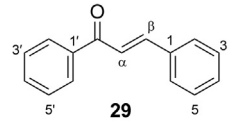

29

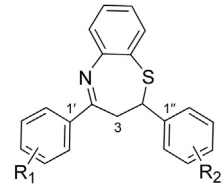

30 R_1=2-OH, R_2=H
31 R_1=2-OH, R_2=4-F
32 R_1=2-OH, R_2=4-MeO
33 R_1=2-OH, R_2=4-Me

Figure 3.5 Chalcone and benzothiazepine derivatives. *Reproduced from U. Ghani, Re-exploring promising α-glucosidase inhibitors for potential development into oral anti-diabetic drugs: finding needle in the haystack, Eur. J. Med. Chem. 103 (2015) 133–162. © 2015 French Société de Chimie Thérapeutique published by Elsevier Masson SAS. All rights reserved.*

inhibit yeast α-glucosidase with IC_{50} values of 15, 12.8, 12, 12, and 12 μM, respectively.

Recently enzymological and computational studies on a series of synthetic furanochalcone derivatives revealed interesting clues to rat intestinal maltase inhibition and interactions with its active site. In these compounds, the number and position of the hydroxyl groups in the B ring of chalcones influenced the level of inhibition (Fig. 3.6). Compound **34** (IC_{50} = 15.2 μM) carrying hydroxyl groups at positions 3 and 4 exhibited more promising activity than others. The activity did not alter much despite a change in the conformation of the furan ring from angular to linear form as long as the hydroxyl groups at positions 3 and 4 remain there (**35**, IC_{50} = 18.9 μM). Removal of the hydroxyl group at position 3 of the angular furanochalcones yielded better inhibitors (**36**, IC_{50} = 10.9 μM). However, removal of the same from the linear furanochalcones weakened their inhibitory activity

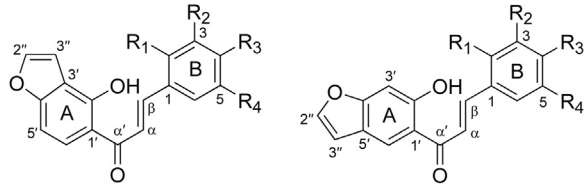

Figure 3.6 The number and position of the hydroxyl groups in the B ring of chalcones determines the potency of α-glucosidase inhibition by these furanochalcone derivatives. *Reproduced from U. Ghani, Re-exploring promising α-glucosidase inhibitors for potential development into oral anti-diabetic drugs: finding needle in the haystack, Eur. J. Med. Chem. 103 (2015) 133–162. © 2015 French Société de Chimie Thérapeutique published by Elsevier Masson SAS. All rights reserved.*

(**37**, $IC_{50} = 14.5\ \mu M$). The results were in agreement with molecular docking studies conducted on the compounds [16].

Chalcones are an interesting class of compounds with potential for antidiabetic drug development since they are known to exert significant antihyperglycemic effects *in vivo* and inhibit α-glucosidase [12–16]. They target pancreatic β-cells where they act as insulin secretagogues to maintain glucose homeostasis upon hyperglycemia. *In vivo* studies on the naphthylchalcones (**38–46**) (Fig. 3.7) demonstrated that they significantly exert rapid and long-term antihyperglycemic effects in glucose-loaded rats.

Furthermore, the effect is accompanied by improvement in the insulin management upon hyperglycemia possibly suggesting that chalcones reduce blood glucose levels through apparent stimulation of insulin from the β-cells. The results also showed that the presence of the nitro group and its position in the phenyl rings are primarily responsible for the antihyperglycemic effects. Example includes compound **39**, which improved glucose tolerance *in vivo* augmented by stimulation of insulin secretion [17].

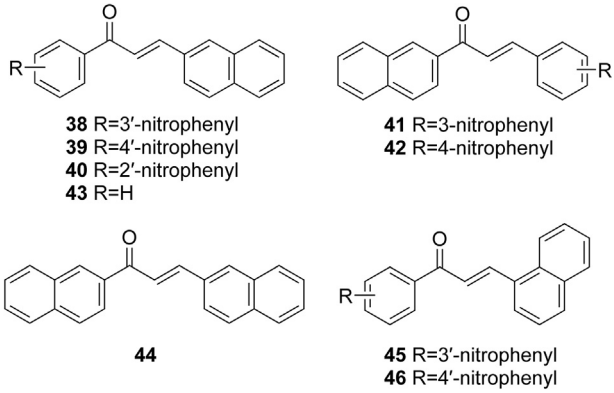

Figure 3.7 The naphthylchalcones reduce blood glucose levels by stimulating insulin and inhibiting α-glucosidase. *Reproduced from U. Ghani, Re-exploring promising α-glucosidase inhibitors for potential development into oral anti-diabetic drugs: finding needle in the haystack, Eur. J. Med. Chem. 103 (2015) 133–162. © 2015 French Société de Chimie Thérapeutique published by Elsevier Masson SAS. All rights reserved.*

3.2 Xanthones

Xanthones (9*H*-xanthen-9-ones) are secondary metabolites found in some bacteria, fungi, and lichens, and in higher plant families including but not limited to Moraceae, Guttiferae, and Polygalaceae. The xanthone skeleton carries a variety of substituents that include hydroxyl, methoxyl, glycosyl, and prenyl groups. Moreover, it also exists as dimer, polycyclic, and xanthonolignoid chemical entities. Xanthones exhibit antiinflammatory, antidiabetic, anticancer, and antioxidant activities including a number of natural and synthetic derivatives that have been identified as α-glucosidase inhibitors [18–21].

Seo et al. [22] reported natural xanthone-derived α-glucosidase inhibitors isolated from *Cudrania tricuspidata*. Although the plant has been previously reported to contain compounds exhibiting antioxidant, antiatherosclerotic, and

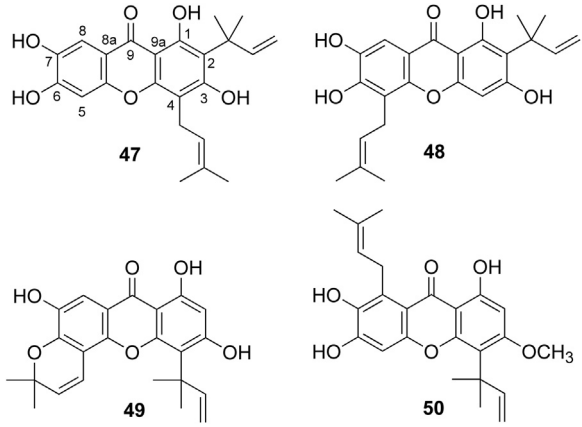

Figure 3.8 Natural derivatives of xanthones isolated from *Cudrania tricuspidata* plant. *Reproduced from U. Ghani, Re-exploring promising α-glucosidase inhibitors for potential development into oral anti-diabetic drugs: finding needle in the haystack, Eur. J. Med. Chem. 103 (2015) 133–162. © 2015 French Société de Chimie Thérapeutique published by Elsevier Masson SAS. All rights reserved.*

antiinflammatory activities [23,24], it is the first report on yeast α-glucosidase inhibition by natural xanthones from the plant. Noteworthy inhibitors include macluraxanthone B (**47**, $K_i = 8.9$ μM), cudraxanthone L (**48**, $K_i = 7.4$ μM), 1,3,7-trihydroxy-4-(1,1-dimethyl-2-propenyl)-5,6-(2-2-dimethylchromeno)xanthone (**49**, $K_i = 5.8$ μM), and cudratricusxanthone F (**50**, $K_i = 7.0$ μM) (Fig. 3.8). Some of the compounds exhibit mixed-type inhibition of the enzyme. Importantly, the activity of cudratricusxanthone F (**50**) significantly reduced due to demethylation leading to a loss of polarity or hydrogen bonding needed to interact with the enzyme residues. Additionally, the alkyl substitution at the position 4 of these compounds was not supportive to potency despite contribution to inhibition by the groups at other positions.

Garcinia mangostana is a tree of Southeast Asian origin commonly known as mangosteen. Its seedcases have been reported to contain a range of oxygenated and prenylated xanthones [25].

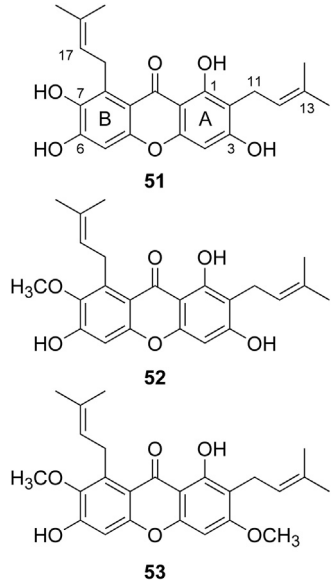

Figure 3.9 Mangostin xanthones: presence of free hydroxyl groups and the type of alkyl substitution are important for α-glucosidase inhibition. *Reproduced from U. Ghani, Re-exploring promising α-glucosidase inhibitors for potential development into oral anti-diabetic drugs: finding needle in the haystack, Eur. J. Med. Chem. 103 (2015) 133–162.*

Ryu et al. [26] reported xanthone inhibitors of yeast α-glucosidase namely mangostins from the plant demonstrating comparable activity to that of deoxynojirimycin (Fig. 3.9). Kinetic studies revealed that the compounds exhibited mixed-type inhibition of the enzyme. The activity of these compounds was exclusively due to dependence on free hydroxyl groups and alkyl substitution. The number of free hydroxyl groups in the A and B rings of mangostin greatly augmented the inhibitory activity as shown in compounds **51**, **52**, and **53** ($IC_{50} = 1.5$, 5.0, and 14.4 μM, respectively). Similarly, compounds yielded much less potency when the C_3 hydroxyl group was masked with a hemiterpene moiety in the A ring.

Additionally, the alkyl substitution is also significant for α-glucosidase inhibition implying that the geranylated xanthones are more active than their prenylated counterparts. Prenylation yielded better inhibitors than the ones with prenyl hydrate substitution.

Swertia mussotii has been used to treat liver diseases in South Asian folklore medicine [27]. Although there are no reports of the plant on treatment of diabetes mellitus, the other species of the same genus have been reported to possess antidiabetic effects [28]. Zheng et al. [29] first reported isolation of 14 xanthones exhibiting yeast α-glucosidase inhibition notably **54**, **55**, and **56** ($IC_{50} = 7.3$, 5.2, and 13.3 μM, respectively; Fig. 3.10). Comparison of the inhibitory activities showed that the nonglycosylated xanthones were more promising than their glycosylated analogs.

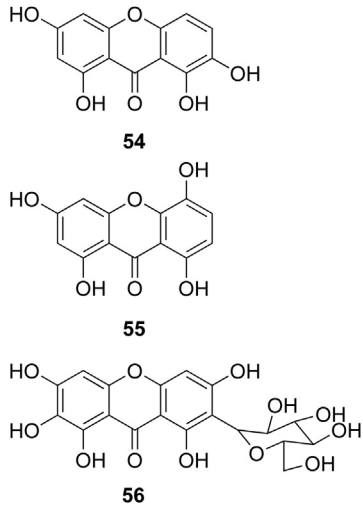

Figure 3.10 Glycosylated and nonglycosylated xanthones. The latter are promising α-glucosidase inhibitors. *Reproduced from U. Ghani, Re-exploring promising α-glucosidase inhibitors for potential development into oral anti-diabetic drugs: finding needle in the haystack, Eur. J. Med. Chem. 103 (2015) 133–162. © 2015 French Société de Chimie Thérapeutique published by Elsevier Masson SAS. All rights reserved.*

Liu et al. [30] synthesized a series of hydroxyxanthones and their acetoxy and alkoxy derivatives, all of which inhibited yeast α-glucosidase with the exception of the parent xanthone. In these polyhydroxyxanthone derivatives, the number and position of the hydroxyl groups dictate their inhibitory activity. Compounds with three hydroxyl groups exhibit more potency than those with a single hydroxyl group. The activity of the hydroxyxanthones was directly proportional to the number of hydroxyl groups. Moreover, incorporation of the acetoxy and alkoxy groups did not exert significant effects on the activity. Liu et al. [31] also synthesized novel xanthone derivatives by inserting one aromatic ring to extend the π-conjugated systems, which resulted in an amplification of α-glucosidase inhibitory activity by several-fold. Although the role of the π-conjugated systems has been tested in other biological activities [32–35], it is the first report that targeted yeast α-glucosidase inhibition. Benzoxanthones, carrying four fused aromatic rings, as shown in Fig. 3.11, possessed more inhibitory

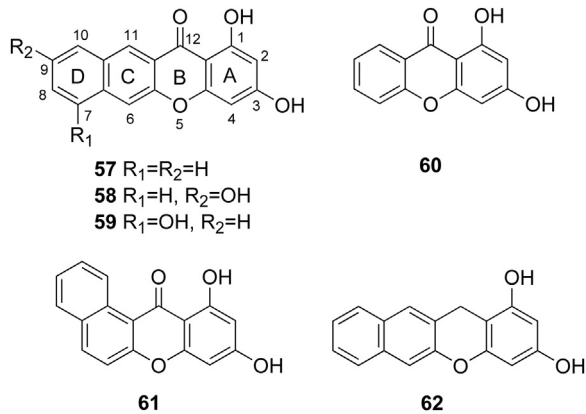

Figure 3.11 Novel xanthone inhibitors of α-glucosidase featuring extended π-conjugated systems. *Reproduced from U. Ghani, Re-exploring promising α-glucosidase inhibitors for potential development into oral anti-diabetic drugs: finding needle in the haystack, Eur. J. Med. Chem. 103 (2015) 133–162. © 2015 French Société de Chimie Thérapeutique published by Elsevier Masson SAS. All rights reserved.*

activity (**57**, **58**, **59**, $IC_{50} = 9.3$, 5.8, 8.0 μM, respectively) than the ones with three rings (**60**, $IC_{50} = 160.8$ μM). Apparently, the enzyme prefers binding to compounds carrying linearly fused aromatic rings than those with angularly fused rings. Interestingly, partially destroying the π-conjugated system in compounds **57** ($IC_{50} = 9.3$ μM) and **61** ($IC_{50} = 39.9$ μM) drastically compromised their inhibitory activities as seen in **62** ($IC_{50} = 27.8$ μM), further confirming the important role of π-stacking in α-glucosidase inhibition.

Investigators from the same laboratory also reported a series of noncoplanar and flexible xanthone derivatives that noncompetitively inhibited yeast α-glucosidase. Similar to their previous work, α-glucosidase inhibition is greatly influenced by both the coplanar and noncoplanar fused π-systems in addition to hydrophobicity and structural flexibility [36].

3.3 Flavonoids and other polyphenols

The branches, leaves, and roots of *Broussonetia papyrifera* have been used as diuretic, tonic, and edema suppressant in Chinese folk medicine. The plant is mainly rich in polyphenols including chalcones, flavans, and flavanols. In addition to the chalcones discussed earlier in the chapter, Ryu et al. [11] also identified 12 polyphenols with yeast α-glucosidase inhibitory activity including two new compounds with a rare 5,11-dioxabenzo-[β]-fluoren-10-one skeleton. All compounds were active notably broussochalcone A (**63**), dimethylally-tetrahydroxyflavonol derivative (**64**), and papyriflavonol A (**65**) (Fig. 3.12). Broussochalcone A (**63**), a prenylated chalcone containing the catechol and resorcinol moieties, noncompetitively inhibited yeast α-glucosidase ($K_i = 5.3$ μM). Its resorcinol moiety is selective to activity over

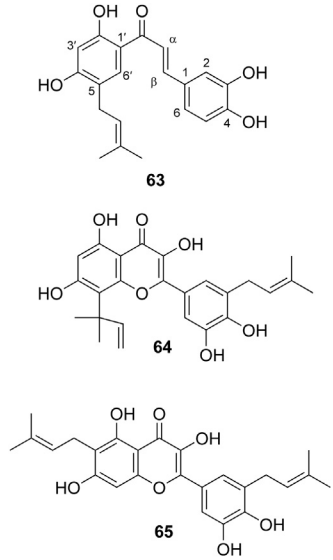

Figure 3.12 Increasing number of prenylation is crucial for the inhibitory activity of these natural polyphenols. *Reproduced from U. Ghani, Re-exploring promising α-glucosidase inhibitors for potential development into oral anti-diabetic drugs: finding needle in the haystack, Eur. J. Med. Chem. 103 (2015) 133–162.*

corresponding moieties present in other compounds. Compounds with one prenyl group on the C ring displayed lowest activity. Compounds **64** ($K_i = 4.2$ μM) and **65** ($K_i = 2.3$ μM) also showed comparable results whose inhibitory activities and the levels of prenylation are similar. The inhibitory activity of these polyphenols depends on increasing number of the prenyl groups.

Plant species in the genus *Dorstenia* are rich in coumarins and flavonoids especially prenylated and geranylated flavonoids. The plants are used for antivenom, antiseptic, and antirheumatic therapy in Africa, Central, and South America. Six new C_4'-triprenylated flavonols called dorsilurins have been isolated from the roots of the Cameroonian plant *Dorstenia psilurus* with yeast

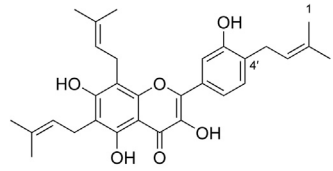

66

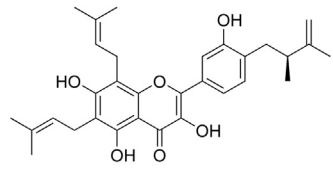

67

Figure 3.13 Dorsilurin F and G flavonols isolated from the roots of the Cameroonian plant *Dorstenia psilurus*. *Reproduced from U. Ghani, Re-exploring promising α-glucosidase inhibitors for potential development into oral anti-diabetic drugs: finding needle in the haystack, Eur. J. Med. Chem. 103 (2015) 133–162. © 2015 French Société de Chimie Thérapeutique published by Elsevier Masson SAS. All rights reserved.*

α-glucosidase inhibitory activity. Dorsilurin F (**66**, $IC_{50} = 4.13$ μM) and dorsilurin G (**67**, $IC_{50} = 7.51$ μM) possessed highest affinities to the enzyme in the series (Fig. 3.13). The former with three native prenyl groups exhibited highest activity compared to those carrying a single native prenyl group. A correlation of the inhibitory activity with the number of native prenylated groups is clearly observed in these compounds as well [37].

Myrcia multiflora is a tree common in Brazil, Peru, Paraguay, and Guianas where its leaves and bark are widely used for treating diabetes thus commonly known as "plant insulin." Studies on the extracts and pure compounds from its leaves showed significant reduction in blood glucose levels in rats including inhibition of intestinal α-glucosidases. Two new flavanone glucosides called myrciacitrins I (**68**) and II (**69**), and two new acetophenone glucosides called myrciaphenones A (**70**) and B (**71**) have been identified (Fig. 3.14). The importance of the medicinal use of the plant for treatment of

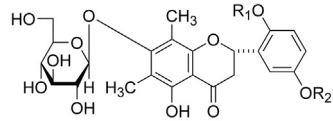

68 $R_1=R_2=H$
69 $R_1=H$, $R_2=CH_3$

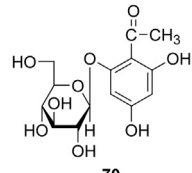

70

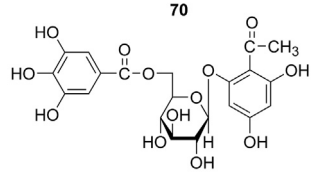

71

Figure 3.14 Flavanone glucosides myrciacitrins I (**68**) and II (**69**), and acetophenone glucosides myrciaphenones A (**70**) and B (**71**) are part of the constituents of *Myrcia multiflora* tree that is widely used for treating diabetes mellitus often called "plant insulin." *Reproduced from U. Ghani, Re-exploring promising α-glucosidase inhibitors for potential development into oral anti-diabetic drugs: finding needle in the haystack, Eur. J. Med. Chem. 103 (2015) 133–162. © 2015 French Société de Chimie Thérapeutique published by Elsevier Masson SAS. All rights reserved.*

diabetes cannot be underestimated despite the weak *in vitro* intestinal maltase and sucrase inhibitory activities of its constituents ($IC_{50} = 100–700\ \mu M$) [38]. This warrants further exploration of the plant for *in vivo* antihyperglycemic activity.

A number of flavonol rhamnoside α-glucosidase inhibitors from the leaf extract of *Machilus philippinensis* have been reported. The acylated rhamnosides (**72**) and (**73**) exhibited potent inhibition of bacterial α-glucosidase from *Bacillus stearothermophilus* ($IC_{50} = 6.1$ and $1.0\ \mu M$, respectively; Fig. 3.15). However, nonacylated rhamnosides such as quercetin-3-*O*-rhamnopyranoside

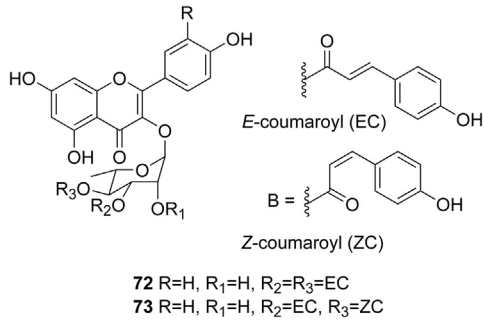

Figure 3.15 The acylated flavonol rhamnosides are more potent inhibitors of α-glucosidase than their nonacylated counterparts. *Reproduced from U. Ghani, Re-exploring promising α-glucosidase inhibitors for potential development into oral anti-diabetic drugs: finding needle in the haystack, Eur. J. Med. Chem. 103 (2015) 133–162.*

and kaempferol-3-*O*-rhamnopyranoside were weak inhibitors of the enzyme ($IC_{50} = 33.05$ and 228.11 μM, respectively). Coumaroylated flavanol mono-rhamnosides inhibited the enzyme more efficiently than those possessing the individual moieties [39]. Acylation has a significant contribution to enzyme inhibition, which is in agreement with previous studies conducted on the α-glucosidase inhibitory activity of acylated anthocyanins and caffeoylquinic acids [40,41].

Studies on the phytochemistry of soybean by Tadera et al. [42] identified a wide variety of flavonoids as α-glucosidase inhibitors. These include genistein (**74**) and dadzein isoflavones (**75**) that potently inhibited yeast α-glucosidase ($IC_{50} = 7$ and 14 μM, respectively) as shown in Fig. 3.16. Methylation and methoxylation have been found to compromise the inhibitory activity of the former [43]. Similar studies on formononetin and afromosin isolated from the leaves of soybean plant have also confirmed that methoxylation at the C_6 position of formononetin significantly reduced its yeast α-glucosidase inhibitory activity [44].

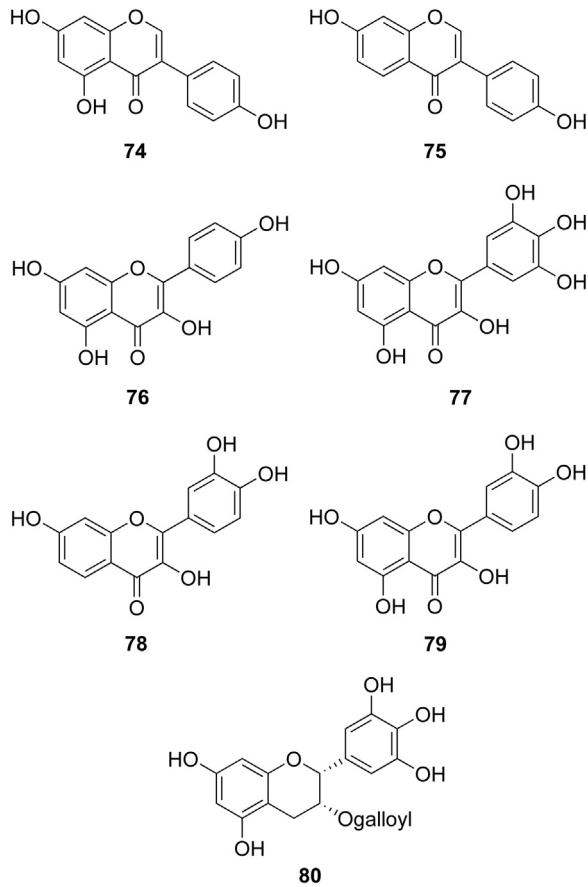

Figure 3.16 The denistein, dadzein, kaempferol, myricetin, fisetin, and quercetin isoflavones.

Furthermore, other phytochemical studies have also identified flavonols such as kaempferol (**76**), myricetin (**77**), fisetin (**78**), and quercetin (**79**) with α-glucosidase inhibitory activities ($IC_{50} = 5-13\ \mu M$). Flavan and flavan-3-ols are abundant in plants including tea and cacao. Their structure contains the 2-phenyl-3,4-dihydro-2*H*-chromen and 3-ol backbones, respectively. Flavan-3-ols bear two chiral carbon atoms at 2 and 3 positions, examples of which include catechin, epicatechin, epicatechin gallate, and theaflavin. Tadera and coworkers

[42] also identified a number of flavan and flavan-3-ols as α-glucosidase inhibitors such as catechin, epigallocatechin, and epigallocatechin gallate (**80**). In these compounds, presence of the galloyl group at 3-position of the flavan moiety augments inhibition of the enzyme as exhibited by epigallocatechin gallate ($IC_{50} = 2\ \mu M$). It is also interesting to mention that the synthetic planar catechin analogs bearing variable alkyl side chain lengths tend to be potent inhibitors of yeast and *B. stearothermophilus* α-glucosidase than the catechin itself.

Recently, Nur-e-Alam et al. [45] isolated and characterized three new derivatives of prenylated flavones namely retamasin C−E, four new derivatives of prenylated isoflavones namely retamasin F−I, and two other new isoflavones isolated from *Retama raetam*. The plant is a bush that belongs to the Fabaceae family, which grows in North Africa, Eastern Mediterranean, and Middle East regions including Saudi Arabia where it is used for treating diabetes mellitus and hypertension in traditional medicine. Studies on the plant extracts have previously confirmed that they lower plasma glucose and lipid levels in normal and diabetic rats [46]. The antidiabetic effects of the plant are correlated to its ability to enhance stimulation of insulin and limit intestinal absorption of glucose [47]. The therapeutic effects of the plant have been further confirmed by the identification of five of the retamasin flavones and isoflavones that enhance glucose-induced insulin secretion by pancreatic islets of mice in addition to α-glucosidase inhibition [45].

Ghani et al. [48] further extended work on the retamasin flavonoids by studying their α-glucosidase inhibition kinetics and docking simulations. Retamasin C, F, and H (compounds **81**, **82**, and **83**, respectively) are especially highlighted since they exhibited higher potency of inhibition than other compounds ($K_i = 19.93$, 14.45, and 12.06 μM, respectively; Fig. 3.17). All three compounds competitively inhibited the

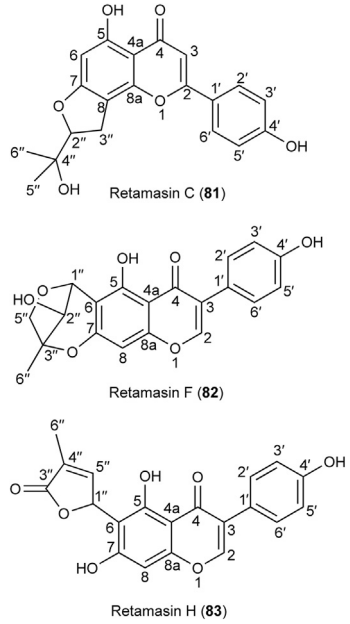

Figure 3.17 The retamasin isoflavones and flavones exert antidiabetic effects by using two different mechanisms of action: α-glucosidase inhibition and enhancement of glucose-induced insulin secretion by pancreatic islets.

enzyme with the exception of retamasin H which showed noncompetitive inhibition. All seven isoflavones and flavones contained various C_6 and C_8 substituent groups, respectively. The activity of the compounds primarily depended on the type of substitutions at these positions in addition to the main skeleton carrying various hydroxyl and methyl groups. The highest potency exhibited by retamasin H appears to be mainly due to presence of the γ-lactone substitution at C_6 position. Moreover, five flavonoids including retamasin C and F enhanced glucose-induced secretion of insulin from the pancreatic islets of mice. Molecular docking simulation of retamasin C and F in complex with modeled yeast α-glucosidase showed that the inhibitors are mainly stabilized by hydrogen bonding interactions with the active site residues. Compounds

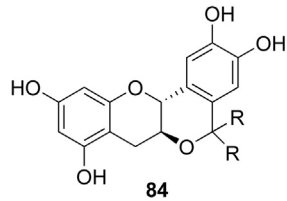

84

R = $(CH_2)_{n-1}$ CH_3 (*n* = 1-6)

Figure 3.18 The analogs of planar catechins carry potential for further development into antidiabetic drugs. *Reproduced from U. Ghani, Re-exploring promising α-glucosidase inhibitors for potential development into oral anti-diabetic drugs: finding needle in the haystack, Eur. J. Med. Chem. 103 (2015) 133–162.*

with dual insulin secretory and α-glucosidase inhibitory activities are highly valuable in drug discovery since they exert the antidiabetic effects by utilizing two separate mechanisms of action for a better control of hyperglycemia in diabetes. Retamasin flavonoids are one such promising example.

Hakamata et al. [49] synthesized planar catechin analogs and identified promising inhibitors of yeast and bacterial α-glucosidase from *B. stearothermophilus* ($IC_{50} = 0.7–47.5$ μM). Example includes compound **84** (Fig. 3.18). Planar catechins are promising α-glucosidase inhibitors than simple catechins.

A number of hydrolysable tannins have been isolated from the petals of *Rosa gallica*. The flower, commonly known as gallic rose or French rose, has been used in Uygur traditional medicine of China for treating diabetes mellitus. Tellimagrandin with an HHDP and three galloyl groups have been identified as yeast α-glucosidase inhibitors specifically tellimagrandin I (**85**) and II (**86**) (Fig. 3.19). The latter is more potent ($IC_{50} = 6$ μM) than the former bearing an HHDP and two galloyl groups ($IC_{50} = 13$ μM). Furthermore, rugosin A and D displayed promising inhibition of α-glucosidase ($IC_{50} = 8$ and 2 μM, respectively), with comparable levels of enzyme

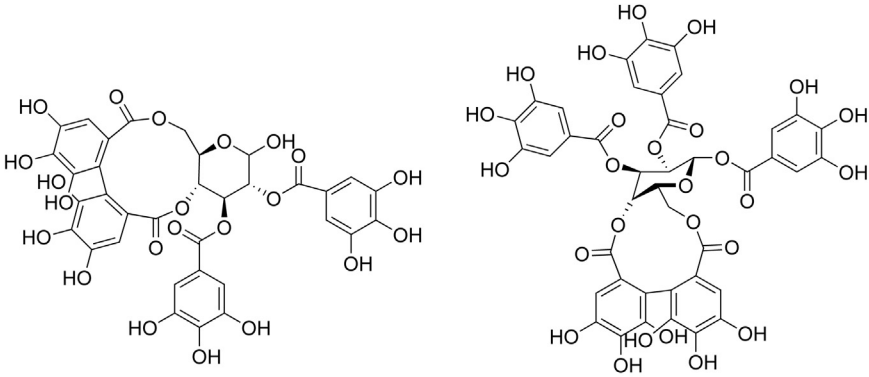

85 86

Figure 3.19 The bulky, hydrolysable tannins such as tellimagrandin I and II are promising inhibitors of α-glucosidase. *Reproduced from U. Ghani, Re-exploring promising α-glucosidase inhibitors for potential development into oral anti-diabetic drugs: finding needle in the haystack, Eur. J. Med. Chem. 103 (2015) 133–162.*

inhibition to acarbose. These studies conclude that the bulky hydrolysable tannins are more promising inhibitors of α-glucosidase than other tannins [50].

The *Edgeworthia chrysantha* plant carries a history of its use in Chinese folklore medicine for treating rheumatism and traumatic injury. Eight daphnodorin monomers have been recently characterized from the stems and twigs of the plant as α-glucosidase inhibitors ($IC_{50} = 3.14–19\ \mu M$). Both monomers and dimers showed comparable activities [51].

Tannins are natural polyphenols that are widely used in food industry for stabilizing and improving color and taste of food products. Gallotannin, also known as tannic acid, is a commercial version of tannins that exhibits anticancer activity at multiple levels. It is regarded as a promising candidate for cancer treatment since it inhibits metastasis, invasion, and proliferation of malignant prostate gland cells. Additionally, it is

also considered as a potential drug for prevention of breast and squamous cell carcinomas. Studies directed toward α-glucosidase inhibition by tannins have recently started to emerge in the literature [52,53]. Gallotannin is a potent mixed-type inhibitor of α-glucosidase ($K_i = 0.41$ μM) as shown by a recent report that conducted enzyme kinetics and molecular docking studies. Computational studies showed that the functional ring structure of gallotannin binds to the substrate-binding pocket of α-glucosidase leading to prevention of substrate catalysis. Additionally, there appears to be a promising role of the phenolic hydroxyl groups of gallotannin in the enzyme inhibition that enhances the binding stability by strongly interacting with the active site residues [54].

Macaranga tanarius leaves and *Terminalia chebula* Retz. plant contain a number of ellagitannins with moderate to strong α-glucosidase inhibitory activity. These types of compounds possess the $^1C_4$ glucose core conjugated by galloyl, HHDP, valoneayl, and/or tanaroyl groups. *T. chebula* Retz. is commonly used in traditional medicine for treating drooling and heartburn [55]. Some ellagitannins isolated from the plant possess promising intestinal maltase inhibitory activity such as chebulinic acid ($IC_{50} = 36$ μM) and chebulagic acid ($IC_{50} = 97$ μM). Structure–activity relationship studies on ellagitannins showed that their activity was directly dependent on the number of flexible galloyl units. For structural details of the compounds discussed in the preceding three paragraphs, please refer to the corresponding references.

Hydroxycinnamic acids are generally composed of a carbon backbone that varies in length from C_6 to C_3 with a variety of substituents such as caffeic acid, chlorogenic acid, and quinic acid. The compounds are abundant in the plant kingdom and are found in blueberry leaves and coffee beans. It is important to highlight three cinnamic acids (**87**, **88**, and **89**) exhibiting promising α-glucosidase inhibitory activity (Fig. 3.20). The rhizomes

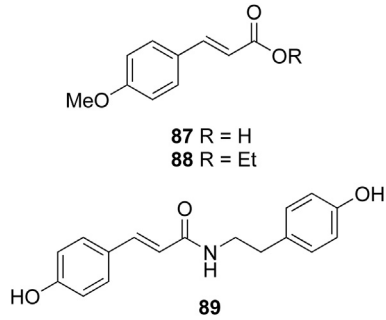

Figure 3.20 Natural hydroxycinnamic acids isolated from the rhizomes of *Kaempferia galangal* plant.

of *Kaempferia galangal* contain *trans*-cinnamic acids **87** and **88** exhibiting microbial α-glucosidase inhibitory activity ($IC_{50} = 40$ and 50 μM, respectively) [56] whereas, *N*-*p*-coumaroyltyramine (**89**), isolated from the methanol extracts of *Allium fistulosum*, commonly called Welsh onion, inhibited yeast α-glucosidase ($K_i = 0.84$ μM) [57].

Proanthocyanidins are widely distributed in plants as phenolic secondary metabolites with oligomeric or polymeric structures. These chains consist of flavan-3-ol monomers bonded mainly through C_4-C_8 or C_4-C_6 (type B) or through C_4-C_8 and C_2-O_7 linkages (type A). The *Pyracantha fortuneana* fruit has been traditionally used in Chinese folklore medicine for treatment of indigestion. Moreover, extracts of various parts of the plant have been reported to exhibit immunoprotective and antioxidant activities, particularly the phenolic extracts that carry α-glucosidase inhibitory activity. A number of proanthocyanidins have been identified from *P. fortuneana* fruit's extract with promising α-glucosidase inhibitory activity [58]. Further details on proanthocyanidins have been provided in the corresponding reference.

Eugenia caryophylata (clove) has been used in natural medicine for treating toothaches, infections, and digestive disorders [59], and as spice. The clove essential oil contains a variety of

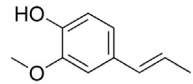

Isoeugenol (**90**)

Figure 3.21 Natural isoeugenol and similar phenolic compounds provide interesting clues to developing potent α-glucosidase inhibitors since they inhibit the enzyme in nanomolar range.

compounds including eugenol, isoeugenol, and eugenyl acetate. Chemically, isoeugenol is 2-methoyxy-4-propenyl-phenol (**90**), which is used as antioxidant, preservative, and sweetener in food and pharmaceutical industry [60], in addition to antimicrobial agent [61]. Isoeugenol (Fig. 3.21) has been recently identified as potent yeast α-glucosidase inhibitor demonstrating noncompetitive inhibition of the enzyme in nanomolar range ($IC_{50} = 19.25$ nM; $K_i = 21$ nM) [62]. Natural phenolic compounds like isoeugenol provide structural and functional clues to synthesis and identification of new similar compounds for promising α-glucosidase inhibition in nanomolar range.

The *Aspergillus flavipes* fungus of marine origin is known to be a rich source of marine natural products. Its secondary metabolites have shown to possess antioxidant, insecticidal, antimicrobial, and antitumor activities [63]. The fungus, collected from the coastal sea sediment samples from Lianyungang in the Jiangsu province of China, contains chemically diverse secondary metabolites. Three new 2,3-disubstituted γ-butenolide derivatives namely flavipesolides A−C (**91**−**93**) have been identified from the fungus exhibiting α-glucosidase inhibitory activity in addition to 13 known compounds [64]. These include compound **94**, aspernolide A (**95**), emodin (**96**), questin (**97**), geodin hydrate (**98**), 7-methyldichloroasterrate (**99**), monomethylosoic acid (**100**), asterric acid (**101**), methyl 3-chloroasterric acid (**102**), and epicoccolide B (**103**) (Fig. 3.22). Compounds **91**−**96**, **98**−**100**, and **103** showed promising α-glucosidase inhibition with lower cytotoxic effects on Caco-2

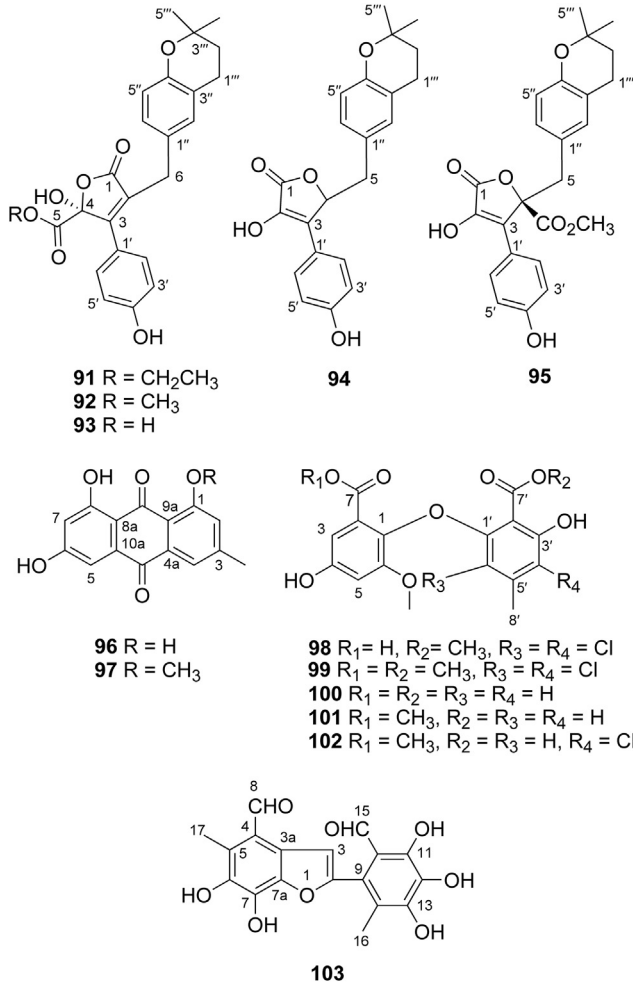

Figure 3.22 The butenolides (flavipesolides A–C) and other flavonoid derivatives.

cells than α-deoxynojirimycin and acarbose. Compounds **94–96** and **99** demonstrated noncompetitive inhibition of the enzyme (K_i values = 0.43, 2.1, 0.79, and 2.8 μM, respectively) whereas compounds **91–93**, **98**, **100**, and **103** were mixed-type inhibitors. Compounds **91** and **92** bearing esterification inhibited the enzyme more potently than compound **93**. However, in the anthraquinones, presence of

O-methylation on the 1-OH group reduced the inhibitory activity by several folds as seen in the structure–activity comparison of compounds **96** and **97**. Moreover, the compounds containing the diphenyl ether group exhibited more inhibition potency than the benzophenone derivatives.

Berries are regarded as an important food for consumption and for beneficial health effects [65–67]. One of the pharmacological effects of berry fruits is inhibition of carbohydrate digestion enzymes leading to reduction of blood glucose levels and increasing insulin sensitivity in diabetes. Previous studies have demonstrated that oral administration of mulberry anthocyanin extracts in diabetic mice improved insulin sensitivity [68]. Anthocyanins are known to inhibit α-glucosidase, however, there is a very limited number of reports that discussed their structure–activity relationship in detail. Synthesis of monomeric anthocyanins is challenging due to presence of the flavylium cation in their skeleton. Therefore, isolation from natural sources is still a preferred method for characterizing anthocyanins.

Xu et al. [69] recently developed an efficient chromatography-based protocol for isolation of natural anthocyanin α-glucosidase inhibitors from plant sources that were subjected to systematic structure–activity relationship studies. This includes 18 monomeric anthocyanins constituting six types of anthocyanidins and five types of glycosyl moieties present in their structures. In particular, natural pelargonidin-3-O-rutinoside (**104**) (Fig. 3.23), a mixed-type α-glucosidase inhibitor, exhibited highest potency of inhibition among other anthocyanins studied in the work ($IC_{50} = 1.69\ \mu M$). Moreover, it also suppressed postprandial hyperglycemia in mice.

Natural lignans are biosynthesized through phenylpropanoid coupling. A variety of lignans with diverse chemical structures and biological activities exist in nature such as neolignans, oxyneolignans, and mixed lignans. Magnolol and honokiol are typical examples of lignans, isolated from the bark of

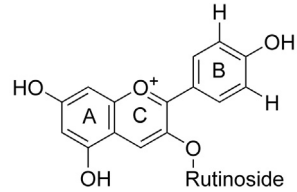

Pelargonidin-3-*O*-rutinoside (**104**)

Figure 3.23 Natural pelargonidin-3-*o*-rutinoside.

Magnolia species of plants, which have been used in Chinese and Japanese traditional medicine for treating anxiety, allergy, and gastrointestinal disorders. The lignan constituents of *Magnolia officinalis* bark have been studied to exhibit a spectrum of biological activities including but not limited to anticancer, antiinflammatory, antidepressant, and antimicrobial effects. In view of their promising and diverse biological effects, several groups of synthetic and medicinal chemists studied synthetic analogs of magnolol and honokiol including bisphenol neolignans with diverse biological activities such as modulation of GABA receptors, antimicrobial, antiinflammatory, and anticancer activities [70–74].

Magnolol (**105**) and honokiol (**106**) have been shown to inhibit α-glucosidase enzyme ($IC_{50} = 2.0$ and 23.0 μM, respectively). Pulvirenti et al. [75] recently synthesized a series of bisphenols based on the magnolol structure using chemoenzymatic methods (Fig. 3.24). The compounds potently inhibited yeast α-glucosidase ($IC_{50} = 0.15–4.1$ μM) particularly 1,1′-dityrosol-8,8′-diacetate (**107**, $IC_{50} = 0.15$ μM). The bisphenol derivatives such as **108**, **109**, and **110** demonstrated comparative enzyme inhibition ($IC_{50} = 0.49$, 0.5, 0.86 μM, respectively). Compound **108**, a catechol analog of magnolol, showed more potency than that of magnolol alone; similar level of activity difference was also observed in compound **109** when compared to **111**. Compounds **107** and **110**, which are devoid of the catechol moiety, also showed considerable

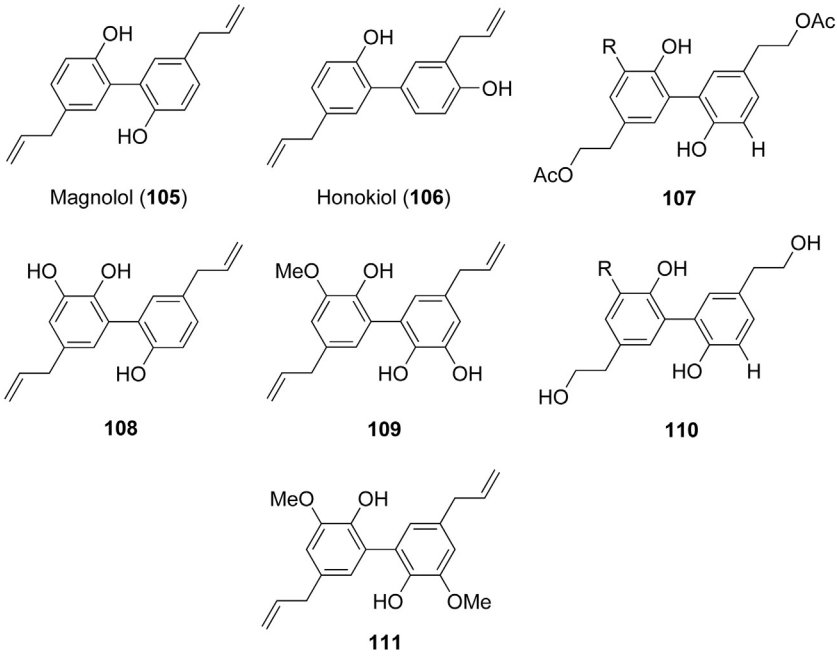

Figure 3.24 Natural lignans including magnolol-based compounds are an emerging class of α-glucosidase inhibitors.

enzyme inhibition, suggesting the importance of the dityrosol structure in enzyme inhibition. The relatively moderate activity of honokiol appears to be due to presence of a hydroxyl group *ortho* to the allyl chain in the ring B. Enzyme inhibition kinetic studies conducted on compound **107** revealed that it is a competitive inhibitor ($K_i = 0.86\ \mu M$). Magnolol-based synthetic derivatives possess potential for antidiabetic drug candidacy.

Salvia miltiorrhiza, commonly called Danshen in China, is used to treat cardiovascular diseases. The chemical constituents of the plant are known to possess antioxidant, antitumor, and antithrombosis activities. Therapeutic preparations containing antidiabetic constituents of the Danshen root have shown to exhibit hypoglycemic effects [76]. Since several α-glucosidase inhibitors have been identified from the plant [77], the hypoglycemic effect is apparently due to inhibition of intestinal

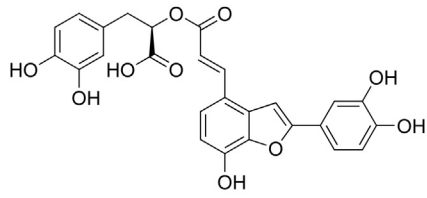

Salvianolic acid C (**112**)

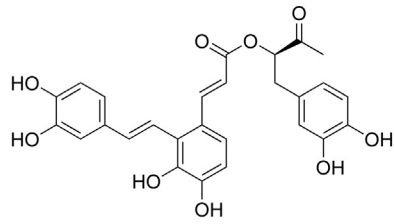

Salvianolic acid A (**113**)

Figure 3.25 Salvianolic acid C and A isolated from *Salvia miltiorrhiza* plant.

α-glucosidase. Tang et al. [78] recently conducted α-glucosidase inhibition assays on some compounds isolated from the plant. Additionally, they also compiled a list of inhibitors isolated from the plant to date, and performed molecular docking studies to validate their interaction with the enzyme. In these studies, two interesting compounds with potent α-glucosidase inhibitory activities were identified namely salvianolic acid C (**112**) and A (**113**) (Fig. 3.25). The former was identified as a mixed-type inhibitor ($IC_{50} = 4.31$ μM) whereas the latter showed competitive inhibition of the enzyme ($IC_{50} = 19.29$ μM).

Bromophenols from marine algae are known to inhibit α-glucosidase [79]. Examples include *bis*-(2,3,6-tribromo-4,5-dihydroxybenzyl) ether, *bis*-(2,3-dibromo-4,5-dihydroxybenzyl) ether [80], 2,3,6-tribromo-4,5-dihydroxybenzyl alcohol [81], and 2,4,6-tribromophenol [82]. *Bis*-(2,3,6-tribromo-4,5-dihydroxybenzyl) ether (**114**, $IC_{50} = 0.03$ μM) and *bis*-(2,3-dibromo-4,5-dihydroxybenzyl) ether (**115**, $IC_{50} = 0.098$ μM), which are potent inhibitors of yeast α-glucosidase (Fig. 3.26).

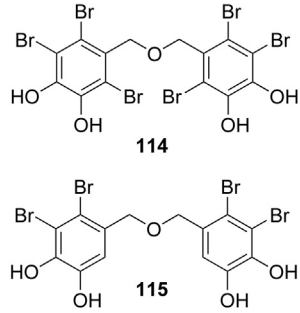

Figure 3.26 Marine bromophenols. *Reproduced from U. Ghani, Re-exploring promising α-glucosidase inhibitors for potential development into oral anti-diabetic drugs: finding needle in the haystack, Eur. J. Med. Chem. 103 (2015) 133–162. © 2015 French Société de Chimie Thérapeutique published by Elsevier Masson SAS. All rights reserved.*

Liu et al. [83] synthesized compound **115** and determined its interactions with yeast α-glucosidase using circular dichroism and molecular docking techniques. The enzyme-inhibitor binding involves a number of hydrophobic interactions and hydrogen bond formation. Moreover, the inhibitor induced minor conformational changes to the enzyme.

Natural curcumin and its related derivatives are found in *Curcuma longa* (turmeric), a very common yellow spice used in Asia. It is effective for treatment of diabetes in Chinese herbal medicine [84] besides its antioxidant, antiinflammatory, and anticancer properties [85]. *C. longa* plant extract inhibits α-glucosidase and lowers blood glucose level in diabetic patients [86]. Interest in this particular property of the plant involves study of curcuminoid and synthetic curcumin analog inhibitors of α-glucosidase. Natural curcumin, demethoxycurcumin, and *bis*-demethoxycurcumin displayed comparable α-glucosidase inhibitory activity to that of acarbose.

Generally, the synthetic curcumin analogs exhibited more potent enzyme inhibitory activity than their natural counterparts. Compounds carrying the tetrahydroxyl groups (**116**, **117**, and **118**) possessed highest inhibitory activity against yeast

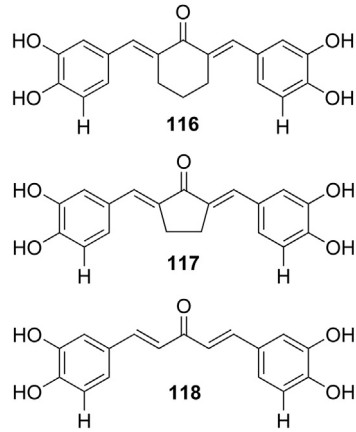

Figure 3.27 Analogs of curcumin. *Reproduced from U. Ghani, Re-exploring promising α-glucosidase inhibitors for potential development into oral anti-diabetic drugs: finding needle in the haystack, Eur. J. Med. Chem. 103 (2015) 133–162. © 2015 French Société de Chimie Thérapeutique published by Elsevier Masson SAS. All rights reserved.*

α-glucosidase ($IC_{50} = 2.8$, 2.6, and 1.6 μM, respectively; Fig. 3.27). Compounds containing a methoxyl group at the *ortho* position of the phenols exhibited much lower activity, in contrast to incorporation of a bromic group at the same position that potentiated the activity. A significant decrease in the activity was observed when the bulky *ortho*-tetrabutyl groups replaced these groups. Interestingly, compounds with no hydroxyl groups were inactive obviously suggesting that the *para* hydroxyl groups in the curcumin analogs are important pharmacophores for α-glucosidase inhibition. Moreover, it is proposed that presence of the *ortho*-dihydroxyl groups may also contribute to higher affinity of the compounds to the enzyme active site.

Noncompetitive inhibitors such as *bis*-demethoxycurcumin and compound **118** were further studied by circular dichroism spectroscopy for their effects on the overall secondary structure of the enzyme. The compounds interact with the enzyme by a mechanism that induces changes in the α-helix

conformation to other forms of secondary structures [87]. Curcuminoids and curcumin analogs can be studied further and developed into potential antidiabetic drug candidates either at preclinical or clinical level.

References

[1] V. Rastija, D. Beslo, S. Nikolic, Two-dimensional quantitative structure–activity relationship study on polyphenols as inhibitors of α-glucosidase, Med. Chem. Res. 21 (2012) 3984–3993.
[2] S.D. Cohen, J.A. Kennedy, Plant metabolism and the environment: implications for managing phenolics, Crit. Rev. Food Sci. Nutr. 50 (2010) 620–643.
[3] D.K. Mahapatra, V. Asati, S.K. Bharti, Chalcones and their therapeutic targets for the management of diabetes: structural and pharmacological perspectives, Eur. J. Med. Chem. 92 (2015) 839–865.
[4] D.A. Israf, T.A. Khaizurin, A. Syahida, N.H. Lajis, S. Khozirah, Cardamonin inhibits COX and iNOS expression via inhibition of p65NF-kB nuclear translocation and Ik-B phosphorylation in RAW 264.7 macrophage cells, Mol. Immunol. 44 (2007) 673–679.
[5] L.B. Salum, et al., Cytotoxic 3, 4, 5-trimethoxychalcones as mitotic arresters and cell migration inhibitors, Eur. J. Med. Chem. 63 (2013) 501–510.
[6] Y. Luo, et al., Design, synthesis, and biological evaluation of chalcone oxime derivatives as potential immunosuppressive agents, Bioorg. Med. Chem. Lett. 22 (2012) 3039–3043.
[7] J.R. Dimmock, D.W. Elias, M.A. Beazely, N.M. Kandepu, Bioactivities of chalcones, Curr. Med. Chem. 6 (1999) 1125–1149.
[8] P. Singh, A. Anand, V. Kumar, Recent developments in biological activities of chalcones: a mini review, Eur. J. Med. Chem. 85 (2014) 758–777.
[9] Z. Nowakowska, A review of anti-infective and anti-inflammatory chalcones, Eur. J. Med. Chem. 42 (2007) 125–137.
[10] T. Tanaka, R. Uehara, K. Nishida, I. Kouno, Galloyl, caffeoyl and hexahydroxydiphenoyl esters of dihydrochalcone glucosides from *Balanophora tobiracola*, Phytochemistry 66 (2005) 675–681.
[11] H.W. Ryu, B.W. Lee, L.J. Curtis-Long, S. Jung, Y.B. Ryu, W.S. Lee, et al., Polyphenols from *Broussonetia papyrifera* displaying potent α-glucosidase inhibition, J. Agric. Food Chem. 58 (2010) 202–208.
[12] W.D. Seo, et al., Sulfonamide chalcone as a new class of α-glucosidase inhibitors, Bioorg. Med. Chem. Lett. 15 (2005) 5514–5516.

[13] S. Wang, et al., Synthesis and evaluation of the α-glucosidase inhibitory activity of 3-[4-(phenylsulfonamido)benzoyl]-2H-1-benzopyran-2-one derivatives, Eur. J. Med. Chem. 45 (2010) 1250–1255.
[14] Y. Wang, T. Zhang, J. Liang, F. Meng, S. Wang, Synthesis and biological evaluation of new substituted 3-[4-(phenylsulfonamido)benzoyl]-*2H*-1-benzopyran-2-one derivatives as α-glucosidase inhibitors, J. Chem. 2014 (2014). Article ID 590129, 6 pages.
[15] F.L. Ansari, et al., Syntheses and biological activities of chalcone and 1,5-benzothiazepine derivatives: promising new free-radical scavengers, and esterase, urease, and α-glucosidase inhibitors, Chem. Biodiversity 2 (2005) 487–496.
[16] R.R. Rao, et al., Synthesis of antihyperglycemic, α-glucosidase inhibitory and DPPH free radical scavenging furanochalcones, Med. Chem. Res. 21 (2012) 760–774.
[17] R.G. Damazio, et al., Antihyperglycemic activity of naphthylchalcones, Eur. J. Med. Chem. 45 (2010) 1332–1337.
[18] K.S. Masters, S. Brase, Xanthones from fungi, lichens, and bacteria: the natural products and their synthesis, Chem. Rev. 112 (2012) 3717–3776.
[19] H.R. El-Seedi, et al., Recent insights into the biosynthesis and biological activities of natural xanthones, Curr. Med. Chem. 17 (2010) 854–901.
[20] L.M.M. Vieira, A. Kijjoa, Naturally-occurring xanthones: recent developments, Curr. Med. Chem. 12 (2005) 2413–2446.
[21] J.S. Negi, V.K. Bisht, P. Singh, M.S.M. Rawat, G.P. Joshi, Naturally occurring xanthones: chemistry and biology, J. Appl. Chem. 621459 (2013) 9.
[22] E.J. Seo, et al., Xanthones from *Cudrania tricuspidata* displaying potent α-glucosidase inhibition, Bioorg. Med. Chem. Lett. 17 (2007) 6421–6424.
[23] K.H. Park, Y.D. Park, J.M. Han, K.R. Im, B.W. Lee, I.Y. Jeong, et al., Anti-atherosclerotic and anti-inflammatory activities of catecholic xanthones and flavonoids isolated from *Cudrania tricuspidata*, Bioorg. Med. Chem. Lett. 16 (2006) 5580–5583.
[24] B.W. Lee, J.H. Lee, S.T. Lee, H.S. Lee, W.S. Lee, T.S. Jeong, et al., Antioxidant and cytotoxic activities of xanthones from *Cudrania tricuspidata*, Bioorg. Med. Chem. Lett. 15 (2005) 5548–5552.
[25] V. Peres, T.J. Nagem, F.F. Oliveira, Tetraoxygenated naturally occurring xanthones, Phytochemistry 55 (2000) 683–710.
[26] H.W. Ryu, J.K. Cho, M.J. Curtis-Long, H.J. Yuk, Y.S. Kim, S. Jung, et al., α-Glucosidase inhibition and antihyperglycemic activity of prenylated xanthones from *Garcinia mangostana*, Phytochemistry 72 (2011) 2148–2154.
[27] Y.C. Yang, Tibetan Medicine, Qinghai People's Publishing House, Xining, 1991, pp. 111–112.

[28] P. Basnet, S. Kadota, M. Shimizu, T. Namba, Bellidifolin: a potent hypoglycemic agent in streptozotocin (STZ)-induced diabetic rats from *Swertia japonica*, Planta Med. 60 (1994) 507–511.
[29] H. Zheng, et al., Xanthones from *Swertia mussotii* as multitarget-directed antidiabetic agents, ChemMedChem 9 (2014) 1374–1379.
[30] Y. Liu, L. Zou, L. Ma, W. Chen, B. Wang, Z. Xu, Synthesis and pharmacological activities of xanthone derivatives as α-glucosidase inhibitors, Bioorg. Med. Chem. 14 (2006) 5683–5690.
[31] Y. Liu, L. Zou, L. Ma, W. Chen, B. Wang, Z. Xu, Synthesis of xanthone derivatives with extended *p*-systems as α-glucosidase inhibitors: insight into the probable binding mode, Bioorg. Med. Chem. 15 (2007) 2810–2814.
[32] C.M. Park, T. Oie, A.M. Petros, H. Zhang, P.M. Nimmer, R.F. Henry, et al., Design, synthesis, and computational studies of inhibitors of Bcl-XL, J. Am. Chem. Soc. 128 (2006) 16206–16212.
[33] J.G. Ding, J.H. Shi, D.F. Cui, L.F. Xu, S.H. Duan, L.H. Guo, et al., Development of peptidic dopamine transporter inhibitors via aromatic modification-mediated conformational restriction, J. Med. Chem. 49 (2006) 4048–4051.
[34] P.J. Berti, J.A.B. McCann, Toward a detailed understanding of base excision repair enzymes: transition state and mechanistic analyses of *N*-glycoside hydrolysis and *N*-glycoside transfer, Chem. Rev. 106 (2006) 506–555.
[35] T. Flatmark, R.C. Stevens, Structural insight into the aromatic amino acid hydroxylases and their disease-related mutant forms, Chem. Rev. 99 (1999) 2137–2160.
[36] G. Li, J. He, A. Zhang, Y. Wan, B. Wang, W. Chen, Toward potent α-glucosidase inhibitors based on xanthones: a closer look into the structure-activity correlations, Eur. J. Med. Chem. 46 (2011) 4050–4055.
[37] T.K. Tabopda, J. Ngoupayo, P.K. Awoussong, A. Mitaine-Offer, M.S. Ali, B.T. Ngadjui, et al., Triprenylated flavonoids from *Dorstenia psilurus* and their α-glucosidase inhibition properties, J. Nat. Prod. 71 (2008) 2068–2072.
[38] M. Yoshikawa, H. Shimada, N. Nishida, Y. Li, I. Toguchida, J. Yamahara, et al., Antidiabetic principles of natural medicines. II. Aldose reductase and alpha-glucosidase inhibitors from Brazilian natural medicine, the leaves of *Myrcia multiflora DC. (Myrtaceae)*: structures of myrciacitrins I and II and myrciaphenones A and B, Chem. Pharm. Bull. (Tokyo) 46 (1998) 113–119.
[39] S.S. Lee, H.C. Lin, C.K. Chen, Acylated flavonol monorhamnosides, α-glucosidase inhibitors, from *Machilus philippinensis*, Phytochemistry 69 (2008) 2347–2353.

[40] T. Matsui, T. Ueda, T. Oki, K. Sugita, N. Terahara, K. Matsumoto, α-Glucosidase inhibitory action of natural acylated anthocyanins. 2. α-Glucosidase inhibition by isolated acylated anthocyanins, J. Agric. Food Chem. 49 (2001) 1952–1956.
[41] T. Matsui, S. Ebuchi, T. Fujise, K. Abesundara, S. Doi, H. Yamada, et al., Strong antihyperglycemic effects of water-soluble fraction of Brazilian propolis and its bioactive constituent, 3,4,5-tri-O-caffeoylquinic acid, Biol. Pharm. Bull. 27 (2004) 1797–1803.
[42] K. Tadera, Y. Minami, K. Takamatsu, T. Matsuoka, Inhibition of α-glucosidase and α-amylase by flavonoids, J. Nutr. Sci. Vitaminol. 52 (2006) 149–153.
[43] C.W. Choi, Y.H. Choi, M.R. Cha, D.S. Yoo, Y.S. Kim, G.H. Yon, et al., Yeast α-glucosidase inhibition by isoflavones from plants of *Leguminosae* as an *in vitro* alternative to acarbose, J. Agric. Food Chem. 58 (2010) 9988–9993.
[44] H.J. Yuk, J.H. Lee, M.J. Curtis-Long, J.W. Lee, Y.S. Kim, H.W. Ryu, et al., The most abundant polyphenol of soy leaves, coumestrol, displays potent α-glucosidase inhibitory activity, Food Chem. 126 (2011) 1057–1063.
[45] M. Nur-e-Alam, et al., New flavonoids from the Saudi Arabian plant *Retama raetam* which stimulates secretion of insulin and inhibits α-glucosidase, Org. Biomol. Chem. 17 (2019) 1266–1276.
[46] M. Maghrani, A. Lemhadri, H. Jouad, J.-B. Michel, M. Eddouks, Effect of the desert plant *Retama raetam* on glycaemia in normal and streptozotocin-induced diabetic rats, J. Ethnopharmacol. 87 (2003) 21–25.
[47] O. Mejri, O. Beji, C. Ben Salem, H. Hmouda, A case-based discussion from the Medical Intensive Care Unit of Sahloul University Hospital of Tunisia: an unusual cause of alveolar hypoventilation in a patient with COPD, Thorax 70 (2015). 1004 LP-1006.
[48] U. Ghani, et al., Natural flavonoid α-glucosidase inhibitors from *Retama raetam*: enzyme inhibition and molecular docking reveal important interactions with the enzyme active site, Bioorg. Chem. 87 (2019) 736–742.
[49] W. Hakamata, et al., Planar catechin analogs with alkyl side chains: a potent antioxidant and an α-glucosidase inhibitor, J. Am. Chem. Soc. 128 (2006) 6524–6525.
[50] S. Ochir, M. Nishizawa, B.J. Park, K. Ishii, T. Kanazawa, M. Funaki, et al., Inhibitory effects of *Rosa gallica* on the digestive enzymes, J. Nat. Med. 64 (2010) 275–280.
[51] T. Zhou, S.W. Zhang, S.S. Liu, H.J. Cong, L.J. Xuan, Daphnodorin dimers from *Edgeworthia chrysantha* with α-glucosidase inhibitory activity, Phytochem. Lett. 3 (2010) 242–247.

[52] H.Z. Xiao, B.G. Liu, H.Z. Mo, G.Z. Liang, Comparative evaluation of tannic acid inhibiting α-glucosidase and trypsin, Food Res. Int. 76 (2015) 605–610.
[53] V. Muccilli, N. Cardullo, C. Spatafora, V. Cunsolo, C. Tringali, α-Glucosidase inhibition and antioxidant activity of an oenological commercial tannin. Extraction, fractionation and analysis by HPLC/ESI–MS/MS and (1)H NMR, Food Chem. 215 (2017) 50–60.
[54] L.M. Yue, J. Lee, L. Zhenga, Y.D. Park, Z.M. Ye, J.M. YangYu, Computational prediction integrating the inhibition kinetics of gallotannin on α-glucosidase, Intl. J. Biolog. Macromol. 103 (2017) 829–838.
[55] H. Gao, Y.N. Huang, P.Y. Xu, J. Kawabata, Inhibitory effect on α-glucosidase by the fruits of *Terminalia chebula* Retz, Food Chem. 105 (2007) 628–634.
[56] S. Adisakwattana, K. Sookkongwaree, S. Roengsumran, A. Petsom, N. Ngamrojnavanich, W. Chavasiri, et al., Structure-activity relationships of trans-cinnamic acid derivatives on alpha-glucosidase inhibition, Bioorg. Med. Chem. Lett. 14 (2004) 2893–2896.
[57] T. Nishioka, J. Watanabe, J. Kawabata, R. Niki, Isolation and activity of N-p-coumaroyltyramine, an α-glucosidase inhibitor in Welsh onion (*Allium fistulosum*), Biosci. Biotechnol. Biochem. 61 (1997) 1138–1141.
[58] M. Wei, W.M. Chai, Q. Yang, R. Wang, Y. Peng, Novel insights into the inhibitory effect and mechanism of proanthocyanidins from *Pyracantha fortuneana* fruit on α-glucosidase, J. Food Sci. 82 (2017) 2260–2268.
[59] I. Gulcin, İ.G. Şat, Ş. Beydemir, M. Elmastaş, Ö.İ. Küfrevioğlu, Comparison of antioxidant activity of clove (*Eugenia caryophylata* Thunb.) buds and lavender (*Lavandula Stoechas* L.), Food. Chem. 87 (2004) 393–400.
[60] Z. Liang-Liang, Z. Li-Fang, X. Jian-Guo, H. Qing-Ping, Comparison study on antioxidant, DNA damage protective and antibacterial activities of eugenol and isoeugenol against several foodborne pathogens, Food Nutr. Res. 61 (2017) 1353356.
[61] I. Gulcin, Antioxidant activity of eugenol: a structure and activity relationship study, J. Med. Food. 14 (2011) 975–985.
[62] F. Topal, Anticholinergic and antidiabetic effects of isoeugenol from clove (*Eugenia caryophylata*) oil, Int. J. Food Prop. 22 (2019) 583–592.
[63] J. Zheng, Z. Xu, Y. Wang, K. Hong, P. Liu, W. Zhu, Cyclic tripeptides from the halotolerant fungus *Aspergillus sclerotiorum* PT06-1, J. Nat. Prod. 73 (2010) 1133–1137.
[64] C. Wang, L. Guo, J. Hao, L. Wang, W. Zhu, α-Glucosidase inhibitors from the marine-derived fungus *Aspergillus flavipes* HN4-13, J. Nat. Prod. 79 (2016) 2977–2981.

[65] W. Chen, H. Su, Y. Xu, T. Bao, X. Zheng, Protective effect of wild raspberry (*Rubus hirsutus* Thunb.) extract against acrylamide-induced oxidative damage is potentiated after simulated gastrointestinal digestion, Food Chem. 196 (2016) 943–952.
[66] Y. Li, T. Bao, W. Chen, Comparison of the protective effect of black and white mulberry against ethyl carbamate-induced cytotoxicity and oxidative damage, Food Chem. 243 (2018) 65–73.
[67] L. Xie, H. Su, C. Sun, X. Zheng, W. Chen, Recent advances in understanding the anti-obesity activity of anthocyanins and their biosynthesis in microorganisms, Trends Food Sci. Technol. 72 (2018) 13–24.
[68] F. Yan, G. Dai, X. Zheng, Mulberry anthocyanin extract ameliorates insulin resistance by regulating PI3K/AKT pathway in HepG2 cells and db/db mice, J. Nutr. Biochem. 36 (2016) 68–80.
[69] Y. Xu, L. Xie, J. Xie, Y. Liub, W. Chen, Pelargonidin-3-*O*-rutinoside as a novel α-glucosidase inhibitor for improving postprandial hyperglycemia, Chem. Commun. 55 (2019) 39–42.
[70] S. Jada, M.R. Doma, P.P. Singh, S. Kumar, F. Malik, A. Sharma, et al., Design and synthesis of novel magnolol derivatives as potential antimicrobial and antiproliferative compounds, Eur. J. Med. Chem. 51 (2012) 35–41.
[71] L. Yang, Z.H. Wang, H. Lei, R.D. Chen, X.L. Wang, Y. Peng, et al., Neuroprotective glucosides of magnolol and honokiol from microbial-specific glycosylation, Tetrahedron 70 (2014) 8244–8251.
[72] B. Lee, et al., Design and synthesis of 4-*O*-methylhonokiol analogs as inhibitors of cyclooxygenase-2 (COX-2) and PGF_1 production, Bioorg. Med. Chem. 20 (2012) 2860–2868.
[73] J.M. Lin, A.S.P. Gowda, A.K. Sharma, S. Amin, In vitro growth inhibition of human cancer cells by novel honokiol analogs, Bioorg. Med. Chem. 20 (2012) 3202–3211.
[74] A. Fuchs, R. Baur, C. Schoeder, E. Sigel, C.E. Muller, Structural analogs of the natural products magnolol and honokiol as potent allosteric potentiators of GABAA receptors, Bioorg. Med. Chem. 22 (2014) 6908–6917.
[75] L. Luana Pulvirenti, V. Muccilli, N. Cardullo, C. Spatafora, C. Tringali, Chemoenzymatic synthesis and α-glucosidase inhibitory activity of dimeric neolignans inspired by magnolol, J. Nat. Prod. 80 (2017) 1648–1657.
[76] T. Wang, D.Q. Zhang, Y.H. Li, H. Liu, Z.B. Liu, C.F. Zhao, et al., Regulation effects on abnormal glucose and lipid metabolism of TZQ-F, a new kind of traditional Chinese medicine, J. Ethnopharmacol. 128 (2010) 575–582.
[77] H.Y. Ma, H.Y. Gao, L. Sun, J. Huang, X.M. Xu, L.J. Wu, Constituents with α-glucosidase and advanced glycation end-product

formation inhibitory activities from *Salvia miltiorrhiza* Bge, J. Nat. Med. 65 (2011) 37–42.
[78] H. Tang, D. Zhaob, Z. Xue, Exploring the interaction between *Salvia miltiorrhiza* and α-glucosidase: insights from computational analysis and experimental studies, RSC Adv. 8 (2018) 24701–24710.
[79] H. Kurihara, T. Mitani, J. Kawabata, K. Takahashi, Two new bromophenols from the red alga *Odonthalia corymbifera*, J. Nat. Prod. 62 (1999) 882–884.
[80] H. Kurihara, T. Mitani, J. Kawabata, K. Takahashi, Inhibitory potencies of bromophenols from *Rhodomelaceae* algae against α-glucosidase activity, Fish Sci. 65 (1999) 300–303.
[81] K.Y. Kim, K.A. Nam, H. Kurihara, S.M. Kim, Potent alpha-glucosidase inhibitors purified from the red alga *Grateloupia elliptica*, Phytochemistry 69 (2008) 2820–2825.
[82] K.Y. Kim, T.H. Nguyen, H. Kurihara, S.M. Kim, Alpha-glucosidase inhibitory activity of bromophenol purified from the red alga *Polyopes lancifolia*, J. Food. Sci. 75 (2010) H145–H150.
[83] M. Liu, W. Zhang, J. Wei, X. Lin, Synthesis and α-glucosidase inhibitory mechanisms of *bis*(2,3-dibromo-4,5-dihydroxybenzyl) ether, a potential marine bromophenol α-glucosidase inhibitor, Mar. Drugs 9 (2011) 1554–1565.
[84] D. Zhang, M. Fu, S. Gao, J. Li, Curcumin and diabetes: a systematic review. Evid.-Based Compl. Altern. Med., 2013, Article ID 636053, 16 pages, http://dx.doi.org/10.1155/2013/636053.
[85] S. Sreejayan, M.N.A. Rao, Curcuminoids as potent inhibitors of lipid peroxidation, J. Pharm. Pharmacol. 46 (1994) 1013–1016.
[86] H.S. Lee, KR Pat. 2003090395 (2003).
[87] Z. Du, R. Liu, W. Shao, X. Mao, L. Ma, L. Gu, et al., α-Glucosidase inhibition of natural curcuminoids and curcumin analogs, Eur. J. Med. Chem. 41 (2006) 213–218.

CHAPTER FOUR

Terpenoids and steroids

Contents

4.1 Terpenoids

Terpenoids are ubiquitous in nature with a range of biological activities including antidiabetic [1], antimalarial [2], and antimicrobial [3] activities. There are about 200 types of triterpenoids with different structural features, most of which are biologically active as antiviral, antitumor, antioxidative, and antiinflammatory agents. Currently, the pentacyclic triterpenoids are of special interest due to their antidiabetic activities [4]. Some dammarane terpenoids have been reported to regulate glucose metabolism with potential for suppressing blood glucose levels in hyperglycemia [5]. Several synthetic approaches involving incorporation of a variety of chemical moieties into the terpenoid skeleton have resulted in the identification of some promising α-glucosidase inhibitors with better efficacy than that of acarbose [6–8].

Recently, a variety of triterpenes isolated from the mangroves have been identified as α-glucosidase inhibitors [9]. Mangroves are halophytes that mainly grow in the tropical and subtropical regions. The plants are part of traditional medicine for treatment of skin infections, tuberculosis, and diarrhea [10]. Studies on the medicinal chemistry of mangroves have led to identification of a number of alkaloids, flavonoids,

Alpha-glucosidase Inhibitors.
DOI: https://doi.org/10.1016/B978-0-08-102779-0.00004-6

triterpenes, and saponins [11,12]. Lopez et al. [9] isolated five pentacyclic triterpene inhibitors of yeast α-glucosidase from *Pelliciera rhizophorae* mangroves of Panama using bioassay-guided fractionation. These include α-amyrine (**1**), β-amyrine (**2**), ursolic acid (**3**), oleanolic acid (**4**), and betulinic acid (**5**), which inhibited the enzyme in a concentration-dependent fashion (IC_{50} values of 1.45, 0.02, 1.08, 0.98, and 2.37 μM, respectively) (Fig. 4.1). The levels of enzyme inhibition

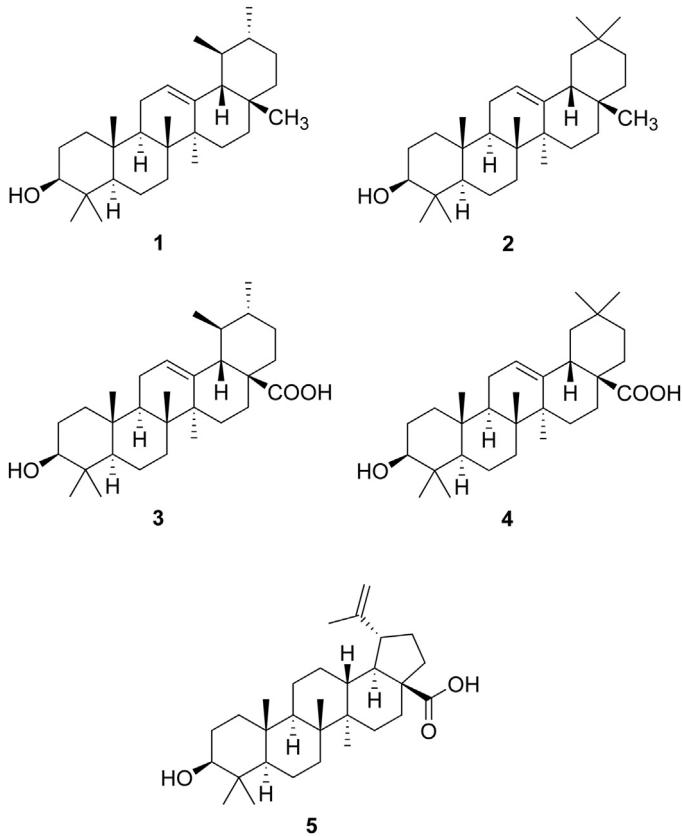

Figure 4.1 Pentacyclic triterpenes: α-amyrime (**1**), β-amyrine (**2**), ursolic acid (**3**), oleanolic acid (**4**), and betulinic acid (**5**). The highest potency of α-glucosidase inhibition by β-amyrine ($IC_{50} = 0.02$ μM) is contributed by the gem dimethyl group and the methyl group at positions 20 and 28, respectively.

exhibited by the compounds were found to be similar to each other since the main pentacyclic moiety contained only minor substitutions with the exception of compound **2** bearing a gem dimethyl group and a methyl group at positions 20 and 28, respectively. It is apparently these two groups that enable them to be potent in the series. All five compounds competitively inhibited yeast α-glucosidase.

Mohamed et al. [13] screened known triterpenes isolated from a number of plants for yeast α-glucosidase inhibition. One of the compounds called lupeol (**6**; $IC_{50} = 2.0$ μM) from *Diospyros mespiliformis* exhibited several-fold activity more than that of acarbose and deoxynojirimycin (Fig. 4.2). Introduction of additional hydroxyl groups and the acetyl functionality to these triterpenes compromised their activity. Furthermore, novel α-amyrin and lupeol hybrids have been synthesized that showed moderate α-glucosidase inhibition ($IC_{50} = 5.0$ μM) and antihyperglycemic activity in diabetic rats [14].

Moreover, report on the constituents of *Lagerstroemia speciosa* leaf extract has shown to contain lupeol-like pentacyclic triterpenes with ability to inhibit yeast α-glucosidase (Fig. 4.3).

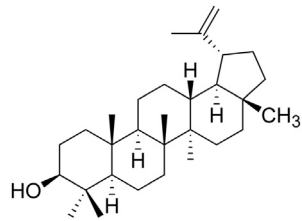

Lupeol (**6**)

Figure 4.2 Lupeol isolated from *Diospyros mespiliformis*. *Reproduced from U. Ghani, Re-exploring promising α-glucosidase inhibitors for potential development into oral anti-diabetic drugs: finding needle in the haystack, Eur. J. Med. Chem. 103 (2015) 133–162. © 2015 French Société de Chimie Thérapeutique published by Elsevier Masson SAS. All rights reserved.*

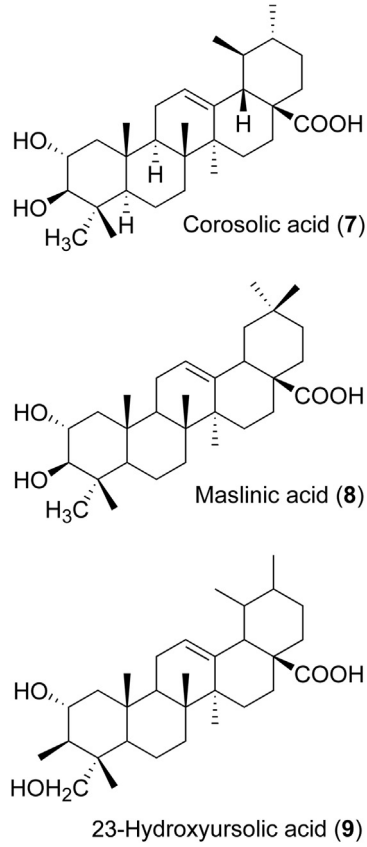

Figure 4.3 Pentacyclic triterpenes from *Lagerstroemia speciosa* leaves: corosolic acid, maslinic acid, and 23-hydroxyursolic acid. *Reproduced from U. Ghani, Re-exploring promising α-glucosidase inhibitors for potential development into oral anti-diabetic drugs: finding needle in the haystack, Eur. J. Med. Chem. 103 (2015) 133–162. © 2015 French Société de Chimie Thérapeutique published by Elsevier Masson SAS. All rights reserved.*

Examples include corosolic acid (**7**; $IC_{50} = 3.53\ \mu M$), maslinic acid (**8**; $IC_{50} = 5.52\ \mu M$), and 23-hydroxyursolic acid (**9**; $IC_{50} = 8.14\ \mu M$) [15].

Alpinia is the largest genus of Zingiberaceae family that includes species such as *Alpinia galangal* notable for antidiabetic effects in Asian traditional medicine [16,17]. Phytochemical

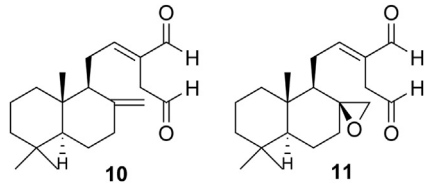

Figure 4.4 The labdane diterpenes I and II noncompetitively inhibit yeast α-glucosidase. *Reproduced from U. Ghani, Re-exploring promising α-glucosidase inhibitors for potential development into oral anti-diabetic drugs: finding needle in the haystack, Eur. J. Med. Chem. 103 (2015) 133–162. © 2015 French Société de Chimie Thérapeutique published by Elsevier Masson SAS. All rights reserved.*

investigations on *Alpinia nigra* (tora seeds), a closest species to *Alpinia galanga*, for potential antidiabetic activity led to isolation of labdane diterpenes I (**10**) and II (**11**) (Fig. 4.4) demonstrating noncompetitive inhibition of yeast α-glucosidase ($K_i = 11.61$ and 11.87 μM, respectively) [18].

Xu et al. [19,20] reported 15-alkylidene andrographolide inhibitors of yeast α-glucosidase (Fig. 4.5). The γ-alkylidene butenolide moiety and the aromatic group at the 3,19-hydroxyls are essential for the activity. Conversely, epoxidation of the double bonds [$\Delta^{8(17)}$] was not favorable to the activity. Examples of potent inhibitors from this class of compounds include 4-methoxylphenylidene derivative (**12**) ($IC_{50} = 16$ μM) and 15-*p*-chlorobenzylidene-14-deoxy-11,12-didehydro-3,19-dinicotinate-andrographolide (**13**) ($IC_{50} = 6$ μM). Additionally, synthetic work by the same investigators on similar derivatives identified a number of α-glucosidase inhibitors including one with the *p*-(*N*,*N*-dimethyl)-C_6H_4 substitution (**14**) ($IC_{50} = 8.3$ μM).

Khusnutdinova et al. [21] synthesized a number of A-ring fused heterocycles of lupine, oleanane, ursane, and dammarane triterpenoids and investigated their α-glucosidase inhibitory activity. Out of these, the indolo- and pyrazino-fused triterpenoids showed more potency of enzyme inhibition than that of

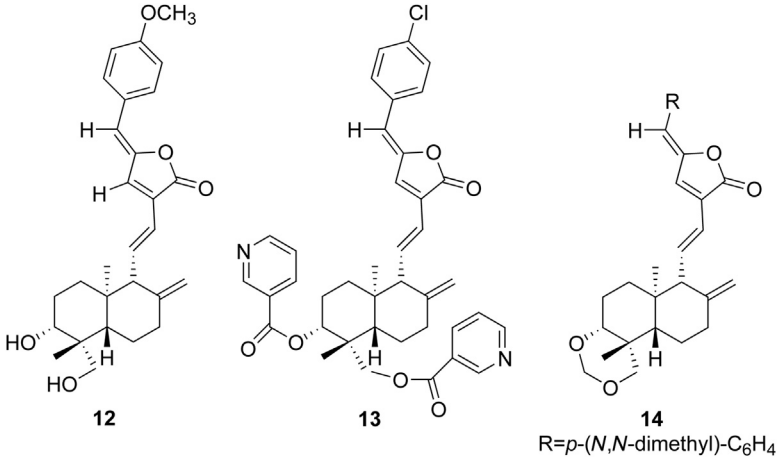

Figure 4.5 The alkylidene andrographolides. *Reproduced from U. Ghani, Re-exploring promising α-glucosidase inhibitors for potential development into oral anti-diabetic drugs: finding needle in the haystack, Eur. J. Med. Chem. 103 (2015) 133–162. © 2015 French Société de Chimie Thérapeutique published by Elsevier Masson SAS. All rights reserved.*

acarbose. Comparison of the activities of the compounds showed that the 2,3-indolotriterpenoids were more efficient inhibitors than the corresponding 3-oxo derivatives. The most potent in the series was 2,3-indolo-lup-20(29)-ene-28-oic acid (**15**; $IC_{50} = 1.8\ \mu M$) that exhibited ten-fold higher activity than that of betulonic acid (**16**; $IC_{50} = 18.4\ \mu M$). The 2,3-indolo-triterpenic acids of oleanone (**17**) and ursane (**18**) were next potent inhibitors of α-glucosidase ($IC_{50} = 5.5$ and $7.9\ \mu M$, respectively) including 3-oxo-oleanolic (**19**) and 3-oxo-ursolic (**20**) acids ($IC_{50} = 6.5$ and $22.5\ \mu M$, respectively). The indoles of lupine (**15**), oleanane (**17**), and ursane (**18**) bearing a carboxyl group at C_{17} showed more activity than the derivatives of allobetulin or dammarane (Fig. 4.6).

Recently, Sun et al. [22] performed chemical-epigenetic modification of the marine algicolous fungus *Aspergillus terreus* yielding biosynthesis of new and structurally diverse meroterpenoids and other natural products. Since the biosynthetic gene

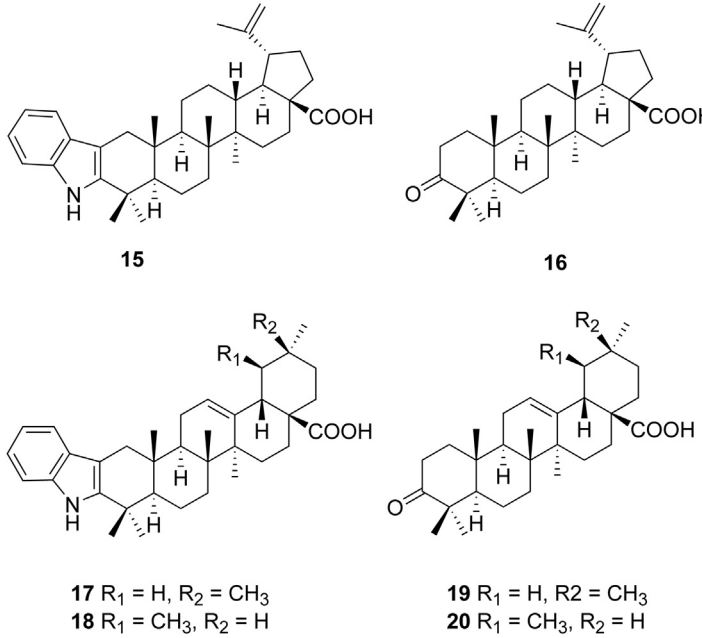

Figure 4.6 All the A-ring fused heterocycles of lupine, oleanane, ursane, and dammarane triterpenoids particularly the indolo- and pyrazino-fused triterpenoids possess promising activity.

pool of microorganisms is merely expressed under the normal culture conditions, it is essential to modify those conditions in order to stimulate transcription of silent genes that might induce biosynthesis of diverse natural products. Some of the identified compounds (Fig. 4.7) showed promising α-glucosidase inhibitory activity including (*R*,*E*)-3-(2,2-dimethylchroman-6-yl)-4-hydroxy-5-((2-(2-hydroxypropan-2-yl)-2,3-dihydrobenzofuran-5-yl)methylene)furan-2(5*H*)-one (**21**; $IC_{50} = 24.8\ \mu M$) and rubrolide S (**22**; $IC_{50} = 1.2\ \mu M$). The latter displayed noncompetitive inhibition of α-glucosidase ($K_i = 1.42\ \mu M$).

Oleanolic acid is a natural pentacyclic triterpenoid found in plants either as a glycoside or free compound with promising antitumor [23], antidiabetic [24], antimicrobial [3], and hepatoprotective activities [25]. It is a noncompetitive inhibitor of

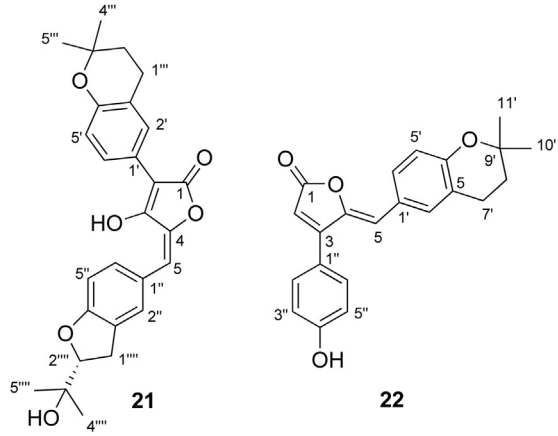

Figure 4.7 The natural meroterpenoids expressed by *Aspergillus terreus* fungus under modified culture conditions.

α-glucosidase with *in vivo* hypoglycemic effects [26,27]. Despite its diverse activity profile, high molecular weight, and hydrophobicity, oleanolic acid has always been a barrier to optimal bioavailability and therapeutic applications. Attempts have been made in the past to structurally modify oleanolic acid and its derivatives in order to increase the solubility and bioavailability while retaining or even improving its biological activities. These include amidation or oxidation of groups at C_3, esterification at C_{28}, and addition of a lactone between C_{12} and C_{28} positions [7,28,29]. Moreover, fluorination has shown to increase the bioavailability of oleanolic acid by enhancing its chemical stability, protein-binding affinity, and membrane permeability [30].

Recently, Zhong et al. [31] synthesized novel oleanolic acid analogs (Fig. 4.8) exhibiting α-glucosidase inhibition and *in vivo* hypoglycemic effects (compounds **23**−**34**). Compounds **23**, **24**, **25**, and **26** noncompetitively inhibited the enzyme ($K_i = 0.52$, 1.49, 0.88, and 1.19 μM, respectively). The condensation modification at the C_2 position was crucial for potent inhibition of α-glucosidase as observed in compound

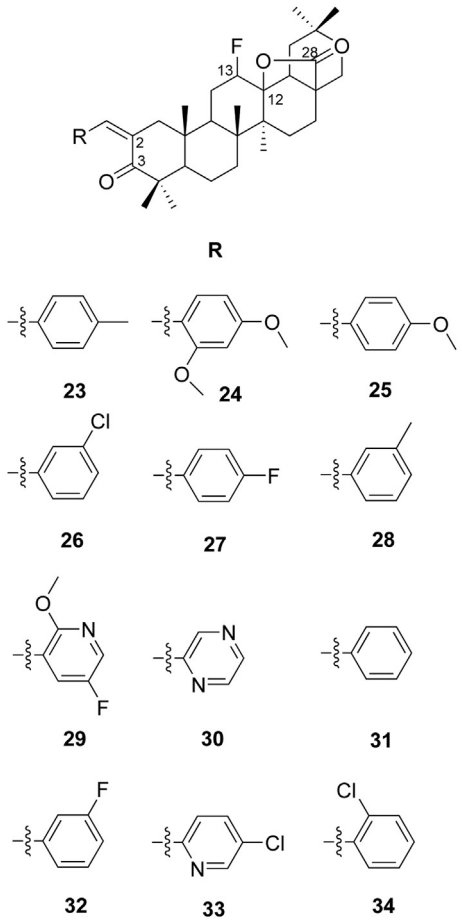

Figure 4.8 Synthetic analogs of oleanolic acid. In these compounds, the condensation modification at C_2 position is pivotal to potent inhibition of α-glucosidase. The compounds showed significant antihyperglycemic effect with ability to resist increase in blood glucose levels for up to 12 days.

23 ($IC_{50} = 0.33\ \mu M$), the most potent inhibitor in the series. Moreover, incorporating substituents at the *para*-position of the phenyl ring resulted in the improvement of inhibitory activity as seen in compounds **27** and **28** ($IC_{50} = 1.92$ and $2.74\ \mu M$, respectively). A comparable level of enzyme inhibition was exhibited by compounds **26**, **29**, **30** and **31**, **25**, **32**

owing to exchange of the phenyl ring at C_2 position with a pyridyl or pyrazine ring. Conversely, **33** and **34** displayed lower potencies apparently due to structural bulkiness introduced by the pyridyl and imidazole rings at the *para*-position of the phenyl ring. The *in vivo* hypoglycemic activity of the potent compounds **23**−**34** was also tested in diabetic mice. The compounds significantly decreased blood glucose levels at nine hours after oral administration except for compound **23**, the effect of which appeared in seven hours. The antihyperglycemic effect of the compounds was generally comparable to that of acarbose. Compound **26** exerted long term effect by maintaining lower blood glucose levels for two hours. Additionally, the target compounds were able to resist increase in blood glucose levels in diabetic mice for up to 12 days of initial administration followed by a decrease in the levels thereafter for up to 18 days. The mice showed significant glucose tolerance as observed in oral glucose tolerance test, with no changes in body weight.

Ursolic acid (**35**) is a triterpenoid natural product found in a number of medicinal plants and fruits (Fig. 4.9). The structural features of ursolic acid provide an important framework for developing and optimizing new derivatives as leads for drug development. Wu et al. [32] synthesized two series of ursolic acid analogs exhibiting α-glucosidase inhibitory activity. The ursolic acid ester analogs inhibited the enzyme with the IC_{50} range of 2.51−15.23 μM, all of which were more potent than ursolic acid alone. In these compounds the type of side chain and presence of large ester group at C_3 position compromised the activity in varying degrees. The second series of compounds (**36**−**39**) inhibited α-glucosidase with an IC_{50} range of 0.71−10.32 μM; their potency of inhibition depended on the type of condensation groups (Fig. 4.9). The activity of ursolic acid improved two-fold when its hydroxyl group was oxidized to a ketone (as in compound **36**; $IC_{50} = 2.47$ μM).

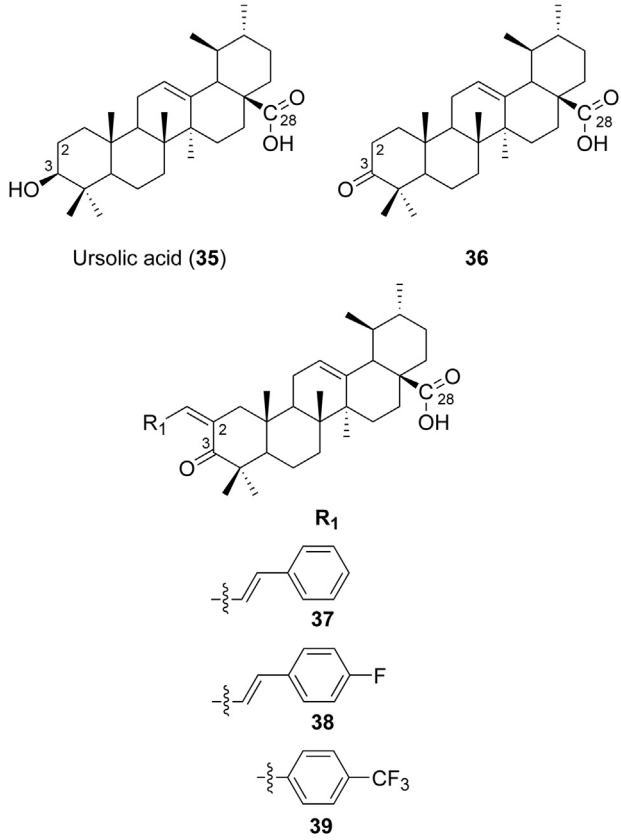

Figure 4.9 Ursolic acid analogs. The type of condensation groups mainly influences the activity of these inhibitors.

Similar analogs were synthesized based on this ketone including compounds **37** ($IC_{50} = 10.32\ \mu M$) and **38** ($IC_{50} = 7.49\ \mu M$), which were more promising than compound **36** indicating noticeable influence of the length of the substituent group on the activity. An inverse correlation was observed with the length of the substituent group and activity. Moreover, replacing the substituent groups at the C_2 position with a phenyl group substantially increased the enzyme inhibition as seen in compound **39** ($IC_{50} = 0.71\ \mu M$) bearing a *p*-trifluoromethyl benzaldehyde substituent.

4.2 Steroid derivatives

Tibolone is a synthetic derivative of 19-nortestosterone that mimics the action of estrogen especially in postmenopausal hormone replacement therapy. It has been shown to decrease blood glucose levels with improvement in insulin sensitivity of cells [33–36]. Atta-ur-Rahman et al. [37] conducted microbial transformation of tibolone by *Cunninghamella elagans* and *Gibberilla fujikuruoi* fungi that yielded a number of derivatives exhibiting promising inhibition of yeast α-glucosidase. Compounds carrying the $\Delta^{4(5)}$ bond with 3-oxo group conjugation, and a 6α- or 15α-hydroxy group exhibited potent inhibitory activity (**40**, **41**; $IC_{50} \leq 0.07$ μM each) (Fig. 4.10). The unconjugated $\Delta^{5(10)}$ compounds with a 6β-hydroxy group also showed comparable levels of activity similar to that of the conjugated ones. Additionally, the same group of investigators also conducted fungal transformation of cedryl acetate that yielded metabolites demonstrating promising α-glucosidase inhibition [38].

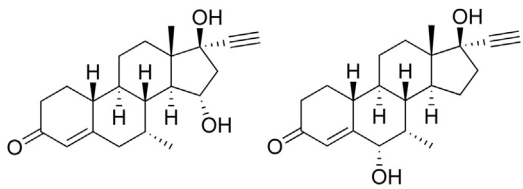

40 **41**

Figure 4.10 Steroids obtained from the microbial transformation of tibolone by *Cunninghamella elagans* and *Gibberilla fujikuruoi* fungi. *Reproduced from U. Ghani, Re-exploring promising α-glucosidase inhibitors for potential development into oral anti-diabetic drugs: finding needle in the haystack, Eur. J. Med. Chem. 103 (2015) 133–162.*

Mangifera plants are widely distributed in the tropical and subtropical regions of Asia. Some of the species of the genus are famous for their delicious mango fruit especially in Pakistan. *Mangifera mekongensis* plant is abundant in the tropical and subtropical areas of Asia including Southeast Asia. It is used in Vietnamese traditional medicine as antidiabetic,

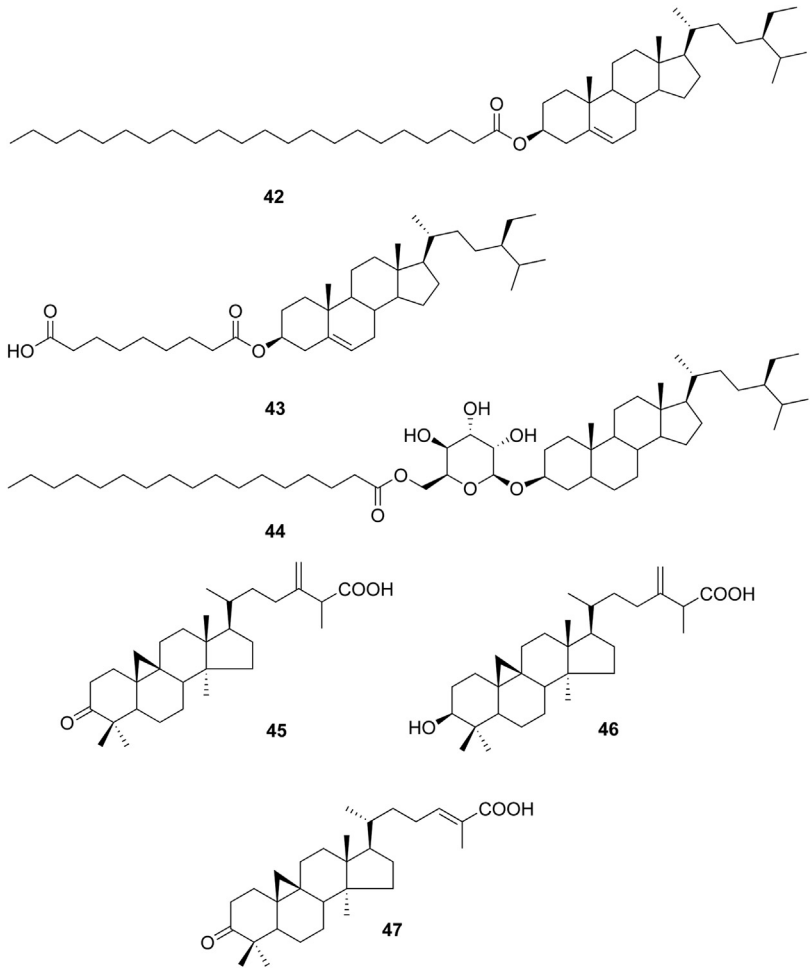

Figure 4.11 Natural steroid α-glucosidase inhibitors isolated from the bark of *Mangifera mekongensis*. Noteworthy inhibitors include mekongsterols B (**43**) and magiferonic acid (**47**).

vermifuge, and antiaging agent [39,40]. Previous work on the constituents of mango fruit identified compounds with antihypoglycemic and α-glucosidase inhibitory activities. The *n*-hexane extract of the bark of *M. mekongensis* has been reported to exhibit promising activity. Studies on natural steroids from the bark of *M. mekongensis* plant have recently identified two new steroids namely mekongsterols A (**42**) and B (**43**), and several known compounds with α-glucosidase inhibitory activity (Fig. 4.11). Sterols with saturated fatty ester chain or sugar group at C_3 (compounds **42**−**44**) showed potent activity. Additionally, the cycloartane triterpenes (compounds **45**−**47**) also showed promising enzyme inhibition. Among these compounds, mekongsterols B (**43**) and magiferonic acid (**47**) ($IC_{50} = 2.5$ and 1.2 μM) offer promising candidature for development of antidiabetic drugs [41].

References

[1] P.P. Wu, K. Zhang, Y.J. Lu, P. He, S.Q. Zhao, In vitro and in vivo evaluation of the antidiabetic activity of ursolic acid derivatives, Eur. J. Med. Chem. 80 (2014) 502−508.

[2] G. Chianese, S.R. Yerbanga, L. Lucantoni, A. Habluetzel, N. Basilico, D. Taramelli, et al., Antiplasmodial triterpenoids from the fruits of neem, *Azadirachta indica*, J. Nat. Prod. 73 (2010) 1448−1452.

[3] S. Fontanay, M. Grare, J. Mayer, C. Finance, R.E. Duval, Ursolic, oleanolic and betulinic acids: antibacterial spectra and selectivity indexes, J. Ethnopharmacol. 120 (2008) 272−276.

[4] F.S.G. Silva, P.J. Oliveira, M.F. Duarte, Oleanolic, ursolic, and betulinic acids as food supplements or pharmaceutical agents for type 2 diabetes: promise or illusion? J. Agric. Food Chem. 64 (2016) 2991−3008.

[5] J. Liu, D. Chen, P. Liu, M. He, J. Li, J. Li, et al., Discovery, synthesis, and structure-activity relationships of 20(S)-protopanaxadiol (PPD) derivatives as a novel class of AMPK α2β1γ1 activators, Eur. J. Med. Chem. 79 (2014) 340−349.

[6] C. Genet, A. Strehle, C. Schmidt, G. Boudjelal, A. Lobstein, K. Schoonjans, et al., Structure-activity relationship study of betulinic acid, a novel and selective TGR5 agonist, and its synthetic derivatives: potential impact in diabetes, J. Med. Chem. 53 (2010) 178−190.

[7] W. Nie, J.-G. Luo, X.-B. Wang, H. Yin, H.-B. Sun, H.-Q. Yao, et al., Synthesis of new α-glucosidase inhibitors based on oleanolic acid incorporating cinnamic amides, Chem. Pharm. Bull. 59 (2011) 1051–1056.
[8] T. Niwa, U. Doi, T. Osawa, Inhibitory activity of corn-derived bisamide compounds against alpha-glucosidase, J. Agric. Food Chem. 51 (2003) 90–94.
[9] D. Lopez, et al., Phytochemical composition, antiparasitic and α-glucosidase inhibition activities from *Pelliciera rhizophorae*, Chem. Cent. J. 9 (2015) 53–63.
[10] M. Spalding, M. Kainuma, L. Collins, World Atlas of Mangroves, Earthscan Ltd, London, 2010.
[11] W.M. Bandaranayake, Bioactivities, bioactive compounds and chemical constituents of mangrove plants, Wetlands Ecol. Manage. 10 (2002) 421–452.
[12] J. Wu, Q. Xiao, J. Xu, M.Y. Li, J.Y. Pan, M.H. Yang, Natural products from true mangrove flora: source, chemistry and bioactivities, Nat. Prod. Rep. 25 (2008) 955–981.
[13] I.E. Mohamed, E. Nur, M.I. Choudhary, S.N. Khan, Bioactive natural products from two Sudanese medicinal plants *Diospyros mespiliformis* and *Croton zambesicus*, Rec. Nat. Prod. 3 (2009) 198–203.
[14] T. Narender, et al., Synthesis of novel triterpene and *N*-allylated/*N*-alkylated niacin hybrids as α-glucosidase inhibitors, Eur. J. Med. Chem. 63 (2013) 162–169.
[15] W. Hou, Y. Li, Q. Zhang, X. Wei, A. Peng, L. Chen, et al., Triterpene acids isolated from *Lagerstroemia speciosa* leaves as alpha-glucosidase inhibitors, Phytother. Res. 23 (2009) 614–618.
[16] M.S. Akhtar, M.A. Khan, M.T. Malik, Hypoglycaemic activity of *Alpinia galanga* rhizome and its extracts in rabbits, Fitoterapia 73 (2002) 623–628.
[17] A.R. Srividya, S.P. Dhanabal, M.N.S. Kumar, P. Bavadia, Antioxidant and antidiabetic activity of *Alpinia Galanga*, Int. J. Pharmacog. Phytochem. Res. 3 (2010) 6–12.
[18] S. Ghosh, L. Rangan, Molecular docking and inhibition kinetics of α-glucosidase activity by labdane diterpenes isolated from tora seeds (*Alpinia nigra B.L. Burtt.*), Appl. Biochem. Biotechnol. 175 (2015) 1477–1489.
[19] H.W. Xu, G.F. Dai, G.Z. Liu, J.F. Wang, H.M. Liu, Synthesis of andrographolide derivatives: a new family of α-glucosidase inhibitors, Bioorg. Med. Chem. 15 (2007) 4247–4255.
[20] H.W. Xu, G. Liu, G. Gui-Fu, C. Wu, H. Liu, Modification of 15-akylidene andrographolide derivatives as alpha-glucosidase inhibitor, Drug Discov. Ther. 1 (2007) 73–77.
[21] E.F. Khusnutdinova, et al., Synthesis and evaluation of 2,3-indolotriterpenoids as new α-glucosidase inhibitors, Med. Chem. Res. 26 (2017) 2737–2742.

[22] K. Sun, G. Zhu, J. Hao, Y. Wang, W. Zhu, Chemical-epigenetic method to enhance the chemodiversity of the marine algicolous fungus, *Aspergillus terreus* OUCMDZ-2739, Tetrahedron 74 (2018) 83–87.
[23] R.P. Zhou, et al., Inhibition of mTOR signaling by oleanolic acid contributes to its anti-tumor activity in osteosarcoma cells, J. Orthop. Res. 29 (2011) 846–852.
[24] C. Tang, Y. Chen, S. Bai, G.Z. Yang, Advances in the study of structural modification and biological activities of oleanolic acid, Chin. J. Org. Chem. 33 (2013) 46–65.
[25] Y.F. Lu, J. Liu, K.C. Wu, C.D. Klaassen, Protection against phalloidin-induced liver injury by oleanolic acid involves Nrf2 activation and suppression of Oatp1b2, Toxicol. Lett. 232 (2015) 326–332.
[26] H.F. Ding, X. Hu, X.M. Xu, G.W. Zhang, D.M. Gong, Inhibitory mechanism of two allosteric inhibitors, oleanolic acid and ursolic acid on alpha-glucosidase, Int. J. Biol. Macromol. 107 (2018) 1844–1855.
[27] K. Kang, Z.K. Yang, J. Sheng, J.B. Liu, Q.Y. Xie, W. Zheng, et al., Oleanolic acid prevents cartilage degeneration in diabetic mice via PPAR gamma associated mitochondrial stabilization, Biochem. Bioph. Res. Co. 490 (2017) 834–840.
[28] C. Tang, et al., Synthesis and biological evaluation of oleanolic acid derivative-chalcone conjugates as alpha-glucosidase inhibitors, RSC Adv. 4 (2014) 10862–10874.
[29] S. Qian, et al., Synthesis and biological evaluation of oleanane triterpenoid with gamma-lactone functionality in ring C, Chem. J. Chin. Univ. 33 (2012) 969–975.
[30] A.S. Leal, R. Wang, J.A.R. Salvador, Y.K. Jing, Semisynthetic ursolic acid fluorolactone derivatives inhibit growth with induction of p21waf1 and induce apoptosis with upregulation of NOXA and downregulation of c-FLIP in cancer cells, ChemMedChem 7 (2012) 1635–1646.
[31] Y.-Y. Zhong, et al., Synthesis and biological evaluation of novel oleanolic acid analogs as potential α-glucosidase inhibitors, Eur. J. Med. Chem. 164 (2019) 706–716.
[32] P.P. Wu, et al., Synthesis and biological evaluation of novel ursolic acid analogs as potential α-glucosidase inhibitors, Sci. Reports 7 (2017) 45578.
[33] H.J.J. Kloosterboer, Tibolone: a steroid with a tissue-specific mode of action, Steroid Biochem. Mol. Biol. 76 (2001) 231–238.
[34] R.M.E. Vos, S.F.M. Krebbers, C.H.J. Verhoever, L.P.C. Delbressine, The in vivo human metabolism of tibolone, Drug Metab. Dispos. 30 (2002) 106–112.
[35] S. Steckelbroeck, Y.B. Oyesanmi, H.J. Kloosterboer, T.M. Penning, Tibolone is metabolized by the 3-alpha/3-beta-hydroxysteroid dehydrogenase activities of the four human isozymes of the aldo-keto reductase

1C subfamily: inversion of stereospecificity with a delta-5-(10)-3-ketosteroid, Mol. Pharmacol. 66 (2004) 1702–1711.
[36] M.J. Reed, H.J. Kloosterboer, Tibolone: a selective tissue estrogenic activity regulator (STEAR), Maturitas 48 (2004) 4–6.
[37] Atta-ur-Rahman, M.I. Choudhary, F.Z. Basha, G. Abbas, S.N. Khan, S.A.A. Shah, Science at the interface of chemistry and biology: discoveries of α-glucosidase inhibitors and antiglycation agents, Pure Appl. Chem. 79 (2007) 2263–2268.
[38] S. Sultan, et al., Fungal transformation of cedryl acetate and α-glucosidase inhibition assay, quantum mechanical calculations and molecular docking studies of its metabolites, Eur. J. Med. Chem. 62 (2013) 764–770.
[39] H.H. Pham, An Illustrated Flora of Vietnam, Youth Publishing House, Hochiminh City, 2000.
[40] B.K. Dang, M.T. Pham, V.Q. Ngo, T.B.O. Dang, Total phenolic content and anti-oxidant capacity of some spices and herbs grown in Vietnam, J. Post Harvest Technol. 1 (2013) 22–28.
[41] H.X. Nguyen, et al., α-Glucosidase inhibitors from the bark of *Mangifera mekongensis*, Chem. Cent. J. 10 (2016) 45–50.

CHAPTER FIVE

Azoles and related derivatives

Contents

Azoles are a group of compounds that contain a five-membered ring with nitrogen and other atoms such as sulfur and oxygen. Although they possess a range of biological activities, they are especially known as antifungal agents commonly prescribed in clinical practice [1]. The azole ring system is chemically diverse comprising thiadiazole, oxadiazole, triazole, imidazole, isoxazole, pyrazole, and other chemically related rings. Thiadiazoles contains a five-membered ring system with a sulfur and two nitrogen atoms. Natural thiadiazoles exist in four isomeric forms 1,3,4-, 1,2,3-, 1,2,5-, and 1,2,4-thiadiazole. Derivatives of 1,3,4-thiadiazole are highly active compounds demonstrating antibacterial, antifungal, anticancer, anticonvulsant, antiinflammatory, antiviral, and antileishmanial properties [2].

The oxadiazole ring system comprises one oxygen and two nitrogen atoms. The forms of oxadiazoles include 1,3,4-, 1,2,3-, 1,2,5-, and 1,2,4-oxadiazole. Substituted oxadiazoles have been identified as antidiabetic, anticonvulsant, anti-HIV, anti-Alzheimer's, antimicrobial, antiinflammatory, immunosuppressant, and anticancer agents. The 1,3,4-oxadiazole ring system

Alpha-glucosidase Inhibitors.
DOI: https://doi.org/10.1016/B978-0-08-102779-0.00005-8

has also been studied for its role in enzyme inhibition targeting cancer and other diseases. In this regard, derivatives of 1,3,4-oxadiazole have been reported to inhibit telomerase, methionine aminopeptidase, histone deacetylase, focal adhesion kinase, and thymidylate synthase enzymes [3].

Triazoles contain a five-membered ring system with three nitrogen and two carbon atoms. The isomeric forms of triazole, primarily conjugated with heterocyclic derivatives, exhibit diverse chemical and biological properties making them promising for drug development and other applications. The two tautomeric forms of the triazole ring namely 1,2,3-triazole and 1,2,4-triazole have attracted attention of the drug development community since they are promising for treatment of a variety of diseases. The ^{1}H and ^{4}H-1,2,4-triazole derivatives have been studied on a number of clinically important targets due to their interesting biological activity profile. The 1,2,4-triazole ring system, incorporated into antimicrobial, antiinflammatory, antimigraine, and CNS stimulatory drugs and their candidates, has been thoroughly studied. Examples include antimycotic drugs such as voriconazole, itraconazole, and fluconazole, anticonvulsant drugs such as estazolam, and antiviral drugs such as ribavirin. Triazole derivatives possess a wide range of biological activities, therefore, they are of focal interest in drug development. A number of 1,2,4-triazole-3-thione and 1,2,4-triazole-3-(4*H*)-thione derivatives have shown to exert promising *in vivo* activities including anticonvulsant, antidepressant, antibacterial, antiviral, anticancer, antifungal, antiinflammatory, analgesic, and antioxidant activities [4].

The biological activity profile of azoles and related derivatives also includes α-glucosidase inhibition. The scientific literature has witnessed a number of reports on azoles exhibiting promising inhibition of the enzyme. This chapter discusses promising azole derivatives and related compounds identified as α-glucosidase inhibitors.

5.1 Thiadiazoles, oxadiazoles, and triazoles

Kashtoh et al. [5] reported synthesis of a series of thiadiazole and oxadiazole derivatives. Although majority of the compounds showed moderate inhibition of yeast α-glucosidase, three oxadiazoles (**1**−**3**) and two thiadiazoles (**4** and **5**) are noteworthy to mention (Fig. 5.1). The former are all noncompetitive inhibitors ($K_i = 12$, 4.36, and 11.2 μM, respectively) whereas the latter are each competitive and noncompetitive inhibitors ($K_i = 6.0$ and 14.3 μM, respectively). The activity of the compounds is primarily dependent on the oxadiazole and thiadiazole moieties, the carbonyl oxygen and the substitutions on the aromatic rings.

The yeast α-glucosidase inhibitory profile of benzothiazole compounds containing the benzohydrazide moiety is also similar to that of thiadiazoles, especially for the compounds **6**, **7**, and **8** ($IC_{50} = 5.55$, 5.58, and 5.31 μM, respectively) (Fig. 5.2). Molecular docking showed strong binding affinity of the compounds to the *C*-terminal domain of α-glucosidase with no significant correlation of binding energies to IC_{50} values. Compounds bearing higher dipole moment and weaker hydrogen bonding interactions displayed lower inhibitory activity [6].

Recently, the synthetic diamine-bridged coumarinyl oxadiazole conjugates have shown to potently inhibit α-glucosidase ($IC_{50} = 0.07-0.76$ μM) [7]. The conjugates were synthesized using three different types of linkers namely phenylenediamine, benzidine, and 4,4′-oxydianiline. Generally, compounds from all the series displayed comparable inhibition of the enzyme. Compound **9** ($IC_{50} = 0.07$ μM) with the 4,4′-oxydianiline linker and the *meta*-bromo substitution on the aryl ring highest affinity to the enzyme in the series. Moreover, compounds possessing the phenylenediamine

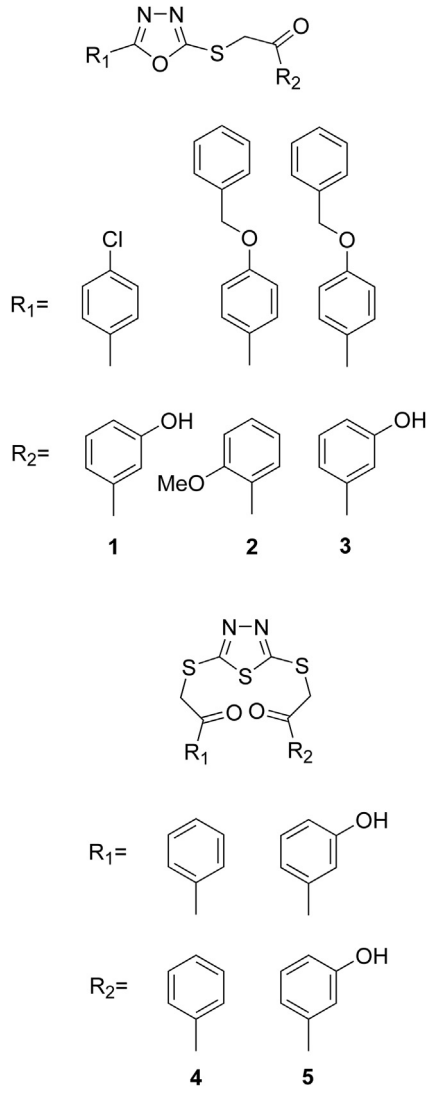

Figure 5.1 The thiadiazole and oxadiazole inhibitors of α-glucosidase. *Reproduced from U. Ghani, Re-exploring promising α-glucosidase inhibitors for potential development into oral anti-diabetic drugs: finding needle in the haystack, Eur. J. Med. Chem. 103 (2015) 133–162.*

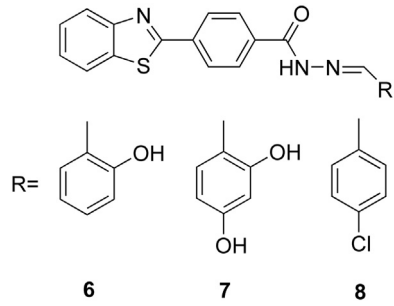

Figure 5.2 Benzothiazole derivatives containing the benzohydrazide moiety. *Reproduced from U. Ghani, Re-exploring promising α-glucosidase inhibitors for potential development into oral anti-diabetic drugs: finding needle in the haystack, Eur. J. Med. Chem. 103 (2015) 133–162. © 2015 French Société de Chimie Thérapeutique published by Elsevier Masson SAS. All rights reserved.*

linker also exhibited promising activity including the ones bearing electron-poor and electron-rich substituents ($IC_{50} = 0.11–2.18\ \mu M$). The position and the type of substituents played a central role in the activity. Conjugates containing the benzidine linker inhibited the enzyme with an IC_{50} range of $0.11–0.76\ \mu M$. Conjugates bearing the 4,4′-oxydianiline linker exhibited relatively higher level of inhibition potency. These include compound **10** ($IC_{50} = 0.09\ \mu M$) carrying a methyl group at the *para*-position of the aryl ring, and compound **11** ($IC_{50} = 0.09\ \mu M$) carrying a chloro substituent at the *ortho* and *para*-positions of the aromatic ring (Fig. 5.3).

A series of 4-substituted 1,2,3-triazoles conjugated with D-xylose, D-galactose, D-allose, and D-ribose sugars have been synthesized and screened for yeast maltase inhibitory activity. Compound **12**, a β-D-ribosyl triazole, exhibited highest potency among other derivatives studied ($IC_{50} = 3.8–24.7\ \mu M$) (Fig. 5.4). Molecular docking suggested that the target inhibitors bind to the enzyme active site by mimicking the transition state of the substrate. Moreover, the role of the N_3 atom in the

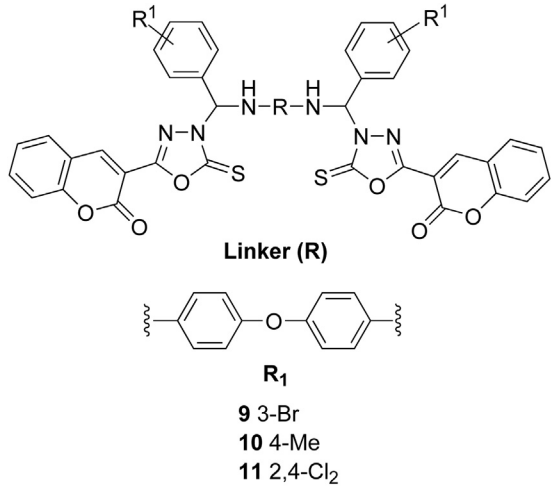

Figure 5.3 The diamine-bridged coumarinyl oxadiazole conjugates. Compounds possessing the phenylenediamine linker exhibited potent activity including the ones bearing electron-poor and electron-rich substituents.

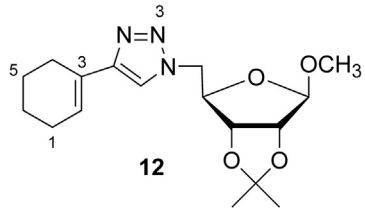

Figure 5.4 β-D-Ribosyl triazole: computational studies show that it acts as a transition state analog of α-glucosidase substrate. *Reproduced from U. Ghani, Re-exploring promising α-glucosidase inhibitors for potential development into oral anti-diabetic drugs: finding needle in the haystack, Eur. J. Med. Chem. 103 (2015) 133–162.*

triazole ring and the R_2 substituent is also important. Oral administration of some of these triazoles to normal rats also suppressed postprandial glucose levels [8].

Wang et al. [9] synthesized and evaluated a series of 5,6-diaryl-1,2,4-triazine thiazole derivatives as α-glucosidase

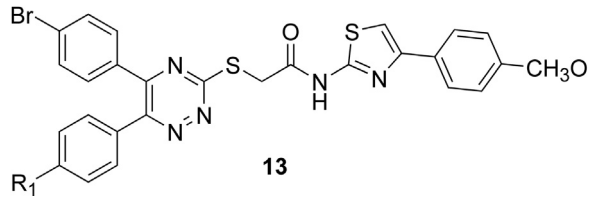

13

Figure 5.5 The 5,6-diaryl-1,2,4-triazine thiazole derivatives. Manipulation of R_1 substitution especially incorporation of electron-withdrawing groups such as fluorine or bromine yielded potent inhibitors of α-glucosidase.

inhibitors. Compound **13** ($IC_{50} = 2.8$ μM) bearing an R_1 bromine and an R_2 methoxy group exhibited highest level of enzyme inhibition (Fig. 5.5). A general comparison of the activities showed that incorporation of electron-withdrawing groups such as fluorine or bromine at R_1 position enhanced the level of inhibition. Therefore, the type of substitution at R_1 position has greater influence on α-glucosidase inhibition than the one at R_2.

5.2 Other related derivatives

5.2.1 Oxindoles

Synthesis and evaluation of oxindole derivatives for yeast α-glucosidase inhibitory activity have identified compounds **14**, **15**, and **16** ($IC_{50} = 2.71$, 11.41, and 14.2 μM, respectively) (Fig. 5.6). Molecular docking using a model of yeast α-glucosidase suggested that the oxindole moiety optimally fits into the active site pocket of the enzyme allowing important interactions with corresponding residues [10].

Luthra et al. synthesized a library of oxindole derivatives by scaffold hopping of known α-glucosidase inhibitors namely synthetic oxindole, natural piperidine and cytidine, and

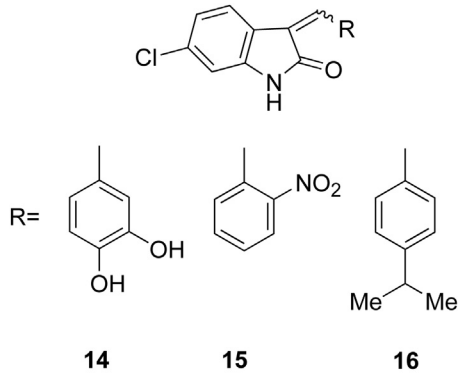

Figure 5.6 The oxindole α-glucosidase inhibitors. *Reproduced from U. Ghani, Re-exploring promising α-glucosidase inhibitors for potential development into oral anti-diabetic drugs: finding needle in the haystack, Eur. J. Med. Chem. 103 (2015) 133–162. © 2015 French Société de Chimie Thérapeutique published by Elsevier Masson SAS. All rights reserved.*

pyridofuranone derivative [11]. The final compounds displayed promising α-glucosidase inhibitory activity with an IC_{50} range of 0.64–10.22 μM (Fig. 5.7). Compound **17** was 3–4 fold more potent than its precursors that were initially used to design the library. The structural motifs in these compounds apparently responsible for α-glucosidase inhibition include the indole moiety, pyridine ring, and the amide group. Also, the C_5 fluoro substitution of the indole ring enhances the potency of inhibition as in compound **17** (a competitive inhibitor), which is three-fold more potent than the compounds **18** and **19**. In contrast, the compounds containing the nitro group (as in **20**) displayed less potency of inhibition probably due to its strong electron-withdrawing properties. Compounds **18** and **21** with amide moieties (pyrrolidine and piperidine) also showed promising enzyme inhibition.

5.2.2 2-Arylquinazolin-4(3*H*)-one derivatives

The yeast α-glucosidase inhibitory activity of 2-arylquinazolin-4(3*H*)-one derivatives is primarily dependent on the

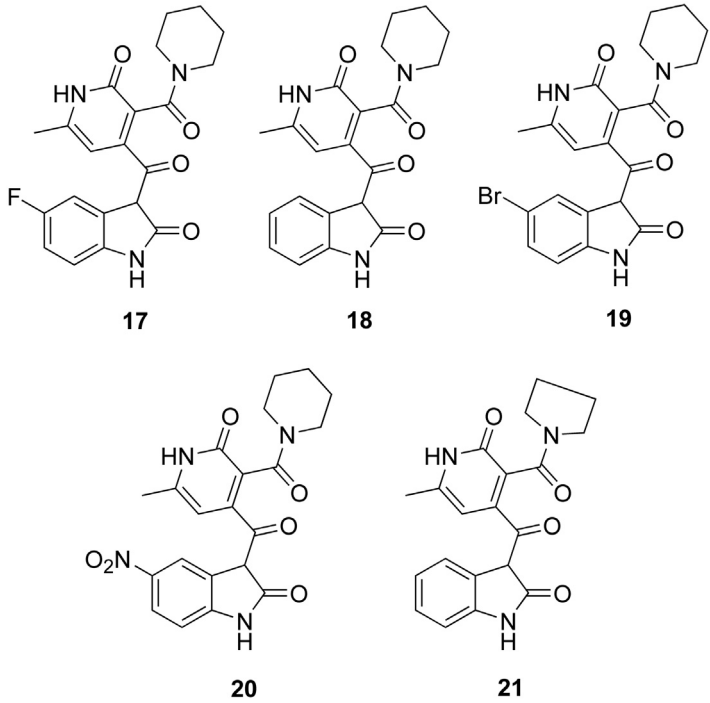

Figure 5.7 The oxindole derivatives synthesized by scaffold hopping of known α-glucosidase inhibitors such as synthetic oxindole, natural piperidine, cytidine, and pyridofuranone derivatives. The indole moiety, pyridine ring, and amide group are the structural motifs responsible for α-glucosidase inhibition.

2-arylquinazolin-4(3*H*)-one skeleton and the benzene ring at C_2 which is substituted with various electron-donating and withdrawing structures. Compound **22**, a competitive inhibitor of the enzyme and the most potent in the series, carries ethoxy and hydroxyl groups at C_3' and C_4' positions of the phenyl ring, respectively ($IC_{50} = 0.3\ \mu M$; $K_i = 0.43\ \mu M$) (Fig. 5.8). In this compound, presence of the two groups is essential for promising enzyme inhibition.

Compound **23** showed activity similar to that of **22** despite being substituted with only one methoxy group at C_4' position ($IC_{50} = 0.4\ \mu M$). However, it inhibited the enzyme

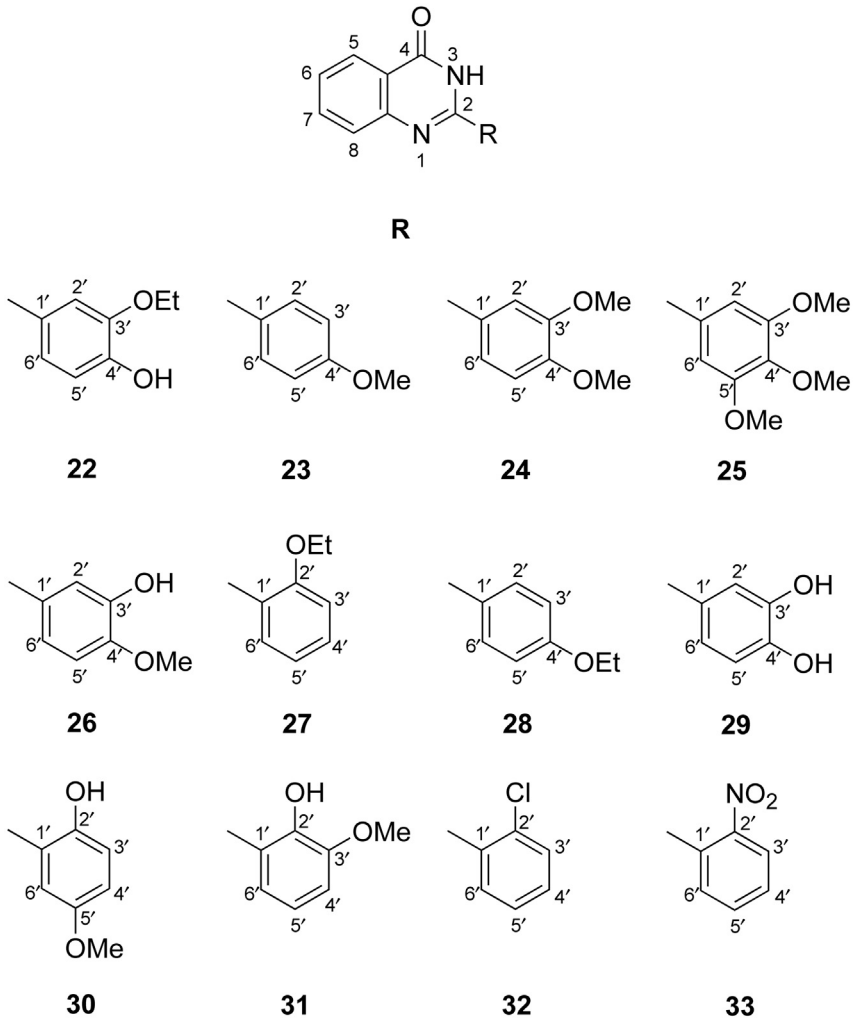

Figure 5.8 The activity of arylquinazoline derivatives primarily depends on their 2-arylquinazolin-4(3*H*)-one skeleton and the benzene ring at C_2 position, substituted with various electron-donating and withdrawing groups.

noncompetitively ($K_i = 0.25$ μM). When substituted with one more methoxy group at C_3' position (as in compound **24**), the activity was compromised by two-fold relative to that of **23** ($IC_{50} = 0.86$ μM; competitive inhibition, $K_i = 0.28$ μM).

Addition of one more methoxy group at C_5' position resulted in a significant loss of inhibitory activity as shown by compound **25** ($IC_{50} = 118$ μM). Replacement of the C_3' methoxy group of compound **24** with a hydroxyl group (as in **26**) suppressed its activity by almost two-fold ($IC_{50} = 1.9$ μM). Since the C_3' ethoxy group partly plays an important role in enabling the compound **22** to exhibit highest affinity to the enzyme, the activity profiling of other positions of the ethoxy group in the same benzene ring would be worth exploring. Example in this regard includes compound **27**, a mixed-type inhibitor substituted by an ethoxy group at C_2' rather than C_3', that also showed promising activity ($IC_{50} = 0.57$ μM; $K_i = 6.6$ μM).

In contrast, the C_4' ethoxy substitution in **28** drastically compromised its activity ($IC_{50} = 3.25$ μM). Interestingly, the dihydroxy substitution at C_3' and C_4' positions also afforded a potent inhibitor, that is, **29** ($IC_{50} = 1.5$ μM). Generally, the dihyroxy-substituted compounds tend to be more potent inhibitors than their monohydroxy counterparts. Moreover, the proportion of the distance between the methoxy and hydroxyl groups also contributed to the activity. Compound **30** ($IC_{50} = 1.15$ μM), which is substituted by the hydroxyl and ethoxy groups at C_2' and C_5', respectively, exhibited more potency than **31**, which is substituted by the same groups at C_2' and C_3', respectively ($IC_{50} = 14.6$ μM).

The chlorine analogs studied in the series also exhibited promising inhibitory activities. Chlorine and nitro substitutions at C_2' position of the phenyl ring were found to be most optimal for the activity within the series as observed in compounds **32** and **33** ($IC_{50} = 1.3$ and 1.45 μM, respectively) [12].

5.2.3 *Bis*-Indolylmethanes

Bis-Indolylmethanes naturally exist as metabolites in a wide range of plant species with aromatase inhibitory effects for cancer treatment, antimicrobial, and anti-HIV activities. They

possess therapeutic effects on estrogen metabolism in humans, and are used for treatment of fibromyalgia and irritable bowel disease [13]. Recently, a series of synthetic *bis*-indolylmethane sulfono-hydrazide derivatives have been identified as α-glucosidase inhibitors ($IC_{50} = 0.1-5.1$ μM) [13]. The activity of the compounds, bearing chloro groups at the phenyl ring, is mainly influenced by their number and position. Same applies to the nitro group-containing compounds in which the α-glucosidase inhibitory activity is mainly driven by the position of the nitro group. The structure and activity details of the compounds are cited in the original article [13].

5.2.4 Metallophthalocyanines

Macrocyclic compounds such as phthalocyanines have multiple applications in clinical, biomedical and analytical devices and procedures including gas sensors, catalysts, electrochromic devices, photosensitizers, and photodynamic cancer therapy [14]. Derivatives of phthalocyanine-containing aminopyrazole moieties are of interest in medicinal and pharmaceutical chemistry due to their wide spectrum of biological activities including antimicrobial activity [14]. Moreover, latest work on the aminopyrazole-substituted metallophthalocyanines has shown that they inhibit α-glucosidase in nanomolar range ($IC_{50} = 2.15-11.01$ nM/$K_i = 1.55-10.85$ nM). The compounds demonstrated much higher potency of α-glucosidase inhibition than that of acarbose especially the phthalonitrile derivative (**34**; $IC_{50} = 11.01$ nM/$K_i = 10.85$ nM) and its metal complex chloromanganese(III) phthalocyanine (**35**; $IC_{50} = 2.15$ nM/$K_i = 1.55$ nM), as shown in Fig. 5.9.

5.2.5 Thiobarbiturates

Barbiturates or malonylurea compounds are commonly used as anesthetics, and for treatment of epilepsy, anxiety, and psychiatric diseases. Similar to thiouracil, they carry various

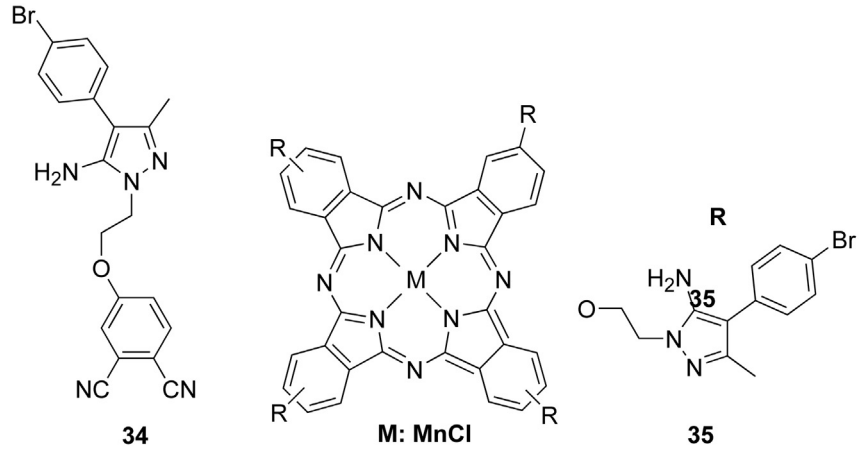

Figure 5.9 The aminopyrazole-substituted metallophthalocyanines inhibit α-glucosidase in nanomolar range.

substituents at C_5 position which influence their activity and lipid solubility [15]. The effects of the C_5 substitution on yeast α-glucosidase inhibitory activity have been explored using various synthetic 5-arylidene-*N*,*N*′-diethylthiobarbituric acid derivatives [15]. The compounds exhibited varying degree of enzyme inhibition with noticeable activities by compounds **36**, **37**, and **38** (Fig. 5.10). Compound **37**, the most potent in the series ($IC_{50} = 0.6$ nM), is a noncompetitive inhibitor carrying three hydroxyl groups at the 2′, 3′, and 4′ positions. It appears that these hydroxyl groups are essential for activity since compounds containing the hydroxyl groups either at 3′ and 4′ positions or at 4′ position alone markedly displayed weak inhibitory activities. Compound **38**, with a naphthyl substitution, showed more potency of inhibition ($IC_{50} = 19.18$ μM) than the one bearing a phenyl substitution. Interestingly, introduction of a nitro group at 3′ position of the phenyl substitution dramatically enhanced the potency as seen in compound **36** ($IC_{50} = 18.91$ μM). However, presence of a nitro group at other positions of the phenyl substitution did not yield promising inhibitors.

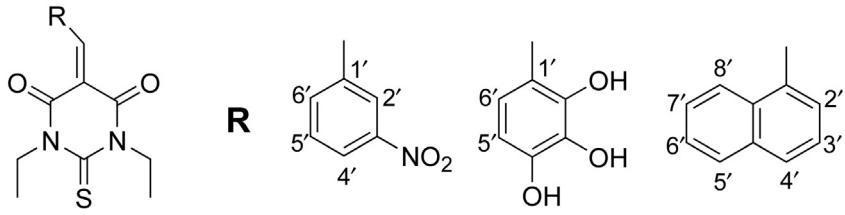

36 **37** **38**

Figure 5.10 The 5-arylidene-*N*,*N*′-diethylthiobarbituric acid derivatives. Presence of hydroxyl groups in compound **37** ($IC_{50} = 0.6$ nM) is essential for promising enzyme inhibition.

5.2.6 Carbazoles and hydrazone-bridged thiazole-pyrrole derivatives

Carbazoles and hydrazone-bridged thiazole-pyrrole derivatives have been previously synthesized and reported as antimicrobial agents [16–18]. The compounds are an emerging class of α-glucosidase inhibitors, and the literature has started to witness reports on 1,2,4-triazine-carbazoles [19], 1,2,3-triazole-carbazoles [20], thiosemicarbazines [21], and chromone-hydrazone derivatives [22].

Ghani et al. [23] recently identified carbazoles and hydrazone-bridged thiazole-pyrrole derivatives as α-glucosidase inhibitors that add new structural diversity to α-glucosidase inhibitors discovered to date (Fig. 5.11). The carbazole series of derivatives were identified as noncompetitive inhibitors of yeast α-glucosidase. The most potent inhibitor in the series was **39** containing the 2-benzoimidazole substitution ($K_i = 0.17$ μM) that appears to play a primary role in the enzyme inhibition. A substantial loss of the inhibitory activity was observed when the 2-benzoimidazole group was replaced by a 2-benzothiazole group (**40**; $K_i = 8.25$ μM). The rings of both substitutions differ only by a nitrogen and a sulfur atom, which markedly discriminated their activities. The –NH group of the benzoimidazole moiety is highly selective for

enzyme inhibition apparently due to its participation in forming important hydrogen bonds with the enzyme active site. Compound **41** ($K_i = 11.75\ \mu M$) bearing the 2-benzoxazole ring exerts inhibitory effects similar to that of compound **40**. Moreover, compounds **42** and **43** also exhibited similar levels of inhibition ($K_i = 14.53$ and $14.35\ \mu M$, respectively). In the

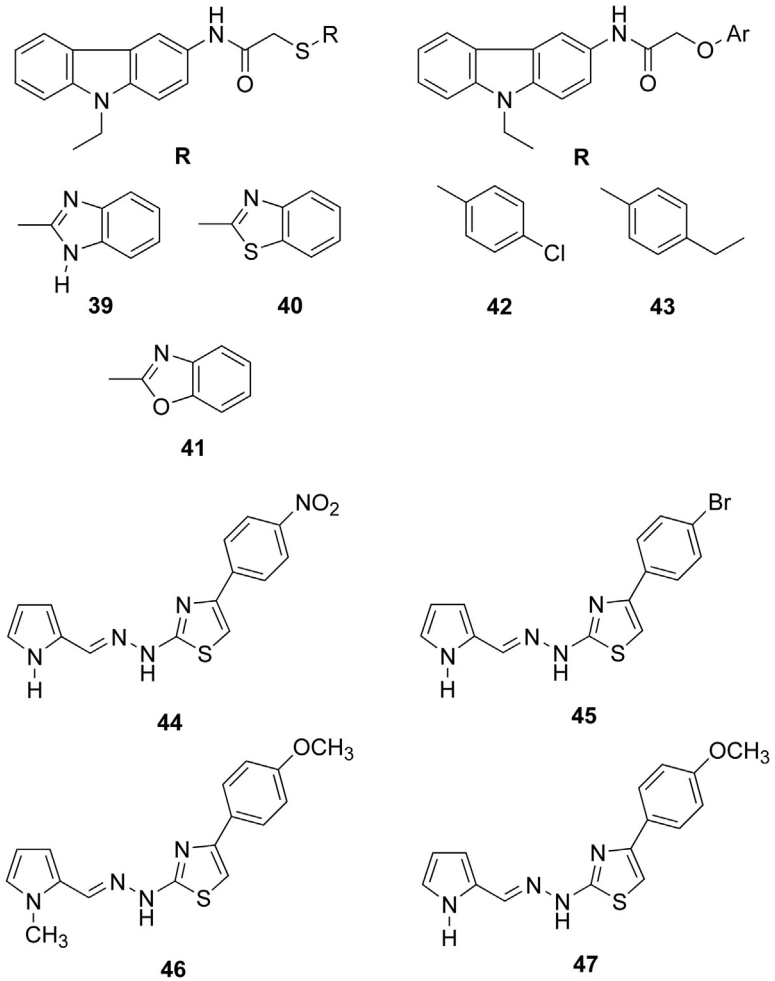

Figure 5.11 The carbazoles (**39**–**43**) and hydrazone-bridged thiazole-pyrrole inhibitors (**44**–**47**) of α-glucosidase offer new structural diversity to antidiabetic drug development.

carbazole series of compounds, the order of potency is based on the type of the substituent ring, that is, imidazole > thiazole > oxazole.

Ghani et al. [23] also studied hydrazone-bridged thiazole-pyrrole derivatives which demonstrated competitive enzyme inhibition. Promising inhibitors in this series include compounds **44** bearing a 4-nitrophenyl group ($K_i = 3.03$ μM), and **45** with a 4-bromophenyl group ($K_i = 3.18$ μM). Both compounds exhibited similar levels of activity despite being different only by a nitro and a bromo group. Moreover, compounds **46** ($K_i = 9.18$ μM) and **47** ($K_i = 6.7$ μM), which are chemically different only by a methyl group on the pyrrole ring, exhibited different levels of potencies. Comparison of their activities showed that the absence of the methyl group in compound **47** is substantially favorable for α-glucosidase inhibition. The carbazoles and hydrazone-bridged thiazole-pyrrole inhibitors of α-glucosidase offer new structural diversity that can be further explored for antidiabetic drug development.

References

[1] D. Allen, D. Wilson, R. Drew, J. Perfect, Azole antifungals: 35 years of invasive fungal infection management, Expert Rev. Anti Infect. Ther. 13 (2015) 787–798.

[2] A.K. Jain, et al., 1,3,4-Thiadiazole and its derivatives: a review on recent progress in biological activities, Chem. Biol. Drug Des. 81 (2013) 557–576.

[3] A. Zarghi, Z. Hajimahdi, Substituted oxadiazoles: a patent review (2010–2012), Expert Opin. Ther. Patents 23 (2013) 1209–1232.

[4] S.G. Küçükgüzel, P. Çıkla-Süzgün, Recent advances bioactive 1,2,4-triazole-3-thiones, Eur. J. Med. Chem. 97 (2015) 830–870.

[5] H. Kashtoh, et al., Oxadiazoles and thiadiazoles: novel α-glucosidase inhibitors, Bioorg. Med. Chem. 22 (2014) 5454–5465.

[6] M. Taha, et al., Synthesis of novel inhibitors of α-glucosidase based on the benzothiazole skeleton containing benzohydrazide moiety and their molecular docking studies, Eur. J. Med Chem. 92 (2015) 387–400.

[7] M. Kazmi, et al., A new entry into the portfolio of α-glucosidase inhibitors as potent therapeutics for type 2 diabetes: design, bioevaluation and

one-pot multi-component synthesis of diamine-bridged coumarinyl oxadiazole conjugates, Bioorg. Chem. 77 (2018) 190–202.
[8] S.B. Ferreira, et al., Synthesis, biological activity, and molecular modeling studies of *1H*-1,2,3-triazole derivatives of carbohydrates as α-glucosidases inhibitors, J. Med. Chem. 53 (2010) 2364–2375.
[9] G. Wang, Z. Peng, Z. Gong, Y. Li, Synthesis, biological evaluation, and docking studies of novel 5,6-diaryl-1,2,4-triazine thiazole derivatives as a new class of α-glucosidase inhibitors, Bioorg. Chem. 78 (2018) 195–200.
[10] M. Khan, et al., Discovery of novel oxindole derivatives as potent α-glucosidase inhibitors, Bioorg. Med. Chem. 22 (2014) 3441–3448.
[11] T. Luthra, K.N. Lalitha, R. Agarwal, A. Uma, S. Sen, Design, synthesis and in vitro study of densely functionalized oxindoles as potent α-glucosidase inhibitors, Bioorg. Med. Chem. 26 (2018) 4996–5005.
[12] K. Javaid, et al., 2-Arylquinazolin-4(*3H*)-ones: a new class of α-glucosidase inhibitors, Bioorg. Med. Chem. 23 (2015) 7417–7421.
[13] M. Gollapalli, et al., Synthesis of bis-indolylmethane sulfonohydrazides derivatives as potent α-glucosidase inhibitors, Bioorg. Chem. 80 (2018) 112–120.
[14] E. Guzel, et al., Aminopyrazole-substituted metallophthalocyanines: preparation, aggregation behavior, and investigation of metabolic enzymes inhibition properties, Arch. Pharm. Chem. Life Sci. 352 (2019) e1800292.
[15] M. Khan, et al., Synthesis, molecular modeling and biological evaluation of 5-arylidene-N,N-diethylthiobarbiturates as potential α-glucosidase inhibitors, Med. Chem. 15 (2019) 175–185.
[16] Z.A. Kaplancikli, Synthesis of some novel carbazole derivatives and evaluation of their antimicrobial activity, Marmara Pharm. J. 15 (2011) 105–109.
[17] Z.A. Kaplancikli, et al., Synthesis, antimicrobial activity and cytotoxicity of some new carbazole derivatives, J. Enz. Inh. Med. Chem. 27 (2012) 868–874.
[18] L. Yurttaş, Y. Özkay, Z.A. Kaplancıklı, Y. Tunalı, H. Karaca, Synthesis and antimicrobial activity of some new hydrazone-bridged thiazole-pyrrole derivatives, J. Enz. Inh. Med. Chem. 28 (2013) 830–835.
[19] G. Wang, et al., Synthesis and biological evaluation of novel 1,2,4-triazine derivatives bearing carbazole moiety as potent α-glucosidase inhibitors, Bioorg. Med. Chem. Lett. 26 (2016) 2806–2809.
[20] S. Iqbal, et al., New carbazole linked 1,2,3-triazoles as highly potent non-sugar α-glucosidase inhibitors, Bioorg. Chem. 74 (2017) 72–81.
[21] M. Wos, et al., Novel thiosemicarbazide derivatives with 4-nitrophenyl group as multi-target drugs: α-glucosidase inhibitors with antibacterial and antiproliferative activity, Biomed. Pharmacother. 93 (2017) 1269–1276.

[22] G. Wang, et al., Synthesis, biological evaluation and molecular docking studies of chromone hydrazone derivatives as α-glucosidase inhibitors, Bioorg. Med. Chem. Lett. 27 (2017) 2957–2961.
[23] U. Ghani, A. Albarrag, L. Yurttaş, F. Demirci, Z.A. Kaplancikli, Carbazoles and hydrazone-bridged thiazole-pyrrole derivatives as new inhibitors of α-glucosidase, Chem. Select 3 (2018) 7921–7925.

CHAPTER SIX

Cyclitols and miscellaneous inhibitors

Contents

6.1 Cyclitols

As discussed in Chapter 2: Natural and synthetic sugar mimics, the *Salacia* plant species is known to possess *in vivo* antidiabetic effects [1]. *Salacia reticulata*, commonly known as kothala-himbutu in Southeast Asia [2], is also reported to contain thiocyclitol (**1**) (Fig. 6.1). It is a novel compound with a 13-membered ring structure first isolated by Oe and Ozaki [3] exhibiting potent α-glucosidase inhibitory activity (IC_{50} rat intestinal maltase = 0.23 μM; rat intestinal sucrase = 0.19 μM)

Alpha-glucosidase Inhibitors.
DOI: https://doi.org/10.1016/B978-0-08-102779-0.00006-X

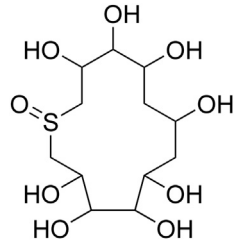

1

Figure 6.1 The thiocyclitol demonstrates significant α-glucosidase inhibitory activity and antihyperglycemic effects in maltose and sucrose-loaded rats. *Reproduced from U. Ghani, Re-exploring promising α-glucosidase inhibitors for potential development into oral anti-diabetic drugs: finding needle in the haystack, Eur. J. Med. Chem. 103 (2015) 133–162. © 2015 French Société de Chimie Thérapeutique published by Elsevier Masson SAS. All rights reserved.*

comparable to that of salacinol. Additionally, it showed significant antihyperglycemic effects in maltose and sucrose-loaded rats. Muraoka et al. [4] redetermined the structure of thiocyclitol and claimed that it was actually the de-*O*-sulfonated kotalanol as supported by spectral data but with a subtle deviation allowing to consider with a fair degree of confidence that these two compounds are either the same or have similar structure [4].

Pluchea indica, a traditional herb ubiquitous in South Asia carries antioxidant, antiulcer, and antiinflammatory properties. The leaves of the herb have been used as tea to treat diabetes, which is scientifically supported by *in vivo* experiments on diabetic rats [5]. Arsiningtyas et al. [6] identified five derivatives of caffeoylquinic acid from the herb leaves carrying rat intestinal maltase inhibitory activity. In these compounds, the increasing number of caffeoyl groups bound to quinic acid is central to high affinity to rat intestinal α-glucosidase. Furthermore, the methyl esterification of the quinic acid carboxylic group has important contribution to inhibition of the enzyme. Examples include 3,4,5-tri-*O*-caffeoylquinic acid methyl ester, 3,4,5-tri-*O*-caffeoylquinic acid, and 1,3,4,5-tetra-*O*-caffeoylquinic acid ($IC_{50} = 2.0$, 13, and 11 μM, respectively).

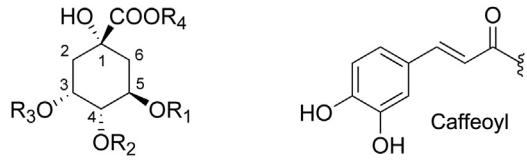

2 R_1=H, R_2=R_3=caffeoyl, R_4=Me
3 R_1=R_2=caffeoyl, R_3=H, R_4=Me

Figure 6.2 In the methylated derivatives of dicaffeoylquinic acid, the number and position of the caffeoyl groups primarily determine the potency of α-glucosidase inhibition. *Reproduced from U. Ghani, Re-exploring promising α-glucosidase inhibitors for potential development into oral anti-diabetic drugs: finding needle in the haystack, Eur. J. Med. Chem. 103 (2015) 133–162. © 2015 French Société de Chimie Thérapeutique published by Elsevier Masson SAS. All rights reserved.*

Gynura divaricata is used for treatment of diabetes in Chinese traditional medicine. Detailed phytochemical analysis of the plant identified caffeoylquinic acid derivatives possessing yeast α-glucosidase inhibitory activity. The methylated derivatives of dicaffeoylquinic acid such as methyl-3,4-dicaffeoylquinate (**2**) (IC_{50} = 12.23 μM) and methyl 4,5-dicaffeoylquinate (**3**) (Fig. 6.2) (IC_{50} = 13.08 μM) were more potent than their non-methylated counterparts, confirming previous studies that suggested that the number and position of the caffeoyl groups in the quinic acid derivatives primarily determine their potency of enzyme inhibition [5].

6.2 Polycyclitols

Novel synthetic bicyclitols featuring conduritol and carbasugar hybrid molecules have been reported to selectively inhibit yeast α-glucosidase (Fig. 6.3). The decalin-based carbasugar analog (**4**; K_i = 12 μM) showed more promising activity than the hydrindane-based polyol (**5**; K_i = 84 μM).

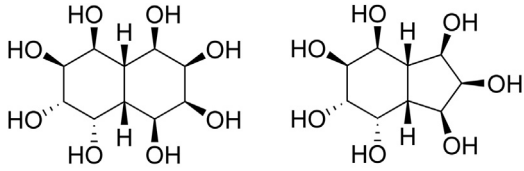

4 5

Figure 6.3 Bicyclitols: the conduritol and carbasugar hybrid molecules are highly selective to α-glucosidase inhibition. *Reproduced from U. Ghani, Re-exploring promising α-glucosidase inhibitors for potential development into oral anti-diabetic drugs: finding needle in the haystack, Eur. J. Med. Chem. 103 (2015) 133–162.*

However, both of the compounds including other diastereomeric isomers were inactive against almond β-glucosidase, galactosidases, and mannosidases. The apparent selective affinity of the inhibitors for α-glucosidase can be explained by the influence of subtle stereochemical variations in their structures [7].

6.3 Aminocyclitols

Two new diastereomeric amine-linked diquercitols (**6** and **7**) from natural (+)-*proto*-quercitol have been synthesized by Worawalai et al. [8] (Fig. 6.4). The compounds inhibited rat intestinal maltase ($IC_{50} = 3.1$ and 3.6 μM, respectively) and sucrase ($IC_{50} = 3.7$ and 4.0 μM, respectively) more potently than yeast α-glucosidase ($IC_{50} = 32.3$ and 40.1 μM, respectively). The cyclitol moiety and the *N*-linked glycosidic bond make these compounds more promising than the original aminoquercitol.

Additionally, the bioconjugates of (+)-*proto*-quercitol and cinnamic analogs called quercitylcinnamates also have been synthesized that selectively inhibited rat intestinal maltase and

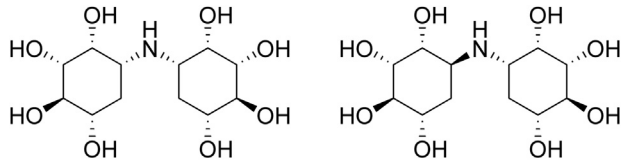

Figure 6.4 The cyclitol moiety and the *N*-linked glycosidic bond make diastereomeric amine-linked diquercitols more potent than the native aminoquercitol. *Reproduced from U. Ghani, Re-exploring promising α-glucosidase inhibitors for potential development into oral anti-diabetic drugs: finding needle in the haystack, Eur. J. Med. Chem. 103 (2015) 133–162. © 2015 French Société de Chimie Thérapeutique published by Elsevier Masson SAS. All rights reserved.*

sucrase with higher potency than their precursors. The conjugates were identified as mixed-type inhibitors of the target enzymes [9].

6.4 Conduritols

Recently, four novel conduritol derivatives containing the indoline and indole moieties have been synthesized as bacterial (*Bacillus stearothermophilus*) α-glucosidase inhibitors (IC_{50} range = 11–18 μM) (Fig. 6.5). Variations in the activities of these indole conduritols (**8**–**11**) are primarily due to the type of groups in the *ortho*, *meta* and *para* positions to the OAc and OH moieties [10].

6.5 Inositols

Inositol is one of the most common members of naturally occurring cyclitols. *Myo*-inositol, a stereoisomer of inositol plays essential roles in cellular function and metabolism [11–13].

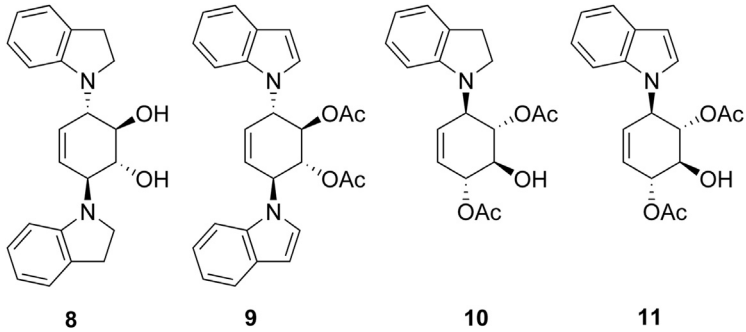

Figure 6.5 The novel conduritol derivatives bearing indoline and indole moieties. *Reproduced from U. Ghani, Re-exploring promising α-glucosidase inhibitors for potential development into oral anti-diabetic drugs: finding needle in the haystack, Eur. J. Med. Chem. 103 (2015) 133–162. © 2015 French Société de Chimie Thérapeutique published by Elsevier Masson SAS. All rights reserved.*

Four new isomeric hydroxy-skipped *bis*-homoinositol analogs have been synthesized from both enantiomers of 5-hydroxymethyl-2-cyclohexenone. Three of these compounds (**12**–**14**) inhibited yeast α-glucosidase with IC_{50} values of 16, 18.5 and 6.5 μM, respectively (Fig. 6.6). The structures of the compounds mimic the transition state of glucosidase substrate [14].

6.6 Miscellaneous derivatives

6.6.1 Anthraquinones

Yang et al. [15] studied four anthraquinones from the extract of *Polygonum multiflorum* plant namely emodin (**15**), aloe-emodin (**16**), physcion (**17**) and rhein (**18**) (IC_{50} = 4.12, 4.56, 5.32, 5.68 μM, respectively) (Fig. 6.7), by employing a new assay method for yeast α-glucosidase inhibitory activity with maltose as a substrate using LC-MS.

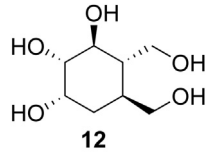

12

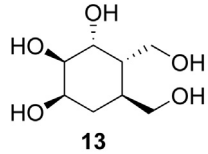

13

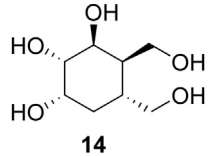

14

Figure 6.6 The homoinositol analogs mimic the transition state of glucosidase substrate. *Reproduced from U. Ghani, Re-exploring promising α-glucosidase inhibitors for potential development into oral anti-diabetic drugs: finding needle in the haystack, Eur. J. Med. Chem. 103 (2015) 133–162. © 2015 French Société de Chimie Thérapeutique published by Elsevier Masson SAS. All rights reserved.*

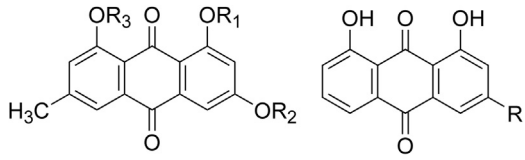

15 R_1=H, R_2=H, R_3=H
16 R=CH_2OH
17 R_1=H, R_2=CH_3, R_3=H
18 R=COOH

Figure 6.7 Natural anthraquinones: emodin, aloe-emodin, physcion and rhein. *Reproduced from U. Ghani, Re-exploring promising α-glucosidase inhibitors for potential development into oral anti-diabetic drugs: finding needle in the haystack, Eur. J. Med. Chem. 103 (2015) 133–162. © 2015 French Société de Chimie Thérapeutique published by Elsevier Masson SAS. All rights reserved.*

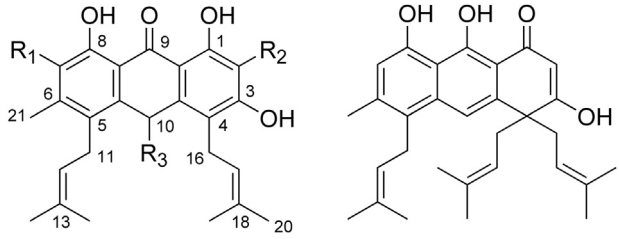

19 R_1=H, R_2=prenyl, R_3=OH
21 R_1=prenyl, R_2=H, R_3=H

20

Figure 6.8 Natural anthranols and quinones. The prenyl group at the C_2 position is central to potent α-glucosidase inhibition by kenganthranol B (**19**). *Reproduced from U. Ghani, Re-exploring promising α-glucosidase inhibitors for potential development into oral anti-diabetic drugs: finding needle in the haystack, Eur. J. Med. Chem. 103 (2015) 133–162. © 2015 French Société de Chimie Thérapeutique published by Elsevier Masson SAS. All rights reserved.*

The stem bark of *Harungana madagascariensis* contains anthranol and quinone α-glucosidase inhibitors. Kouam et al. (2006) [16] reported a number of yeast α-glucosidase inhibitors that include kenganthranol B (**19**), harunganin (**20**) and harunganol B (**21**) (IC_{50} = 6.3, 6.0 and 12 μM, respectively) (Fig. 6.8). Kenganthranol B was most potent among the compounds; its activity was primarily dependent on the prenyl group at C_2 position when compared to relatively less potent harunganol B carrying the prenyl group at C_7 position.

6.6.2 Sarcoviolins and terphenyl derivatives

Natural terphenyls are mainly *p*-terphenyls composed of C_{18} tricyclic or polycyclic aromatic structure that commonly possess an aromatic or a *p*-quinone group in the central ring with an additional oxygen atom. One of their functions is to provide pigmentation to mushrooms and other fungi. Their biosynthesis in fungi involves the shikimate-chorismate pathway which finally leads to arylpyruvic acid. The *p*-terphenyls

possess a range of biological activities including antioxidant, neuroprotective, antimicrobial, cytotoxic and immunosuppressive effects. Ma et al. [17] the isolated two sarcoviolins and seven terphenyl derivatives from the edible mushroom *Sarcodon leucopus*. Sarcoviolin β (**22**) presented highest yeast α-glucosidase inhibitory activity ($IC_{50} = 0.58\ \mu M$) compared to that of epi-sarcoviolin β (**23**) ($IC_{50} = 1.07\ \mu M$) and other compounds ($IC_{50} = 1-10\ \mu M$). Sarcoviolins with $N_1\beta$ and $C_2\beta$ configurations have important contribution to enzyme inhibition. Compounds with *cis* configuration at $N_1\beta$ and $C_2\beta$, as in sarcoviolin β (**22**) and sarcodonin α (**24**) ($IC_{50} = 1.23\ \mu M$) were more potent than those with *trans* configuration. The activity of the *p*-terphenyl derivatives (**25**−**27**) directly correlated to increasing number of hydroxyl groups. The compound structures are presented in Fig. 6.9. A comprehensive list and discussion on the natural terphenyls with α-glucosidase inhibitory activity can be accessed from the original reference [18].

6.6.3 Stilbenes

Stilbenoids, namely 13-hydroxykompasinol A (**28**) and scirpusin C (**29**), isolated from the seeds of *Syagrus romanzoffiana* show strong inhibitory activity against bacterial α-glucosidase from *B. stearothermophilus* ($IC_{50} = 6.5$ and $5.0\ \mu M$, respectively). Additionally, kompasinol A (**30**) and 3,30,4,5,50-pentahydroxytrans-stilbene (**31**) (Fig. 6.10) isolated from the same plant were also able to lower postprandial blood glucose levels *in vivo* [19].

6.6.4 Stilbene-based urea derivatives

Kim et al. [20] designed and synthesized novel stilbene-based achiral (*E*)-1-phenyl-3-(4-strylphenyl)urea derivatives that competitively inhibited yeast α-glucosidase (Fig. 6.11). The rationale is based on the structural analogy of stilbenes to resveratrol (**32**), a noncompetitive inhibitor of α-glucosidase ($K_i = 21.5\ \mu M$) [19]. The urea derivatization of stilbene-based

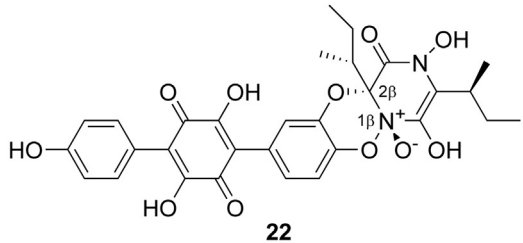

22

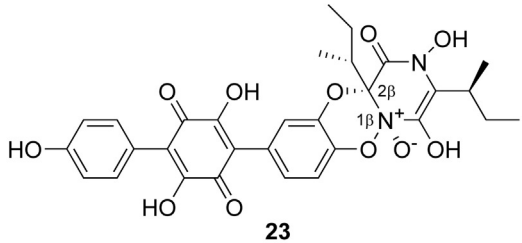

23

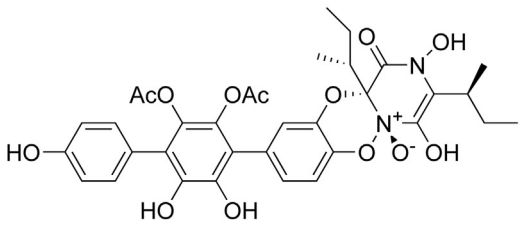

24

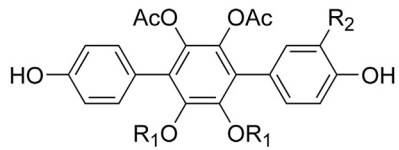

25 R_1=Ac, R_2=H
26 R_1=R_2=H
27 R_1=H, R_2=OH

Figure 6.9 Natural sarcoviolins and terphenyl derivatives. Sarcoviolins with *cis* configuration at $N_1\beta$ and $C_2\beta$ are more potent than those with *trans* configuration. The activity of the *p*-terphenyl derivatives has a direct correlation to increasing number of hydroxyl groups. *Reproduced from U. Ghani, Re-exploring promising α-glucosidase inhibitors for potential development into oral anti-diabetic drugs: finding needle in the haystack, Eur. J. Med. Chem. 103 (2015) 133—162.*

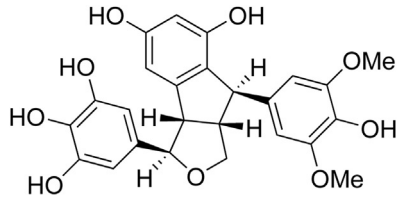

28

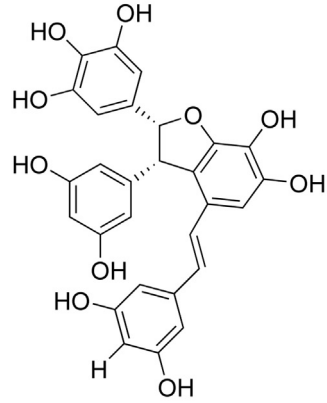

29

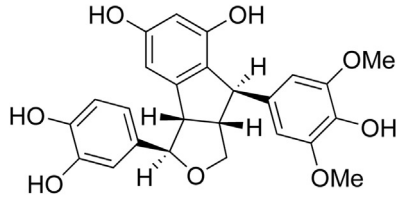

30

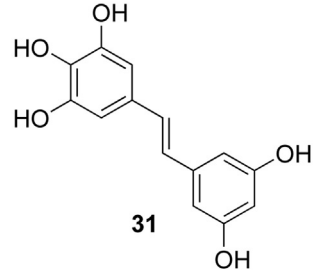

31

Figure 6.10 The natural stilbene inhibitors of α-glucosidase. Kompasinol A (**30**) and 3,30,4,5,50-pentahydroxytrans-stilbene (**31**) also lower postprandial blood glucose levels *in vivo*. *Reproduced from U. Ghani, Re-exploring promising α-glucosidase inhibitors for potential development into oral anti-diabetic drugs: finding needle in the haystack, Eur. J. Med. Chem. 103 (2015) 133—162. © 2015 French Société de Chimie Thérapeutique published by Elsevier Masson SAS. All rights reserved.*

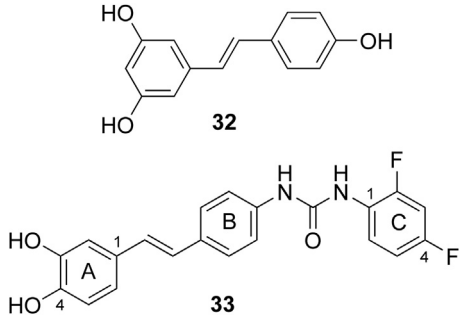

Figure 6.11 The stilbene-based urea derivatives. Urea is found to augment the inhibitory activity due to important contribution of its 1-phenyl moiety ensuring competitive and selective inhibition of α-glucosidase. *Reproduced from U. Ghani, Re-exploring promising α-glucosidase inhibitors for potential development into oral anti-diabetic drugs: finding needle in the haystack, Eur. J. Med. Chem. 103 (2015) 133–162. © 2015 French Société de Chimie Thérapeutique published by Elsevier Masson SAS. All rights reserved.*

compounds is found to augment the inhibitory activity due to important contribution of its 1-phenyl moiety thus ensuring competitive and selective inhibition of the enzyme. Additionally, the substituents on both the terminal phenyl groups are proposed to contribute to enzyme inhibition. Example includes compound **33** ($IC_{50} = 8.4\ \mu M$; $K_i = 3.2\ \mu M$), which is a competitive and selective α-glucosidase inhibitor.

6.6.5 Depsidones

Ngoupayo et al. [21] studied four new depsidones called brevipsidones from the stem bark of *Garcinia brevipedicellata* with yeast α-glucosidase inhibitory activities ($IC_{50} = 7.04–59.64\ \mu M$) (Fig. 6.12). In these compounds, the prenyl group plays an important role in the activity as observed in brevipsidone D (**34**) ($IC_{50} = 7.04\ \mu M$). Compounds lacking the prenyl group or carrying both the prenyl and the 2,2-dimethylchromene groups exhibited weak inhibitory activity.

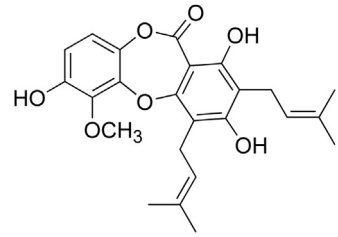

34

Figure 6.12 Brevipsidone D isolated from the stem bark of *Garcinia brevipedicellata*. Its prenyl group is important for enzyme inhibition. *Reproduced from U. Ghani, Re-exploring promising α-glucosidase inhibitors for potential development into oral anti-diabetic drugs: finding needle in the haystack, Eur. J. Med. Chem. 103 (2015) 133–162. © 2015 French Société de Chimie Thérapeutique published by Elsevier Masson SAS. All rights reserved.*

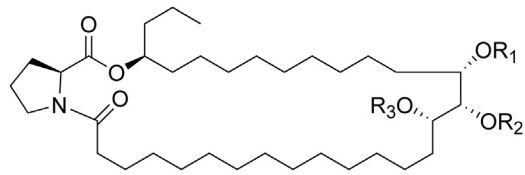

35 $R_1=R_2=R_3=SO_3Na$
36 $R_1=R_2=R_3=H$

Figure 6.13 The macrolide inhibitors of α-glucosidase. *Reproduced from U. Ghani, Re-exploring promising α-glucosidase inhibitors for potential development into oral anti-diabetic drugs: finding needle in the haystack, Eur. J. Med. Chem. 103 (2015) 133–162. © 2015 French Société de Chimie Thérapeutique published by Elsevier Masson SAS. All rights reserved.*

6.6.6 Macrolides

Gao et al. [22] conducted first convergent total synthesis of penarolide sulfate A_2 (**35**), a 31-membered macrolide bearing a proline residue and three sulfate groups (Fig. 6.13). The compound and its desulfated derivative (**36**) are reported to inhibit yeast α-glucosidase with IC_{50} values of 4.87 and 10.74 μM, respectively.

6.6.7 Peptides

Peptides are a rare entry to the battery of α-glucosidase inhibitors. They may offer potentially safer and cheaper alternative to treatment of type 2 diabetes mellitus. Since acarbose, miglitol, and voglibose are sugars or sugar-based derivatives which exert unwanted gastrointestinal side effects, nonsaccharide inhibitors such as peptides may offer better and safer solutions to treatment of hyperglycemia in type 2 diabetes with minimal unwanted side effects. Reports on the peptide α-glucosidase inhibitors are rare and this area needs more attention in terms of screening, identification and development of promising inhibitors. Eichler and coworkers [23] identified cyclic hexapeptide lactam molecules from 26 unique synthetic combinatorial libraries of cyclic peptides with significant yeast α-glucosidase inhibitory activity. All other libraries showed little or moderate activity with the exception of the cyclic hexapeptide library (Fig. 6.14).

The libraries other than that of the hexapeptide lactam that differed only in the order of L- and D-amino acid mixture positions, showed no activity. Interestingly, only cyclic analogs of the libraries were active; the linear ones were inactive. Some of the active analogs of the libraries displayed more potency than *N*-methyl-DNJ ($K_i = 6.75\ \mu M$). These include cyclo[iWyRyN] (**37**), cyclo[iWyRwN], cyclo[iWyRvN] and cyclo[iWyRiN] with K_i values of 1.7, 4.3, 5.1, 6.4 μM, respectively.

Another example of peptide inhibitors of α-glucosidase include work by Yu et al. [24] who isolated eight promising antidiabetic linear peptides from egg white, which were later synthesized by Fmoc solid phase method. The RVPSLM (arginine−valine−proline−serine−leucine−methionine; $IC_{50} = 23.07\ \mu M$) and TPSPR (threonine−proline−serine−proline−arginine; $IC_{50} = 40.02\ \mu M$) peptides showed highest activity. Based on their *in vivo* antidiabetic and α-glucosidase inhibitory

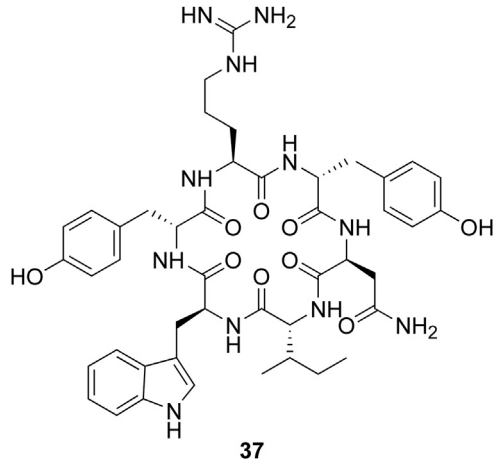

37

Figure 6.14 Only cyclic analogs of the combinatorial library of hexapeptide lactams are active against α-glucosidase. *Reproduced from U. Ghani, Re-exploring promising α-glucosidase inhibitors for potential development into oral anti-diabetic drugs: finding needle in the haystack, Eur. J. Med. Chem. 103 (2015) 133–162. © 2015 French Société de Chimie Thérapeutique published by Elsevier Masson SAS. All rights reserved.*

activities, the peptides offer new avenues for exploring their antidiabetic drug candidacy.

Furthermore, the identification and characterization of sericin peptide by Xie et al. is worth highlighting [25]. The work includes α-glucosidase inhibitory activity of sericin with special focus on its interaction with the enzyme, study of thermodynamic parameters and molecular modeling. Sericin inhibited α-glucosidase ($IC_{50} = 2.9\ \mu M$) in a noncompetitive fashion ($K_i = 1.0\ \mu M$); it binds to the enzyme at a site other than that for acarbose. Moreover, the binding resulted in a conformational change of the enzyme's secondary structure. A detailed discussion on the sericin kinetics and mechanism of inhibition will follow in Chapter 7: Computational and structural biology of α-glucosidase-inhibitor complexes: clues to drug optimization and development.

6.6.8 Ganomycin I and its derivatives

In China, a variety of mushrooms belonging to the *Ganoderma* species are used as food and elixir in traditional medicine. Chemically, ganomycin I (**38**) is a meroterpene-type compound isolated from the *Ganoderma* species that carries dual α-glucosidase and HMG-CoA reductase inhibitory activities. It demonstrates *in vivo* hypoglycemic, hypolipidemic and insulin-sensitizing activities making it a promising candidate for treatment of metabolic syndrome and features associated with it including hyperglycemia and hyperlipidemia. Despite all these promising effects, ganomycin I (**38**) is chemically unstable due to presence of the *para*-dihydroxylbenzene moiety, which imposes a major obstacle in its synthesis and drug development. Recently, Wang et al. [26] synthesized chemically stable derivatives of ganomycin I (**38**) that also demonstrated dual α-glucosidase and HMG-CoA reductase inhibitory activities (Fig. 6.15). Notably, compound **39** exhibited most potent dual inhibitory activity in the series with *in vivo* hypoglycemic, hypolipidemic and weight loss effects on both *ob/ob* and DIO mice. Compounds **39**, **40**, **41**, and **42** demonstrated more promising α-glucosidase inhibitory activity than that of ganomycin I (**38**). Compound **43** exhibited weaker dual activity despite sharing similar structural features with compound **39**, indicating that it is highly selectivity to α-glucosidase inhibition. Moreover, it is chemically more stable than genomycin I (**38**), and toxicologically safer to use even after long-term administration in mice. It effectively decreased fasting and postprandial blood glucose levels along with HbA1c levels in a dose-dependent manner. Additionally, it also improved glucose tolerance by reducing insulin resistance and enhancing insulin sensitivity of cells.

Another significant therapeutic effect of compound **39** was on lipid metabolism; the *ob/ob* mice also significantly lost fat mass as indicated by their reduced body weight compared to

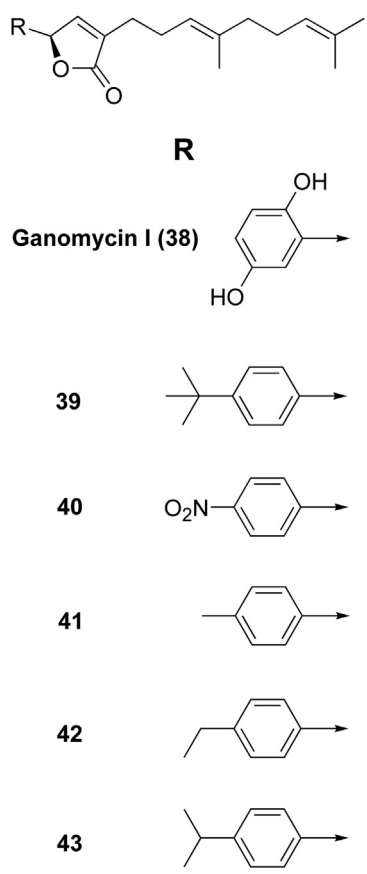

Figure 6.15 The ganomycin I derivatives are promising candidates for antidiabetic drug development due to their dual α-glucosidase and HMG-CoA reductase inhibitory activities in addition to reducing postprandial blood glucose levels *in vivo*.

acarbose which exhibited weaker effects on the body weight. The mice reduced 68% of body weight when compared to controls without treatment. Administration of compound **39** in *ob/ob* mice resulted in the reduction of serum cholesterol, free fatty acids, and triglycerides levels in a dose-dependent manner. Drugs with dual therapeutic effects on the glucose and lipid metabolism are of special focus for the treatment of metabolic syndrome that includes diabetes and glucose intolerance as

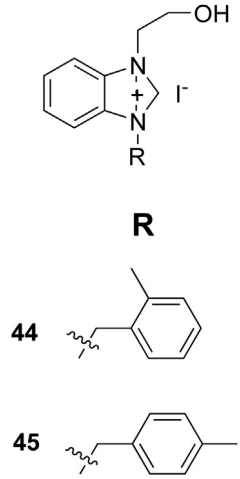

Figure 6.16 The 2-hydroxyethyl substituted *N*-heterocyclic carbene derivatives (IC_{50} = 1.73−7.96 nM/K_i = 0.3−9.22 nM).

its primary components. Compound **39** is a promising and safe drug candidate for treatment of diabetes and metabolic syndrome with significant therapeutic benefits including weight loss, reversal of hepatic steatosis, and hypolipidemic and hypoglycemic effects.

6.6.9 Carbenes

A series of 2-hydroxyethyl substituted *N*-heterocyclic carbene derivatives were recently synthesized that inhibited a number of clinically important enzymes including α-glucosidase in nanomolar range (IC_{50} = 1.73−7.96 nM/K_i = 0.3−9.22 nM) [27]. Lead inhibitors in the series were compounds **44** and **45** (K_i = 1.42 and 0.3 nM, respectively) (Fig. 6.16).

6.6.10 Pyranoquinolinyl-acrylic acid diastereomers

Four types of new pyranoquinolinyl/furoquinolinyl-acrylic acid derivatives, demonstrating α-glucosidase inhibition, have been synthesized utilizing a highly diastereoselective strategy [28]. The exo-diastereomers of pyranoquinolinyl-acrylic acid

adducts (**46**−**49**) inhibited the enzyme with an IC_{50} range of 0.62−4.2 μM, especially compound **47** (Fig. 6.17). In these compounds, the trimethoxy and fluoro substitutions greatly influenced the activity. The exoisomers demonstrated more promising enzyme inhibition than the other diastereomers; compound **50** ($IC_{50} = 0.4$ μM) is one example of this class (Fig. 6.17). Furthermore, the endo-diastereomers of the pyranoquinolinyl-acrylic acid series showed more promising α-glucosidase inhibition than the exo-diastereomers. In contrast, the activity of the nitro-substituted pyranoquinolinyl-acrylic acid endo-diastereomers were more promising than the exo-diastereomers. Importantly, the oxygen atom in the pyranoquinolinyl ring is crucial for potent enzyme inhibition since replacing it with a carbon atom significantly suppressed the activity.

6.6.11 *N,N′-bis*-Cyanomethylamine and alkoxymethylamine derivatives

In an effort to explore the chemical and biological properties of *N,N′-bis*-cyanomethylamines and alkoxymethylamines, Taslimi et al. synthesized novel derivatives of these compounds, which inhibited α-glucosidase in nanomolar range ($IC_{50} = 0.73$−38.5 nM/$K_i = 0.15$−13.31 nM) [29]. Compounds **51** and **52** ($K_i = 0.62$ and 0.15 nM, respectively) are presented in Fig. 6.18.

Transition metal complexes are known to inhibit α-glucosidases [30]. Schiff base transition metal complexes may provide new avenues for α-glucosidase inhibition. Amino acid Schiff bases containing the C = O, C = N groups and S, O, and N atoms have shown to act as metal chelators. Synthesis of a series of salicylaldehyde-amino acid Schiff bases and silver(I) complexes of the 2,4-dihydroxybenzaldehyde-amino acid Schiff bases were conducted which were evaluated for yeast α-glucosidase inhibitory activity. The silver complexes (**53**−**67**) (Fig. 6.19),

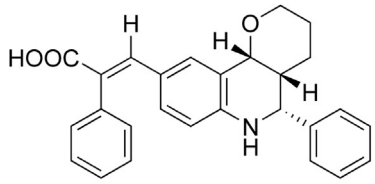

46

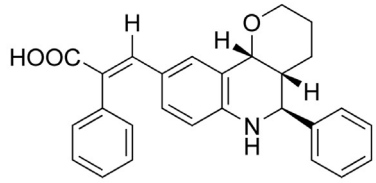

47

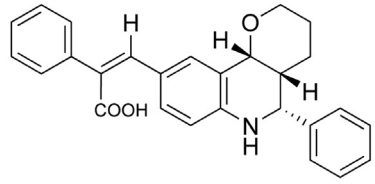

48

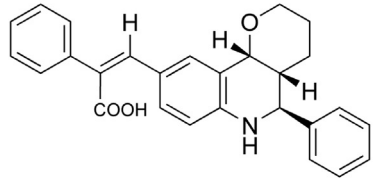

49

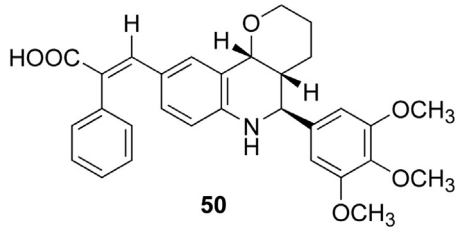

50

Figure 6.17 The pyranoquinolinyl/firoquinolinyl-acrylic acid derivatives.

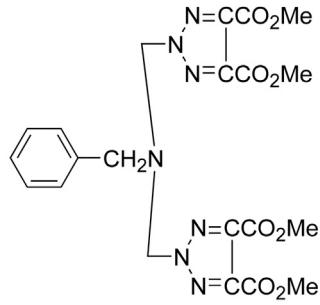

51

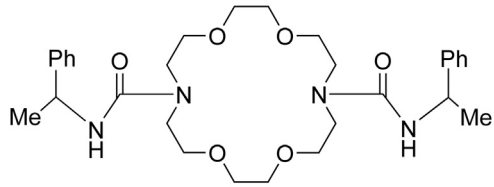

52

Figure 6.18 The *N,N′-bis*-cyanomethylamine and alkoxymethylamine derivatives inhibit α-glucosidase in nanomolar range.

possessing structural similarity to flavones and xanthones, strongly inhibited the enzyme ($IC_{50} = 0.0092-0.246\ \mu M$).

The metal-free amino acid Schiff bases were inactive with the exception of tyrosine and alanine derivatives. Within the silver complexes, those with aliphatic amino acid side chains (**59**, **60**, **62**, and **64**) displayed best activity ($IC_{50} = 0.0168$, 0.0202, 0.0455, and 0.0769 μM, respectively). Nevertheless, other compounds such as **61** ($IC_{50} = 0.00973\ \mu M$) and **67** ($IC_{50} = 0.00922\ \mu M$) showed promising inhibitory activity [31]. In these compounds the amino group of the corresponding amino acids appears to play a crucial role in enzyme inhibition. This is in agreement with the previous studies suggesting an important role of amines in the potent inhibition of various glucosidases [32]. Furthermore, contribution of the silver ligand and the corresponding amino acid side chains to enzyme inhibition is also acknowledged.

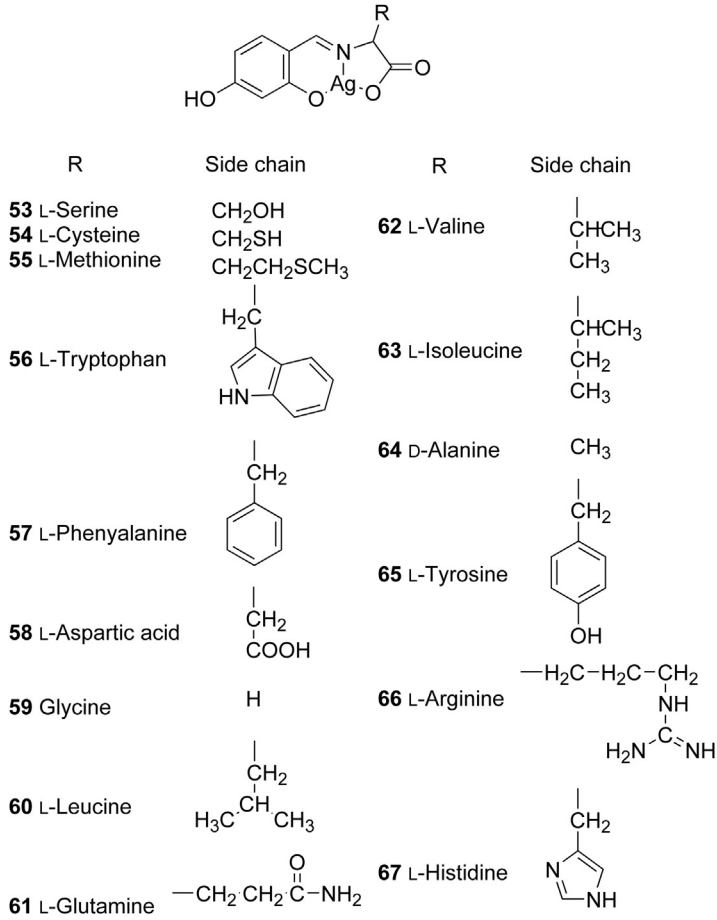

Figure 6.19 The silver(I) complexes of 2,4-dihydroxybenzaldehyde-amino acid. Schiff bases are a new class of potent α-glucosidase inhibitors. *Reproduced from U. Ghani, Re-exploring promising α-glucosidase inhibitors for potential development into oral anti-diabetic drugs: finding needle in the haystack, Eur. J. Med. Chem. 103 (2015) 133–162. © 2015 French Société de Chimie Thérapeutique published by Elsevier Masson SAS. All rights reserved.*

In vivo and *in vitro* inhibition of α-glucosidase by insulinomimetic metal ions has also confirmed that metal ions are catalytically involved in the enzyme inhibition process [30]. Some of the representative compounds (**56**, **64**, and **67**) from the

silver complexes exhibited noncompetitive inhibition of yeast α-glucosidase [31], which complies with a previous report on the role of metal ions in noncompetitive inhibition of yeast α-glucosidase [30]. Since silver(I) complexes of the 2,4-dihydroxybenzaldehyde-amino acid Schiff bases are entirely a new class of promising α-glucosidase inhibitors, further insight into their mechanism of inhibition and *in vivo* studies would provide important clues to development of new antidiabetic drug candidates.

References

[1] M. Yoshikawa, T. Murakami, K. Yashiro, H. Matsuda, Kotalanol, a potent alpha-glucosidase inhibitor with thiosugar sulfonium sulfate structure from anti-diabetic ayurvedic medicine *Salacia reticulata*, Chem. Pharm. Bull. (Tokyo) 46 (1998) 1339–1340.

[2] R.J. Marles, N.R. Farnsworth, Antidiabetic plants and their active constituents, Phytomedicine 2 (1995) 137–189.

[3] H. Oe, S. Ozaki, Hypoglycemic effect of 13-membered ring thiocyclitol, a novel α-glucosidase inhibitor from Kothala-himbutu (*Salacia reticulate*), Biosci. Biotechnol. Biochem. 72 (2008) 1962–1964.

[4] O. Muraoka, W. Xie, G. Tanabe, M. Amer, T. Minematsu, M. Yoshikawa, On the structure of the bioactive constituent from ayurvedic medicine *Salacia reticulata*: revision of the literature, Tetrahedron Lett. 49 (2008) 7315–7317.

[5] K.C. Pramanik, P. Bhattacharya, R. Biswas, D. Bandyopadhyay, M. Mishra, T.K. Chatterjee, Hypoglycemic and antihyperglycemic activity of leaf extract of *Pluchea indica Less*, Orient Pharm. Exp. Med. 6 (2006) 232–236.

[6] I.S. Arsiningtyas, D.P.T. Maria, G. Puteri, E. Kato, J. Kawabata, Identification of α-glucosidase inhibitors from the leaves of *Pluchea indica Less.*, a traditional Indonesian herb: promotion of natural product use, Nat. Prod. Res. 28 (2014) 1350–1353.

[7] G. Mehta, S.S. Ramesh, Polycyclitols - novel conduritol and carbasugar hybrids as new glycosidase inhibitors, Can. J. Chem. 83 (2005) 581–594.

[8] W. Worawalai, S. Wacharasindhu, P. Phuwapraisirisan, Amine-linked diquercitols as new α-glucosidase inhibitors, Bioorg. Med. Chem. Lett. 24 (2014) 5530–5533.

[9] E. Rattanangkool, et al., Quercitylcinnamates, a new series of antidiabetic bioconjugates possessing α-glucosidase inhibition and antioxidant, Eur. J. Med. Chem. 66 (2013) 296–304.

[10] H. Çavdar, O. Talaz, D. Ekinci, Synthesis of novel mono and *bis*-indole conduritol derivatives and their α/β-glycosidase inhibitory effects, Bioorg. Med. Chem. Lett. 22 (2012) 7499–7503.
[11] M.J. Berridge, R.F. Irvine, Inositol trisphosphate, a novel second messenger in cellular signal transduction, Nature 312 (1984) 315–321.
[12] M.J. Berridge, Inositol trisphosphate and calcium signalling, Nature 361 (1993) 315–325.
[13] R.F. Irvine, M.J. Schell, Back in the water: the return of the inositol phosphates, Nat. Rev. Mol. Cell Biol. 2 (2001) 327–338.
[14] T. Mahapatra, S. Nanda, Asymmetric synthesis of hydroxy-skipped *bis*-homo-inositols as potential glycosidase inhibitors, Tetrahedron: Asymmetry 21 (2010) 2199–2205.
[15] D. Yang, J. Zhao, S. Liu, F. Song, Z. Liu, The screening of potential α-glucosidase inhibitors from the *Polygonum multiflorum* extract using ultrafiltration combined with liquid chromatography-tandem mass spectrometry, Anal. Methods 6 (2014) 3353–3359.
[16] S.F. Kouam, et al., α-Glucosidase inhibitory anthranols, kenganthranols A-C, from the stem bark of *Harungana madagascariensis*, J. Nat. Prod. 69 (2006) 229–233.
[17] K. Ma, J. Han, L. Bao, T. Wei, H. Liu, Two sarcoviolins with antioxidative and α-glucosidase inhibitory activity from the edible mushroom *Sarcodon leucopus* collected in Tibet, J. Nat. Prod. 77 (2014) 942–947.
[18] W. Li, X.-B. Li, H.-X. Lou, Structural and biological diversity of natural p-terphenyls, J. Asian Nat. Prod. Res. 20 (2018) 1–13.
[19] S.H. Lam, J.M. Chen, C.J. Kang, C.H. Chen, S.S. Lee, Alpha-glucosidase inhibitors from the seeds of *Syagrus romanzoffiana*, Phytochemistry 69 (2008) 1173–1178.
[20] J.Y. Kim, et al., A novel competitive class of α-glucosidase inhibitors: (*E*)-1-phenyi-3-(4-styrylphenyl)urea derivatives, ChemBioChem 11 (2010) 2725–2737.
[21] J. Ngoupayo, T.K. Tabopda, M.A. Ali, E. Tsamo, α-Glucosidase inhibitors from *Garcinia brevipedicellata* (*Clusiaceae*), Chem. Pharm. Bull. 56 (2008) 1466–1469.
[22] Y. Gao, Q. Shan, J. Liu, L. Wanga, Y. Du, The first convergent total synthesis of penarolide sulfate A_2, a novel α-glucosidase inhibitor, Org. Biomol. Chem. 12 (2014) 2071–2079.
[23] J. Eichler, A.W. Lucka, C. Pinilla, R.A. Houghten, Novel α-glucosidase inhibitors identified using multiple cyclic peptide combinatorial libraries, Mol. Divers. 1 (1995) 233–240.
[24] Z. Yu, Y. Yin, W. Zhao, Y. Yu, B. Liu, J. Liu, et al., Novel peptides derived from egg white protein inhibiting alpha-glucosidase, Food Chem. 129 (2011) 1376–1382.

[25] F. Xie, S. Wang, L. Zhang, J. Wu, Z. Wang, Investigating inhibitory activity of novel synthetic sericin peptide on α-D-glucosidase: kinetics and interaction mechanism study using a docking simulation, J. Sci. Food Agric. 98 (2018) 1502–1510.
[26] K. Wang, et al., Structural modification of natural product ganomycin I leading to discovery of a α-glucosidase and HMG-CoA reductase dual inhibitor improving obesity and metabolic dysfunction in vivo, J. Med. Chem. 61 (2018) 3609–3625.
[27] F. Erdemir, et al., 2-Hydroxyethyl substituted NHC precursors: synthesis, characterization, crystal structure and carbonic anhydrase, α-glycosidase, butyrylcholinesterase, and acetylcholinesterase inhibitory properties, J. Mol. Struct. 1155 (2018) 797–806.
[28] G. Lavanya, K. Venkatapathy, C.J. Magesh, M. Ramanathan, R. Jayasudha, The first target specific, highly diastereoselective synthesis, design and characterization of pyranoquinolinyl acrylic acid diastereomers as potential α-glucosidase inhibitors, Bioorg. Chem. 84 (2019) 125–136.
[29] P. Taslimi, et al., Synthesis and discovery of potent carbonic anhydrase, acetylcholinesterase, butyrylcholinesterase, and α-glycosidase enzymes inhibitors: The novel N,N′-bis-cyanomethylamine and alkoxymethylamine derivatives, J. Biochem. Mol. Toxicol. 32 (2018) e22042.
[30] Y. Yutaka, H. Ryoko, Y. Hiroyuki, S. Hiromu, Alpha-glucosidase inhibitory effect of anti-diabetic metal ions and their complexes, Biochimie 91 (2009) 1339–1341.
[31] J. Zheng, L. Ma, Silver(I) complexes of 2,4-dihydroxybenzaldehyde–amino acid Schiff bases-novel noncompetitive α-glucosidase inhibitors, Bioorg. Med. Chem. Lett. 25 (2015) 2156–2161.
[32] K. Bharatham, N. Bharatham, K.H. Park, K.W. Lee, Binding mode analyses and pharmacophore model development for sulfonamide chalcone derivatives, a new class of alpha-glucosidase inhibitors, J. Mol. Graph. Model. 26 (2008) 1202–1212.

CHAPTER SEVEN

Computational and structural biology of α-glucosidase-inhibitor complexes: clues to drug optimization and development

Contents

7.1 Crystal structure of human MGAM-C in complex with acarbose

Inhibition of the *C*-terminal human maltase glucoamylase (MGAM-C) (EC 3.2.1.20 and 3.2.1.3) is a target for treatment

Alpha-glucosidase Inhibitors.
DOI: https://doi.org/10.1016/B978-0-08-102779-0.00007-1

of type 2 diabetes and obesity [1]. Interest in the development of MGAM-C inhibitors in the past led to the identification of acarbose since it is a potent inhibitor of the enzyme. Human MGAM-C (molecular weight ~100 kDA) demonstrates higher catalytic activity than its counterpart *N*-terminal human maltase glucoamylase (MGAM-N). In fact, its activity is highest among all of the maltase subunits [2]. The crystal structures of free MGAM-C and in complex with acarbose have been solved, which provide important structural insights into the substrate specificity and catalytic mechanism of MGAM-C and related enzymes including MGAM-N and *N*-terminal sucrase-isomaltase (SI-N; EC 3.2.148 and 3.2.10) [3]. The global conformation of MGAM-C is very similar to that of MGAM-N and SI-N; its structure is composed of five domains, namely trefoil type-P, *N*-terminal, catalytic, proximal *C*-terminal, and distal *C*-terminal domains (Fig. 7.1C).

Acarbose is a pseudotetrasaccharide competitive inhibitor of MGAM-C that contains an acarviosine group connected to a maltose via the α-1,4-linkage. Binding of acarbose to the MGAM-C active site does not induce significant conformational changes to the enzyme. The inhibitor occupies the −1 to +3 subsites exposing its nonreactive *N*-linked bond into the catalytic center, hence forming numerous hydrogen bonds and hydrophobic interactions with the active site residues (Fig. 7.2). The cyclitol moiety of acarbose forms hydrogen bonds with the His1584 NE2 and Asp1279 OD2 through its hydroxyl groups at C_3 and C_4 positions, respectively. The first sugar ring forms hydrophobic interactions with the side chains of Tyr1251, Trp1523, and Trp1418. The 4,6-dideoxy-4-amino-*D*-glucose moiety of acarbose is stabilized in the subsite +1 by engaging in hydrogen bonding interactions with the side chain of Asp1157 through its hydroxyl groups at C_2 and C_3 positions. Moreover, the hydroxyl group at C_3 position of the second ring interacts with the Arg1510 NH1. The first

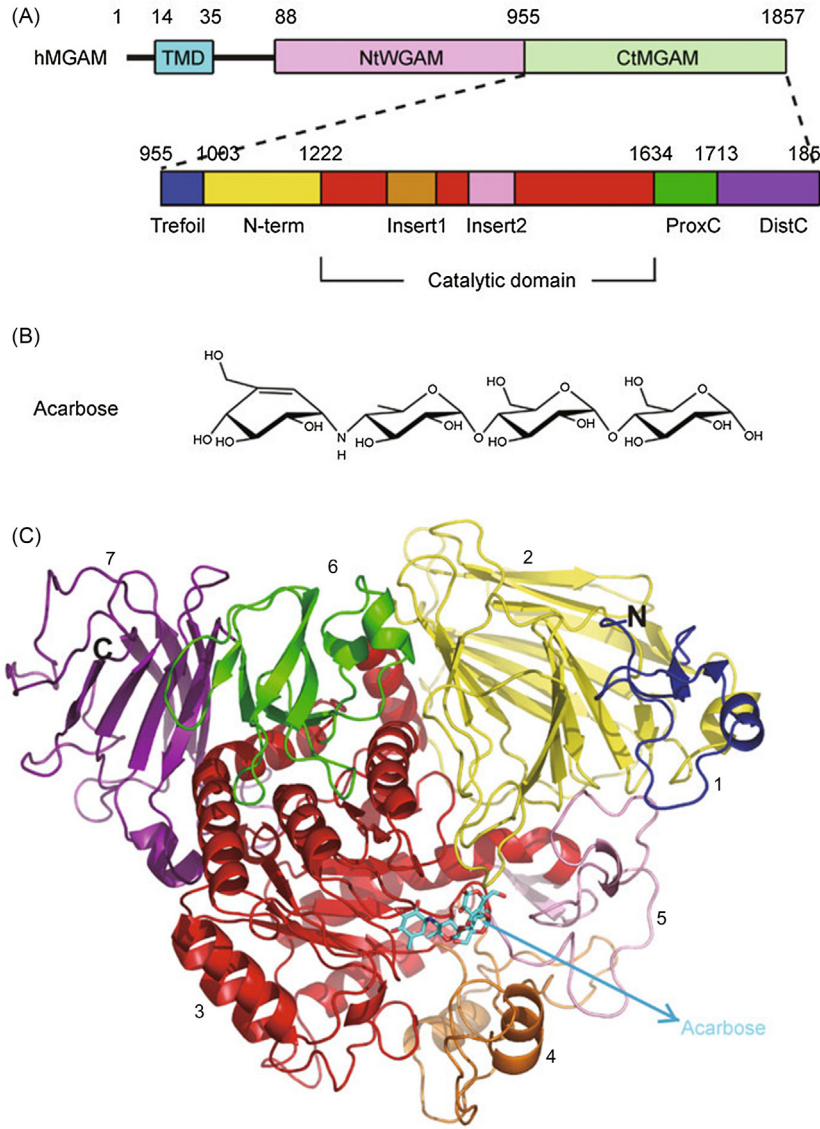

Figure 7.1 (A) Location of each MGAM-C domain in its primary structure. (B) The structure of acarbose. (C) The global structure of MGAM-C in complex with acarbose. The bound acarbose is shown as sticks. The enzyme domains are numbered as follows: 1. trefoil type-P domain; 2. *N*-terminal domain; 3. catalytic $(\beta/\alpha)8$ domain; 4. catalytic domain insert 1; 5. catalytic domain insert 2; 6. proximal *C*-terminal domain; 7. distal *C*-terminal domain. *Reprinted by permission from Springer Nature: L. Ren, et al., Structural insight into substrate specificity of human intestinal maltase-glucoamylase, Protein Cell 2 (2011) 827–836* ©*2011.*

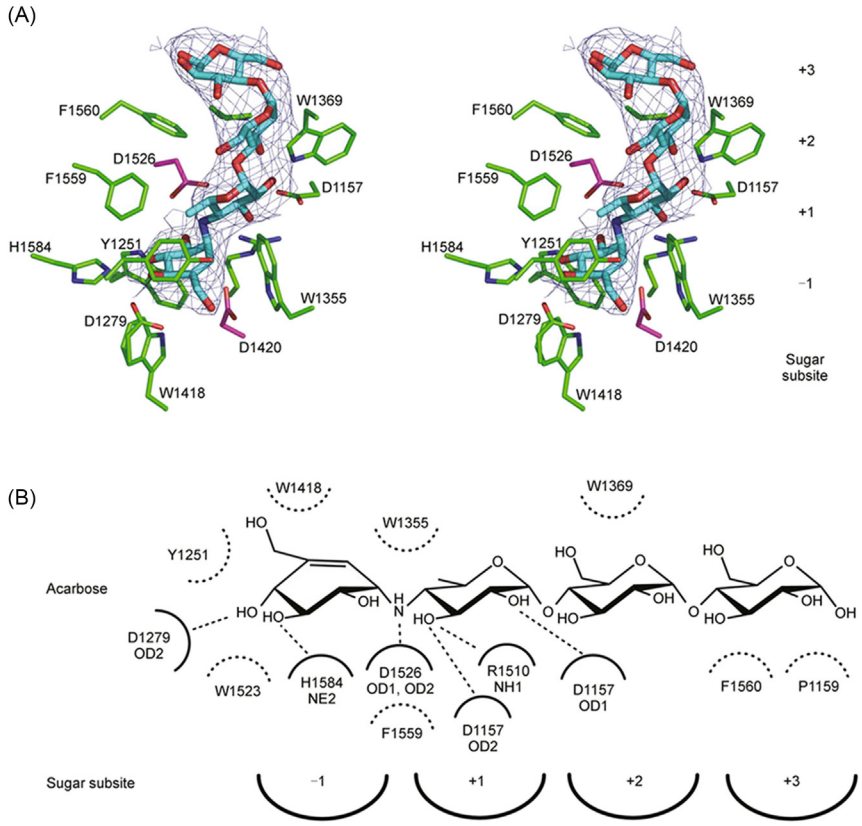

Figure 7.2 Structural details of MGAM-C-acarbose interactions. (A) Electron density map of the complex. Acarbose is shown in the electron density surrounded by the active site residues. (B) The inhibitor occupies the −1 to +3 subsites exposing its nonreactive *N*-linked bond into the catalytic center, and forming numerous hydrogen bonds (represented as *dashed lines*) and hydrophobic interactions (represented as *dashed-lined semicircles*) with the active site residues. *Reprinted by permission from Springer Nature: L. Ren, et al., Structural insight into substrate specificity of human intestinal maltase-glucoamylase, Protein Cell 2 (2011) 827–836 ©2011.*

and second rings are further stabilized by stacking effects from the Trp1355 and Phe1559 residues. The N4B atom of the inhibitor forms hydrogen bond with Asp1526—a potential acid: base residue for catalysis. The third ring (at the subsite +2) and

fourth ring (at the subsite +3) of acarbose are stacked by the side chains of Trp1369, and Phe1560/Pro1159, respectively.

The MGAM-C prefers to bind to oligosaccharide substrates containing 3−6 glucose rings compared to MGAM-N that binds to 2−7 rings, suggesting high substrate specificity and binding affinity of the enzyme for longer substrates—a property of the enzyme supported by structural evidence from the crystal structure. Sequence alignment of MGAM-C, *C*-terminal sucrase-isomaltase (SI-C), MGAM-N, and SI-N showed that the first insert of MGAM-C and SI-C contains an additional segment of 21 amino acids which is absent in MGAM-N and SI-N (Fig. 7.3A). These extra amino acids are part of the active site that form an α-helix and a loop, all of which along with other residues constitute the +2 and +3 subsites. The presence of the extra 21 amino acids clearly justifies stabilization of the third acarbose ring at the +2 subsite through Trp1369, which is part of the extra segment (Fig. 7.3B). Deletion of this extra segment from the MGAM-C sequence resulted in a mutant enzyme devoid of the subsites +2 and +3 that demonstrated preference for shorter substrates similar to that for MGAM-N with five- to ten-fold decrease in the binding affinities to substrates containing 4−6 glucose units. Therefore, the extra segment in the MGAM-C active site is essential for high substrate specificity and affinity. Moreover, studies on the type of substrate catalysis by MGAM-C, SI-C, MGAM-N, and SI-N have confirmed that all enzymes hydrolyze linear α-1,4-linked maltose except SI-N that hydrolyzes branched α-1,6-linked isomaltose [4].

Despite having a high sequence identity ranging from 40−60% and similar carbohydrate digestion profile, these enzymes have evolved differently in terms of substrate specificities and catalytic activities. Preference for longer substrates is mainly a feature of MGAM-C and SI-C enzymes, whereas SI-N exhibits additional catalytic activity for α-1,6-linked

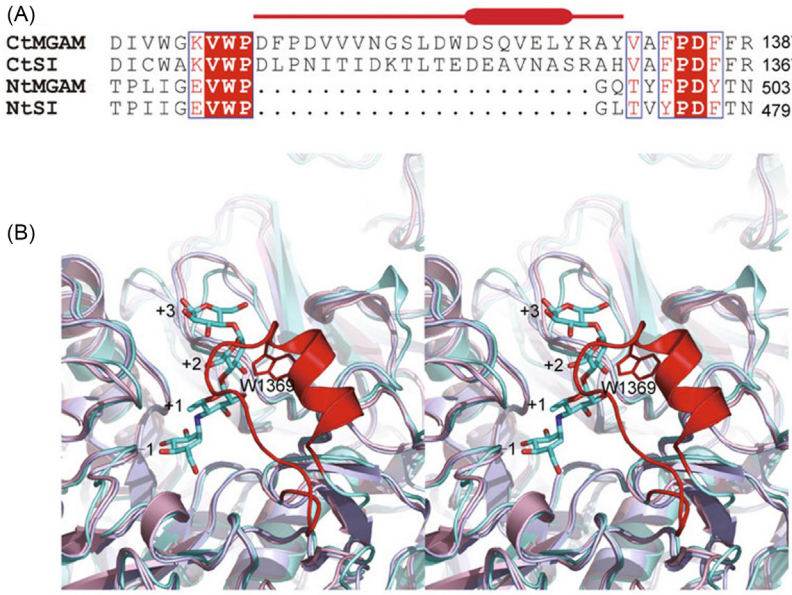

Figure 7.3 (A) Sequence alignment of MGAM-C, SI-C, MGAM-N, and SI-N showing that the first insert of MGAM-C and SI-C contains an additional segment of 21 amino acids which is absent in MGAM-N and SI-N. (B) The MGAM-C-acarbose superimposition on the MGAM-N (*medium gray*) and SI-N (*light gray*) active sites. The extra 21 amino acids form an α-helix loop (*dark gray*) in the active site, which along with other residues constitute the +2 and +3 subsites, justifying stabilization of the third acarbose ring at the +2 subsite through Trp1369. *Reprinted by permission from Springer Nature: L. Ren, et al., Structural insight into substrate specificity of human intestinal maltase-glucoamylase, Protein Cell 2 (2011) 827–836 ©2011.*

substrates. Since the distribution ratio of α-1,4 to α-1,6-linked substrates in human diet is 19:1, there needs to be a proportional distribution of the enzymes with α-1,4 and α-1,6 catalytic activities in accordance with the carbohydrate contents of the human diet, that is, more α-1,4 catalytic activity than α-1,6. The proportionality and activities of these four enzymes are in harmony with starch digestion in humans because all of them hydrolyze α-1,4-linkages with an additional α-1,6 catalytic

activity specific to SI-N only; the enzymes act in concert for optimal digestion and metabolism of starch. In this regard, the drug discovery community needs to focus more on developing antidiabetic candidates that inhibit α-1,4 hydrolytic enzymes rather than α-1,6 hydrolytic enzymes by appreciating this naturally balanced process of carbohydrate digestion in humans.

7.2 Crystal structures of human MGAM-N in complex with acarbose, miglitol, and salacinol

Acarbose is a weak inhibitor of human MGAM-N with poor binding capabilities to the enzyme active site. The 1.9 Å resolution crystal structure of human MGAM-N in complex with acarbose showed that the enzyme active site is composed of the −1 and +1 subsites to which the substrate or inhibitor binds. In the crystal structure, the two nonreducing rings of acarbose namely the acarviosine rings bind to the subsites via hydrogen bonds with Asp327, Asp203, His600, Arg526, and Asp542 residues (Fig. 7.4A). The other two rings do not interact with any residues since they do not fit well in the active site as their atoms show higher B-factor values [5].

Miglitol binds only to the −1 subsite of MGAM-N active site and interacts with the side chains of Asp327, His600, and Asp542 residues similar to that of acarbose. The Asp443 somewhat stabilizes the ring nitrogen of the inhibitor through hydrogen bonding. Due to its shorter structure, miglitol does not reach the +1 subsite, therefore, it does not interact with Asp203 and Arg526 residues (Fig. 7.4B). Moreover, the *N*-hydroxyethyl chain with a hydroxyl group does not form any contacts with the active site as revealed in the crystal structure [5].

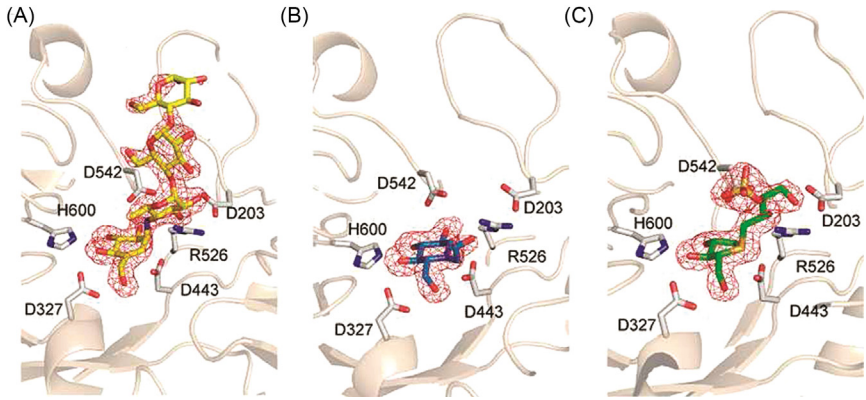

Figure 7.4 MGAM-N in complex with (A) acarbose, (B) miglitol, and (C) salacinol. The catalytic nucleophile Asp443, acid/base catalyst Asp542 and other active site residues are represented as sticks. *Reprinted with permission from L. Sim, et al., New glucosidase inhibitors from an Ayurvedic herbal treatment for type 2 diabetes: structures and inhibition of human intestinal maltase-glucoamylase with compounds from* Salacia reticulata, *Biochemistry 49 (2011) 443–451. ©2011. American Chemical Society.*

Salacinol binds to the −1 and +1 subsites of MGAM-N since it is relatively larger in structure than miglitol. The side chains of Asp327 and H600 residues stabilize the inhibitor in the −1 subsite via hydrogen bonds whereas in the +1 subsite, the side chains of Asp203, Arg526, and the acid–base catalyst Asp542 interact with the acyclic chain of salacinol through its hydroxyl groups. The sulfate group on the same chain remains free of any interactions with the active site residues. Furthermore, the sulfonium ion of salacinol makes electrostatic contacts with Asp443, which is a catalytic nucleophile of the enzyme (Fig. 7.4C). All inhibitors bind to two active site water molecules via hydrogen bonds; each of which forms tight hydrogen bonds with Asp366, Asp443/Asp571, and Trp539, respectively (Fig. 7.5).

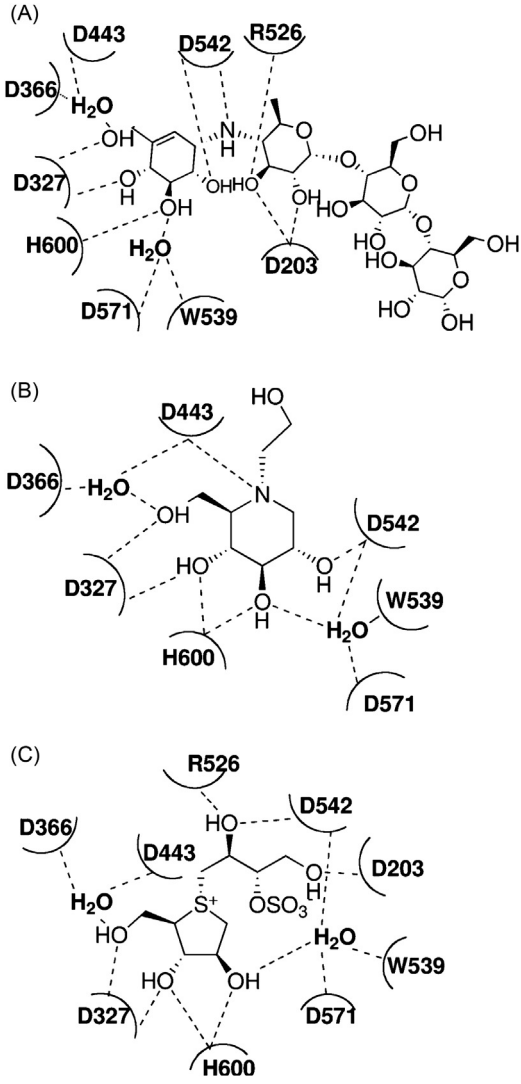

Figure 7.5 The hydrogen bonding interactions (displayed as dotted lines) between MGAM-N and (A) acarbose, (B) miglitol, and (C) salacinol. *Reprinted with permission from L. Sim, et al., New glucosidase inhibitors from an Ayurvedic herbal treatment for type 2 diabetes: structures and inhibition of human intestinal maltase-glucoamylase with compounds from* Salacia reticulata*, Biochemistry 49 (2011) 443−451. ©2011. American Chemical Society.*

7.3 Comparison of the MGAM-N-inhibitor complexes

Acarbose has largest structure with weaker inhibition of the enzyme due to the fact that MGAM-N does not have extended +2 and +3 sugar binding subsites. This in contrast to MGAM-C which possesses these subsites where acarbose can bind and inhibit the enzyme with more potency. Miglitol and salacinol are potent inhibitors of MGAM-N since they have smaller structures compared to acarbose. Presence of the +2 and +3 subsites is not needed for these inhibitors since their structural features are optimal for binding to the −1 and +1 subsites only [5].

Superimposition of all three enzyme-inhibitor complex structures, presented in Fig. 7.6A, revealed comparative clues to how these inhibitors bind to the −1 and +1 subsites. Miglitol and the valienamine ring of acarbose align well at the −1 subsite including their C_2−C_4 and C_6 hydroxyl groups. The C_2, C_3, and C_5 ring hydroxyl groups of salacinol (a five-membered ring inhibitor) align well with the C_3, C_4, and C_6 hydroxyl groups of its six-membered counterparts. A high level of similarity exits between these structures only at the −1 subsite; the binding of the inhibitors markedly differed beyond this subsite. Miglitol mainly binds to the −1 subsite due to its smaller structure, and its *N*-hydroxyethyl group is free without involving in any interaction with the active site. Moreover, this group moves the side chain of Trp406 by extending into the side of the active site and enlarges it. The resulting conformational change causes the active site Met444 to take the space created by shifting of the Trp406 side chain. Additionally, miglitol binding also shifts the catalytic nucleophile Asp542 by ∼0.4 Å [5].

The acarbose and salacinol bind very differently to the +1 subsite of MGAM-N, however, the Arg526, Asp203, and

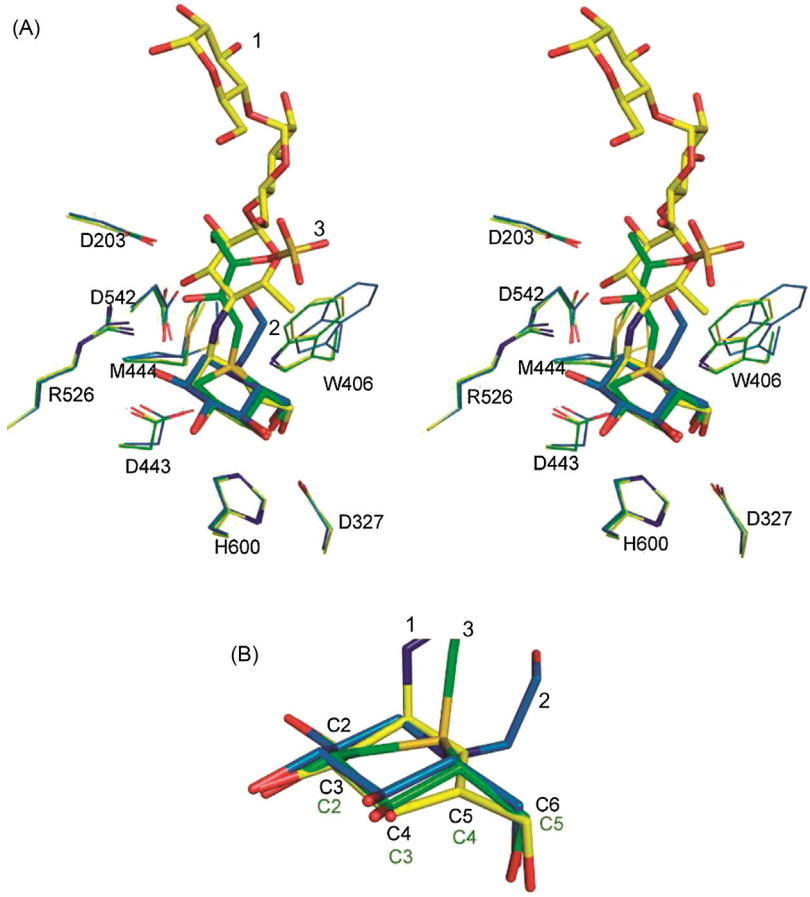

Figure 7.6 (A) Superimposition of MGAM-N active site complexes and their respective interactions with acarbose (1), miglitol (2), and salacinol (3) for comparison purposes. (B) Binding of the inhibitors to the −1 subsite is compared. The carbon ring atom numbers are represented in black for acarbose and miglitol, and light gray for salacinol. *Reprinted with permission from L. Sim, et al., New glucosidase inhibitors from an Ayurvedic herbal treatment for type 2 diabetes: structures and inhibition of human intestinal maltase-glucoamylase with compounds from* Salacia reticulata*, Biochemistry 49 (2011) 443−451. ©2011. American Chemical Society.*

Asp542 residues that are involved in hydrogen bonding, align well. In both structures, the Asp203 residue shares hydrogen bonds with the C_2 of acarbose and C_4' of salacinol hydroxyl groups. In contrast, the C_3 acarbose hydroxyl group forms hydrogen bond with Arg526 only, whereas the C_2' salacinol hydroxyl group also interacts with Asp542 in addition to Arg526. Significant differences of binding of the three inhibitors has been noted in the −1 subsite (Fig. 7.6B). The structure of a GH31 xylosidase and its catalytic mechanism provides important clues to understanding the mechanism of inhibition of MAGAM-N by acarbose, miglitol, and salacinol. In this family of enzymes, the substrate binds to the active site as a covalent enzyme−substrate intermediate utilizing the $^4C_1-^4H_3-^1S_3$ conformation [2]. The mechanism of inhibition of MGAM-N by miglitol involves the $^4C_1$ structure which undergoes a transition state similar to predicted substrate-binding conformation which is different from the charged oxacarbenium ion-like transition state. Salacinol uses the $^3T_2$ conformation in the MGAM-N active site which is same as its unbound conformation [6]. The $^3T_2$ conformation of the salacinol ring bears maximal resemblance to the $^4H_3$ conformation of the predicted transition state when the respective C_2-C_4 of salacinol rings and C_3-C_5 of a glucopyranose ring were superimposed. Moreover, the sulfonium ion−Asp443 interaction mimics the charged oxacarbenium ion-like transition state and the carboxylate in the hydrolysis.

The valienamine acarbose ring acquires a $^2H_3$ half-chair conformation which is unlike that of miglitol and salacinol, which appears to be a reasonable explanation for the weak inhibition of MGAM-N by acarbose. This conformation influences the posture of C_3-C_5 of the valienamine ring that changes the positions of their respective CH_2OH or OH groups. It is not clear if acarbose is a real transition-state analog or just a tight binding inhibitor of MGAM-N. Evidence from the kinetic

studies on the active site mutants of cyclodextrin glucanotransferase from the GH13 family have demonstrated that acarbose is most likely a transition-state analog [7]. However, studies on the GH15 family of inverting glucoamylase enzymes imply the opposite [8]. Salacinol and miglitol do not reach out to the +2 and +3 subsites of MGAM-N due to their smaller molecular size than acarbose. Exploring extension of the inhibitor to these subsites might provide clues to increasing their inhibitory activities against MGAM-C enzyme. In this connection, extended acyclic chain-containing derivatives of salacinol have been synthesized that demonstrated inhibitory activities comparable to that of inhibition of MGAM-N by salacinol. Structural modifications of miglitol such as exchanging its *N*-hydroxyethyl group with the acyclic chain of salacinol resulted in the deterioration of its inhibitory activity mainly due to the reason that the *N*-hydroxyethyl group in miglitol alone displaces some active site amino acids rather than extending into the +1 subsite.

7.4 The human MGAM-N-salacinol derivative complexes

A number of reports have been published on the synthesis and α-glucosidase inhibitory activity of a variety of salacinol derivatives [9]. Noteworthy to mention are kotalanol and its de-*O*-sulfonated analog featuring extended acyclic chains. Crystal structure of the compounds in complex with MGAM-N suggested potential role of stereochemistry, sulfate group, and the length of the acyclic polyhydroxylated chain in enzyme inhibition. Previous reports on systematic investigation of the influence of inhibitor chain lengths and their stereochemistry concluded that *S* and *R* configurations for C_2' and

C_4' centers, respectively, are essential for potent inhibition. Also, the longer acyclic chains constituting more than four carbons and stereochemistry of sulfate at C3′ do not exert significant effects on the inhibition. These studies were mainly conducted utilizing synthetic and kinetic approaches, which were later confirmed and concluded by structural evidence. These include synthesis of a series of salacinol derivatives with varying acyclic chain lengths including the role of sulfate group, and stereochemistry in MGAM-N inhibition.

The NR4-8, NR4-8II, salacinol and kotalanol structures were compared; kotalanol carry an extended 7-carbon polyhydroxylated side chain with *S*, *S*, *R*, *R*, and *S* stereoconfigurations at $C_2'-C_6'$, respectively. The 2.1-Å resolution crystal structure of kotalanol in complex with MGAM-N revealed that the salacinol and kotalanol complexes are conserved, and both structures align well with each other with the exception of the $C_4'-C_7'$ hydroxyl groups that the salacinol molecule lacks. The polyhydroxylated side chain of kotalanol forms some more hydrogen bonds with the Asp203 residue of the enzyme through its C_6' hydroxyl group, and Trp205 and Asp203 through water with the $C_5'-C_7'$ (Fig. 7.7A). Despite these extra interactions, the K_i value of kotalanol remained unchanged which is identical to that of salacinol (0.19 μM). Furthermore, the NR4-8 and NR4-8II derivatives with *S*, *S* and *S*, *R* configurations also showed similar levels of inhibition ($K_i = 0.13$ and 0.10 μM, respectively) [10]. In both the crystal structures of MGAM-N in complex with NR4-8 and NR4-8II, the $C_5'-C_7'$ chain of the former appears to be disordered, whereas the latter binds to the enzyme in a conformation other than that of kotalanol. This structural evidence is enough to draw a conclusion that the $C_5'-C_7'$ chain of NR4-8 is not essential for high affinity to the enzyme.

Derivatives featuring ring stereoconfigurations other than those present in salacinol or related derivatives were able to

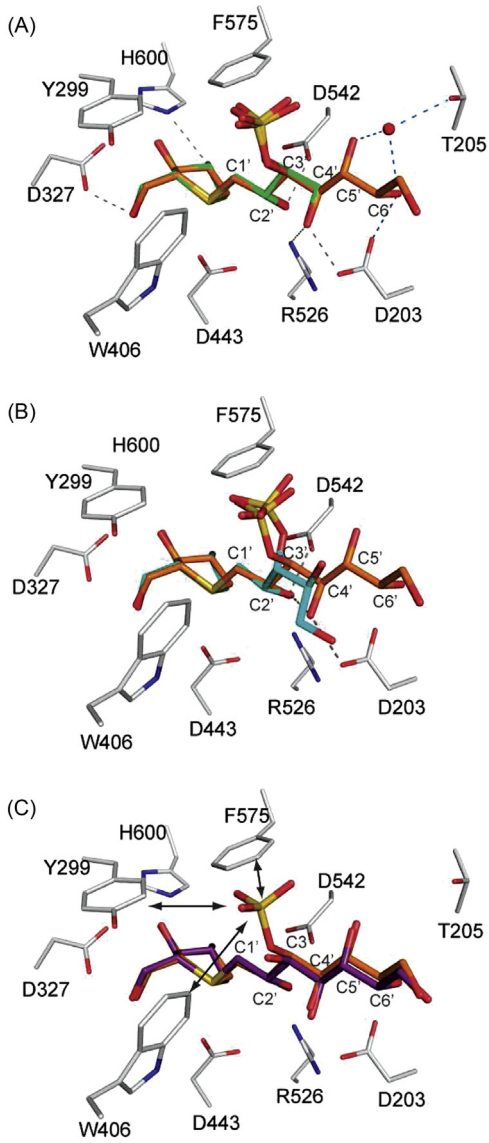

Figure 7.7 Comparison of MGAM-N-salacinol complex and its derivatives. The structures of (A) salacinol and kotalanol, (B) kotalanol and BJ2661 derivative, and (C) kotalanol and de-*o*-sulfonated kotalanol are superimposed. *Reprinted with permission from L. Sim, et al., New glucosidase inhibitors from an Ayurvedic herbal treatment for type 2 diabetes: structures and inhibition of human intestinal maltase-glucoamylase with compounds from* Salacia reticulata*, Biochemistry 49 (2011) 443−451. ©2011. American Chemical Society.*

bind to the enzyme active site. The *R* configuration at C_4' was not as important as it was at C_2'. The BJ2661 derivative bears *S*, *R*, and *S* stereoconfigurations at $C_2'-C_4'$ positions, respectively. Its crystal structure in complex with MGAM-N showed undefined electron density at $C_1'-C_3'$, ring C_1 and at $C_4'-C_5'$ hydroxyl groups indicating that it is a weaker inhibitor of MGAM-N. Comparison of its structure with kotalanol revealed no conformational changes in the MGAM-N active site with good alignment of the inhibitor ring up to the C_2' hydroxyl group (Fig. 7.7B). However, the C_3' center features a conformation other than that of kotalanol. Their sulfate groups are conserved in both structures which do not interact with the active site apart from affording constraining effects from the distant bulky hydrophobic residues that include Phe575, Trp406, and Tyr299 (Fig. 7.7C).

The C_4' hydroxyl group appears to stabilize the orientation of the C_2' hydroxyl group through internal hydrogen bonding. The *S* configuration at the C_4' in BJ2661 derivative, which is different from that of salacinol, kotalanol, and de-*O*-sulfonated kotalanol derivatives (all have *R* configuration), abolishes hydrogen bonding with Asp203. This reorientation from Asp203 to the C_4' hydroxyl group and to the C_2' hydroxyl group is not found in BJ2661 derivative crystal structure, and is probably a cause for undefined electron density from C_1' to C_3' of the inhibitor.

The de-*O*-sulfonated derivative of kotalanol ($K_i = 0.03$ μM) is most potent inhibitor of MGAM-N. Surprisingly, removal of the sulfate group increases its activity by seven-fold, whereas its stereoconfiguration at C_3' does not change its potency of inhibition [9]. The 1.9-Å crystal structures of de-*O*-sulfonated derivatives in complex with MGAM-N were compared with that of kotalanol to investigate the role of sulfate group in enzyme inhibition. The structures superimpose up to C_3', and without the sulfate group, the C_3' hydroxyl group acquires a

different position. Removal of the sulfate group also resulted in the relief of constraints around C_3' by the bulky hydrophobic residues that in turn culminated in more favorable interactions with the active site.

7.5 Comparison of the crystal structures of acarbose in complex with MGAM-C, MGAM-N, and SI-N

The crystal structures of acarbose in complex with MGAM-C, MGAM-N and SI-N were compared to determine structural and functional differences between these enzymes [3]. All complexes exhibited almost identical binding of the inhibitors' first ring groups to the −1 subsite. The amino acids constituting this site are conserved in all enzymes with the exception of one amino acid that is Tyr1251 in MGAM-C. Its counterparts in MGAM-N and SI-N include Tyr299 and Trp327, respectively (Fig. 7.8). These amino acid differences determine the substrate binding and specificity of the enzymes. From these

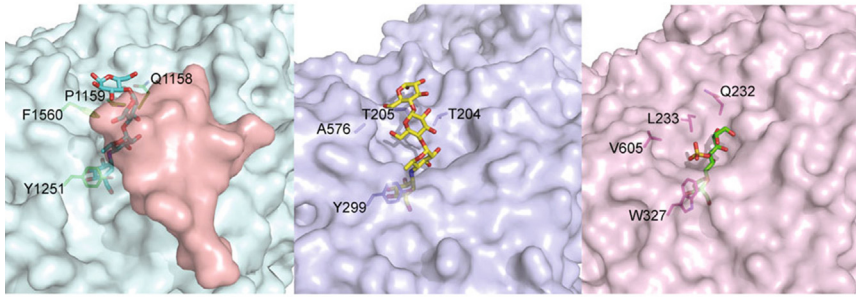

Figure 7.8 Surface diagrams of the MGAM-C-acarbose, MGAM-N-acarbose, and SI-N-kotalanol active site complexes (from left to right). The extra 21 amino acid segment in MGAM-C is shown in dark gray (first left). *Reprinted by permission from Springer Nature: L. Ren, et al., Structural insight into substrate specificity of human intestinal maltase-glucoamylase, Protein Cell 2 (2011) 827–836 ©2011.*

differences, it was proposed that presence of the bulky hydrophobic side chain of Trp327 in SI-N occupies the subsite −1 space to tether the flexible branched α-1,6-linked sugar moiety for catalysis compared to smaller size of Tyr1251 and Tyr299 side chains that cannot restrict the α-1,6-linked sugar in the active sites of MGAM-C and MGAM-N. The MGAM-C and MGAM-N mutants containing tryptophan instead of tyrosine in their active sites exhibited α-1,6 catalytic activities. The MGAM-N mutant demonstrated three-fold more affinity to α-1,6 substrate than its native form. Moreover, both mutants exhibited ten- and three-fold reduced catalytic activity for linear α-1,4 substrates [3].

7.6 Important structural and functional clues to human MGAM-N inhibition

A number of important structural features that significantly contribute to potent inhibition of MGAM-N can be derived from these studies.

1. The long hydroxylated side chains of kotalanol, NR4-8, and NR4-8II derivatives featuring varying configurations at the $C_5'-C_7'$ appear distorted. These chains do not potentiate or weaken the inhibitory activity of the compounds since they do not interact with the MGAM-N active site.
2. The C_2' and C_4' stereoconfigurations are crucial for tight binding because the C_2' hydroxyl group forms essential hydrogen bonds with Arg526 and Asp542 residues in concert with the C_4' hydroxyl group. The BJ2661 derivative lacks this interaction, therefore, it appears disordered.
3. Although their C_3' stereoconfigurations are in contrast to each other, the sulfate groups of BJ2661 and kotalanol superimpose precisely.

4. Truncation of the sulfate groups from the compounds yielded more efficient inhibitors of MGAM-N.
5. The detailed kinetic, structural, and mechanistic analyses of MGAM-N inhibition by salacinol, kotalanol, and related derivatives provide framework for developing new promising inhibitors of α-glucosidase for potential treatment of type 2 diabetes mellitus and other diseases.

7.7 The human MAGAM-N-casuarine complex

The crystal structure of casuarine in complex with MGAM-N has been solved at a resolution of 2.1 Å [11]. As presented in Fig. 7.9, casuarine binds to the −1 subsite with two A and B pyrrolidine rings acquiring an envelope configuration namely 2E and E6, respectively. Since casuarine carries rings which are highly hydroxylated, it tightly binds to the enzyme active site residues constituting the −1 subsite, mainly through hydrogen bonding interactions (Fig. 7.10). The C_2 and C_8 hydroxyl groups form hydrogen bonds with the side chain of Asp327, the C_1 and C_2 hydroxyl groups with His600,

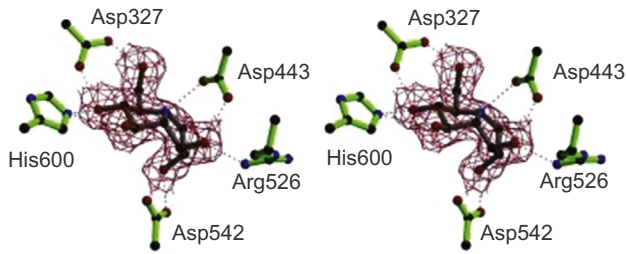

Figure 7.9 The crystal structure of MGAM-N in complex with casuarine. *Reprinted by permission from John Wiley & Sons. F. Cardona, et al., Total syntheses of casuarine and its 6-o-α-glucoside: complementary inhibition towards glycoside hydrolases of the GH31 and GH37 families, Chem. A Eur. J. 15 (2009) 1627–1636. ©2009. John Wiley & Sons.*

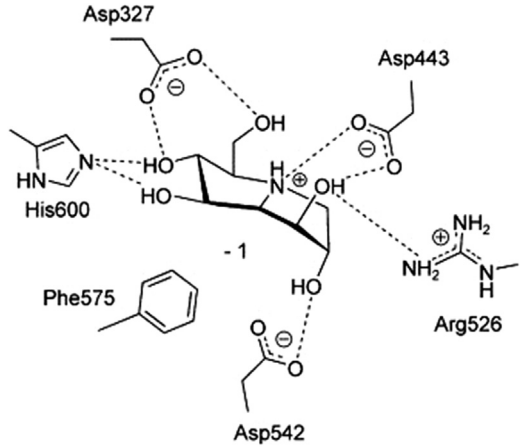

Figure 7.10 Interaction of casuarine with the MGAM-N active site. *Reprinted by permission from John Wiley & Sons. F. Cardona, et al., Total syntheses of casuarine and its 6-o-α-glucoside: complementary inhibition towards glycoside hydrolases of the GH31 and GH37 families, Chem. A Eur. J. 15 (2009) 1627–1636. ©2009. John Wiley & Sons.*

the C_7 hydroxyl group and the pyrrolidine nitrogen with Asp443, the C_6 hydroxyl group with Asp542, and the C_7 hydroxyl group with Arg526.

Comparison of the casuarine complex structure with that of casuarine-6-*o*-glucoside showed that it weakly binds to the active site mainly by involving in unfavorable interactions with the +1 subsite. Moreover, its binding affinity to the −1 subsite is much weaker than that of casuarine. Binding of casuarine-6-*o*-glucoside to MGAM-N was also studied using docking simulation, revealing that the casuarine moiety of the glucoside fits in the −1 subsite, whereas its glucose moiety fits in the +1 subsite. The crystal structure of casuarine complex (Fig. 7.11A) and the modeled casuarine part of its glucoside (Fig. 7.11C) showed no optimal overlapping that is probably due to presence of the 1,1-linkage rather than the 1,4-linkage that is abundant in natural substrates. The hydrogen bonding in the modeled casuarine glucoside complex is solely contributed

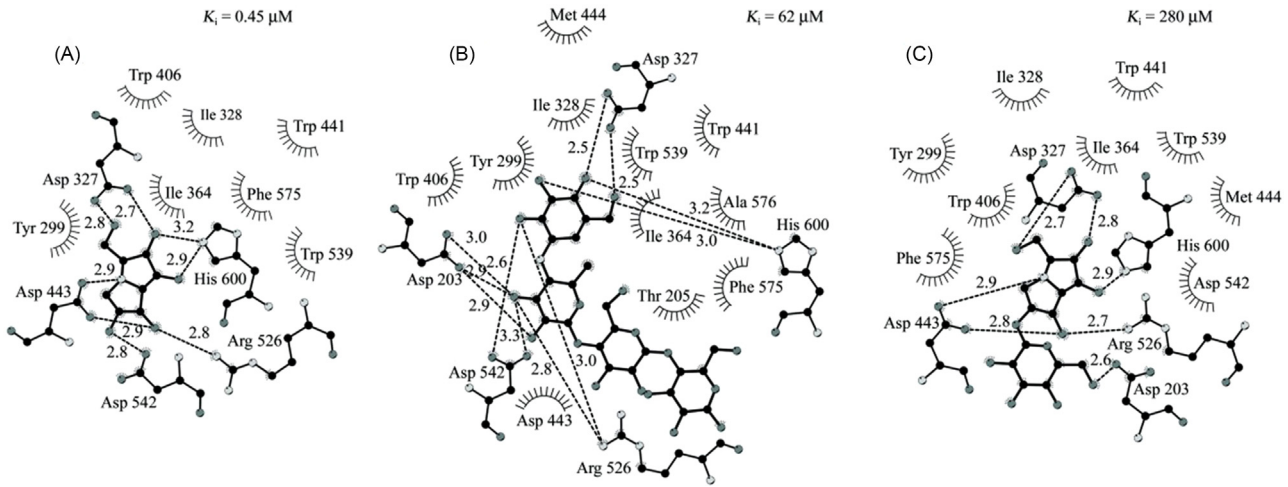

Figure 7.11 Interactions of MGAM-N active site with (A) casuarine, (B) acarbose in the crystal structure, and (C) casuarine 6-*o*-α-Glucoside in the docking simulation. *Reprinted by permission from John Wiley & Sons. F. Cardona, et al., Total syntheses of casuarine and its 6-*o*-α-glucoside: complementary inhibition towards glycoside hydrolases of the GH31 and GH37 families, Chem. A Eur. J. 15 (2009) 1627—1636. ©2009. John Wiley & Sons.*

by the casuarine moiety of the glucoside with the exception of the C_6 hydroxyl group interaction with Asp542 due to presence of the glucosidic bond in that location. The +1 subsite, where the glucose moiety binds, is involved in some hydrogen bonding interactions with the residues exposed by the solvent, including residues around the −1 subsite (Fig. 7.11C). Since MGAM-N hydrolyzes the α-1,4-linkages in starch-based dextrins, the weaker inhibitory profile of casuarine-6-*o*-glucoside is mainly due to its low specificity to the enzyme. As discussed earlier, in the crystal structure of MGAM-N-acarbose complex, acarbose is involved in the electrostatic interaction with Asp542 residue without forming any hydrogen bonds with Asp443 residue (Fig. 7.11B). In contrast, casuarine interacts with both of these residues explaining its two-fold higher potency of MGAM-N inhibition than acarbose. Inhibition of MGAM-N by casuarine provides promising clues to synthesis of novel α-glucosidase inhibitors [11].

7.8 Crystal structures of free isomaltase and in complex with maltose

Isomaltase (EC 3.2.1.10) is an oligo-1,6-glucosidase that catalyzes the hydrolysis of α-1,6-glucosidic linkage in dextran and isomalto-oligosaccharides. The enzyme, which belongs to the GH13 family of glycoside hydrolases, is not specific to carbohydrates containing the α-1,4-glucosidic linkage which is in contrast to α-1,4-glucosidases (2). *Saccharomyces cerevisiae* expresses α-1,4-glucosidase (maltase) and oligo-1,6-glucosidase (isomaltase) enzymes. Crystal structure of the former is yet to be determined, whereas the latter has been studied in great details. The crystal structure of free isomaltase and in complex with its inhibitor maltose has been solved at high resolutions

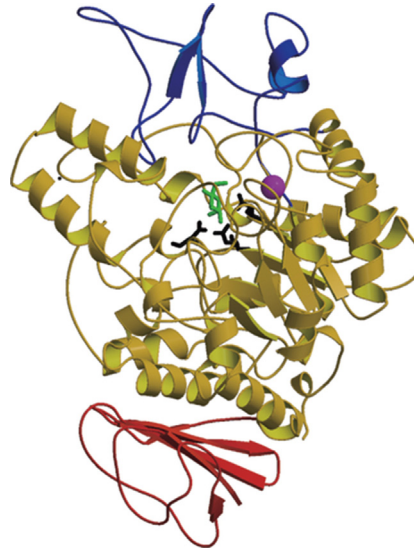

Figure 7.12 The global structure of isomaltase in complex with maltose. *Reprinted by permission from John Wiley & Sons. K. Yamamoto, H. Miyake, M. Kusunoki, S. Osaki, Crystal structures of isomaltase from Saccharomyces cerevisiae and in complex with its competitive inhibitor maltose, FEBS J. 277 (2010) 4205–4214. ©2010. John Wiley & Sons.*

of 1.3 Å and 1.6 Å, respectively [12]. The structure of isomaltase features three domains, namely A, B, and C (Fig. 7.12). The catalytic residues Asp215, Glu277, and Asp352 are located in the domain A which consists of eight alternating parallel α-helices and β-strands. Since maltose is not a specific substrate for isomaltase, its α-1,4 bond remains unhydrolyzed in the active site as competitive inhibitor. The free active site contains five water molecules which are dislodged by substrate or inhibitor binding. The nonreducing end of the glucose moiety occupies the −1 subsite, located at the bottom of the active site, where it is stabilized by nine hydrogen bonds and stacking effect from Tyr72. Maltose shares hydrogen bonds with the three catalytic residues mentioned above. The O_6, O_1, and O_3 atoms of the glucose moiety are involved in hydrogen bond formation with the OD2 of Asp215, Glu277,

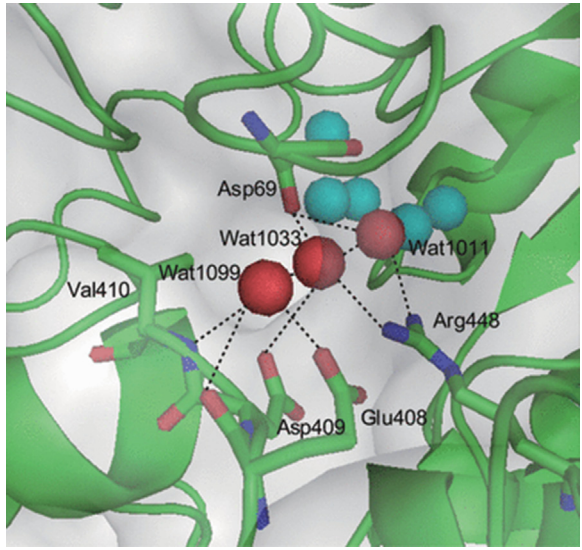

Figure 7.13 The isomaltase active site contains a water path (dark gray spheres: Wat 1099, 1033, and 1011) at its bottom. *Reprinted by permission from John Wiley & Sons. K. Yamamoto, H. Miyake, M. Kusunoki, S. Osaki, Crystal structures of isomaltase from Saccharomyces cerevisiae and in complex with its competitive inhibitor maltose, FEBS J. 277 (2010) 4205–4214. ©2010. John Wiley & Sons.*

and the OD1 of Asp532 residues, respectively. In the GH13 family of enzymes, seven of the nine hydrogen bonds between the glucose moiety and the enzyme are conserved while remaining two are specific to oligo-1,6-glucosidases [13]. Isomaltase mainly recognizes the nonreducing end of glucose moiety through these two hydrogen bonds that are shared by the O_4 of glucose, OD of Asp69, and NH1 of Arg 442.

The active site also contains numerous water molecules arranged almost like a path. One path, located at the bottom, is composed of three water molecules lined up from the bottom to the other side of the active site entrance (Fig. 7.13). These include Wat1011, Wat1033, Wat1099, Wat713, Wat734, and Wat779 in free and bound isomaltase. Additionally, five more water molecules are found in the free

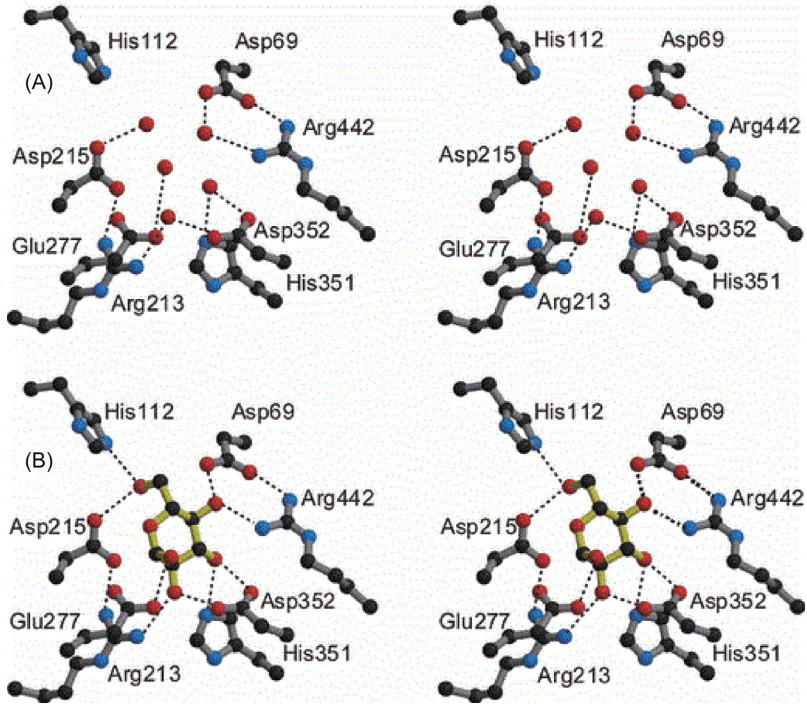

Figure 7.14 Hydrogen bonding network in the isomaltase active site before (A) and after maltose binding (B). *Reprinted by permission from John Wiley & Sons. K. Yamamoto, H. Miyake, M. Kusunoki, S. Osaki, Crystal structures of isomaltase from Saccharomyces cerevisiae and in complex with its competitive inhibitor maltose, FEBS J. 277 (2010) 4205–4214. ©2010. John Wiley & Sons.*

isomaltase active site, which must be dislodged upon substrate or inhibitor binding (Fig. 7.14). The active site cannot accommodate both the ligand and water molecules at the same time due to its narrow space. Hence the water path acts as a drain that pushes water molecules out of the active site to facilitate ligand binding. The second water path (Wat707, Wat751, Wat720, Wat922, Wat708, and Wat701) is located in proximity to the catalytic residues of free and bound isomaltase active sites, which has been proposed to act as a water reservoir for substrate hydrolysis [12].

Maltose binding in the −1 subsite of isomaltase is undifferentiated from that of other members of the GH13 family. However, the inability of yeast isomaltase to catalyze maltose hydrolysis appears to be due to: (1) flexing of the maltose reducing end, (2) differences of binding mechanisms of glycosidic bond to the enzyme, and (3) differences of binding mechanisms of the reducing end of glucose to the subsite +1 from other enzyme members of the GH13 family. Maltose cannot attain transition state since its glycosidic bond's dihedral angle lacks adequate energy to proceed with catalysis.

7.9 Insights into the α-glucosidase mechanism of inhibition

Enzymatic addition or removal of carbohydrate moieties is an essential step in cellular processes [14–16]. In this regard, glycoside hydrolases including α-glucosidases are an important class of enzymes that catalyze such reactions. These enzymes contain catalytic aspartic acid and/or glutamic acid residues that work through two steps. They catalyze generation of a covalent glycosyl–enzyme intermediate followed by its hydrolysis. During catalysis by the GH13 α-glucosidases, substrates undergoing transition state for addition or removal of glucose moieties feature pyranosylium ion-like properties with an $^{4}H_{3}$ half-chair conformation, whereas the six-membered ring goes through a number of possible conformations [17,18]. To better understand the catalytic events taking place in the GH13 α-glucosidases, two carbonic analogs of D-glucose (inhibitors **1** and **2**) were synthesized and their mechanism of inhibition was studied in detail (Fig. 7.15). The compounds form a covalent complex with the active site residues of yeast α-glucosidase (Fig. 7.16) [19]. Moreover, the rate constants for

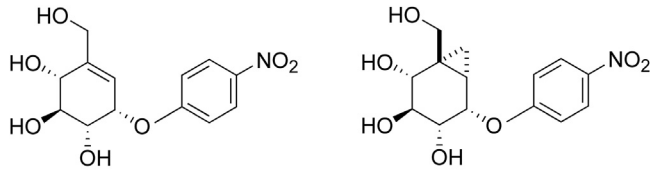

Inhibitor 1 **Inhibitor 2**

Figure 7.15 The carbonic analogs of D-glucose (inhibitors **1** and **2**) used as probes to explore the catalytic mechanism of inhibition of α-glucosidase.

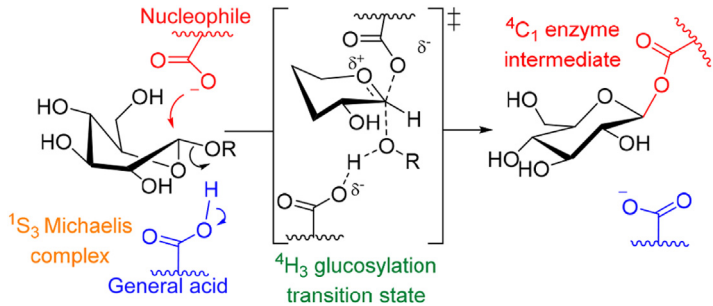

Figure 7.16 Proposed catalytic mechanism of a GH13 α-glucosidase. The Michaelis complex ($^1S_3$) undergoes glucopyranosylium ion-like transition state ($^4H_3$) that results in enzyme-bound intermediate ($^4C_1$). *Reprinted with permission from S. Shamsi Kazem Abadi, et al., New class of glycoside hydrolase mechanism-based covalent inhibitors: glycosylation transition state conformations, J. Am. Chem. Soc. 139 (2017) 10625−10628. ©2017. American Chemical Society.*

catalysis involving pseudoglycosylation and deglycosylation are different, which gives further insights into the conformational profile of the GH family of α-glucosidases. Mass spectrometry of the complex revealed the presence of a portion of the inhibitors' carbon skeleton that required unique conformations of both inhibitors to accomplish carbocation of the enzyme. For natural substrates, the conformation features a π-type molecular orbital that facilitates the C−O bond hydrolysis, which takes place through an oxygen *n*-type lone pair. The inhibitor **2**, a pseudoequatorial aglycone, is needed to proceed for catalysis

with a σ-bond participation, however, in case of inhibitor **1**, a pseudoaxial algycone conformation is needed [19].

The GH family of enzymes have been reported to stabilize the pyranosylium ion-like $^{4}H_{3}$ transition states that originate from the $^{1}S_{3}$ Michaelis complex. Based on this proposal, the inhibitor **2** forms a bicyclobutonium ion from bisected geometry similar to that of hydrolysis catalyzed by the GH13 family of enzymes. The enzyme stabilized the inhibitor **1** by forming an allylic cation-like transition state with five coplanar carbon atoms. Therefore, it binds to the enzyme in an $^{2}H_{3}$ half-chair conformation followed by catalysis that leads to an E3 allylic cation or allylic cation-like transition state similar to the $^{4}H_{3}$ glycosylation transition states. The σ-bond of inhibitor **2** requires a bisected geometry which results in a cation that retains the same geometry because of the high amount of rotational hindrance in bicyclobutonium ions [20]. Therefore, the reaction coordinates for covalent binding of inhibitor **1** resemble more closely to that of natural substrates. These reversible covalent inhibitors of α-glucosidases can be used as biological probes to study cellular processes involving time-dependent changes in glucosidase activity, and as tools for selecting better carbasugar analogs for antidiabetic drug development.

7.10 Computational simulations of α-glucosidase-inhibitor interactions

7.10.1 The 3′-benzylated analog of 3′-*epi*-neoponkoranol

Ponkoranol and its various analogs are a widely studied class of compounds with special focus on α-glucosidase inhibition. Recent work on the docking simulation of the 3′-benzylated analog of 3′-*epi*-neoponkoranol (BAN) with MGAM-N revealed important clues to how the inhibitor interacts with

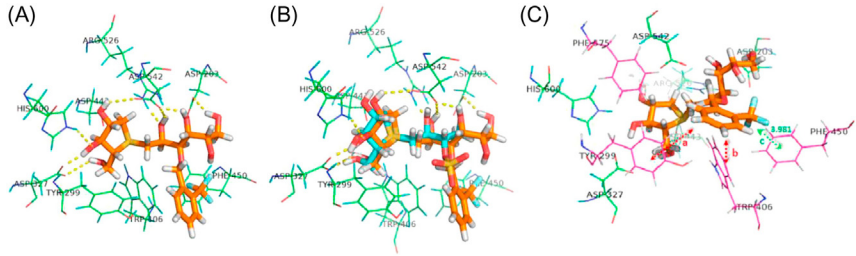

Figure 7.17 (A) Interaction of BAN with the MGAM-N active site. (B) Superimposition of salacinol and BAN. (C) Interaction of the trifluoromethyl group with amino residue Phe450. *Reproduced from D. Liu, et al., Design, synthesis and biological evaluation of 3′-benzylated analogs of 3′-epi-neoponkoranol as potent α-glucosidase inhibitors. Eur. J. Med. Chem. 110 (2016) 224–236. ©2015. French Société de Chimie Thérapeutique published by Elsevier Masson SAS. All rights reserved.*

the enzyme active site [21]. Its C_4' hydroxyl group is engaged in hydrogen bonding with Asp542 unlike MGAM-N-salacinol interaction in which its C_4' hydroxyl group binds to Asp203, whereas its C_2 hydroxyl group also interacts with Asp542. Additionally, the Asp542 residue is also involved in forming two hydrogen bonds with the C_2' hydroxyl group. It appears that the Asp542 residue is crucial for potent inhibition of MGAM-N since it allows hydrogen bonding interactions with both the C_2' and C_4' hydroxyl groups of BAN. The C_6' hydroxyl group of the inhibitor forms hydrogen bonds with Asp203 that is in agreement with the MGAM-N-kotalanol crystal structure (Fig. 7.17A).

The C_3' atom features an inverse stereoconfiguration that allows the *ortho*-substituted benzyl group to orient itself in a conformation similar to that of the sulfate group of salacinol (Fig. 7.17B). As discussed earlier, the sulfate group does not interact with any residues of the MGAM-N active site. However, the benzyl group of BAN contributed to inhibitory activity by involving in the van der Waals interactions with the

hydrophobic residues such as Tyr299, Trp406, and Phe450 (Fig. 7.17C). Noteworthy to mention is the *ortho*-substituted trifluoromethyl group, which most likely forms hydrophobic contacts with the phenyl ring of Phe450 at a distance of 3.98Å as it is oriented near that residue thus increasing the binding affinity of the inhibitor. The docking simulation of this class of compounds provides structural and functional evidence as to which derivatives demonstrate more inhibition of α-glucosidase. These studies suggest that sulfonium salts with an *ortho*-substituted benzyl group at 3′ position possess better enzyme affinities than their *meta* or *para*-substituted counterparts [21].

7.10.2 Fluorescent DNJ derivatives

The structure–activity relationship of fluorescent DNJ derivatives has been discussed in Chapter 2: Natural and synthetic sugar mimics (compounds **75–79**). Hatano et al. (2017) also computationally evaluated the compounds for their binding to MGAM-N active site [22]. The binding pattern of the compounds is similar to that of miglitol with the exception of the fluorescent moiety that moves freely on the surface of the active site owing to free rotation of the linker group (Fig. 7.18). Repulsion between the hydrophilic side chains on

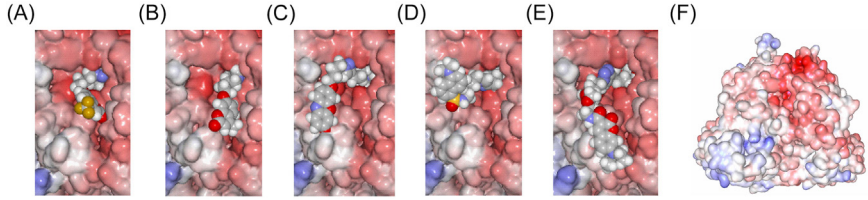

Figure 7.18 Binding simulations of fluorescent DNJ derivatives (A–E) to human MGAM-N (Chapter 2: Natural and synthetic sugar mimics, compounds **75–79**). (F) The global structure of MGAM-N. *Reprinted from A. Hatano, et al., Synthesis and characterization of novel, conjugated, fluorescent DNJ derivatives for α-glucosidase recognition, Bioorg. Med. Chem. 25 (2017) 773–778, with permission from Elsevier ©2017.*

the enzyme surface and the hydrophobic fluorescent moieties did not affect binding affinities of the compounds to the active site, which is in agreement with previous studies [23]. The kinetic data on the inhibition of rat intestinal maltase and sucrase by the target derivatives share similar pattern of inhibition of the enzymes by miglitol.

7.10.3 The 5-arylidene-*N*,*N*-diethylthiobarbiturate derivatives

The α-glucosidase inhibitory activity of 5-arylidene-*N*, *N*-diethylthiobarbiturate derivatives has been discussed in Chapter 5: Azoles and related derivatives. In this section, the molecular docking of the 2,3,4-trihydroxybenzylidene derivative (Chapter 5, compound **37**) is highlighted. The compound showed highest potency of *Saccharomyces cerevisiae* α-glucosidase inhibition among other derivatives ($IC_{50} = 0.6$ nM). Since no crystal structure of yeast α-glucosidase is available to date, a homology model of the enzyme was built based on the crystal structure of yeast isomaltase (PDB identifier 3AJ7) to which 2,3,4-trihydroxybenzylidene derivative was docked. The inhibitor forms hydrogen bonds with the Asp68, Asp214, GLu276, Asp349, and Arg439 residues. These interactions form a strong network of hydrogen bonds essentially contributing to its high affinity binding. In fact, the inhibitor shares the highest number of hydrogen bonds with the active site compared to other inhibitors studied in the series. The phenyl ring hydroxyl groups of the inhibitor form three hydrogen bonds with the active site residues, which is highest among all inhibitors. Generally, the potency of inhibition exhibited by the inhibitors in this series depends on the number of hydrogen bonds with the enzyme active site [24].

7.10.4 The 3′-*o*-neopentyl derivative of salacinol

Structural studies on MGAM-N inhibition by a variety of compounds provide an essential framework for exploring avenues to designing new inhibitors. One such study includes docking simulation of the 3′-*o*-neopentyl derivative of salacinol (Fig. 7.19) in complex with human MGAM-N and its comparison with the MGAM-N-salacinol crystal structure (Fig. 7.20) [25]. Since the physicochemical properties of the target compounds from the *Salacia* plant species greatly influence their inhibitory activities, this property was also reflected in the docking studies. Despite bearing negative binding effects between the aromatic residues and the sulfonate oxygens of salacinol, van der Waals interactions still prevailed between the neopentyl group and the hydrophobic residues (Phe575, Tyr299, and Trp406). The residues were in optimal range of distance to form van der Waals contacts with the hydroxyl groups of the neopentyl moiety. Binding data suggested that compounds with long alkyl chains interacted with the MGAM-N active site more efficiently than the 3′-*o*-neopentyl derivative despite exhibiting lower degree of inhibition than the derivative alone (data not shown). This appears to be attributed to lack of rotational movement of the straight alkyl chain.

7.10.5 Salvianolic acids C and A

The *Salvia miltiorrhiza* plant is a rich source of compounds with medicinal value. Tang et al. (2018) compiled a

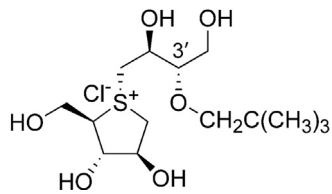

Figure 7.19 The 3′-*o*-neopentyl derivative of salacinol.

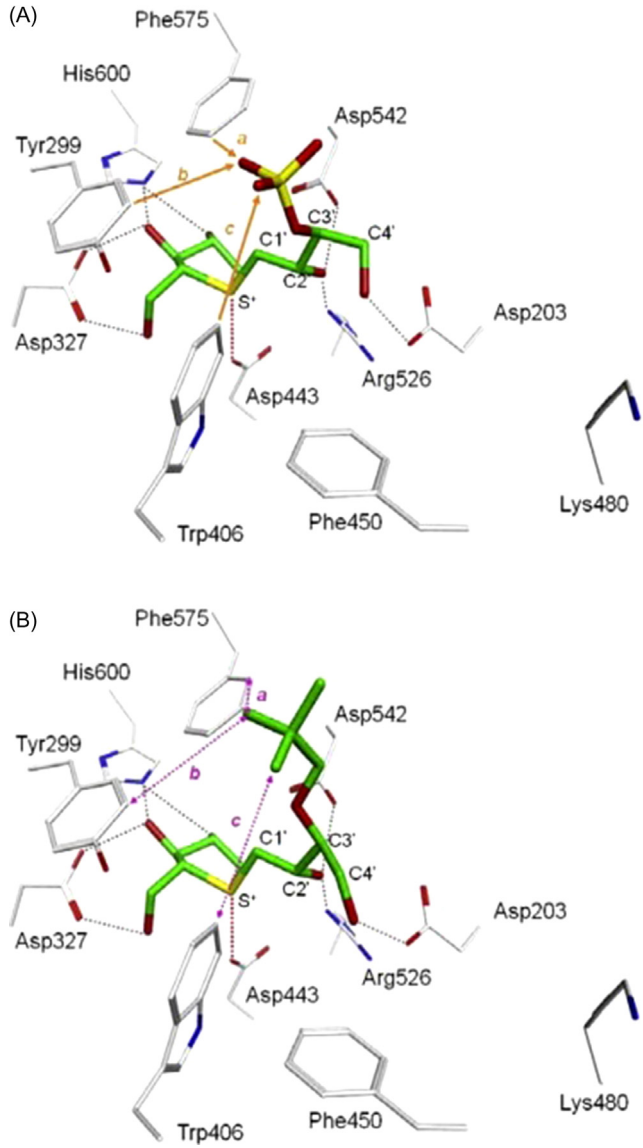

Figure 7.20 Docking of (A) salacinol and (B) 3′-*o*-neopentyl derivative of salacinol in the MGAM-N active site. Hydrogen bonds are shown as dotted lines. *Reprinted from G. Tanabe, et al., Hydrophobic substituents increase the potency of salacinol, a potent α-glucosidase inhibitor from Ayurvedic traditional medicine 'Salacia', Bioorg. Med. Chem. 24 (2016) 3705−3715, with permission from Elsevier* ©*2016.*

comprehensive list of α-glucosidase inhibitors isolated from the plant and studied them *in silico* [26]. Using the crystal structure of isomaltase as a model, the target compounds were docked into its active site. A number of important active site residues interacting with the ligands were identified. This includes Asp69, Tyr72, His112, Phe159, Gln182, Val216, Glu277, Gln279, His351, Asp352, Glu411, and Arg442 sharing several hydrogen bonds with the compounds. A list of key enzyme residues interacting with the inhibitors, and their hydrogen bonding scores have been provided in the original reference [26].

The docking study of salvianolic acid C (SAC) and salvianolic acid A (SAA) (Compounds **112** and **113**, respectively; Chapter 3: Polyphenols) revealed that they exhibit similar enzyme binding pattern by interacting with the Tyr72, Tyr158, Phe159, Gln182, Asp215, Val216, Glu277, Gln279, Phe303, Asn350, Asp352, and Arg442 residues (Fig. 7.21), and through several nonpolar interactions with their aromatic and aliphatic moieties. Moreover, the π-stacking of SAC and SAA with the Phe303, Phe159, Phe178, and Phe301 residues was also detected along with several hydrophobic interactions. The compounds also interacted with two of the catalytic residues of isomaltase active site that include Asp215 and Glu277. The hydrogen bond network that the inhibitors form is different from that of maltose–isomaltase complex; SAC forms seven hydrogen bonds with Asp215, Glu277, Glan279, Asp307, and Asn350 residues through its hydroxyl and carbonyl groups, whereas SAA does so by interacting with Asp215, Glu277, Gln279, Thr306, Gln353, and Glu411 with a total of nine hydrogen bonds. The docking scores for SAC (7.781) and SAA (8.0625) suggested that they are selective to the enzyme. Other phenolic compounds identified from the herb as α-glucosidase inhibitors demonstrated similar pattern of binding to the active site suggesting a common mechanism of

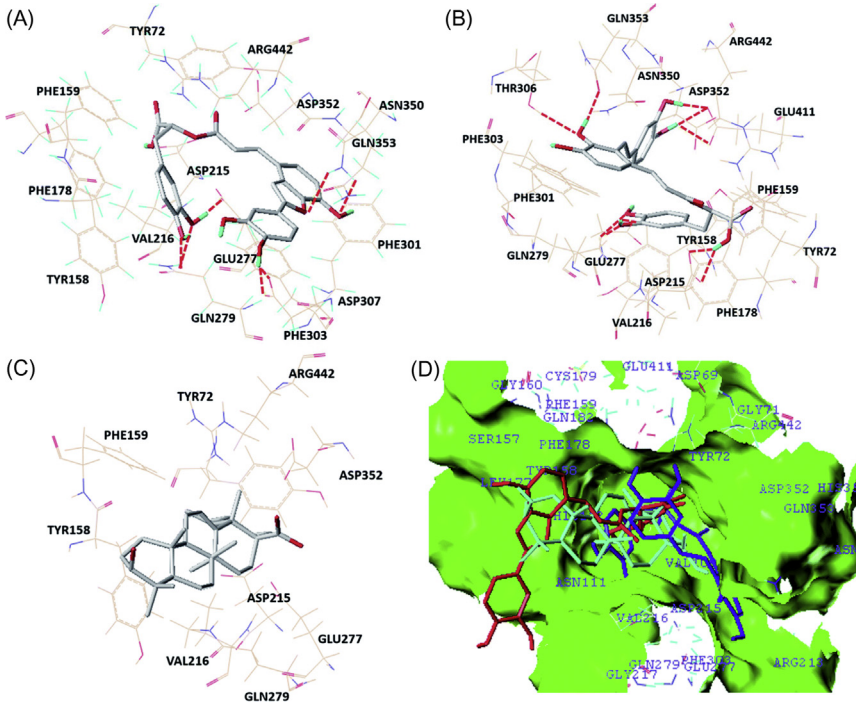

Figure 7.21 Docking simulations of (A) salvianolic acid C, (B) salvianolic acid A, and (C) ursolic acid. (D) Superimposition of the inhibitors bound to the enzyme active site. The amino acid residues are represented as sticks, and the hydrogen bonding interactions are shown as dotted lines. *Republished with permission of Royal Society of Chemistry from H. Tang, D. Zhao, Z. Xue, Exploring the interaction between Salvia miltiorrhiza and α-glucosidase: insights from computational analysis and experimental studies, RSC Adv. 8 (2018) 24701–24710. Permission conveyed through Copyright Clearance Center, Inc.*

α-glucosidase inhibition shared by the compounds isolated from the *Salvia miltiorrhiza* plant [26].

7.10.6 Pelargonidin-3-*o*-rutinoside and analogs

Recently, a number of pelargonidin-3-*O*-rutinoside and its analogs have been computationally studied using docking simulations [27]. The pelargonidin-3-*O*-rutinoside, modeled into the yeast α-glucosidase active site, forms electrostatic interactions

(π anion) with the catalytic residues of the enzyme (Asp214, Glu276, and Asp349). Moreover, it also forms a number of hydrogen bonds with several residues of the pocket that include Asp68, Ser156, His279, Arg312, Asp408, Asn412, and Arg439 in addition to one hydrogen bond with the catalytic residue Glu276. A number of hydrophobic interactions were also detected that include Tyr71 (π − π), Ala278 (π -alkyl), and His279 (π -alkyl).

For comparative purposes, four anthocyanins with potent α-glucosidase inhibitory activities (M3A, Peo3A, D3A, and Pg3G) and four with weaker activities (C3S, D3S, C3G, and C3R) were also docked into the active site. The M3A, Peo3A, D3A, and Pg3G inhibitors were able to reach deep into the active site through their A and C rings (Fig. 7.22) by forming hydrophobic interactions with Glu276, Asp214, Ala278, Tyr71, AND Asp349 residues (Fig. 7.23). The inhibitors also formed hydrogen bonds with Asp408 through their algycone moieties. However, the aglycone moieties of the weaker inhibitors (in particular D3S and C3S) could not access the deep active site pocket that resulted in the loss of all respective interactions mention above for the stronger inhibitors. Therefore, anthocyanins potently inhibit α-glucosidase mainly through hydrophobic interactions of their aglycone moieties with the Glu276, Asp214, Ala278, Tyr71, and Asp349 residues, and through hydrogen bonding interactions of their glycoside moieties with the Asp408 and Glu276 residues. The compound code numbers, referring to pelargonidin-3-*O*-rutinoside and its analogs in the text and in Figs. 7.22 and 7.23, have been adapted from the original reference. For complete structural details on the compounds, please refer to the original article [27].

7.10.7 Sericin peptide

Sericin peptide (sequence: SEDSSEVDIDLGN) is a product of silk protein hydrolysis which competitively inhibits α-glucosidase.

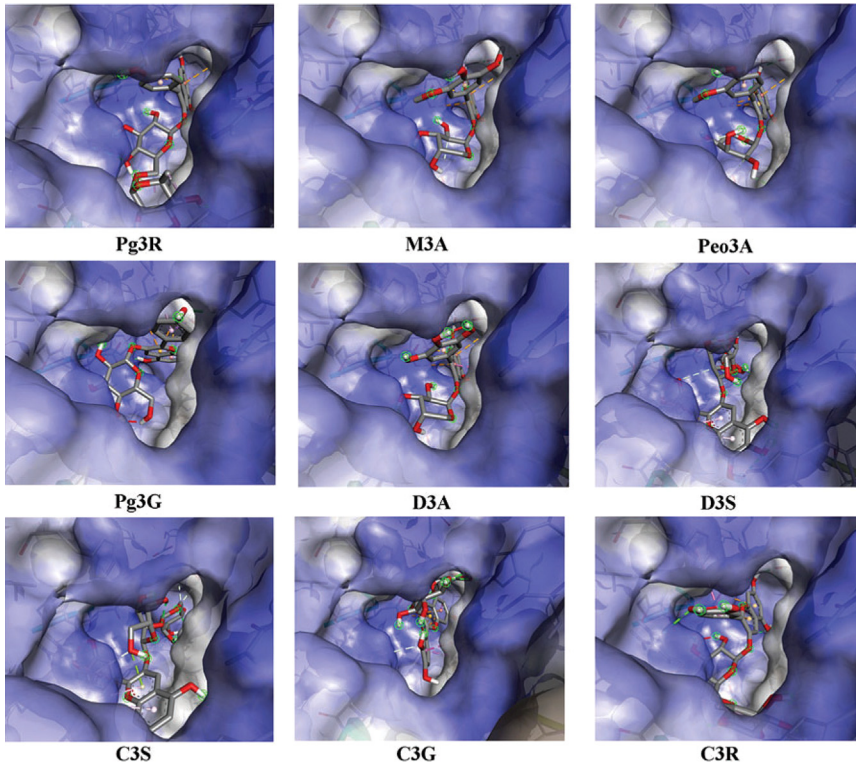

Figure 7.22 Pelargonidin-3-*o*-rutinoside (Pg3R) and its analogs reach deep into the α-glucosidase active site through their A and C rings. *Republished with permission of Royal Society of Chemistry from Y. Xu, L. Xie, J. Xie, Y. Liu, W. Chen, Pelargonidin-3-o-rutinoside as a novel α-glucosidase inhibitor for improving postprandial hyperglycemia, Chem. Commun. 55 (2019) 39–42. Permission conveyed through Copyright Clearance Center, Inc.*

Detailed analysis of its kinetics, mechanism of inhibition, thermodynamic properties, conformational changes, and molecular docking has been conducted recently [28]. Since α-glucosidase contains phenylalanine, tryptophan, and tyrosine residues that possess intrinsic fluorescence characteristics, binding of the peptide to the enzyme resulted in a suppression of intrinsic fluorescence in a concentration-dependent manner. Additionally, the peptide binding increased the polarity around the tryptophan and tyrosine

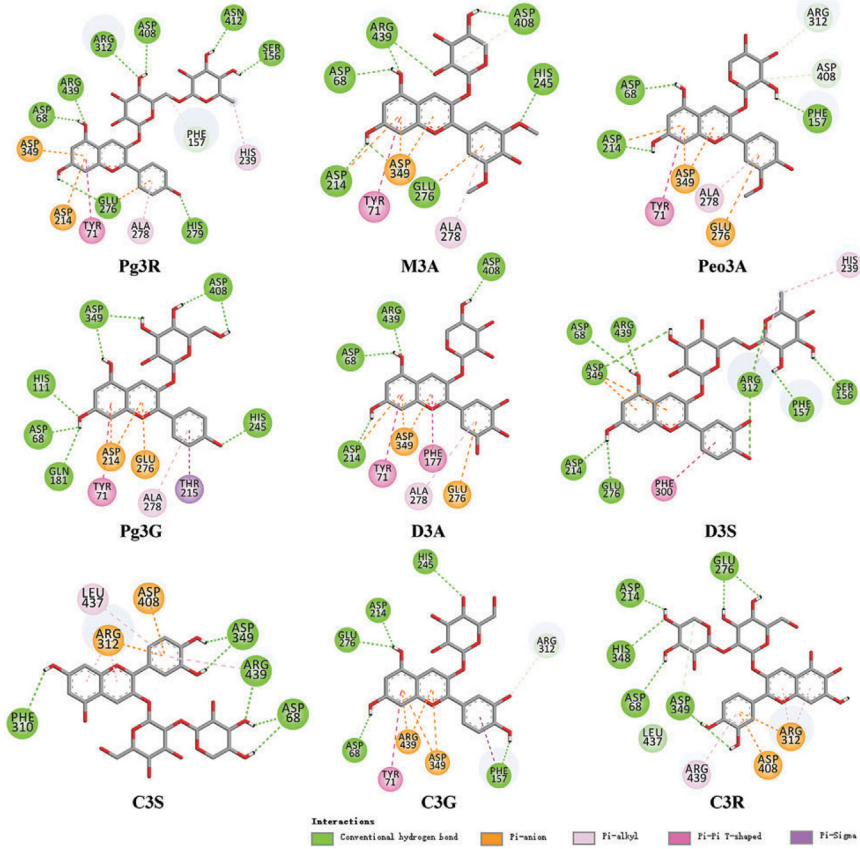

Figure 7.23 Interactions of pelargonidin-3-*o*-rutinoside (Pg3R) and its analogs with the α-glucosidase active site. *Republished with permission of Royal Society of Chemistry from Y. Xu, L. Xie, J. Xie, Y. Liu, W. Chen, Pelargonidin-3-o-rutinoside as a novel α-glucosidase inhibitor for improving postprandial hyperglycemia, Chem. Commun. 55 (2019) 39–42. Permission conveyed through Copyright Clearance Center, Inc.*

residues, implying that the peptide increased the surface or active site hydrophobicity of the enzyme. Analysis of the thermodynamic properties and binding forces showed that the van der Waals, hydrogen bonding, hydrophobic and electrostatic forces play important roles in the peptide binding. These forces define spontaneous binding of sericin which directly depends on

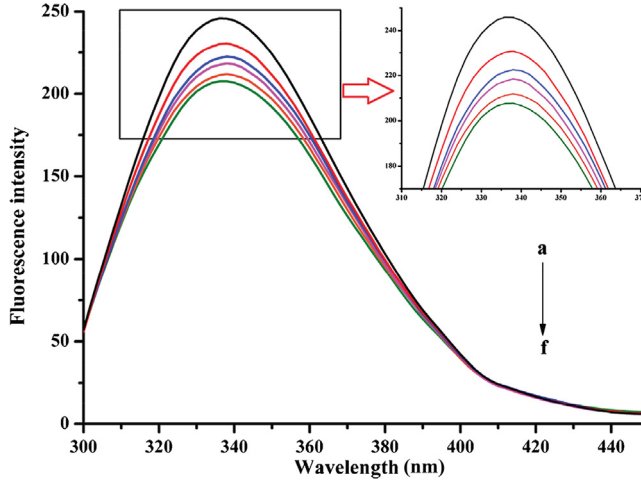

Figure 7.24 Circular dichroism spectra of α-glucosidase bound to sericin peptide. Binding of the peptide at two different concentrations resulted in a decrease of enzyme helicity. *Reprinted by permission from John Wiley & Sons. F. Xie, S. Wang, L. Zhang, J. Wu, Z. Wang, Investigating inhibitory activity of novel synthetic sericin peptide on α-D-glucosidase: kinetics and interaction mechanism study using a docking simulation, J. Sci. Food Agric. 98 (2018) 1502–1510. ©2018.*

increasing temperature. Moreover, the hydrophobic interactions play a major role in enzyme binding. Further work on the α-glucosidase-sericin interactions includes circular dichroism (CD) analysis that provides information on the effects of the peptide binding on the α-glucosidase structure. The enzyme features a high proportion of α-helix secondary structure. Binding of the peptide at two different concentrations resulted in a decrease of enzyme helicity (Fig. 7.24) [28].

Sericin was also subjected to molecular docking into the modeled α-glucosidase active site (Fig. 7.25A). The peptide forms four hydrogen bonds with the residues located in close proximity to the active site which include Thr310, Ser31, and Asn317. Moreover, the Asp242, Ser304, Asp307, Asp325, and Glu332 residues stabilized the peptide (Fig. 7.25B). Unlike acarbose, the peptide did not make any contacts with the

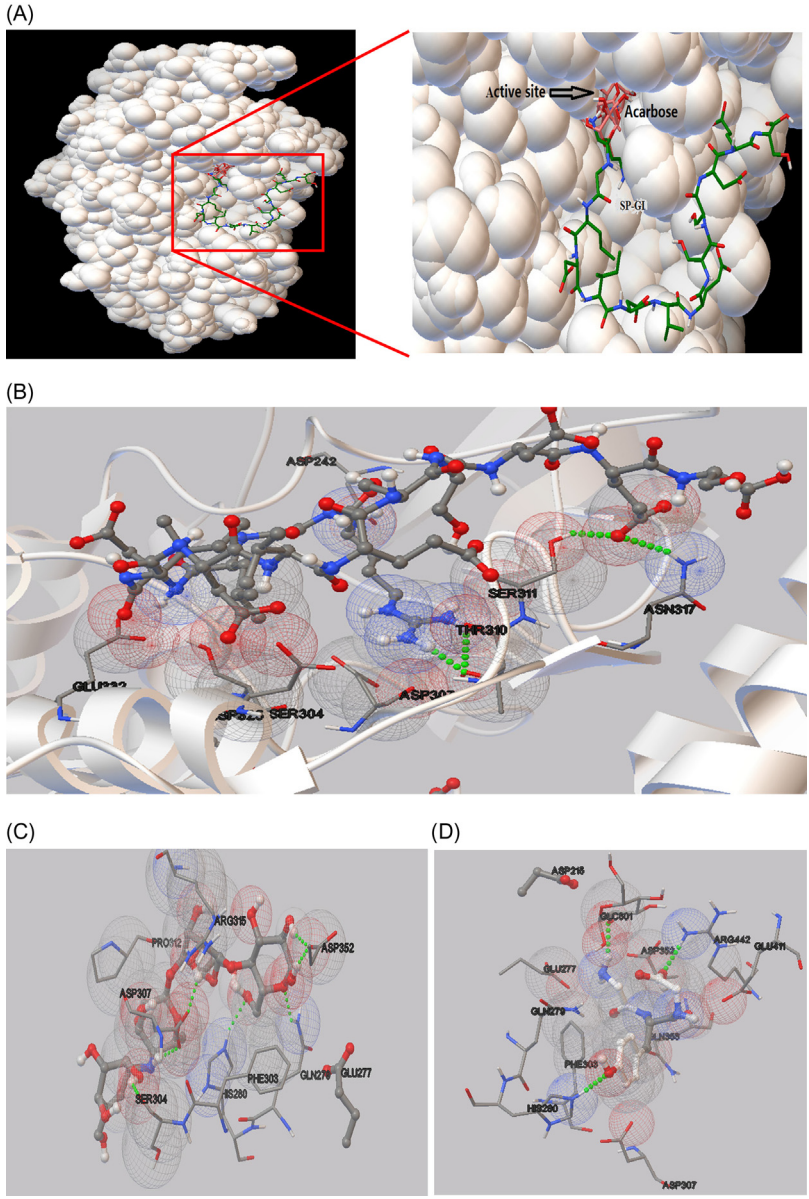

Figure 7.25 (A) Surface diagram of α-glucosidase comparing predicted binding of acarbose and sericin peptide. Interactions of sericin peptide (B), acarbose (C), and GYG peptide (D) with the active site residues. *Reprinted by permission from John Wiley & Sons. F. Xie, S. Wang, L. Zhang, J. Wu, Z. Wang, Investigating inhibitory activity of novel synthetic sericin peptide on α-D-glucosidase: kinetics and interaction mechanism study using a docking simulation, J. Sci. Food Agric. 98 (2018) 1502–1510. ©2018.*

catalytic residues Glu277 and Asp352 (Fig. 7.25B and C). However, the van der Waals forces and hydrogen bonds are central to inhibitor binding. In fact, the peptide binds to the substrate entry site close to the active site; one side of the peptide is positioned in such a way that it blocked the entry of substrate into the active site, whereas the other side is exposed near the surface of the enzyme. Comparison of sericin docking simulation with that of a tripeptide (GYG), identified from a silk cocoon hydrolysate [29], showed that both peptides bind around the same site of α-glucosidase (Fig. 7.25D). The GYG peptide shared three hydrogen bonds with the His280, Arg442, and Glc601 residues while being surrounded by the Asp215, Glu277, Gln279, Phe303, Asp307, Asp352, Gln353, and Glu411 residues. The positions of these amino acids were similar within the two enzymes, however, their composition and sequence was different.

Sericin peptides usually have polar side chains formed by the hydroxyl, carboxyl, and amino groups. The target sericin peptide bears polar side chains contributed by the asparagine and serine amino acids, which form multiple hydrogen bonds with the enzyme residues that is essential for α-glucosidase inhibition. This is in agreement with previous studies on a peptide inhibitor of α-glucosidase confirming that the polar side chains of the peptide play a crucial role in α-glucosidase inhibition [30].

References

[1] E.J. Rossi, et al., Inhibition of recombinant human maltase glucoamylase by salacinol and derivatives, FEBS J. 273 (2006) 2673–2683.
[2] R. Quezada-Calvillo, et al., Luminal starch substrate "brake" on maltase-glucoamylase activity is located within the glucoamylase subunit, J. Nutr 138 (2008) 685–692.
[3] L. Ren, et al., Structural insight into substrate specificity of human intestinal maltase-glucoamylase, Protein Cell 2 (2011) 827–836.
[4] G.M. Gray, B.C. Lally, K.A. Conklin, Action of intestinal sucrase-isomaltase and its free monomers on an alpha-limit dextrin, J. Biol. Chem. 254 (1979) 6038–6043.

[5] L. Sim, New glucosidase inhibitors from an Ayurvedic herbal treatment for type 2 diabetes: structures and inhibition of human intestinal maltase-glucoamylase with compounds from *Salacia reticulata*, Biochemistry 49 (2010) 443–451.
[6] X. Wen, Y. Yuan, D.A. Kuntz, D.R. Rose, B.M. Pinto, A combined STD-NMR/molecular modeling protocol for predicting the binding modes of the glycosidase inhibitors kifunensine and salacinol to Golgi R-mannosidase II, Biochemistry 44 (2005) 6729–6737.
[7] C.R. Berland, B.W. Sigurskjold, B. Stoffer, T.P. Frandsen, B. Svensson, Thermodynamics of inhibitor binding to mutant forms of glucoamylase from Aspergillus niger determined by isothermal titration calorimetry, Biochemistry 34 (1995) 10153–10161.
[8] H. Liu, R. Nasi, K. Jayakanthan, L. Sim, H. Heipel, D.R. Rose, et al., New synthetic routes to chain-extended selenium, sulfur, and nitrogen analogues of the naturally occurring glucosidase inhibitor salacinol and their inhibitory activities against recombinant human maltase glucoamylase, J. Org. Chem. 72 (2007) 6562–6572.
[9] S. Mohan, B.M. Pinto, Zwitterionic glycosidase inhibitors: salacinol and related analogues, Carbohydr. Res. 342 (2007) 1551–1580.
[10] R. Nasi, B.O. Patrick, L. Sim, D.R. Rose, B.M. Pinto, Studies directed toward the stereochemical structure determination of the naturally occurring glucosidase inhibitor, kotalanol: synthesis and inhibitory activities against human maltase glucoamylase of seven-carbon, chain-extended homologues of salacinol, J. Org. Chem. 73 (2008) 6172–6181.
[11] F. Cardona, et al., Total syntheses of casuarine and its 6-*O*-α-glucoside: complementary inhibition towards glycoside hydrolases of the GH31 and GH37 families, Chem. Eur. J. 15 (2009) 1627–1636.
[12] K. Yamamoto, H. Miyake, M. Kusunoki, S. Osaki, Crystal structures of isomaltase from Saccharomyces cerevisiae and in complex with its competitive inhibitor maltose, FEBS J. 277 (2010) 4205–4214.
[13] B. Svensson, Regional distant sequence homology between amylases, α-glucosidases, and transglucanosylases, FEBS Lett 230 (1988) 72–76.
[14] M.D. Witte, G.A. van der Marel, J.M. Aerts, H.S. Overkleeft, Irreversible inhibitors and activity-based probes as research tools in chemical glycobiology, Org. Biomol. Chem. 9 (2011) 5908–5926.
[15] K.W. Moremen, M. Tiemeyer, A.V. Nairn, Vertebrate protein glycosylation: diversity, synthesis and function, Nat. Rev. Mol. Cell Biol. 13 (2012) 448–462.
[16] R.L. Schnaar, R. Gerardy-Schahn, H. Hildebrandt, Sialic acids in the brain: gangliosides and polysialic acid in nervous system development, stability, disease, and regeneration, Physiol. Rev. 94 (2014) 461–518.
[17] G.J. Davies, A. Planas, C. Rovira, Conformational analyses of the reaction coordinate of glycosidases, Acc. Chem. Res. 45 (2012) 308–316.

[18] M.L. Sinnott, Catalytic mechanism of enzymic glycosyl transfer, Chem. Rev. 90 (1990) 1171–1202.
[19] S. Shamsi Kazem Abadi, et al., New class of glycoside hydrolase mechanism-based covalent inhibitors: glycosylation transition state conformations, J. Am. Chem. Soc. 139 (2017) 10625–10628.
[20] D.S. Kabakoff, E. Namanworth, Nuclear magnetic double resonance studies of the dimethylcyclopropylcarbinyl cation. Measurement of the rotation barrier, J. Am. Chem. Soc. 92 (1970) 3234–3235.
[21] D. Liu, et al., Design, synthesis and biological evaluation of 3′-benzylated analogs of 3′-epi-neoponkoranol as potent α-glucosidase inhibitors, Eur. J. Med. Chem. 110 (2016) 224–236.
[22] A. Hatano, et al., Synthesis and characterization of novel, conjugated, fluorescent DNJ derivatives for α-glucosidase recognition, Bioorg. Med. Chem. 25 (2017) 773–778.
[23] N. Ardes-Guisot, et al., Selection of the biological activity of DNJ neoglycoconjugates through click length variation of the side chain, Org. Biomol. Chem. 9 (2011) 5373–5388.
[24] M. Khan, et al., Synthesis, molecular modeling and biological evaluation of 5-arylidene-N,N-diethylthiobarbiturates as potential α-glucosidase inhibitors, Med. Chem. 15 (2019) 175–185.
[25] G. Tanabe, et al., Hydrophobic substituents increase the potency of salacinol, a potent α-glucosidase inhibitor from Ayurvedic traditional medicine 'Salacia', Bioorg. Med. Chem. 24 (2016) 3705–3715.
[26] H. Tang, D. Zhao, Z. Xue, Exploring the interaction between *Salvia miltiorrhiza* and α-glucosidase: insights from computational analysis and experimental studies, RSC Advances 8 (2018) 24701–24710.
[27] Y. Xu, L. Xie, J. Xie, Y. Liu, W. Chen, Pelargonidin-3-O-rutinoside as a novel α-glucosidase inhibitor for improving postprandial hyperglycemia, Chem. Commun. 55 (2019) 39–42.
[28] F. Xie, S. Wang, L. Zhang, J. Wu, Z. Wang, Investigating inhibitory activity of novel synthetic sericin peptide on α-D-glucosidase: kinetics and interaction mechanism study using a docking simulation, J. Sci. Food Agric. 98 (2018) 1502–1510.
[29] H.J. Lee, H.S. Lee, J.W. Choi, K.S. Ra, J.M. Kim, H.J. Suh, Novel tripeptides with α-glucosidase inhibitory activity isolated from silk cocoon hydrolysate, J. Agric. Food Chem. 59 (2011) 11522–11525.
[30] Y. Ren, et al., Identification and characterization of two novel α-glucosidase inhibitory oligopeptides from hemp (*Cannabis sativa* L.) seed protein, J. Funct. Foods 26 (2016) 439–450.

APPENDIX

A comprehensive list of promising α-glucosidase inhibitors with the activity data discussed in the book

Compound	IC_{50} (μM)	K_i (μM)	*In vivo* activity*	References
Chapter 2. Natural and synthetic sugar mimics				
1	0.15[a] 5.8[b]		Yes	[16]
2	0.71[a] 91.0[b]			
3	0.79[f] 4.7[b] 5.0[d]			
4	22.0[f] 65.0[b]			
5	0.19[b] 0.38[d] 8.8[c] 2.0[f]	0.081[b]	Yes	[17]
6	0.08[b]			[18]
7	0.032[d] 0.2[b]			[20]
8	0.71[b] 0.19[d]			
9	0.51[b] 0.11[d]			
10	0.38[b] 0.24[d]			
11	0.32[b] 0.45[d]			
12	0.22[b] 0.026[d]			[22]
13	6.70[a]			[23]
14	9.30[a]			
15	1.40[a]			[24]
16	4.90[a]			
17	See Ref. [24]			
18	See Ref. [24]			
19	3.30[a]			[25]
20	1.50[a]			
21	See Ref.			[26]
22	See Ref. [26]			
23	0.33[b]			

(*Continued*)

(Continued)

Compound	IC_{50} (μM)	K_i (μM)	*In vivo* activity*	References
24	0.53[b]			
25	See Ref.			[27]
26	47 nM[b]		Yes	
27	See Ref. [27]			
28	3.5[b] 3.4[d]			
29	7.9[f] 1.6[b] 3.1[d]			
30–34	0.028–5.0[f]	0.083–3.0[f]		[28]
35	0.5[a]			[29]
36	2.4[a]			
37	0.7[a]			
38	See Ref. [29]			
39	See Ref. [29]			
40	0.2[i]			[30]
41	0.4[i]			
42	See Ref. [30]			
43	4.7[f]			[38]
44	0.7[b] 1.2[f]			[40]
45	1.1[b]			
46	47 nM[f]	57 nM[f]		[45]
47	107[f]			
48	0.26[f]			
49	0.79[f]			
50	2.2[f]			[46]
51	52 nM[f]	31 nM[f]		
52	1.5[f]			
53	2.3[f]			
54	2.3[f]			
55	0.72[b]			[52]
56	5.53[b]			
57–64	See Ref.			[49]
65	0.11[g]	0.19[h]		[53]
66	17 nM[g]	0.3[h]		
67	17 nM[h]			
68–74	0.025–7.3[b,d,f]			[54]
75–79	See Ref.			[55]

(*Continued*)

(Continued)

Compound	IC_{50} (μM)	K_i (μM)	*In vivo* activity*	References
80	6.0[e]			[58]
81	2.3[a]			[59]
82	5.6[a]			
83	7.7[b] 15.9[d]			
84	5.1[b] 10.4[d]	4.8[b] 17.1[d]		
85	12.0[g,h]			
86		0.18[b]		[65]
87		0.31[b]		[66]
		0.47[c]		
		0.32[d]		
88	3.9[e]			[67, 68]
89	3.9[e]			
90	5.0[e]			
91	4.0[e]			
92−95		0.015−0.073[e]	Yes	[69]
96		0.043[e]		[70]
97		0.015[e]		
98		0.5[e]		
99−109	See Ref.			[73]
110	12.0[a]			[75]
111	31.0[a]			
Chapter 3. Polyphenols				
1	0.4[a]			[10]
2	0.8[a]			
3	1.1[a]			
4	1.8[a]			
5	1.6[a]			
6−10	11.1−19.1	9.7−16.2		[11]
11	12.4[a]			[12]
12	15.6[a]			
13	0.98[a]			
14	0.4[a]			
15	7.18[a]			[13]
16	3.28[a]			
17	7.13[a]			
18	5.76[a]			
19	0.19[a]			

(*Continued*)

(Continued)

Compound	IC_{50} (μM)	K_i (μM)	*In vivo* activity*	References
20	1.12[a]			
21	0.34[a]			
22	0.0645[a]			
23	0.075[a]			[14]
24	0.025[a]			
25	0.014[a]			
26	0.036[a]			
27	0.073[a]			
28	0.018[a]			
29	15.0[a]			[15]
30	12.8[a]			
31	12.0[a]			
32	12.0[a]			
33	12.0[a]			
34	15.2[b]			[16]
35	18.9[b]			
36	10.9[b]			
37	14.5[b]			
38–46	See Ref.		Yes	[17]
47		8.9[a]		[22]
48		7.4[a]		
49		5.8[a]		
50		7.0[a]		
51		1.5[a]		[26]
52		5.0[a]		
53		14.4[a]		
54	7.3[a]			[29]
55	5.2[a]			
56	13.3[a]			
57	9.3[a]			[31]
58	5.8[a]			
59	8.0[a]			
60	See Ref. [31]			
61	39.9[a]			
62	27.8[a]			
63		5.3[a]		[11]

(*Continued*)

(Continued)

Compound	IC_{50} (μM)	K_i (μM)	*In vivo* activity*	References
64		4.2[a]		
65		2.3[a]		
66	4.13[a]			[37]
67	7.51[a]			
68−71	100−700[b]		Yes	[38]
72	6.1[i]			[39]
73	1.0[i]			
74	7.0[a]			[42]
75	14.0[a]			
76−79	5−13[a]			
80	2.0[a]			
81		19.93[a]		[48]
82		14.45[a]		
83		12.06[a]		
84	0.7−47.5[a,i]			[49]
85	13.0[a]			[50]
86	6.0[a]			
87	40.0[i]			[57]
88	50.0[i]			
89		0.84[i]		
90	0.0193[a]	0.021[a]		[62]
91−103	See Ref.			[64]
104	1.69[b]			[69]
105	2.0			[70−74]
106	23.0			
107−111	0.15−4.1[a]			[75]
112	4.31[a]			[78]
113	19.29[a]			
114	0.03[a]			[83]
115	0.098[a]			
116	2.8[a]			[87]
117	2.6[a]			
118	1.6[a]			
Chapter 4. Terpenoids and steroids				
1	1.42[a]			[9]
2	0.02[a]			
3	1.08[a]			

(*Continued*)

(Continued)

Compound	IC_{50} (μM)	K_i (μM)	*In vivo* activity*	References
4	0.98[a]			
5	2.37[a]			
6	2.0[a]		Yes	[13]
7	3.53[a]			[15]
8	5.52[a]			
9	8.14[a]			
10		11.61[a]		[18]
11		11.87[a]		
12	16.0[a]			[19, 20]
13	6.0[a]			
14	8.3[a]			
15	1.8[a]			[21]
16	18.4[a]			
17	5.5[a]			
18	7.9[a]			
19	6.5[a]			
20	22.5[a]			
21	24.5			[22]
22	1.2	1.42		
23–34	See Ref.		Yes	[31]
35–39	0.71–10.32[a]			[32]
40–41	<0.07[a]			[37]
42–47	See Ref.		Yes	[41]
Chapter 5. Azoles and related derivatives				
1		12.0[a]		[5]
2		4.36[a]		
3		11.2[a]		
4		6.0[a]		
5		14.3[a]		
6	5.55[a]			[6]
7	5.58[a]			
8	5.31[a]			
9	0.02[b]			[7]
10	0.09[b]			
11	0.09[b]			
12	3.8		Yes	[8]
13	2.8[a]			[9]

(*Continued*)

(Continued)

Compound	IC_{50} (μM)	K_i (μM)	*In vivo* activity*	References
14	2.71[a]			[10]
15	11.41[a]			
16	14.2[a]			
17−21	0.64−10.22[a]			[11]
22	0.3[a]	0.43[a]		[12]
23	0.4[a]	0.25[a]		
24	0.86[a]	0.28[a]		
25	11.8[a]			
26	1.9[a]			
27	0.57[a]	6.6[a]		
28	3.25[a]			
29	1.5[a]			
30	1.15[a]			
31	14.6[a]			
32	1.3[a]			
33	1.45[a]			
34	0.011	0.1085		[14]
35	0.00215	0.0015		
36	18.91[a]			[15]
37	0.6 nM[a]			
38	19.18[a]			
39		0.17[a]		[23]
40		8.25[a]		
41		11.75[a]		
42		14.53[a]		
43		14.35[a]		
44		3.03[a]		
45		3.18[a]		
46		9.18[a]		
47		6.70[a]		
Chapter 6. Cyclitols and miscellaneous inhibitors				
1	0.23[b] 0.19[d]		Yes	[3]
2	12.23[a]			[5]
3	13.08[a]			
4		12.0[a]		[7]
5		84.0[a]		
6	3.1[b] 3.7[d]			[8]

(*Continued*)

(Continued)

Compound	IC_{50} (μM)	K_i (μM)	*In vivo* activity*	References
7	3.6[b] 4.0[d]			
8–11	11–18[i]			[10]
12–14	6.5–18.5[a]			[14]
15–18	4.12–5.68[a]			[15]
19–21	6.0–12.0[a]			[16]
22	0.58[a]			[17]
23	1.07[a]			
24	1.23[a]			
25–27	1.0–10.0[a]			
28	6.5[i]			[19]
29	5.0[i]			
30	See Ref. [19]		Yes	
31	See Ref. [19]		Yes	
32		21.5[a]		
33	8.4[a]	3.2[a]		
34	7.04[a]			[21]
35	4.87[a]			[22]
36	10.74[a]			
37		1.7[a]		[23]
38–43	See Ref.		Yes	[26]
44		1.42 nM		[27]
45		0.3 nM		
46–49	0.62–4.2			[28]
50	0.4			
51		6.2 nM[a]		[29]
52		0.15 nM[a]		
53–67	0.0092–0.246[a]			[31]

*Antihyperglycemic activity in mice/rats.
α-Glucosidase inhibited:
[a]Yeast (*Saccharomyces cerevisiae*)
[b]Rat intestinal maltase
[c]Rat intestinal isomaltase
[d]Rat intestinal sucrase
[e]Human intestinal maltase-glucoamylase (MGAM)
[f]Rice
[g]Rat liver α-glucosidase I
[h]Rat liver α-glucosidase II
[i]Bacterial (*Bacillus stearothermophilus*)

Index

Note: Page numbers followed by "*f*" refer to figures

D

E

F

Alpha-Glucosidase Inhibitors

Clinically Promising Candidates for Antidiabetic Drug Discovery

An extensive compilation of 390 promising α-glucosidase inhibitors for potential development into antidiabetic drugs

Key Features:

- Identifies and presents promising α-glucosidase inhibitors of natural and synthetic origins from a variety of chemical classes
- Discusses detailed structural and biological activity data that will be useful for researchers in selecting inhibitors for further work
- Highlights potential avenues and challenges in the development of new α-glucosidase inhibitors based on their activity data

Over 400 million people worldwide have been diagnosed with diabetes and the numbers continue to rise, highlighting the growing necessity for novel treatment options. Promising α-glucosidase inhibitors identified to date offer a wide chemical diversity, making them good candidates for further development into antidiabetic drugs. However, those in current use are marred by efficacy problems and unwanted side effects. *Alpha-Glucosidase Inhibitors: Clinically Promising Candidates for Antidiabetic Drug Discovery* aims to support researchers in addressing these issues, highlighting a host of leads for development into novel oral antidiabetic drugs with improved efficacy and fewer side effects.

This book begins with a discussion of the challenges and huge potential of α-glucosidase inhibitors for new antidiabetic drug development. The author reviews a range of natural and synthetic α-glucosidase inhibitors, provides chemical structures, background information, and *in vivo* and *in vitro* biological activity data. The book explores new structural and functional avenues that facilitate faster development and more diverse adaptations of oral antidiabetic drugs. Drawing on the author's expert research in the field, this book is an invaluable resource for antidiabetic drug development researchers.

About the Author:

Dr. Usman Ghani is a biochemist with education and training from the University of Karachi, Pakistan and University of Alberta, Canada. Currently, he is Associate Professor of Biochemistry at the Clinical Biochemistry Unit, Department of Pathology, College of Medicine, King Saud University, Saudi Arabia. His research interests include enzymology, cellular processes, and endothelial function and repair in disease. Dr. Ghani's current research also involves screening and identification of clinically important enzyme inhibitors and studies on their mechanism of inhibition. His team has identified a number of synthetic and natural inhibitors of α-glucosidase and other enzymes that may become potential candidates for development into drugs for the treatment of diabetes mellitus and other diseases. Dr. Ghani has been awarded numerous research grants and publishes his research in high impact journals of international repute.

ISBN 978-0-08-102779-0

9 780081 027790

ELSEVIER elsevier.com/books-and-journals